Université de Montréal

Consequences of local and global chromatin mechanics to adaption and genome stability in the budding yeast *Saccharomyces cerevisiae*

Par

Lidice González López

Département de biochimie et médecine moléculaire

Faculté de médecine

Thèse présentée en vue de l'obtention du grade de *Philosophiae Doctor* (PhD)

en Biochimie

Avril 2022

Université de Montréal

Département de biochimie et médecine moléculaire

Faculté de médecine

Cette thèse est intitulée

Consequences of local and global chromatin mechanics to adaption and genome stability in the budding yeast *Saccharomyces cerevisiae*

Présentée par

Lidice González López

Évaluée par un jury composé des membres suivants

John Pascal
Président-rapporteur

Stephen W Michnick
Directeur de recherche

Éric Milot
Membre du jury

Stephanie Weber
Examinateur externe

Audrey Claing
Représentant du Doyen

Résumé

Le génome de la levure de boulanger *Saccharomyces cerevisiae* a évolué à partir d'un ancêtre chez lequel une profonde décompaction du génome s'est produite à la suite de la perte de la méthylation de la lysine 9 de l'histone H3, il y a environ 300 millions d'années. Il a été proposé que cette décompaction du génome a entraîné une capacité accrue des levures à évoluer par des mécanismes impliquant des taux de recombinaison méiotique et de mutation exceptionnellement élevés. La capacité à évoluer accrue qui en résulte pourrait avoir permis des adaptations uniques, qui en ont fait un eucaryote modèle idéal et un outil biotechnologique. Dans cette thèse, je présenterai deux exemples de la façon dont les adaptations locales et globales du génome se reflètent dans les changements des propriétés mécaniques de la chromatine qui, à leur tour, indiquent un phénomène de séparation de phase causée par les modifications post-traductionnelles des histones et des changements dans les taux d'échange des histones.

Dans un premier manuscrit, je présente des preuves d'un mécanisme par lequel la relocalisation du locus *INO1*, gène actif répondant à la déplétion en inositol, du nucléoplasme vers l'enveloppe nucléaire, augmente la vitesse d'adaptation et la robustesse métabolique aux ressources fluctuantes, en augmentant le transport des ARNm vers le cytosol et leur traduction. La répartition d'*INO1* vers l'enveloppe nucléaire est déterminée par une augmentation locale des taux d'échange d'histones, ce qui entraîne sa séparation de phase du nucléoplasme en une phase de faible densité plus proche de la périphérie nucléaire. J'ai quantifié les propriétés mécaniques de la chromatine du locus du gène dans les états réprimé et actif en analysant le déplacement de 128 sites LacO fusionnés au gène liant LacI-GFP en calculant diffèrent paramètres tel que la constante de ressort effective et le rayons de confinement du locus. De plus, j'ai mesuré l'amplitude et le taux d'expansion en fonction du temps du réseau LacO et j'ai observé une diminution significative du locus à l'état actif, ce qui est cohérent avec le comportement de ressort entropique de la chromatine décompactée. J'ai montré que les

séquences d'éléments en cis dans le promoteur du locus, essentielles à la séparation de phase, sont des sites de liaison pour les complexes de remodelage de la chromatine effectuant l'acétylation des histones. Ces modifications de la chromatine entraînent une augmentation des taux d'échanges des sous-unités des complexes d'histones, et une séparation de phase locale de la chromatine. Enfin, je présente l'analyse de simulations *in silico* qui montrent que la séparation de phase locale de la chromatine peut être prédite à partir d'un modèle de formation/disruption des interactions multivalentes protéine-protéine et protéine-ADN qui entraîne une diminution de la dynamique de l'ADN. Ces résultats suggèrent un mécanisme général permettant de contrôler la formation rapide des domaines de la chromatine, bien que les processus spécifiques contribuant à la diminution de la dynamique de l'ADN restent à étudier.

Dans un second manuscrit, je décris comment nous avons induit la « retro-évolution » de la levure en réintroduisant la méthylation de la lysine 9 de l'histone H3 par l'expression de deux gènes de la levure *Schizosaccaromyces pombe Spswi6* et *Spclr4*. Le mutant résultant présente une augmentation de la compaction de la chromatine, ce qui entraîne une réduction remarquable des taux de mutation et de recombinaison. Ces résultats suggèrent que la perte de la méthylation de la lysine 9 de l'histone H3 pourrait avoir augmenté la capacité à l'évoluer. La stabilité inhabituelle du génome conférée par ces mutations pourrait être utile pour l'ingénierie métabolique de *S. cerevisiae*, dans laquelle il est difficile de maintenir des gènes exogènes intégrés pour les applications de nombreux processus biotechnologiques courants tels que la production de vin, de bière, de pain et de biocarburants. Ces résultats soulignent l'influence des propriétés physiques d'un génome sur son architecture et sa fonction globales.

Mots clés : relocalization des gènes, séquences de recrutement de gènes, propriétés mécaniques de la chromatine, séparation de phase, compaction du génome, taux de mutation, taux de recombinaison, stabilité génétique

Abstract

The genome of the budding yeast *Saccharomyces cerevisiae* evolved from an ancestor in which a profound genome decompaction occurred as the result of the loss of histone H3 lysine 9 methylation, approximately 300 million years ago. This decompaction may have resulted in an increased capacity of yeasts to evolve by mechanisms that include unusually high meiotic recombination and mutation rates. Resultant increased evolvability may have enabled unique adaptations, which have made it an ideal model eukaryote and biotechnological tool. In this thesis I will present two examples of how local and global genome adaptations are reflected in changes in the mechanical properties of chromatin.

In a first manuscript, I present evidence for a mechanism by which partitioning of the active inositol depletion-responsive gene locus *INO1* from nucleoplasm to the nuclear envelope increases the speed of adaptation and metabolic robustness to fluctuating resources, by increasing mRNA transport to the cytosol and their translation. Partitioning of *INO1* to the nuclear envelope is driven by a local increase in histone exchange rates, resulting in its phase separation from the nucleoplasm into a low-density phase closer to the nuclear periphery. I quantified the mechanical properties of the gene locus chromatin in repressed and active states by monitoring mean-squared displacement of an array of 128 LacO sites fused to the gene binding LacI-GFP and calculating effective spring constants and radii of confinement of the array. Furthermore, I measured amplitude and rate of time-dependent expansion of the LacO array, and observed a significant decrease for the active-state locus which is consistent with entropic spring behavior of decompacted chromatin. I showed that cis element sequences in the promoter and upstream of the locus that are essential to phase separation are binding sites for chromatin remodeling complexes that perform histone acetylation among other modifications that result in increased histone complex exchange rates, and consequent local chromatin phase separation. Finally, I present analytical simulations that show that

local phase separation of chromatin can be predicted from a model of formation/disruption of multivalent protein-protein and protein-DNA interactions that results in decreased DNA dynamics. These results suggest a general mechanism to control rapid formation of chromatin domains, although the specific processes contributing to the decreased DNA dynamics remain to be investigated.

In a second manuscript, I describe how we retro-evolutionarily engineered yeast by reintroducing histone H3 lysine 9 methylation through the expression of two genes from the yeast *Schizosaccaromyces pombe Spswi6* and *Spclr4*. This mutant shows an increase in compaction, resulting in remarkable reduced mutation and recombination rates. These results suggest that loss of histone H3 lysine 9 methylation may have increased evolvability. The unusual genome stability imparted by these mutations could be of value to metabolically engineering *S. cerevisiae,* in which it is difficult to maintain integrated exogenous genes for applications for many common biotechnological processes such as wine, beer, bread, and biofuels production. These results highlight the influence of the physical properties of a genome on its overall architecture and function.

Key words: gene relocalization, gene recruitment sequences, chromatin mechanical properties, chromatin remodeling, phase separation, genome compaction, mutation rate, recombination rate, genetic stability

Table of Contents

List of figures

List of tables

List of abbreviations

3C: chromosome conformation capture

5-FOA: 5-fluoroorotic acid

ACN: acetonitrile

AID: auxin-inducible degron

ATP: adenosine triphosphate

BioGrid: Biological General Repository for Interaction Datasets

BioID: Proximity-dependent Biotin Identification

Can^r $5FOA^r$: canavanine- and 5-fluoroorotic acid (5FOA)-resistant mutants

Can^r: canavanine-resistant mutants

CFTR: cystic fibrosis transmembrane conductance regulator

CFUs: Colony-forming units

CHD: chromodomain-helicase-DNA binding complex

ChIP-chip: Chromatin immunoprecipitation (ChIP) followed by microarray hybridization

ChIP-qPCR: Chromatin Immunoprecipitation followed by real time PCR

ConA: Concanavalin A

Ct: cycle threshold

CTCF: CCCTC-binding factor

DAPI: 4',6-diamidino-2-phenylindole

dCas9: catalytically dead Cas9

DNA: deoxyribonucleic acid

FA: formic acid

FACT: facilitates chromatin transactions complex

FISH: fluorescence in situ hybridization

GCR: gross chromosomal rearrangement

GRS: gene recruitment sequence

H3K14ac: histone H3 lysine 14 acetylation

H3K18ac: histone H3 lysine 18 acetylation

H3K4me3: histone H3 lysine 4 tri-methylation

H3K56ac: histone H3 lysine 56 acetylation

H3K9ac: histone H3 lysine 9 acetylation

H3K9me: histone H3 lysine 9 methylation

H4K12ac: histone H4 lysine 12 acetylation

H4K5ac: histone H4 lysine 5 acetylation

HAT: histone acetyltransferase

HDAC: histone deacetylase

Hi-C: high-throughput chromosome conformation capture

HP1: heterochromatin protein 1

IAA: indole-3-acetic acid

IgG: Immunoglobulin G

indel: insertion/deletion

INO80: inositol requiring 80 complex

ISWI: imitation switch complex

k_s: effective spring constant

LacI: Lac repressor

LacO: Lac operator sequence

LADs: lamina-associated domains

LC-MS/MS: liquid chromatography-tandem mass spectrometry

LLPS: liquid-liquid Phase Separation

L_p: persistence length

mRNA: messenger RNA

MRS: memory recruitment sequence

MSD: mean squared displacement

NE: nuclear envelope

NPC: Nuclear Pore Complex

ORF: Open reading frame

PBS: phosphate-buffered saline

PCR: polymerase chain reaction

PML: promyelocytic leukemia

Pol II: RNA polymerase II

PPPS: polymer-polymer phase separation

PTMs: post-translational modifications

R_c: radius of confinement

RNA: ribonucleic acid

RSC: Remodeling the Structure of Chromatin complex

SAGA: Spt-Ada-Gcn5-acetyltransferase complex

SGD: Saccharomyces Genome Database

sgRNA: single guide RNA

SIM: Structured illumination microscopy

SMC: structural maintenance of chromosomes complex

SPB: Spindle Pole Body

SWI/SNF: switch/sucrose-non-fermenting complex

TADs: topologically associating domains

TBS: Tris-buffered saline

TetO: Tet operator sequence

TetR: Tet repressor

TFIID: Transcription factor II D complex

TSS: transcriptional start site

UAS: upstream activating sequences

WGD: whole-genome duplication

YPD: yeast extract peptone dextrose

Acknowledgements

First, I would like to thank my supervisor Steve for taking me in as a grad student, supporting my work and always being available for any kind of discussion. You provided me with the right amount of guidance but also encouraged me to be independent and creative. Your passion for science is certainly an inspiration, I will never stop learning from you.

To Kerry, I am very grateful to have had the opportunity to count with your incredible knowledge for this work. Thanks also for being so kind, listening carefully and answering all my questions.

To the members of my thesis committee, Professors Daniel Zenklusen and Luis A Rokeach, thanks for every debate about my project and for all the support.

During these years, I was very lucky to being able to work at different research units and laboratories and learn and take advice from the best. I would like to thank all the members of Professors François Robert, Marlene Oeffinger and Daniel Zenklusen labs, especially Celia, Carolina, Christian, Pascal, and Pierre. Your help designing, executing, and analyzing different experiments was invaluable and the work done here is in many ways thanks to all of you.

Thanks to all past and current members of the Michnick lab, especially Jacqueline, Sinan, LP, Bram, Diala, Nozhat, Luz, Alessandra, Lara, Shelly, Hamed, Pouria, Konstantin, Emily, Poonam, Minoo, Ziwen, Sherry, Rini, and Philippe. We are an unconventional bunch, thanks for that as well. You aided make this journey lighter and all the more interesting. Thanks for the funny discussions, the help, and the laughs.

I want also to especially thank Nicolas Stifani for the assistance and advice with microscopy work. We all appreciate so much what you do.

To my closest friends and family, your constant support and encouragement no matter the project makes it all worth it, thank you. My girls at the university: Ney, Lorea, Yulemi, and Juliana, thanks for making me feel that home was close. To my friends outside the university, thanks for all the years and good memories together: Vicky, Denny, Maray, Elaine, Laura, Yoyo, Eric, Heidi, Carmen, Orlando, Gretel. Thanks especially to my best friends Vicky and Ney for always being there for me. We have shared many crazy rides including this PhD. Thanks to Philippe and his family for the love and support during these years, I'm incredibly grateful to have you in my life. To my parents, the best part of me, thanks for the unconditional love all the way. Dad, thanks for all the good lessons and especially the kindness. I wish you were still here.

Finally, I want to thank the members of the jury for accepting to evaluate my work and for the time invested on it, Professors John Pascal, Éric Milot, Stephanie Weber, and Audrey Claing.

“The most exciting phrase to hear in science, the one that heralds new discoveries, is not, ‘Eureka!’ but ‘That's funny...’”

Isaac Asimov, 1987

Chapitre 1 Introduction

One of the main mysteries of the beginning of life is how genomes originated. It has been suggested that gene cooperation made this possible. The fact is that genomes constitute an integral unit that strictly controls itself and contains all the genetic information living beings require to survive and propagate. This chapter provides an overview about some of the organizing features of the genome and new concepts about biochemical and physical mechanisms that underlie these features.

1.1 Nuclear organization in eukaryotes and *Saccharomyces cerevisiae* as a model organism

DNA organization and compaction are essential to control genome function. Eukaryotic cells are defined by the presence of a membrane-bound nucleus containing most of the genetic material in the cell. Gene expression regulation inside the nucleus is achieved through many different organizational units that go from the several levels of compaction of the chromatin to the compartmentalization of some nuclear functions in specific membraneless organelles (Figure 1.1 A). For example, each chromosome is known to occupy a certain “territory”, and each territory contains diverse chromatin domains that can interact with each other or with other nuclear structures (Bolzer et al., 2005; Cremer and Cremer, 2001; Duan et al., 2010). Individual genes can dynamically change position according to developmental and environmental contexts, which generally reflects in their transcriptional state (Brickner and Walter, 2004; Casolari et al., 2004; Ferrai et al., 2010; Randise-Hinchliff et al., 2016). Moreover, regulatory proteins for several nuclear processes can cluster in specific regions of the nucleus. The nucleolus for instance is a known landmark in the nuclear environment where proteins involved in the synthesis of ribosomal RNA and subunits converge and many other processes take place (Iarovaia et al., 2019). The components and interconnections of most of these well-defined domains and compartments have been extensively studied in the last decades; however, ideas of

how this nuclear order is maintained are only beginning to be explored. Here I provide brief summaries of our current knowledge of some of these nuclear organization features with emphasis on observations from the model organism, the budding yeast *Saccharomyces cerevisiae* (*S. cerevisiae*).

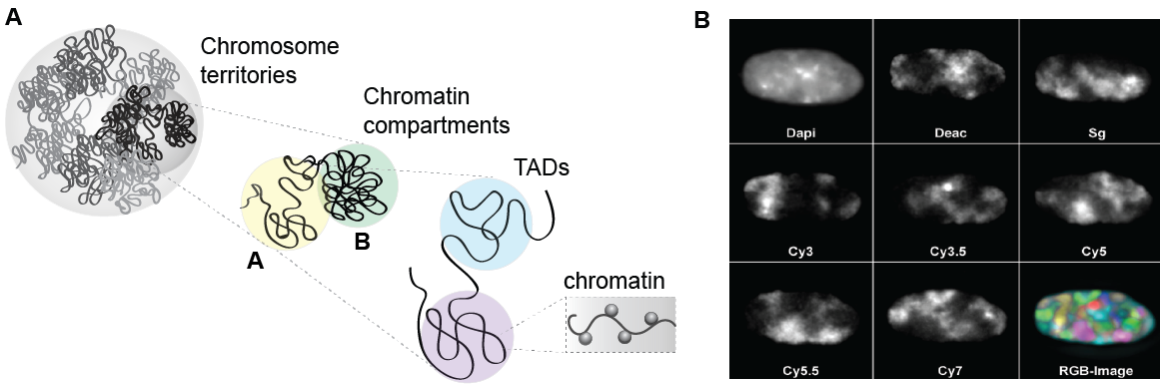

Figure 1.1 Genome compaction and organization in eukaryotes

*(**A**) Schematic representation of the hierarchical folding of chromatin in the eukaryotic nucleus. Each chromosome occupies a specific area inside the nucleus generating so-called chromosome territories. Chromatin in each of these territories also partitions into different compartments denominated A and B corresponding to active or repressed gene regions, respectively. At a lower level of compaction different domains can be formed that can reach up to hundreds of kilobases and that are defined by preferential intrachromosomal interactions, designated as topologically associating domains (TADs). The thinnest level of folding for the DNA is the chromatin fiber that corresponds to the DNA molecule wrapping at different intervals histone octamers forming the nucleosomal array. (**B**) This panel shows chromosome territories observed using 3D FISH in the nucleus of a Human fibroblast in G0 phase. Eight different channels are presented from wide-field microscopy, each one representing different subset of these territories. The combination*

and superposition of all these labels enabled the visualization of the 24 chromosome types (1–22, X, and Y) as shown in the bottom right panel as an RGB image (Bolzer et al., 2005).

1.1.1 Nuclear bodies

One of the main features of the eukaryotic nucleus is the presence of different membraneless compartments whose functions have been suggested to be in the regulation of gene expression (Stanek and Fox, 2017; Zhu and Brangwynne, 2015). Recent studies show that the majority of these assemblies are formed through phase separation in order to organize the proteins that assemble components of and catalyze particular processes and control the efficiency of the underlying chemical reactions (Nott et al., 2015; Weber and Brangwynne, 2015; Zhu and Brangwynne, 2015). There are several of these structures in the eukaryotic nucleus and possibly many more to discover, each one associated with a specific process and some only present in certain cell types and under particular conditions (Stanek and Fox, 2017; Zhu and Brangwynne, 2015). Examples of commonly studied nuclear bodies are the Cajal bodies, the Promyelocytic leukemia (PML) bodies, the transcription and replication factories, the heterochromatin bodies as well as the nucleoli. Yeast nuclei lack of most of these structures and their associated functions such as extensive splicing and editing of mRNA, with the exception of a single nucleolus.

The nucleolus is the largest and prototypical body found in the nucleus and also the most extensively studied (Hernandez-Verdun et al., 2010; Iarovaia et al., 2019). There are many aspects of this compartment that remain to be understood, however until now its main function is considered to be the transcription of the ribosomal DNA (rDNA) repeats and the assembly of pre-ribosomal subunits (Iarovaia et al., 2019). The main components of the nucleolus are the rDNA, their transcripts and all the proteins involved in this process. Even so, there are many more proteins whose function is just starting to be understood and that apparently participate in a broad range of processes inside and outside the nucleolus including mRNA transcription, telomere maintenance, stress response, DNA repair and apoptosis (Boulon et al., 2010; Ogawa and Baserga, 2017; Scott and Oeffinger,

2016). Several studies have shown evidence that this structure behaves as a liquid phase of nucleic acids and proteins which strongly influences the way this compartment functions (Brangwynne et al., 2011; Feric and Brangwynne, 2013; Frottin et al., 2019; Weber and Brangwynne, 2015). Results with chromosome conformation capture (3C) techniques show that the nucleolus seems to be completely separated from the rest of the chromatin (Duan et al., 2010). More interestingly, this behavior has also been observed with synthetic chromosomes; in this case, when the rDNA repeats were repositioned to the middle of another chromosome arm, it was observed that this region split into two non-interacting domains (Mercy et al., 2017). In budding yeast, as well as many other eukaryotes, there is only one nucleolus that occupies almost one-third of the nuclear volume and constitutes an essential landmark defining the topology and function of the nucleus (Figure 1.2 A, B) (Berger et al., 2008; Bystricky et al., 2005).

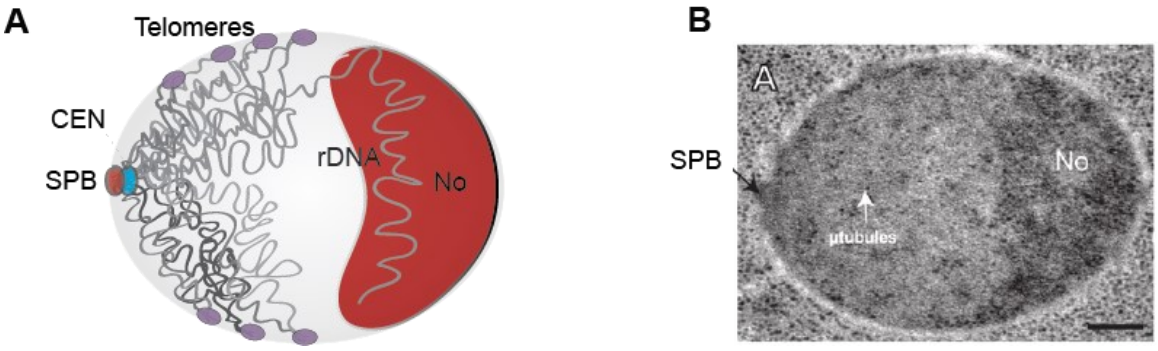

Figure 1.2 Yeast nuclear configuration

*(**A**) The yeast nucleus is represented in this schematic perspective containing the chromosomes (grey lines) and different landmarks that define its organization including a single nucleolus (red bean shape structure) positioned at one extreme of the nucleus and diametrically opposite to the Spindle pole body and Centromeres (red and blue ellipses, respectively), and the telomeres (purple ellipses) localized in close proximity to the nuclear envelope. Centromeres anchoring at the nuclear periphery with arms following behind and telomeres also distributed at the nuclear envelope resembles the Rabl configuration described over a hundred years ago. Figure inspired by several observations of the yeast*

*nucleus components **(B)** Electron micrograph showing a cryofixed yeast nucleus. Main structures in the nucleus are visible, including the nucleolus (No) and the Spindle pole body (Sáez-Vásquez and Gadal, 2010).*

1.1.2 Chromosomal territories

In mammalian nuclei, chromosomes in interphase are arranged into specific spatial conformations denominated "chromosomal territories" (Figure 1.1 B) (Bystricky et al., 2005; Cremer and Cremer, 2001; Heard and Bickmore, 2007; Heun et al., 2001a). This spatial arrangement is defined by different proteins including the interaction with functional aggregates such as the transcription and replication factories, and the association with nuclear landmarks such as the centromeres interaction with the spindle pole body or the telomeres interaction with the lamina and other lamina-associated domains (LADs) (Guelen et al., 2008; Spector, 2003).

In budding yeast, despite the lack of some of the structures found in higher eukaryotes, the spatial orientation of the chromosomes also depends on the interaction with different structures inside the nucleus. Chromosomes in this organism as well as in many other eukaryotes, adopt a Rabl configuration. Centromeres cluster on one side of the nuclear envelope (NE) adjacent to the spindle pole body and opposite to the nucleolus while telomeric regions position also near the NE at non-random locations that depend on the length of the chromosome arm (Berger et al., 2008; Bystricky et al., 2005; Duan et al., 2010; Rabl, 1885). The same study showing the nucleolus acting as a barrier for DNA interaction with other DNA domains outside this compartment also showed that chromosomes in budding yeast occupy specific territories even though this spatial organization is not as well defined as in other eukaryotes (Duan et al., 2010).

1.1.3 Chromatin Compartments

3C techniques have revolutionized the study of genome topology not only by helping to confirm known features such as the chromosome territories but also allowing the discovery of new ones (Dekker et al., 2002). It was previously known that distantly separated regions of the chromosomes can interact with each other to form loops, which can be relevant for different nuclear functions, such as enhancer-promoter interactions. These interactions can occur at different scales within the chromatin fiber and are considered an important feature shaping the nuclear architecture. 3C methods, particularly the high-throughput version (Hi-C) have enabled the characterization of the genome-wide landscape of these interactions, leading to the discovery of new features in the genome folding schemes at large and short length scales (Lieberman-Aiden et al., 2009; Rao et al., 2014; Wang et al., 2016). The establishment of long-range and large scale (megabase) interactions has shown that the genome is partitioned into two main compartments (called A and B) enriched in loose or compact chromatin structure, respectively (Lieberman-Aiden et al., 2009; Rao et al., 2014). Compartment A contains open chromatin and actively transcribed genes. This is usually correlated with a an enrichment of acetylated histone H3 lysines K9 and K27 and high GC content (Guelen et al., 2008). Conversely, compartments B contains repressed genes and double and triple methylated H3 lysines K9 and K27 (Guelen et al., 2008). Both compartments are localized to specific regions in the nucleus. For example, in mammalian cell nuclei, A compartment chromatin is found towards the interior of the nucleus while B compartment chromatin interacts with the nuclear lamina at the nuclear envelope (Ou et al., 2017; Solovei et al., 2009; Stevens et al., 2017). Additionally, observations from electron microscopy have shown that heterochromatin appears to be distributed in close proximity to the nuclear lamina in many cell types (Ou et al., 2017). Interestingly, for some specialized types of cells such the rod photoreceptor cells in nocturnal mammals, this arrangement of A and B chromatin is inverted (Solovei et al., 2009). This interaction of B compartment chromatin with the lamina is a remarkable trait largely found in mammals referred to as

lamina associated domains (LADs), that encompass more than 30 % of the genome (Kind et al., 2015). Yeast nuclei does not contain a lamina, but compact and open DNA are also partitioned, as described in the following sections.

1.1.4 Chromatin loop formation and TADs

At lower scales, in the order of tens to hundreds of kilobases, chromosomes preferentially interact among themselves than with each other generating domains denominated topologically associating domains (TADs) (Dixon et al., 2012; Nora et al., 2012; Sexton et al., 2012). These domains, found in most eukaryotes, are believed to constitute regulatory regions defined by specific contacts between different elements such as enhancers, promoters, heterochromatin components among others (Crane et al., 2015; Dong et al., 2018; Lieberman-Aiden et al., 2009; Sexton et al., 2012). The disruption of the contacts between regulatory elements and gene promoters by impairment of the TADs boundaries can lead to defects in gene expression and disease (Flavahan et al., 2016; Franke et al., 2016; Hnisz et al., 2016; Lupianez et al., 2015). These contact domains and their boundaries differ from one species to another as well as the mechanisms from which they arise. A remarkable feature of TADs boundaries in mammalian and other vertebrates is the presence of the CCCTC-binding factor (CTCF) colocalizing with the structural maintenance of chromosomes (SMC) cohesin complex (Dixon et al., 2012; Phillips-Cremins et al., 2013; Rao et al., 2014; Vietri Rudan et al., 2015). These proteins seem to define the formation of loops between boundaries as well as to delimit the position of the boundaries (Rao et al., 2014), however they are not present or their role does not seem to be significant in other organisms such as some plants and yeasts (Ong and Corces, 2009).

Hi-C studies in yeast have revealed TAD-like structures for *Schizosaccharomyces pombe* (*S. pombe*) (Mizuguchi et al., 2014) but not for *S. cerevisiae* (Duan et al., 2010). For *S. pombe* results even showed the presence of boundaries enriched with cohesin and depict

the importance of this protein in the maintenance of these boundaries. In the case of *S. cerevisiae,* although initial analysis failed to visualize TAD-like domains, more recent studies employing a variation of the Hi-C method called Micro-C allowed to find the existence of much shorter self-associating regions with an approximate size of 5 kb (Hsieh et al., 2015). The boundaries for these smaller domains are apparently enriched for highly transcribed gene promoters and regions with rapid histone turnover. Protein complexes such as the Remodeling the Structure of Chromatin (RSC) ATP-dependent complex, the Mediator and the acetyltransferase Rtt109 seem to play important roles in these folding mechanism (Hsieh et al., 2015).

1.1.5 Relocalization of chromosomal domains

As mentioned above, many studies have shown that chromosomes occupy different territories within the nucleus (Bystricky et al., 2005; Cremer and Cremer, 2001; Duan et al., 2010; Heard and Bickmore, 2007; Heun et al., 2001a). Nevertheless, it is also known that gene loci can change position under different conditions and that specific localization appears associated to chromatin state as well as rate of recombination and transcription. Gene positioning in most of the cases is considered an adaptation mechanism to both stress and differentiation processes (Ferrai et al., 2010). Different silenced regions of the genome in mammalian cells localize near the nuclear lamina while several actively transcribed genes move to the interior of the nucleus or the periphery of their territories (Kosak et al., 2002; Meister et al., 2010; Orsztynowicz et al., 2017; Ragoczy et al., 2006; Zink et al., 2004). A known example of this phenomenon is the human cystic fibrosis transmembrane conductance regulator (CFTR) region that comprises three consecutive loci. This region is inactive in neuroblastoma cells where it is located near the nuclear lamina, but when actively transcribed in adenocarcinoma cells, its position changes to the interior of the nucleus (Zink et al., 2004). Additional analyses have shown that the transcriptional activation of these loci depends not only on their position but also on their chromatin state and surrounding environment that apparently relies on the activity of

histone acetylases/deacetylases (Muck et al., 2012). Many other silenced genes related to developmental events in different cell systems seem to be positioned to the nuclear periphery (Brown et al., 1999; Kim et al., 2004; Kosak et al., 2002; Skok et al., 2001; Williams et al., 2006). More recent studies continue showing this behavior in mammalian cells; the loci encoding two lineage specific genes in mammalian embryos relocate to the periphery of their chromosome territory at stages associated with increased expression (Orsztynowicz et al., 2017).

Gene relocalization phenomenon and the molecular mechanisms behind it have been studied in different species and particularly in the model organism *S. cerevisiae.* In this yeast, despite the lack of the lamina structure, silenced regions such as the mating-type loci *HMR* and *HML* (HM loci) and the telomeres are found near the nuclear periphery (Gasser, 2001). The mechanism here involves mainly the action of the Sir proteins as well as other associated proteins (Gasser, 2001). Gene repositioning at the NE had been considered mainly a repression feature until several studies demonstrated that it also could play roles in gene activation. Several inducible genes in *S. cerevisiae*, including *GAL1*, *INO1*, *HSP104*, *HXK1* and *TSA2*, relocate from the nucleoplasm to the nuclear periphery when activated (Figure 1.3) (Brickner et al., 2012; Brickner and Walter, 2004; Cabal et al., 2006; Casolari et al., 2004; Taddei et al., 2006). It has been suggested that this relocalization couples transcription to the mRNA export and consequently increases the efficiency of the gene expression in response to environmental stimuli. This notion was based on Günther Blobel's "gene gating" hypothesis in which specific gene loci somehow are associated to specific nuclear pore complexes (Blobel, 1985). There have been attempts to attribute this repartitioning of active gene loci to the NE to specific protein-protein-DNA interactions with specific DNA motifs, however as explained below, results supporting this hypothesis are ambiguous (Ahmed et al., 2010; Brickner et al., 2012).

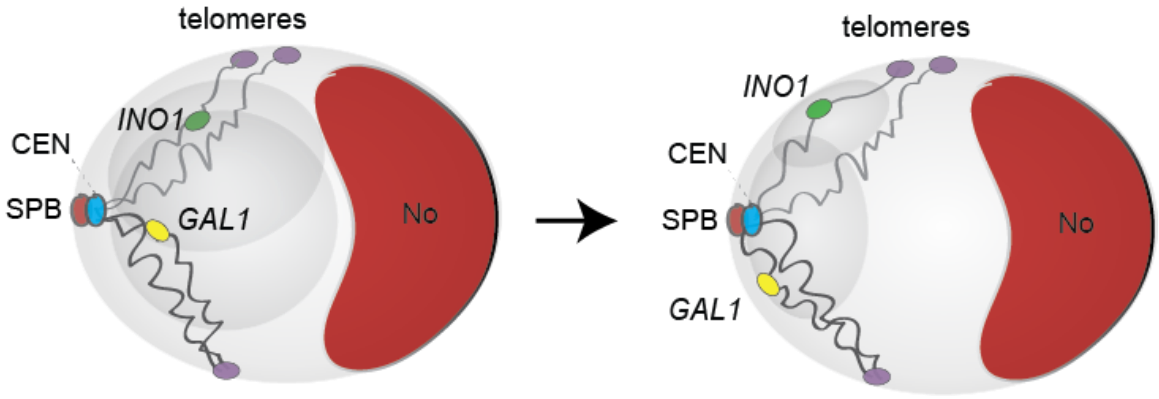

Figure 1.3 Gene repositioning from nucleoplasm to the nuclear envelope in yeast

Schematic depiction of the relocalization of two genes following activation in response to nutrient starvation. Both INO1 (green ellipse) and GAL1 (yellow ellipse) under repressing conditions are widely distributed in the nucleoplasm (grey circles inside the nucleus, left panel) but when activated, reposition to confined regions towards the nuclear periphery (grey ellipses inside the nucleus, right panel). Consequently, there is an increase in the efficiency of gene expression due to the coupling of transcription and export of the mRNA to the cytoplasm. The nucleus is represented by a grey ellipse containing the nucleolus (No, red bean shape structure), the SPB and centromeres (red and blue ellipses at the periphery of the nucleus, opposite to the nucleolus), representative chromosomes arms (grey lines), and representative telomeres at the periphery of the nucleus (purple ellipses).

1.1.5.1 *INO1* locus relocalization at the nuclear periphery

The *INO1* locus is one of the most studied examples of stress-inducible genes that exhibits relocalization to the nuclear periphery once activated and persistence of relocalization (transcriptional memory) following inactivation (Ahmed et al., 2010; Brickner et al., 2012; Brickner and Walter, 2004; Randise-Hinchliff et al., 2016). Both relocalization and memory depend on the presence of specific nucleotide sequences called gene recruitment sequences (GRS) or “zip codes”, which are found in or further upstream to the promoter of the gene (Ahmed et al., 2010). There are two identified GRSs (GRS I and GRS II) that

account for *INO1* relocalization after activation (Ahmed et al., 2010). These sequences are redundant since mutation of either element alone does not affect the peripheral targeting of the gene but loss of both GRS I and GRS II abolishes the process (Ahmed et al., 2010). GRS I (5´-GGGTTGGA-3´) and GRS II (5´-GAATGATTGCTGGGAAGAAT-3´) are not apparently related and do not match to any known binding site (Ahmed et al., 2010). An analysis of the yeast genome revealed 280 GRS I sequences of which 94 are in promoters. This analysis also showed that several of the genes containing this sequence in the promoter were related to the cellular response to heat stress (Ahmed et al., 2010). The working hypothesis for active gene relocalization has been that the zip codes are specific binding sites for proteins that in activated genes, will bind to proteins bound to nuclear pores. In this regard, the deletion of several proteins of the nuclear pore complex (NPC) and NPC related basket proteins, such as elements of the SAGA histone acetyltransferase complex, seem to affect gene relocalization (Ahmed et al., 2010), but no additional evidence of molecular mechanisms physically linking the gene and the NPC have been described. More recent studies have identified two transcription factors, Put3 and Cbf1 that bind to GRS I and GRS II respectively, although no role for these interactions in *INO1* relocalization has been reported (Brickner et al., 2012; Randise-Hinchliff et al., 2016). The first of these studies revealed that *INO1* relocalization to the NE is not as focused as it would be expected for a defined complex, but appears as a change in the statistical distribution of the locus towards the NE when measured in a population of thousands of cells, similar to what has been observed for the *GAL* genes (Berger et al., 2008; Brickner et al., 2012). Furthermore, different transcriptional repressors can block GRS-dependent *INO1* relocalization through an Rpd3(L) histone deacetylase-dependent mechanisms (Randise-Hinchliff et al., 2016). This study also showed that *INO1* relocalization is blocked by histone deacetylase activity. These results suggest that chromatin remodeling accompanying activation of the *INO1* gene must somehow be required for is relocalization to the NE, but how remains unknown.

1.2 Chromatin structure

1.2.1 DNA and histones

DNA molecules encode the genetic information that is passed along to every living organism's offspring. DNA can exist in different arrangements and particularly in eukaryotes, can be found in condensed forms known as chromatin (Becker and Horz, 2002). The basic folding unit of chromatin is the nucleosome, which consists of a core of four pairs of histone proteins wrapped by approximately 146 base pairs (bp) of DNA fiber (Kornberg, 1974).

Histones are a family of small basic proteins present in eukaryotic cells which package and order DNA into nucleosomes (Kornberg and Thomas, 1974; Phillips and Johns, 1965). Five major classes of histones exist: H2A, H2B, H3, H4, and H1; the first four are known as the core histones while H1 is called the linker histone (Phillips and Johns, 1965). There are also other variants within these classes that play other roles on different DNA related processes (Talbert and Henikoff, 2010).

The common features of core histones are the presence of the histone-fold domain and unstructured N-terminal tails of 20–35 residues that account for almost a quarter of their mass (Arents et al., 1991; Arents and Moudrianakis, 1995; Pepenella et al., 2014). These histone N-terminal tails are essential regulators of histone interactions with the DNA and with other protein complexes that determines the local chromatin function. These interaction patterns depends mainly on post-translational modifications of these N-terminal tails (Pepenella et al., 2014).

Linker histone H1, on the other hand, is more abundant in higher eukaryotes where its major role is thought to be the maintenance of higher order chromatin structures by connecting different nucleosomes (Hergeth and Schneider, 2015; McBryant et al., 2010).

H1 binds the nucleosome at the DNA entry and exit sites and its ability to bridge nucleosomes is attributed to the presence of two DNA binding domains in its structure (McBryant et al., 2010). In general, H1 histones are small proteins (~200 amino acids) with a small unstructured N-terminal region, a central globular domain, and a long basic and unstructured C terminal tail (Roque et al., 2005). These unstructured regions undergo phase separation *in vitro*, which is thought to be relevant in the formation of functional compartments (Turner et al., 2018). Lower eukaryotes contain linker histone-like proteins such as the Hho1 protein in *S. cerevisiae*, which is apparently involved in DNA repair and has also been linked to transcriptional silencing (Downs et al., 2003; Yu et al., 2009).

1.2.2 The nucleosome

As mentioned above, the nucleosome is the basic unit of chromatin and it is composed of the four core histones forming pairs and wrapped by DNA (Figure 1.4 A, B) (Kornberg, 1974; Luger et al., 1997; Richmond and Davey, 2003). The histone-fold domain of these four core histones, which is basically three alpha helices separated by two loops, enables these proteins to form dimers H2A-H2B and H3-H4 (Luger et al., 1997; Wood et al., 2005). In addition, the H3-H4 dimers interact with each other to form a tetramer that is sandwiched with two pairs of H2A-H2B to form an octamer that will be wrapped by approximately 1.65 left-handed turns of DNA (Luger et al., 1997; Richmond and Davey, 2003; Wood et al., 2005). These particles of around 6.5 nm diameter are separated by linker DNA that can vary on length forming what is known as the beads on a string structure or 11 nm (Kornberg, 1974). This wrapping of the DNA around the nucleosome allows a level of compaction of approximately 6-fold. There are several high resolution solved structures of the nucleosome and different interacting proteins and DNA sequences revealing that the array of histones remains almost unchanged while the DNA wrapping the octamer appears to be dynamic in solution (Luger et al., 1997; Richmond and Davey, 2003; Wood et al., 2005). These and other studies have also shown that the positively charged histones of the nucleosome have more than 120 points of interaction

with the negatively charged DNA, which makes the complex very stable, even at 65°C (Van Holde et al., 1980). The N-terminal tails of the histones, whose crystal structure have not been solved, are flexible regions that flank the sides of the octamer extending out of the DNA turns (Arents et al., 1991; Arents and Moudrianakis, 1995).

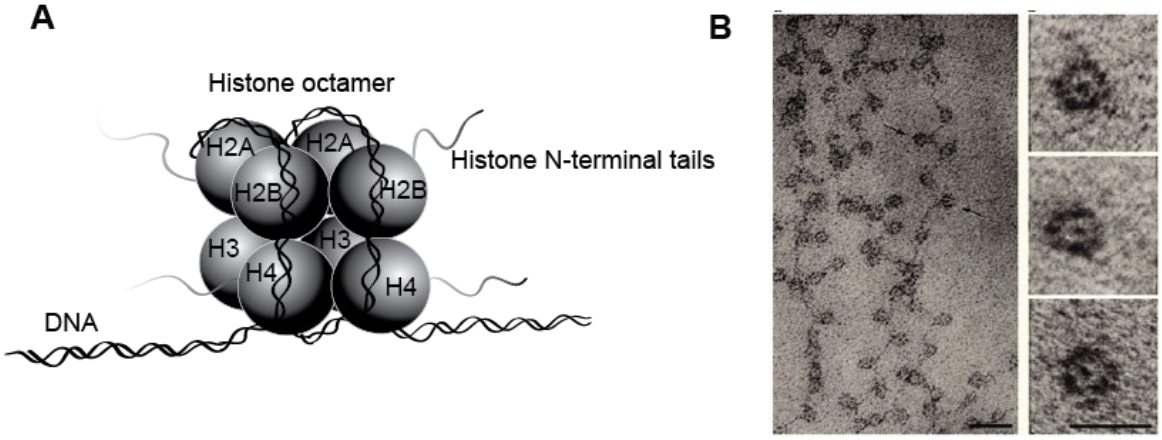

Figure 1.4 Nucleosome structure

*(**A**) Representation of the nucleosome configuration where an octamer composed of histones, 4 pairs of each class H2A, H2B, H3 and H4 are wrapped twice by DNA, forming a solenoid-like structure. The N-terminal tails of each histone in the octamer can be covalently modified with different chemical groups, which determine the degree of interaction of the DNA with the octamer particle and between the histones in the nucleosome. (**B**) Electron micrographs of the chromatin and the nucleosome particle. The left panel shows the "beads on string" configuration of the chromatin while the right panels present three different nucleosomes isolated from chromatin digested with nucleases. Scale bars represent 30 nm and 10 nm, respectively (Olins and Olins, 2003).*

1.2.2.1 Nucleosome positioning and occupancy

Nucleosome positioning constitutes another layer of genome regulation, not only by ensuring DNA compaction but also by controlling the access of polymerases and other proteins to the genetic information (Hughes and Rando, 2014; Lieleg et al., 2015; Yuan et al., 2005). The term positioning refers to the specific location a nucleosome tends to be found in the genome. Nucleosomes are considered well positioned if they appear at the same genomic region in a population of cells (Hughes and Rando, 2014; Lieleg et al., 2015; Yuan et al., 2005). Occupancy, on the other hand, indicates the density of nucleosomes in a certain region of the genome (Lieleg et al., 2015). For more than 30 different species, genome-wide nucleosome maps have been determined, which has allowed deciphering some common features (Heintzman et al., 2007; Hughes and Rando, 2014; Lee et al., 2007; Mavrich et al., 2008; Schones et al., 2008; Yuan et al., 2005). For all these species, promoters and other regulatory sites appear depleted of nucleosomes (Hughes and Rando, 2014). Conventional nucleosome numbering locates the +1 nucleosome at transcriptional start sites (TSS) with numbers increasing positively downstream and negatively increasing upstream of these sites. In general, both parameters, positioning and occupancy, depend on different factors including DNA sequence patterns, sequence-specific regulatory binding proteins and histone modifications that can recruit chromatin remodeling complexes (Heintzman et al., 2007; Hughes and Rando, 2014; Lee et al., 2007).

The positioning of nucleosomes in the genome appears to be partially determined by DNA sequence patterns, a fact that has been observed *in vitro* (Kaplan et al., 2009; Lowary and Widom, 1998; Satchwell et al., 1986) and *in vivo*, from genome-wide studies (Heintzman et al., 2007; Lee et al., 2007). This phenomenon is believed to be influenced by the correlation between energy cost of the DNA deformation and specific sequences (Lee et al., 2007; Thastrom et al., 2004; Widom, 2001). Thus, some features of the DNA sequence have greater affinity to the histone core *in vitro* (Lowary and Widom, 1998). One feature that appears to favor nucleosome formation is a periodic presence of AA-TT-TA dinucleotide sequences occurring at one helical turn of the DNA fiber or approximately

10 bp (Ioshikhes et al., 2006; Satchwell et al., 1986; Segal et al., 2006). Other sequence patterns favoring nucleosome assembly are repeats of the CTG trinucleotide (Godde and Wolffe, 1996; Wang et al., 1994; Wang and Griffith, 1995). On the other hand, sequences that seems to be negatively related to the assembly of nucleosomes are the poly-A or poly-T tracts (Kaplan et al., 2009; Yuan et al., 2005). Genome-wide studies in yeast have revealed that the presence of these tracts in different promoters seems to make then resistant to the incorporation of nucleosomes (Field et al., 2008; Thastrom et al., 2004; Yuan et al., 2005). Changing the length, composition and location of these poly-A/poly-T sequences in different gene regulation sites affects gene expression (Raveh-Sadka et al., 2012).

1.2.2.2 Histone variants

In addition to the typical core histones that assemble the nucleosome, there are some histone variants that can substitute for them (Talbert and Henikoff, 2010; Zlatanova et al., 2009). These variants can be very similar to the core histones but play additional roles in nucleosome function such as altering the histones-DNA interactions and consequently the nucleosome stability, affecting transcription, chromosome segregation and DNA repair (Talbert and Henikoff, 2010). These histone variants are generally deposited in the nucleosomes at different stages of the cell cycle, while the deposition of most of the core histones occurs during S phase (Henikoff, 2009).

H2A and H3 variants are the more common histone variants that can be found in chromatin (Talbert and Henikoff, 2010). In this group the H2A.Z (yeast Htz1) types have been one of the most studied, mainly due to its role in transcriptional regulation and high sequence conservation from yeast to humans (Giaimo et al., 2019; Petty et al., 2009). H2A.Z appears to be deposited more frequently in transcription start sites, which have been linked to transcriptional activation (Albert et al., 2007; Raisner et al., 2005; Zhang et al., 2005). Other studies have also suggested the role of H2A.Z in transcriptional memory

such as observed for the *INO1* gene in *S. cerevisiae* (Brickner et al., 2007). Moreover, H2A.Z has been linked to the prevention of heterochromatin spreading into regions of euchromatin (Abbott et al., 2001; Meneghini et al., 2003). This histone also appears to be enriched at transcriptionally inactive sites, such as telomeres and the mating type loci in yeast where it is believed they contribute to maintaining these sites in a silenced state (Abbott et al., 2001). Other histone variants comprise the centromeric H3 variant (CENPA in mammals, Cse4 in yeast), crucial for kinetochore assembly (Henikoff and Furuyama, 2012). Finally, variants H3.3 is also involved in transcriptional activation (Henikoff, 2009), and H2A.X plays a role in DNA repair at double-strand breaks (van Attikum and Gasser, 2009).

1.2.2.3 Histone post-translational modifications

Histones are known to undergo post-translational modifications (PTM) that alter chromatin state and trigger diverse nuclear processes (Kouzarides, 2007; Ng and Cheung, 2016; Strahl and Allis, 2000). These modifications comprise acetylation, methylation, phosphorylation, ubiquitination, ADP-ribosylation, sumoylation, deimination, and proline *cis-trans* isomerization (Figure 1.5) (Bannister and Kouzarides, 2011; Kouzarides, 2007; Ng and Cheung, 2016). Furthermore, arginine and lysine methylation can occur in a variety of mono- or di-methylation forms for arginine and mono-, di-, or tri-methylated forms of lysine. Because all the histones that assemble the nucleosome can be modified at different residues in both unstructured N-terminal tails and the globular domains, the number of potential patterns of PTMs is very large (Kouzarides, 2007; Ng and Cheung, 2016).

Different PTM patterns are recognized by regulatory proteins that bind to chromatin and recruit proteins involved in different processes (Kouzarides, 2007; Mersfelder and Parthun, 2006; Ng and Cheung, 2016; Strahl and Allis, 2000). For instance, certain chromatin binding domains can recognize only some types of histone modification.

Examples of the more commonly studied of these domains are methylation-recognizing chromo-like and PHD domains, and acetylation (bromodomains), and phosphorylation (14-3-3) recognizing domains (Bannister and Kouzarides, 2011; Kouzarides, 2007). The highly studied heterochromatin protein 1 (HP1) has a chromodomain that binds specifically to a tri-methylated lysine (K9)-containing peptide motif of the histone H3; a function that is considered essential to the formation of higher order heterochromatin and that is observed in many eukaryotes from yeasts to mammals (Bannister et al., 2001; Eissenberg and Elgin, 2014; Lachner et al., 2001; Sanulli et al., 2019).

Genome wide mapping of histone modifications mainly in *S. cerevisiae* has made possible the analysis of the association between combinations of modifications and different nuclear processes (Bernstein et al., 2005; Liu et al., 2005; Pokholok et al., 2005). These studies have also shown how certain combinations of these modifications are more frequently found at specific genomic regions, such as promoters and coding regions (Rando, 2007). For example, independent of transcriptional status, it is known that different acetylation and methylation patterns appear to be depleted in the few nucleosomes present in many promoters (Liu et al., 2005; Pokholok et al., 2005). However, other distinctive modification patterns are found in different sections of the coding regions, which also depends on the transcriptional status of a given locus. Many of the modifications that have been analyzed in all these studies appear in delimited regions encompassing less than ten nucleosomes. This is the case for most acetylated histones and H3K4me3 that appears at the 5' region of actively transcribed genes (Liu et al., 2005; Pokholok et al., 2005; Rando, 2007).

Among proteins that recognize distinct patterns of histone N-terminal tails are included chromatin remodeling complexes that regulate transcription, replication, recombination and DNA repair (Dion et al., 2005; Jenuwein and Allis, 2001; Kouzarides, 2007; Martin et al., 2004; Ng and Cheung, 2016; Parra et al., 2006; Rando, 2007). Histone tail acetylation is considered to have the greatest potential to alter the structure of chromatin due to the

neutralization of positive charges of lysine and arginine residues, resulting in reduced affinity of histones for DNA backbone phosphates and disruption of nucleosome–nucleosome interactions (Kouzarides, 2007). Most of the histone acetylation takes place in their N-terminal tails and the enzymes involved can modify more than one site (Kouzarides, 2007; Sterner and Berger, 2000). Different examples of these acetylated lysine such as H3K9ac, H3K14ac, H3K18ac, H4K5ac and H4K12ac, are present at the beginning of coding regions and are commonly associated with increased transcriptional activity (Liu et al., 2005; Pokholok et al., 2005). On the other hand, regulatory proteins associated with transcriptional repression, including HP1 and Polycomb proteins, bind methylated residues in these tails (Bannister et al., 2001; Lachner et al., 2001). In general, modifications at the N-terminal tails of the histones result in maintenance of the higher order structure of chromatin, which influences the access of these sites to transcription factors (Kouzarides, 2007; Ng and Cheung, 2016).

The globular domains of the histones also contain several residues that are modified, effecting the structural stability of nucleosome particles (Hyland et al., 2005; Xu et al., 2005). Acetylation of some residues in these histone folded domains, for example K115 and K122 in H3, are believed to induce disassembly of nucleosomes (Manohar et al., 2009). The H3K56ac modification is associated with nucleosome assembly in newly synthesized and repaired double strand break DNA by increasing histone turnover in nucleosomes, independent of replication (Chen et al., 2008; Driscoll et al., 2007; Li et al., 2008; Rufiange et al., 2007; Topal et al., 2019).

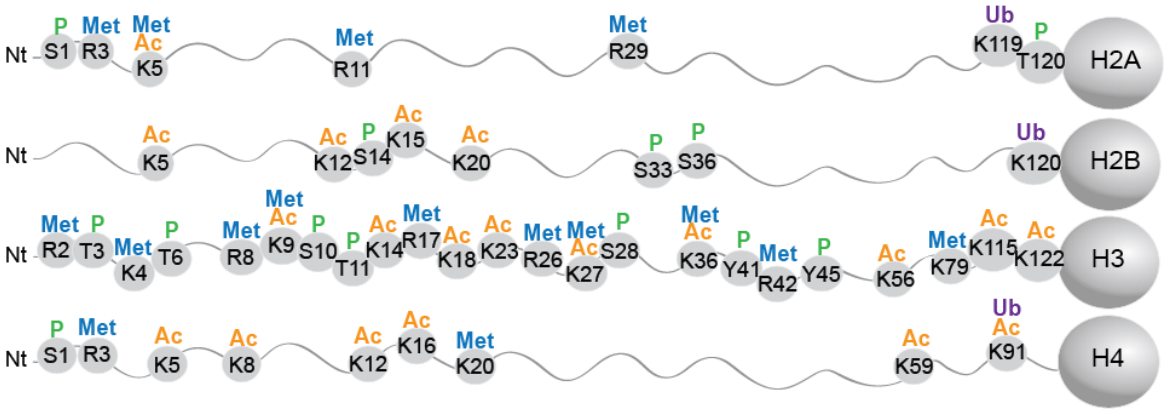

Figure 1.5 Histone post-translational modifications

Examples of the more common covalent modifications of each histone in the nucleosome, mainly in their N-terminal tails. Lysine acetylation, lysine or arginine methylation, phosphorylation on serine, threonine, or tyrosine residues, and lysine ubiquitylation.

1.3 Chromatin remodeling proteins

Through the activities of several proteins and complexes, chromatin structure can be altered in many ways including changes in nucleosome positioning, composition, and conformation, as well as by directly binding to DNA. Access to different regions in the genome for different functions is affected by these activities. According to their type of action, two main categories of chromatin remodeling proteins have been described: those that act by covalently modifying the histones and those that reorganize nucleosomes. Other proteins involved in chromatin remodeling include the heterogenous group of histone chaperones such as components of the FACT complex and the ubiquitous protein Asf1 in yeast (Ransom et al., 2010).

1.3.1 Histone modifying enzymes

The complexes that modify histones act by catalytically adding or removing chemical groups such as acetyl, methyl, and others mentioned above (Bannister and Kouzarides, 2011; Kouzarides, 2007; Ng and Cheung, 2016). The first enzymes discovered with these activities were a histone deacetylase (HDAC) and a histone acetyltransferase (HAT) with high homology to known transcriptional regulators in yeast (Rpd3 and Gcn5, respectively) (Brownell et al., 1996; Taunton et al., 1996). Many more HATs and HDACs have been described since then, as well as other types of enzymes, including methyltransferases and demethylases (Chang et al., 2007; Chen et al., 1999; Rea et al., 2000; Tsukada et al., 2006), kinases (Sassone-Corsi et al., 1999; Thomson et al., 1999), ubiquitinases, and de-ubiquitinases (Emre et al., 2005; Henry et al., 2003; Robzyk et al., 2000).

Acetylation is often a necessary precursor to other modifications, such as phosphorylation, methylation and ubiquitylation (Yang and Seto, 2008a; Yang and Grégoire, 2007). There are two main types of HATs according to their localization (cytoplasm or nucleus); cytoplasmic HATs acetylate free histones that have been recently synthesized before they are transported to the nucleus while nuclear HATs modify histones and other proteins inside the nucleus (Wapenaar and Dekker, 2016). There are distinct families of HATs based on sequence homology, and most of them are conserved from yeast to humans (Vernarecci et al., 2010). Among these families, the two largest and most studied are GNAT and MYST, with yeast examples Gcn5 and Esa1 being common catalytic components of large HAT complexes in the nucleus, including SAGA and NuA4, respectively. Interestingly, some HATs do not belong to any family and are not subunits of large chromatin remodeling complexes (Vernarecci et al., 2010). This is the case for Rtt109, which causes increased histone turnover by acetylating lysine 56 in histone 3 (Chen et al., 2008; Driscoll et al., 2007; Li et al., 2008; Rufiange et al., 2007; Topal et al., 2019). HDACs on the other hand, consist of four main classes by sequence homology, three of which depend on Zn^{2+} for deacetylase activity and one that relies on NAD^{+}

cofactor (Li et al., 2020). The yeast Rpd3 deacetylase is a highly conserved member of the Class I HDACs, and it has been the most studied among these enzymes. Rpd3 can be part of two complexes (Rpd3L and Rpd3S) that play different functions inside the nucleus (Yang and Seto, 2008b). Among the functions of this enzyme is the transcriptional repression of several known genes, including *INO1*, where it has been shown to associate with a specific DNA sequence in the promoter of the gene *via* a DNA binding protein (Kadosh and Struhl, 1998). Recent studies show that Rpd3 can also block the action of gene relocalization elements for this locus (Randise-Hinchliff et al., 2016).

1.3.2 ATP-dependent chromatin remodelers

Chromatin remodelers that rely on ATP for their activity use mechanical work coupled to hydrolysis of ATP to restructure nucleosomes with consequent changes of access to DNA. All these molecules share an ATPase catalytic domain that has homology with helicases although they only act as DNA translocases due to the lack of a motif necessary for strand separation (Singleton et al., 2007; Tyagi et al., 2016). Four families of remodelers have been described: SWI/SNF (switch/sucrose-non-fermenting), ISWI (imitation switch), CHD (chromodomain-helicase-DNA binding) and INO80 (inositol requiring 80) (Erdel and Rippe, 2011; Gerhold and Gasser, 2014; Liu et al., 2011; Tyagi et al., 2016). Most of these complexes are conserved among eukaryotes (Clapier and Cairns, 2009). Apart from the common ATPase domain, all these families have distinct domains that define the type of interaction they make with the nucleosomes and how ATPase domain function is regulated (Clapier and Cairns, 2009; Erdel and Rippe, 2011; Gerhold and Gasser, 2014; Liu et al., 2011; Tyagi et al., 2016). These include bromodomains, chromodomains, and domains that bind to actin or actin related proteins. A large number of studies have and continue to explore the roles of all the different variants of these molecules as well as the different combinations of complexes that exist according to the types of subunits that form them. Many studies relate the activity of these complexes to transcriptional regulation although roles in DNA replication, repair and other functions in the genome

are also considered relevant (Erdel and Rippe, 2011; Gerhold and Gasser, 2014; Kawaguchi et al., 2015; Langst and Manelyte, 2015; Pulice and Kadoch, 2017).

1.4 Phase separation and nuclear organization

Many biochemical processes in the cell occur in membraneless organelles or more generally, biomolecular condensates, which serve to organize the components involved in specific reactions (Brangwynne et al., 2009; Brangwynne et al., 2011; Dao et al., 2018; Elbaum-Garfinkle et al., 2015; Kedersha et al., 2013; Nott et al., 2015; Weber and Brangwynne, 2015; Zhu and Brangwynne, 2015). The nucleus contains several of these compartments, including those involved in synthesis, processing, and storage of different types of RNAs. These compartments include nucleoli, paraspeckles, Cajal bodies, PML bodies and nuclear speckles (Stanek and Fox, 2017; Zhu and Brangwynne, 2015). Phase separation of chromatin may also underlie the dilute or dense states of eu- and heterochromatin, respectively and transcription and replication machinery (Erdel and Rippe, 2018; Hnisz et al., 2017; Larson et al., 2017a; Sanulli et al., 2019; Strom et al., 2017). Understanding the assembly and dynamics of these compartments has been an intensely studied topic in the last decade (Alberti et al., 2019; Banani et al., 2017; Bergeron-Sandoval et al., 2016).

One mechanism shown to drive to drive the formation of some of these structures is liquid-liquid phase separation (LLPS) (Altmeyer et al., 2015; Brangwynne et al., 2009; Dao et al., 2018; Elbaum-Garfinkle et al., 2015; Hnisz et al., 2017; Larson et al., 2017a; Sanulli et al., 2019; Shin et al., 2018; Strom et al., 2017; Turner et al., 2018; Weber and Brangwynne, 2015). LLPS involves demixing of the components of these compartments to form dense liquid phases at equilibrium with the surrounding environment that exhibit different chemical and physical properties (Banani et al., 2017; Boeynaems et al., 2018). One of the common features of proteins that phase separate into biomolecular condensates is that they contain low complexity amino acid composition domains (LCD)

such as the prion-like domains (PLD), which contain polar residues and are usually depleted of charged ones (Holehouse et al., 2021; Wang et al., 2018; Zhu and Brangwynne, 2015). These LCDs are most likely intrinsically disordered, sampling multiple conformations depending on the physical characteristics of the amino acid composition and their distribution within the polypeptide. The inter- and intramolecular interactions between these proteins can be affected as well by posttranslational modifications (PTMs) that alter charge (phosphorylation, methylation, or acetylation), and block distributions of amino acids of particular types or distinct domains(Zhu and Brangwynne, 2015). Biomolecular condensates generated as result of phase separation can exhibit liquid-like properties, including fast dynamic exchange of components with the surrounding environment (Brangwynne, 2013; Malinovska et al., 2013; Toretsky and Wright, 2014; van der Lee et al., 2014). Condensate size and stability can be altered by small changes in conditions such as the concentrations of proteins, nucleic acids, and different ions, which can cause either formation or disintegration of the condensate (Banani et al., 2017; Bergeron-Sandoval et al., 2016; Boeynaems et al., 2018). These features provide the cell with a mechanism to respond to internal and external changes in a fast manner by simply liquid-demixing without the need for membrane barriers.

In addition to LLPS, other mechanisms have been described to be involved in the formation of biomolecular condensates. For example, chromatin-related domains are also suggested to form by bridging different DNA regions through soluble binding factors in what has been called polymer-polymer phase separation (PPPS) (A and Weber, 2019; Erdel and Rippe, 2018). In this case, chromatin binding proteins are suggested to drive the collapse of the regions they associate with (Brackley et al., 2016; Erdel and Rippe, 2018; Michieletto et al., 2017). This mechanism is said to not require interactions between bridging proteins. Moreover, the liquid composition in the collapsed regions is similar to the surrounding medium which implies that the size of these bodies does not rely on the nucleoplasmic composition (Dormidontova et al., 1992; Erdel and Rippe, 2018; Michieletto et al., 2017). Another important feature of PPPS condensates in comparison

with LLPS condensates, is that the former depend on the number of binding sites in the chromatin scaffold (Erdel and Rippe, 2018).

1.4.1 Chromatin phase separation

The study of global ensemble average 3D architecture of genomes has been possible by chromatin conformation capture combined with FISH techniques, among others (Bolzer et al., 2005; Cremer and Cremer, 2001; Duan et al., 2010; Finn et al., 2019; Hsieh et al., 2015; Lieberman-Aiden et al., 2009). However, the studies that employ more advanced super-resolution imaging are those that have made possible to analyze the dynamics of the different states of the chromatin under different conditions (Miron et al., 2020; Shaban et al., 2018; Shaban and Seeber, 2020). The notion of chromatin phase separation has been proposed (Iborra, 2007; Maeshima et al., 2016), and more recently studied (Gibson et al., 2019; Quail et al., 2021; Sanulli et al., 2019; Shin et al., 2018; Strom et al., 2017). For instance, it was shown that reconstituted nucleosomal arrays phase separate in the presence of physiological concentrations of salts and that chromatin phase separation also depends among other factors, on the acetylation of histone tails (Figure 1.6 A, B) (Gibson et al., 2019). Specifically, they showed that histone acetylation dissolved nucleosome array condensates, but if bromodomains are added, a distinct phase separated state is observed. These results indicate that chromatin could partition into different phases depending on patterns of histone PTMs and association of DNA and histone binding proteins. Additionally, evidence that liquid-liquid phase separation (LLPS) of chromatin, particularly heterochromatin domains, is essential to chromatin dynamics, have led to the suggestion that LLPS is an important mechanism by which genome architecture and function is controlled (Larson et al., 2017b; Sanulli et al., 2019; Strom et al., 2017).

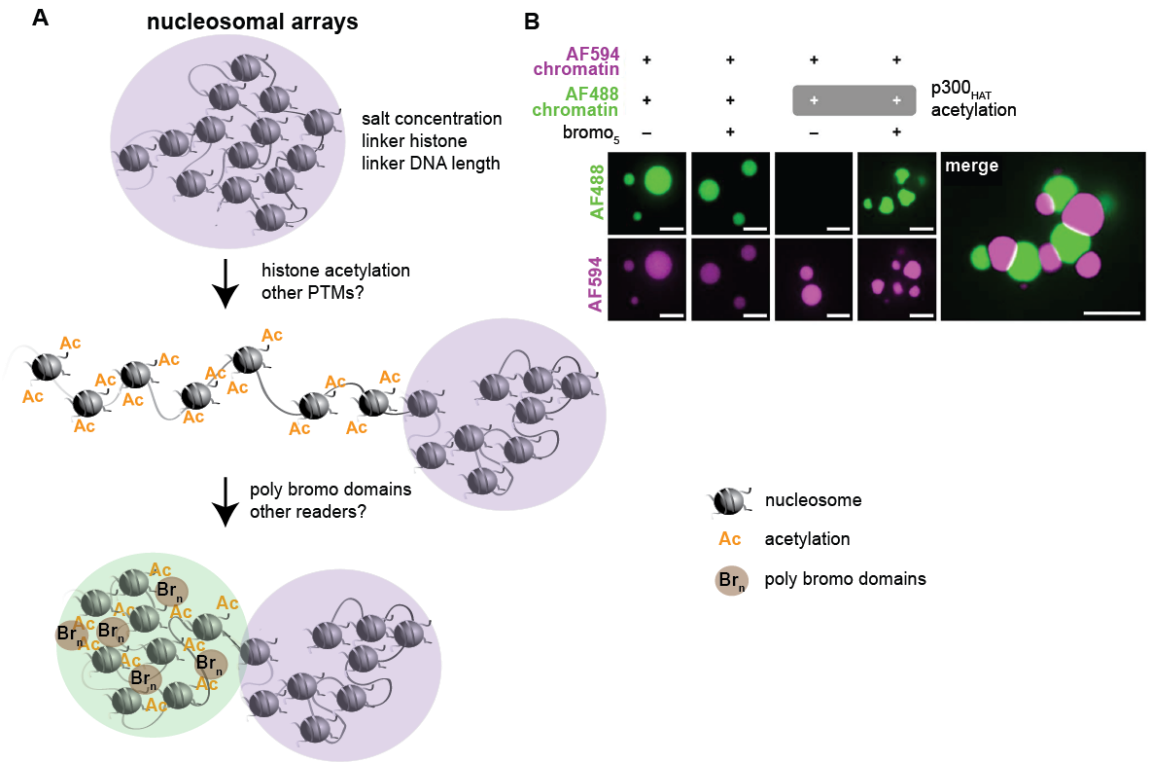

Figure 1.6 Phase separation of nucleosomal arrays

*(**A**) Chromatin domains can arise by phase separation (purple circles) through interactions between the different components that form the chromatin and depending on other variables such as the concentrations of specific ions in the surrounding environment, the positioning of the nucleosomes in the fiber and the binding of different proteins to each other such as occurs between the linker histones. Additionally, post-translational modifications of histones can disrupt or favor the formation of these domains, as well as the chromatin binding proteins that recognize these modifications. An example is depicted from the observation that histone acetylation disrupts nucleosomal array condensates, while polybromo domain proteins can bind to acetylated histones to induce LLPS to form a condensate that does not mix with the deacetylated nucleosome array condensate. These and other variable could give rise to a variety of condensates with different properties. Figure inspired by the results of Gibson et al., 2019 (Gibson et al., 2019). (**B**) Fluorescently labeled histone-deacetylated (purple) and histone-acetylated plus poly*

bromo domain-associated (green) nucleosomal array condensates that do not mix. Scale bars 10 µm. (Gibson et al., 2019).

1.4.2 HP1 proteins and their role in heterochromatin phase separation

An essential role has been demonstrated for the HP1 protein family in driving chromatin compaction and exclusion of proteins that induce gene expression (Lomberk et al., 2006). Recently it has been shown that in addition to mediating compaction of chromatin, HP1 maintains and regulates heterochromatin domains that are formed by LLPS (Larson et al., 2017b; Sanulli et al., 2019). HP1 proteins are highly conserved from Ascomycota yeasts such as *S. pombe* to metazoans, but lost in other yeasts, including the subphylum of Saccharomycotina to which the model eukaryote budding yeast *Saccharomyces cerevisiae* belongs (Hickman et al., 2011). These proteins have a chromodomain that recognizes and binds to the histone H3 methylated at lysine 9 (H3K9me) and a chromoshadow domain that homodimerizes and facilitates nucleosome bridging and binding to other proteins (Bannister et al., 2001; Eissenberg and Elgin, 2014; Lachner et al., 2001; Larson et al., 2017b; Sanulli et al., 2019; Strom et al., 2017). HP1 proteins have intrinsically disordered regions that are essential to HP1 undergoing LLPS *in vitro* and *in vivo* (Figure 1.7 A, B) (Larson et al., 2017b; Strom et al., 2017). More interestingly, it has been shown that HP1 protein and its *S. pombe* homolog Swi6 are sufficient to drive LLPS in reconstituted nucleosomal arrays containing H3K9me (Sanulli et al., 2019). It has been proposed that by reshaping the nucleosomes core, HP1/Swi6 generate multivalent interactions among nucleosomes, thus promoting phase separation. This may constitute a general mechanism by which chromatin organization is driven beyond heterochromatin.

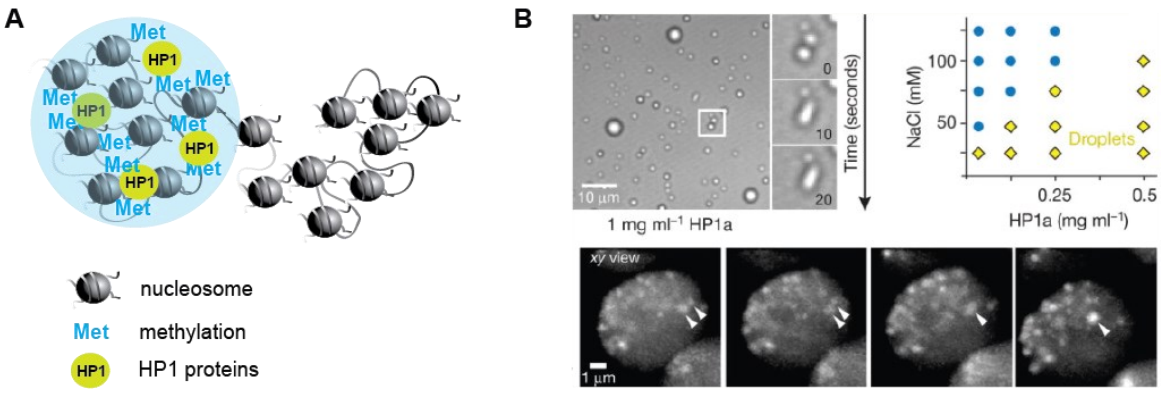

Figure 1.7 HP1 heterochromatin formation through phase separation

*(**A**) The heterochromatin protein 1 (HP1) and homolog Swi6 in S. pombe have been suggested to form chromatin domains through LLPS. The model proposes that the interactions of HP1/Swi6 (green circle) with the methylated lysine 9 at histone 3 (blue notations) will cause a loosening of the contacts between the histones in the nucleosome and with the DNA, and consequently the dynamics within the octamer (grey spheres) will increase. This will also increase the accessibility of the histone core so that there will be more chances for the nucleosomes to form multivalent weak interactions with other nucleosomes due to a higher probability of rearrangements between the different conformations the nucleosomes can adopt. All this will favor the formation of condensates (light blue sphere). Figure inspired by the results of Strom et al., 2017 (Strom et al., 2017) and Sanulli et al., 2019 (Sanulli et al., 2019). (**B**) The liquid behavior of Drosophila HP1a is shown both in vitro and in vivo. The left upper panel presents the formation and fusion of liquid droplets by the HP1a protein in vitro while the lower panel shows the same process but in nuclei of Drosophila embryos. In the upper right panel, a phase diagram of the droplet formation at specific concentrations of protein and salt is represented (Strom et al., 2017).*

1.5 Integrating polymer theory and experimental techniques to better understand chromatin structure and dynamics

To understand how dynamics of chromatin is related to phase separation to explain genome organization, it is necessary to understand the driving forces that control chromatin organization. Polymer theory provides simple and intuitive models that can aid in comprehending the complex dynamics of the interactions between chromatin, RNA, and proteins inside the nucleus. Even within a single chromosome, it is possible that phase separation can occur between one region and another. For example, it has been stated that a polymer chain with reversible interactions with adsorbable ligands at multiple sites will form a dense phase; and if ligands are removed from one segment of the polymer, that segment will phase-separate from the rest to form a "dilute" phase (Figure 1.8) (Dormidontova et al., 1992).

Studying the dynamics of local genomic regions has also allowed insights about how the physical properties of chromatin dictate organization and do work on chromatin in the nucleus (Backlund et al., 2014; Neumann et al., 2012; Verdaasdonk et al., 2013). By probing the spatiotemporal dynamics of chromatin and applying polymer theory, it is possible to measure mechanical properties that explain chromatin behavior. These can be probed by introducing arrays of operator DNA binding motifs–repressor-DNA binding proteins systems such as the LacO-LacI or TetO-TetR with the proteins fused to fluorescent proteins (Heun et al., 2001c). *S. cerevisiae* chromatin spatiotemporal dynamics have been extensively studied this way (Backlund et al., 2014; Cabal et al., 2006; Neumann et al., 2012; Taddei et al., 2006; Verdaasdonk et al., 2013). It has been shown that gene loci in *S. cerevisiae* are in constant movement in a confined territory that depends on the constraints and positioning of tethering to both sides of the chromosome arms as well as the metabolic state of the cells (Berger et al., 2008; Verdaasdonk et al., 2013). Studies of different regions of chromatin in the yeast genome have demonstrated changes in mechanical variables, including effective spring constants and radii of confinement, associated with changes in local or global chromatin structure

accompanying mitosis or gene expression (Backlund et al., 2014; Neumann et al., 2012; Verdaasdonk et al., 2013). These changes in physical properties reflect the local or global modifications of protein-protein and protein-DNA interactions that accompany nuclear processes including transcription, ribosomal RNA synthesis, mitosis, and others (Bloom, 2008; Vasquez et al., 2016; Verdaasdonk et al., 2013).

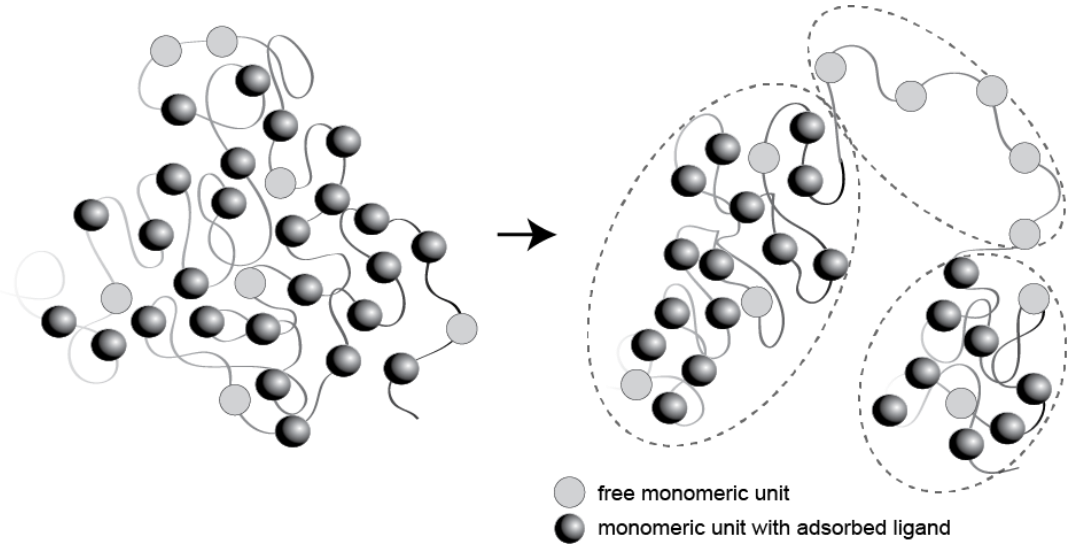

Figure 1.8 Segmental phase separation of a polymer chain through changes in occupancy of binding ligands

Represented is a single polymer chain containing two types of monomeric units, one in which ligands are bound to the polymer (dark gray circle) and those where they are not bound (light gray circle). In this case the ligands binding to the polymer is reversible and favors interactions among themselves in the chain, while the free monomeric unit interactions are repulsive. Thus, due to the interacting ligands this section of the chain will partition into a globular region from the section with more free monomeric units that will partition as a more open configuration. Intramolecular phase separation occurs and the chain behaves as a copolymer with each section displaying different physical properties. Figure modified from Dormidontova et al., (Dormidontova et al., 1992).

1.5.1 Modeling chromatin as long chain polymers

It has been a challenge to model chromatin structure and dynamics in living cells because of the complexity of the nuclear environment, including the effects of active processes on chromatin by chromatin remodelling complexes, DNA and RNA polymerases, or condensins and cohesins. In general, most of the information about genome organization comes from analyzing populations of fixed cells including recent conformation capture techniques showing as suggested before non random spatial distribution of chromatin regions. These studies corroborate the presence of territories and show new topologically associated domains (TADs). However, single cell analyses have proven that adding dynamics to the system changes the view on predicted principles that govern this organizational design.

Simplified polymer models have been powerful tools to formulate hypotheses about the origins of spatiotemporal dynamics and ensemble average topologies of the chromatin. Particularly useful have been 'bead-spring' models, which represent the nucleosomal arrays as beads joined by springs (Cheng et al., 2015; Rouse, 1953; Verdaasdonk et al., 2013). One of the simplest examples for this representation is the Rouse model in which single chains move through a friction-less medium without excluded volume, or confinement (Rouse, 1953). Motion of the beads are treated as thermally driven, while active processes involving molecular motors, such as condensins and cohesins, or DNA and RNA polymerases are not explicitly represented. Other models comprise more factors such as the interactions with complexes that shape the chromosomes (Cheng et al., 2015), as well as excluded volume, wall and chain interactions and tethers, including centromere-spindle and telomere-membrane protein interactions (Verdaasdonk et al., 2013).

Polymer models have performed well at reproducing experimental observations, predicting chromatin topology and excluding unrealistic models. For instance, following the discovery of the nucleosome in the mid 70's (Kornberg and Klug, 1981), data

suggesting that compacted chromatin formed 30 nm thick fibers were proposed but did not stood the test of time (Maeshima et al., 2019). Polymer models, however, could account for higher order chromatin topology observed with by HiC (contact mapping strategies) and live cell microscopy of fluorescent spots in the chromosomes in interphase and mitosis (fluorescence reporter operator spots, FROS) to the relocalization of active gene loci to the nuclear periphery as described in this thesis.

Beyond their use in formulating hypothesis, our current understanding of mechanisms driving the dynamics and topology means that polymer models can be built upon to include the effects of active processes. Polymer models also remain useful to empirically describe observations of chromatin dynamics. For instance, in this thesis, we took advantage of the quantitative methods used to characterize the dynamics and mechanical properties of chromatin as a quantitative reporter assay for chromatin states. For the purposes of interpreting our results, no specific model needed to be assumed. However, we thought it would be interesting and instructive to see whether a simple model of a chain with different persistence lengths could reproduce the dynamic of the *INO1* gene locus we study here and spontaneously phase separate from each other as we propose occurs for the active *INO1* locus in the yeast nucleus. Modeling each chromosome arm as a double tethered bead spring chain with excluded volume interactions and nuclear wall confinement, has captured chromosome locus motions observed in experiments (Verdaasdonk et al., 2013). This model allows us to explore the dynamics of distinct chromatin regions (near the centromere or telomere ends, or in the middle) by analyzing the mean squared displacement (MSD) of beads in the region and calculate effective spring constants from time-dependent MSD trajectories. MSD measurements of chromatin loci *in vivo* show the expected subdiffusive behaviour of a segment of a polymer chain with MSD ~ τ^{α}, $\alpha \approx 0.4$ (Verdaasdonk et al., 2013; Weber et al., 2010, 2012). This behaviour is influenced by crowding and confinement effects of the nuclear environment and provides insight into the range of motion different chromatin regions can exhibit. The range of motion can be measured as radius of confinement (R_c) from the

plateau values of the MSDs at large timescales. The motion is confined due to encapsulation by the nuclear envelope. R_c values are different depending on the position of the bead with respect to centromeres and telomeres, which are tethered respectively, to microtubules or the nuclear envelope. Loci in the middle of the chromosome have more degrees of freedom than loci at the tethered ends. In the case of effective spring constants, values can be quantified from the standard deviation of the bead positions (Verdaasdonk et al., 2013), and it has been observed that these values are inversely related to the plateaus of the MSD curves. It is beneficial to have multiple strategies to estimate these physical parameters. In the case of MSD, the acquisition of time lapse measurements may not be sufficient for the time required to reach a plateau value. In addition to the position of the bead in the tethered chain, spring constant values depend on the nature of the nucleoplasm, including crowding. The power of the bead-spring model is that perturbations that are expected to influence the characteristics of the chain (e.g., histone exchange and cohesin activity) can be included. Changes in parameters including persistence length of the bead-spring model are sufficient to describe variations in motion following nucleosomal depletion (Verdaasdonk et al., 2013). Changes in persistence length (L_p) are predicted to be inversely related to the spring constant of the chain, reducing L_p results in a stiffer spring constant. Upon histone depletion, the increase in less occupied DNA is expected to reduce the overall L_p of the chain due the relatively low L_p of decompacted (50 nm) compared to compacted chromatin (200 nm). The correspondence between the experimental results and the model provides the rationale for using this simple reporter of chain behavior. We recognize that the model provides a simple representation and not a detailed description of the physical processes that act on chain motion. For instance, the addition of parameters that simulate compaction (histones) or loop extrusion (condensin) leads to unexpected behavior, such as the non-monotonic relationship between L_p and MSD (Bloom and Kolbin, 2022; He et al., 2020). This type of model can also provide insight into interactions among chromosomes by measuring mean squared distances between beads and generating contacts maps (Vasquez and Bloom, 2014). Models in general need to include more information to

account for other drivers of chromatin dynamics given by new experimental data. Nonetheless, their critical contribution is that even in a reductionist form, they are much better than any intuition we can possibly have about the motion of a chain in the viscoelastic crowded environment of the nucleus.

1.6 Structure of this thesis

This dissertation presents the research projects I have worked on to study two different chromatin adaptations on local and global levels. More specifically my aim was to understand how histone modifications regulate the mechanical properties of chromatin and how these result in its partitioning into different phases.

The thesis is divided into four chapters; Chapter 1 describes our current understanding of genome organization and the mechanisms that determine this organization, including recent ideas about chromatin phase separation.

In Chapter 2, I present an original study of how an active gene locus partitions out of the nucleoplasm to form a confined object close to the nuclear envelope. This is an adaptation by which transcription is efficiently coupled to mRNA transport-translation for a number of stress-activated genes. I use the *INO1* locus as a model to study and identify a general mechanism to explain this behavior. I show how local histone acetylation at the promoter of the gene, near specific DNA sequence motifs cause the mechanical properties of the chromatin to change resulting in a polymer-polymer phase separation mechanism with implications for other chromatin organization events and chromatin domain formation. This work has been recently revised and resubmitted to the journal "Nature Communications" and it is currently under review.

In Chapter 3, I present an original study to analyze the consequences of retro-engineering the genome of *S. cerevisiae* to reconstitute a mechanism of heterochromatin compaction that has been lost in the Sacharomycotina subphylum. I show that expressing homologs

of the lost genes from the fission yeast *S. pombe* heterochromatin proteins *Sp*Swi6 and *Sp*Clr4 in *S. cerevisiae* results in a global increase in chromatin compaction that causes a significant increase in the stability of the genome as measured by significantly decreased mutation and recombination rates. This work has possible implications for the synthetic biology by offering a resource to maintain insertions and modifications of genes into strains that have been engineered for various purposes. This manuscript is ready to be submitted. Finally, in Chapter 4, I discuss implications of the findings in this work, work that remains and perspectives on future research paths.

Chapitre 2 Adaptive partitioning of the *INO1* locus to the nuclear envelope is driven by polymer-polymer phase separation of the chromatin

2.1 Context of the research

Changes in gene locus spatial organization in response to environmental signals is a common occurrence, observed from lower eukaryotic to metazoan cells. To better understand this phenomenon and other chromatin organization processes, it has become essential to understand the biochemical and physical processes that underlie the organization and dynamics of chromatin in the nucleus. Recent studies have shown that the biochemical changes that take place in local chromatin segments are induced by post-translational modifications in histones that constitute the nucleosome core. These modifications cause disruptions of histone-histone and histone-DNA interactions that change the material properties of chromatin concomitant with their phase separation. In this work we use the stress inducible *INO1* gene in *S. cerevisiae* as a model to study reorganization of a gene locus. Gene recruitment sequences (GRSs) are genetic elements in or upstream of the promoter of this gene and their presence is essential to a transition of the locus from having a wide spatial distribution in the repressed state, to a confined site near the nuclear envelope in its active state. The biochemical and physical mechanisms that cause this change in localization are unknown. We hypothesized that the *INO1* locus undergoes a phase separation from nucleoplasm mainly due to histone acetylation and accompanying disruption of histone-DNA and histone-histone interactions that maintain the chromatin in the dense nucleoplasmic phase. Resulting separation causes the locus to partition with dilute phase chromatin at the periphery, adjacent to the nuclear envelope. We measured this transition by monitoring the locus chromatin dynamics with an array of 128 DNA protein binding motifs (LacO) bound to binding protein LacI-GFP. We demonstrate that *INO1* activation causes a predicted increase in effective spring stiffness and confinement of chromatin at the nuclear envelope, associated with histone modifications and measured increased histone

exchange rates. Using conditional knockout studies and a novel CRISPR-dCas9-BirA∗ method, we identify chromatin remodeling enzymes associated with the GRSs, which we propose modify and catalyze exchange of histones at the active *INO1* locus. Finally, we discuss an analytical model and perform numerical simulations with a simple bead-spring model to show that we can reproduce phase separation and associated changes in mechanical properties of a segment of a chain.

2.2 Authors contributions

S.W.M. and L.G. did research conceptual design and all data analysis with exception of numerical simulations and mass spectrometric data. L.G. generated all the strains used in the study. Statistical mapping and particle tracking were done by L.G. ChIP assays were designed by F.R., C.J, L.G and performed by L.G. HATs depletion employing an Auxin Degron System was designed and performed by L.G. The CRISPR-dCas9-BirA∗ system was designed and generated by L.G. For the dCas9-BioID assays, the streptavidin affinity purification was performed by L.G. and the mass spectrometry and data analysis were done by C.T. Chromatin polymer numerical simulations were designed and performed by K.B. and D.K. All authors wrote and reviewed the manuscript.

Article 1. Adaptive partitioning of the *INO1* locus to the nuclear envelope is driven by polymer-polymer phase separation of the chromatin

Authors: Lidice González[1], Daniel Kolbin[2], Christian Trahan[1,3,4], Célia Jeronimo[3], François Robert[1,3,4], Marlene Oeffinger[1,3,4], Kerry Bloom[2], Stephen W. Michnick[1]*

[1]Département de Biochimie, Université de Montréal, C.P. 6128, Succursale centre-ville, Montréal, Québec H3C 3J7, Canada

[2]Department of Biology, University of North Carolina at Chapel Hill, Chapel Hill, NC 27599, USA

[3]Institut de Recherches Cliniques de Montréal, 110 Avenue des Pins Ouest, Montréal, Québec H2W 1R7, Canada

[4]Faculty of Medicine, Division of Experimental Medicine, McGill University, Montréal, Québec H3A 1A3, Canada

*Correspondence: stephen.michnick@umontreal.ca

2.3 Text of the article

2.3.1 Abstract

Partitioning of active gene loci to the nuclear envelope (NE) is a mechanism by which organisms increase the speed of adaptation and metabolic robustness to fluctuating resources in the environment. In the yeast *Saccharomyces cerevisiae*, adaptation to nutrient depletion or other stresses, results from relocalization of active gene loci from nucleoplasm to the NE, resulting in more efficient transport and translation of mRNA. The mechanism by which this partitioning occurs remains a mystery. Here, we demonstrate that the yeast inositol depletion-responsive gene locus *INO1* partitions to the nuclear envelope, driven by local histone acetylation-induced polymer-polymer phase separation from the nucleoplasmic phase. This demixing is consistent with recent evidence for chromatin phase separation by acetylation-mediated dissolution of multivalent histone association and fits a physical model where increased bending stiffness of acetylated chromatin polymer causes its phase separation from de-acetylated chromatin. Increased chromatin spring stiffness could explain nucleation of transcriptional machinery at active gene loci.

2.3.2 Introduction

Genes relocalize to specific regions inside the nucleus depending on whether they are active or repressed, including the nuclear periphery or the periphery of their chromosomal territories, a phenomenon observed in many different eukaryotes from budding yeast to mammalian cells (Ahmed et al., 2010; Brickner et al., 2012; Brickner et al., 2016; Brickner and Walter, 2004; Brown et al., 2008; Cabal et al., 2006; Casolari et al., 2004; Kalverda et al., 2010; Kosak et al., 2002; Rohner et al., 2013; Taddei et al., 2006; Williams et al., 2006; Zink et al., 2004). This has been particularly studied for *Saccharomyces cerevisiae* gene loci, for which several stress response genes, including nutrient related genes such as the *GAL* loci and heat shock response genes, translocate to the nuclear periphery upon activation (Brickner and Walter, 2004; Cabal et al., 2006; Casolari et al., 2004; Taddei et al., 2006). These genes remain at the periphery after returning to their repressed condition, a form of transcriptional memory, which primes the genes to be more rapidly transcribed, translocated to the cytosol and translated, as nutrients vary between being depleted and enriched in a fluctuating environment (Ahmed et al., 2010; Brickner et al., 2007).

The *INO1* gene has been among the most studied to determine a molecular mechanism for gene locus translocation (Brickner et al., 2012; Brickner and Walter, 2004; Randise-Hinchliff et al., 2016). Efforts to understand locus localization to the nuclear envelope (NE) have focused on attempts to identify protein-protein or protein-DNA interactions that could account for physical tethering of chromatin to the NE (Ahmed et al., 2010; Brickner et al., 2012). Thus, interactions of component proteins of the Nuclear Pore Complex (NPC) or associated components such as subunits of the SAGA complex have been suggested to induce, or their deletion has been shown to prevent *INO1* translocation(Ahmed et al., 2010; Brickner et al., 2012). However, so far, there are no direct evidence that these proteins are involved in physical tethering of the *INO1* locus to the NE. Furthermore, 5' *cis* elements in the *INO1* locus called Gene Recruitment Sequences (GRS) or "Zip Codes", have been shown to be essential to *INO1* and now other loci translocations (Ahmed et al.,

2010; Brickner et al., 2012; Brickner et al., 2016). It has been proposed that GRSs could be anchoring sites for the tethering of gene loci to the NE *via* protein-DNA or protein-protein interactions (Ahmed et al., 2010; Brickner et al., 2012; Brickner et al., 2016). To date, however, evidence of interactions between GRSs and proteins at the NE have not been reported. Furthermore, studies of the statistical distributions of translocated genes among populations of cells, as well as gene tracking measurements, show that instead of being bound at the NE, as are, for instance, the NPC or Spindle Pole Body, activated gene loci are simply statistically more tightly distributed towards the NE (Berger et al., 2008; Brickner et al., 2012; Cabal et al., 2006; Taddei et al., 2006). These observations led us to postulate that active gene locus translocation could be the result of differential partitioning of active gene loci to the periphery by a local phase transition of the chromatin caused by histone acetylation and other modifications, resulting in increased rates of histone exchange and associated decompaction of the chromatin. Here we present evidence that the GRSs are sites of association of chromatin remodeling complexes, including HATs, which catalyze histone H3 acetylation and consequently increased H3 exchange between nucleosomes and nucleoplasm within and surrounding the activated *INO1* locus. This increase in H3 exchange causes dissociation of nucleosomes; and resulting decompaction of chromatin manifests as an increase in spring stiffness and spatial dynamics that reflects phase separation of the *INO1* locus from compacted chromatin compartment found in the nucleoplasm of the yeast nucleus to the decompacted chromatin compartment found adjacent to the nuclear envelope.

2.3.3 Results

Translocation of the activated *INO1* locus and decompaction of its chromatin were studied as follows: first, we obtained a yeast strain in which 128 LacO binding motifs are integrated into the gene and expression of the LacO binding protein LacI fused to GFP (Brickner et al., 2012). Furthermore, reference markers for the nuclear envelope (Nup49-GFP) and nucleolus (Nop1-mCherry) are also expressed. This strain could then be used to monitor and compare the statistical distribution of *INO1* in cells grown in the presence

(inactive *INO1*) or absence (active *INO1*) of inositol (Figure 2.1 a, b). Next, we could monitor the phase transition of active chromatin based on the observation that the consequent decompaction of the chromatin, is reflected in changes in its mechanical properties and geometric organization (Bloom, 2008; Verdaasdonk et al., 2013). These changes can be understood as follows: first, the persistence length (L_p) of DNA, as for all polymers, is the length over which a thermal perturbation would cause it to bend. The L_p for naked DNA is smaller than that of chromatin (5-50 nm *versus* 170-220 nm) (Bystricky et al., 2004; Chi et al., 2013; Cui and Bustamante, 2000; Rechendorff et al., 2009; Smith et al., 1996) given that naked DNA has more degrees of freedom than chromatin (Bloom, 2008; Verdaasdonk et al., 2013). This increase in degrees of freedom implies a higher number of configurations that can be explored per unit time by less occupied DNA so its movements are more confined compared to chromatin. Consequently, chromatin behaves as an "entropic spring" of increasing spring stiffness as it transitions from compact to decompacted states (Bloom, 2008; Verdaasdonk et al., 2013). The spring constant of a polymer (k_s) is inversely proportional to L_p (Equation 1) and consequently k_s is predicted to increase as chromatin decompacts. Furthermore, its trajectories through space are shorter, a characteristic that is determined from the radius of confinement (R_c) of the chromatin (Bloom, 2008; Verdaasdonk et al., 2013). Values for k_s and R_c can be determined from measurements of mean-square displacement (MSD) and localization coordinates of the GFP-labelled LacO array embedded in the *INO1* gene locus (Verdaasdonk et al., 2013).

$$k_S = \frac{k_B T}{L_p^2} \qquad (1)$$

2.3.3.1 Deletion of GRS I and II prevents localization of active *INO1* to the nuclear envelope

The relocalization of the active *INO1* locus to the nuclear periphery is prevented in strains in which the GRSI, and II of the *INO1* locus are both deleted (hereafter referred to as the

GRSI,IIΔ double mutant) (Ahmed and Brickner, 2010). To access the effects of GRS deletions on the statistical distribution of the *INO1* locus in large populations of cells, we used a high-resolution computational approach that generates probabilistic maps of the locus distribution in the nucleus (Figure 2.1 a, b) (Berger et al., 2008). Using the LacI-GFP-labelled LacO array as reporter for the *INO1* locus and, Nop1-mCherry and Nup49-GFP as nucleolus and nuclear envelope reference markers, respectively, we mapped the distribution of the *INO1* locus with respect to these landmarks for the *wild type* and single and double mutants of the GRS sites under repressing (+ inositol) and activating (- inositol) conditions.

Consistent with previous studies, the repressed *INO1* locus was distributed throughout the nucleoplasm, but the activated *INO1* locus was confined to a specific region in the vicinity of the NE (Figure 2.1 c, d) (Brickner et al., 2012). Single GRS deletion mutants reduced and the double mutant GRSI,IIΔ prevented partitioning of the active *INO1* locus towards the NE, as reported previously (Figure 2.1 e-g) (Ahmed and Brickner, 2010). The *INO1* locus was distributed towards, but not fixed at the NE (Brickner et al., 2012). The effects of the mutants do not reflect changes in transcription of *INO1* as disrupting transcription was previously shown to have no effect on *INO1* relocalization (Brickner et al., 2007). Additionally, there was, as previously reported(Ahmed et al., 2010), a subpopulation of cells in which the *INO1* locus was not localized at the NE, corresponding to those in S-phase (Brickner et al., 2012).

The activated *INO1* locus shows a characteristic spatial distribution at the NE that perhaps reflects its position in the middle of the 3' arm of Chromosome X. NE localization of other activated gene loci also reflects their chromosome positions, including the *GAL1-10* locus, which is located closer to the centromere region in Chromosome II and thus close to the Spindle Pole Body (Berger et al., 2008) and the *HXK1* gene locus, located in a subtelomeric region of Chromosome VI, that is localized towards the NE whether active or repressed, but more compact when activated (Taddei et al., 2006).

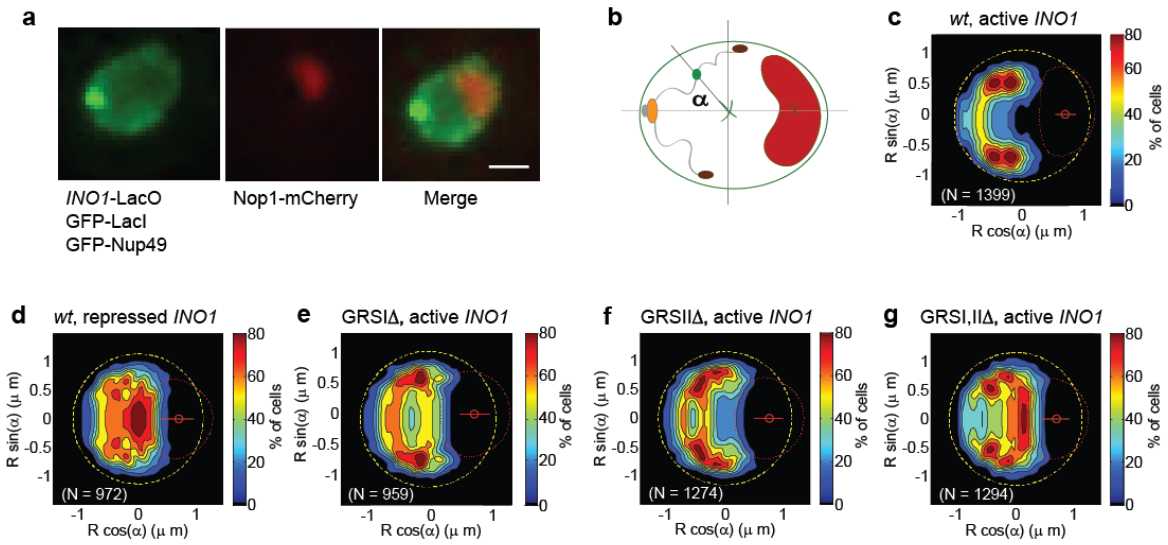

Figure 2.1 Activated INO1 NE localization is disrupted by the deletion of both GRS I and II

a *Representative photomicrographs of yeast nuclei containing the LacO repressor array integrated in the INO1 locus and expressing GFP-LacI allows for visualization of dynamics in the locus with GFP-Nup49-labeled NE and Nop1-mCherry-labeled nucleolus as spatial reference markers (maximum projection of 250 nm Z stacks). Scale bar represents 1 µm.* ***b*** *Yeast nucleus landmarks used as coordinates for this analysis. NE (green ellipsoid), nucleolus (red ellipsoid) and nucleus center (green x). The grey lines represent the central axes of the ellipsoid; α, angle from the longer central axis. Orange, red and green blobs connected by a trace represent the spindle pole body, telomeres and gene locus, respectively.* ***c*** *INO1 probability maps obtained from the analysis of 1399 nuclei of wild type cells grown in the absence of inositol (active), and* ***d*** *972 nuclei of wild type cells in the presence of inositol 100 µM (repressed). Dashed yellow line, NE; dashed red line, position of the nucleolus; the color scale represents the probability density distribution of the locus inside the nucleus.* ***e-g*** *INO1 probability maps obtained from the analysis of 959 (GRSIΔ), 1274 (GRSIIΔ) and 1294 (GRSI, IIΔ) nuclei in cells in which GRS I, GRS II or both GRS I and II are deleted, respectively, and that were grown in the absence of inositol (active).*

2.3.3.2 Deletion of GRSs prevents decompaction of the active *INO1* locus

We measured differences in the mechanical spring stiffness of the *INO1* locus in the repressed and activated states. To do this, we tracked the GFP-LacI-labelled LacO array in the *INO1* locus for 1 minute at intervals of 500 milliseconds and calculated MSD values in each case. The slope and plateaus of the MSD trajectories for the *INO1* locus were markedly reduced under activating *versus* repressed conditions (Figure 2.2 a). In addition, loci closer to the NE appear to be excluded from the interior of the nucleoplasm as observed before for the *GAL1-10* genes (Cabal et al., 2006), which also contain GRS sequences required for relocalization of the *GAL* locus to the NE (Brickner et al., 2016).

We then used established relationships between MSD statistics and R_c and k_s to calculate their values as follows (Verdaasdonk et al., 2013): R_c could be calculated directly from the MSD plateaus (See Methods, Equation M1) (Neumann et al., 2012; Verdaasdonk et al., 2013). R_c could independently be determined from the standard deviation of spot positions, σ, and the average squared deviation from the mean position, $\langle \Delta r_0^2 \rangle$, by applying the equipartition theorem (See Methods, Equation M2) (Scheffold et al., 2010; Uhlenbeck, 1930; Verdaasdonk et al., 2013).

The *INO1* locus in *wild type* strains (Figure 2.2 b) and single GRS mutant cells (Figure 2.2 c, d) showed significantly larger R_c for the repressed *versus* the activated state. The GRSI,IIΔ double deletion, however, resulted in no significant differences in R_c between repressed and activated states (Figure 2.2 e). These results were also consistent with statistical distributions of loci in populations of cells, demonstrating that the observed changes in R_c in single cells are pervasive in the population.

Using the equipartition theorem and standard deviation (σ) for the distribution of steps from the mean we calculated k_s (See Methods, Equation M3) (Scheffold et al., 2010; Verdaasdonk et al., 2013). The k_s of the *INO1* loci significantly increased in cells with active

versus repressed loci in both *wild type* (Figure 2.2 f) and the GRS single deletion strains (Figure 2.2 g, h), suggesting a stiffening of decompacted chromatin. There was no significant change in k_s in the GRSI, IIΔ double deletion strain under activating conditions (Figure 2.2 i).

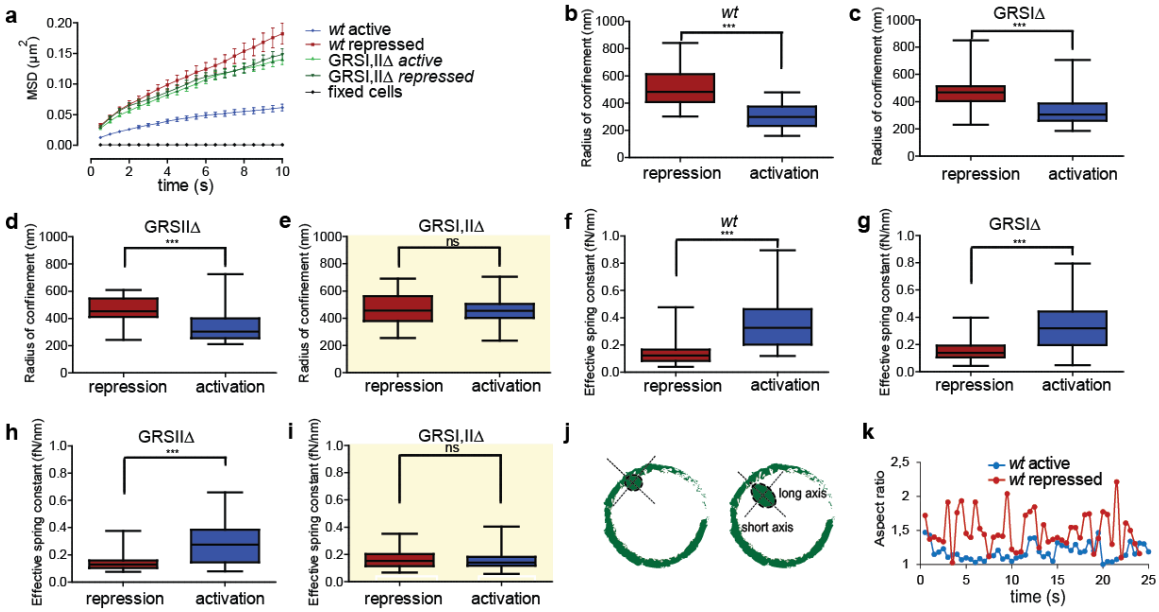

Figure 2.2 INO1 dynamics and material properties depend on the presence of both GRS I and II

a *MSD curves for INO1 locus in wild type (red and blue lines, n = 38 and 34, respectively with SE bars) and the GRSI,IIΔ (dark and light green lines, n = 51 and 45, respectively with SE bars) strains under activating and repressed conditions, and for a population of fixed cells (black line, n = 8, with SE bars).* ***b-d*** *Radius of confinement (R_c) significantly decreases in wild type, GRSIΔ, and GRSIIΔ cells from repressed (red) to activated (blue) conditions.* ***e*** *R_c for GRSI,IIΔ mutant cells under repressing (red) and activating (blue) conditions show no significant differences.* ***f-h*** *Spring constant (k_s) for wild type, GRSIΔ, and GRSIIΔ cells increases significantly from repressing (red) to activating (blue) conditions.* ***i*** *k_s for GRSI, IIΔ mutant shows no significant difference between repressing (red) and activating (blue) conditions.* ***j*** *Schematic of INO1 locus size measurements of aspect ratio variation over time. Green circles represent nuclei of two cells showing loci spots with different long and*

short axes. ***k*** *Aspect ratio change over time for two INO1 loci in cells grown under repressed (red) or activated (blue) conditions measured by Structured Illumination Microscopy. In the box and whisker plots (b-i), the median is indicated as middle line, 25th and 75th percentile as boxes and the whiskers represent minimum and maximum values; n = 38 and 34, respectively (b, f), n = 46 and 51, respectively (c, g), n = 31 (d, h), n = 51 and 45, respectively (e, i). Data were analyzed by unpaired two-sided Student's t-test in b-i. *p < 0.05; **p < 0.01; ***p < 0.001.*

2.3.3.3 The active *INO1* locus behaves as an elastic filament

As discussed above, the increase in spring stiffness of decompacted chromatin reflects in a decrease in the rate and amplitude of *INO1* locus expansion-contraction (Verdaasdonk et al., 2013). This behavior can be visualized with the LacI-GFP-labelled LacO array and quantified by fitting an ellipsoid function to the GFP signal imaged at super-resolution by Structured Illumination Microscopy and calculating the aspect ratio between long and short axes of the ellipsoid (Figure 2.2 j). Consistent with predicted behavior, the *INO1* locus changes shape with higher frequencies and amplitudes in the repressed *versus* the activated states (Figure 2.2 k). These observations are also consistent with previous results in which a decrease in L_p caused by H3 histone depletion resulted in a decrease in the rate and amplitude of expansion of the chromatin (Verdaasdonk et al., 2013).

2.3.3.4 Activation of the *INO1* locus increases rates of exchange of histone H3

To test whether the changes in *INO1* locus mechanical properties follow from an increase in histone exchange, we used a strain to probe changes in histone H3 nucleosome exchange in *wild type* and GRSI, IIΔ double mutant strains. In this strain histones H3 and H4 genes are deleted from the genome and replaced with both constitutively and inducible expressed copies (Figure 2.3 a) (Rufiange et al., 2007). In a galactose inducible cassette, H3 is fused to a FLAG-tag that when expressed can be used to quantify newly synthesized H3 that is incorporated into nucleosomes at specific positions by Chromatin

Immunoprecipitation followed by real time PCR (ChIP-qPCR) to measure nucleosome exchange in different chromatin regions under different conditions. To avoid the contribution of histone incorporation due to DNA replication, cells are also arrested in G1 by the addition of α-factor. We probed H3-FLAG incorporation in several regions in the *INO1* promoter and ORF, plus sites in upstream (*SNA3* and *DAS1*) and downstream (*VPS35*) genes to determine whether changes in histone exchange are confined to the *INO1* locus (Figure 2.3 b, Figure S2.1).

ChIP-qPCR results with an anti-FLAG antibody showed higher incorporation of newly synthesized histone H3 at *INO1* promoter in cells under activated *versus* repressed conditions for the *INO1* promoter and coding region (Figure 2.3 c). Results for repressed cells were consistent with genome-wide ChIP-chip data (Rufiange et al., 2007), validating our method. For the GRSI,IIΔ double mutant, significant reductions in H3 exchange under activated conditions were observed in the *INO1* locus promoter at the GRS I site and in the *SNA3* promoter and coding sequence where GRS II is located but not in the *INO1* coding sequence (Figure 2.3 c). These results suggest that GRS I and II may be HAT and/or other remodeling complex association sites mediating H3 exchange associated with topologically adjacent nucleosomes. The fact that H3 exchange is not affected in the *INO1* coding sequence is consistent with the fact that there are other known remodeling enzymes that bind near the ORF. Thus, consistent with ours and previous results, an increase in nucleosome histone H3 exchange at the *INO1* locus chromatin is associated with an increase in its spring stiffness (Verdaasdonk et al., 2013).

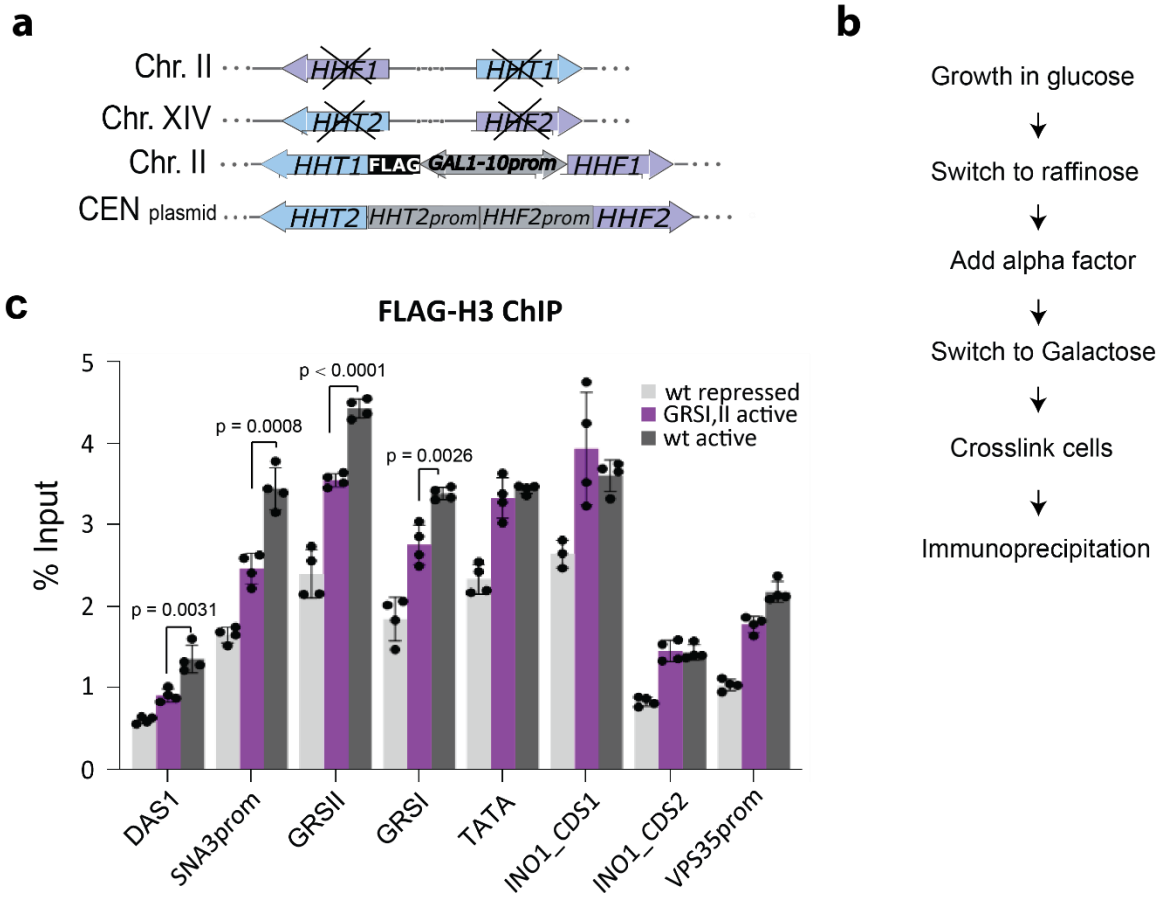

Figure 2.3 H3 exchange increase in activated INO1 is affected when GRS I and II are deleted

a *Schematic representation of the strain used to measure the incorporation of newly synthesized FLAG-H3 into nucleosomes(Rufiange et al., 2007).* ***b*** *Cell sample preparation workflow before ChIP. For the repressed condition, inositol was added in all the media used.* ***c****, FLAG-H3 enrichment, as determined by ChIP-qPCR and expressed in percentage of input, over the vicinity of GRS I and GRS II regions within DAS1, SNA3, INO1 and VPS35 gene loci for wild type strain under repressed (light gray) and activated (gray) conditions, and the GRSI, IIΔ (purple) under activated conditions. Data in panel c represent mean ± SD; n = 4 biological samples. Data were analyzed by unpaired two-sided Student's t-test. p-values are shown for the regions with significant differences between the GRS double mutant and the wild type active gene.*

2.3.3.5 Depletion of yeast HATs prevents active *INO1* locus partitioning to the nuclear envelope

The increase in H3 exchange at the *INO1* locus is consistent with histone post-translational modifications, and specifically lysine acetylation by histone acetyltransferases (HATs) (Bloom, 2008; Driscoll et al., 2007; Rufiange et al., 2007; Topal et al., 2019; Xhemalce et al., 2007). We therefore hypothesized that the GRSs could be association sites for HATs and other chromatin remodeling complexes that alter the rates of histone-nucleosome exchange. Evidence for specific functions of HATs and histone deacetylases in controlling active *INO1* partitioning towards the NE exists. For instance, the Rpd3(L) histone deacetylase blocks partitioning of the *INO1* locus towards the NE and deletion of the gene encoding this deacetylase results in increased acetylation of nucleosome-associated histone complexes in the promoter of *INO1* (Randise-Hinchliff et al., 2016). Additionally, deleting subunits of the SAGA HAT complex decreases active *INO1* locus partitioning to the NE (Ahmed et al., 2010), also observed for the *GAL* loci (Cabal et al., 2006).

Since both GRS I & II, plus other unidentified GRS sites could be associated with HATs, we attempted to identify HATs associated with the *INO1* locus by screening for loss of activated *INO1* locus NE localization in cells in which an auxin-inducible degron (AID) coding sequence was integrated 3' to the ORFs of the 12 known yeast HAT catalytic subunits. The addition of auxin to growth medium then induces targeting of the HAT-AID degron fusion proteins for rapid proteasomal degradation (Figure 2.4 a) (Morawska and Ulrich, 2013). To induce fast degradation of each HAT–AID, cells were treated with 500 µM indole-3-acetic acid (IAA) for 1.5 hours under inositol starvation (*INO1* induction) conditions. This condition was sufficient to reduce the expression of each HAT–AID protein as observed by Western blot (Figure S2.2). After incubation, cells were immobilized on ConA-coated microtiter plate wells and imaged to generate high-resolution probabilistic maps of the localization of the *INO1* locus.

Among the 12 HAT catalytic subunits, depletion of three of these reduced partitioning of the active *INO1* towards the NE: Gcn5, Rtt109, and Taf1 (Figure 2.4 b-g, Figures S2.3, S2.4). Deletion of *GCN5*, coding for a subunit of the SAGA complex, has previously been shown to prevent active *INO1* locus partitioning towards the NE (Ahmed et al., 2010). The SAGA complex has also been implicated directly in the activation of *INO1* through transcription factors that bind the upstream activating sequences (UAS) sites close to the TATA box of *INO1* (Lo et al., 2001). Rtt109 is not part of any known chromatin remodeling complex and has not been implicated in *INO1* gene activation previously. This HAT acetylates lysine 56 on the histone H3 core domain (H3K56), a modification that has been globally observed on newly synthesized histones in *S. cerevisiae* and *S. pombe* (Driscoll et al., 2007; Han et al., 2007; Rufiange et al., 2007; Topal et al., 2019; Xhemalce et al., 2007). Interestingly, H3K56 acetylation also correlates with higher histone exchange rates in global analyses of the *S. cerevisiae* genome (Rufiange et al., 2007). Finally, Taf1 is a subunit of the large TFIID complex, a general transcription initiation factor for RNA polymerase II (Pol II). Taf1 has been shown to have histone acetyltransferase activity during *in vitro* assays, but its role in vivo is less well understood (Durant and Pugh, 2006; Mizzen et al., 1996).

We analyzed the effect of the depletion of each of these three HATs on a specific acetylation mark in the regions surrounding the *INO1* locus including the GRS sites. The H3K14 acetylation is known to be catalyzed by Gcn5 (Duan and Smerdon, 2014; Kuo et al., 1996; Kuo et al., 2000; Smerdon, 1991), and it has been observed *in vitro* that Taf1 also acetylates H3 K14 (Mizzen et al., 1996), although this is more controversial (Durant and Pugh, 2006). Rtt109 has been also observed to acetylate H3K14 in *in vitro* assays (Abshiru et al., 2013; Berndsen et al., 2008). This mark was quantified by ChIP-qPCR on the *INO1* locus and on proximal genes in the AID strains for each of the three HATs. Results are presented as the ratio between each mark and H3 levels in each region analyzed. The regions screened correspond to the same ones used when measuring the rate of incorporation of newly synthesized histones.

The results obtained (Figure 2.4 h), show that there is a significant decrease in the H3K14ac/H3 ratio for the strain where Gcn5 was depleted compared to wild type in all regions analyzed. A significant decrease is also observed for the other two HATs, mainly for the regions close to the GRSII site, however not as significant as for the Gcn5-AID strain. This result indicates that Gcn5 could be the dominant HAT for acetylation in these regions.

We quantified mRNA levels for these loci after depleting each of the HATs in the AID strains. We observed a decrease in *INO1* mRNA levels for Gcn5-AID and Rtt109-AID depletion strains, and a decrease for *SNA3* mRNA levels, in this case for all three HAT-AID strains, although more significantly for Gcn5-AID and Rtt109-AID strains (Figure 2.4 i). For the *DAS1* and *VPS35* loci, there was no apparent difference in mRNA levels between all four strains (Figure 2.4 i). These results indicate that the transcription is affected for *INO1* and the GRS containing upstream locus *SNA3*, when at least two of the three HATs are depleted. Previous results have shown that deleting the GRS sites cause a decrease in *INO1* mRNA levels (Ahmed et al., 2010).

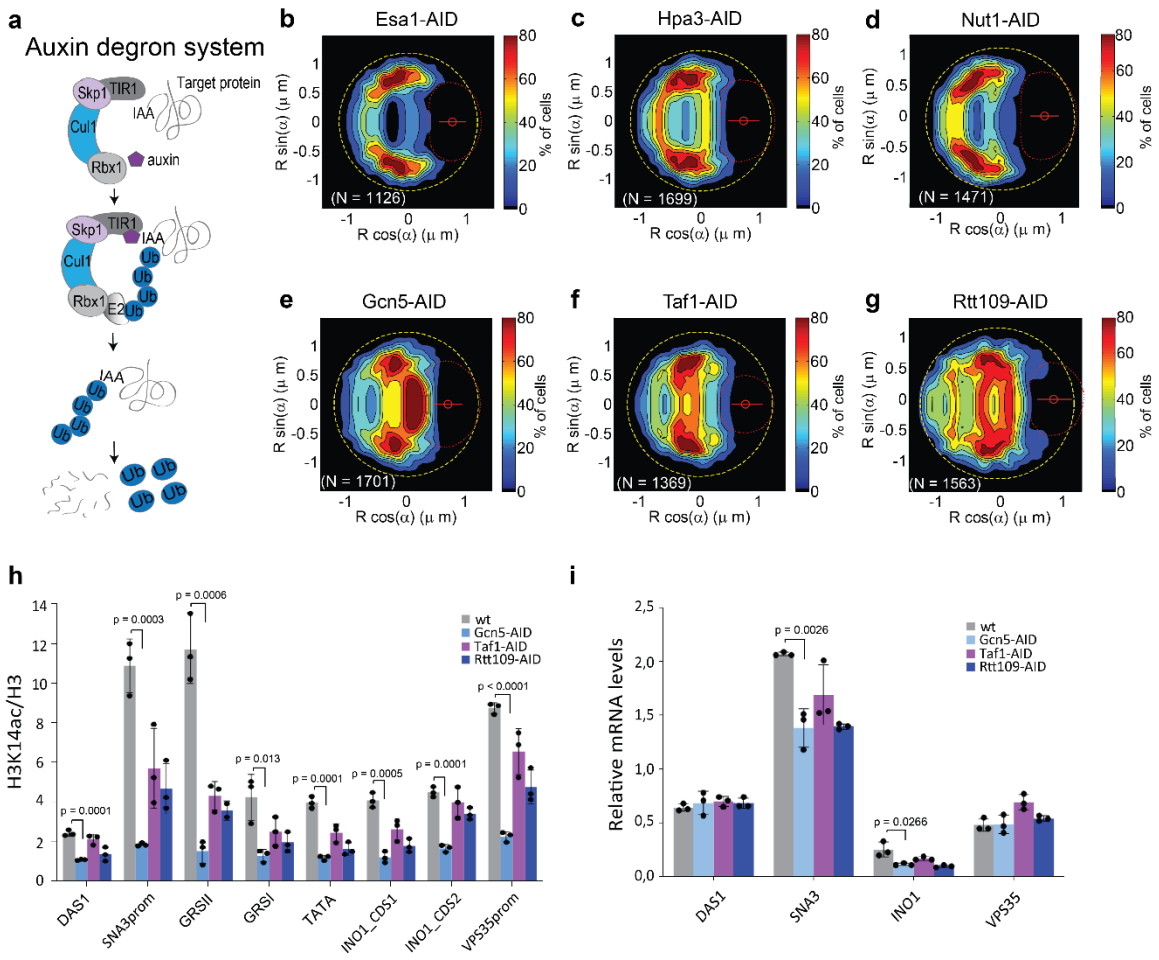

Figure 2.4 Specific histone acetyltransferases (HATs) are required for active INO1 localization

a *Schematic representation of the auxin-inducible degron (AID) system used to deplete targeted HAT catalytic subunits for degradation in the presence of auxin.* ***b-g*** *INO1 probability maps obtained from the analysis of thousands of nuclei in strains with different HATs tagged with the AID degron and grown in the absence of inositol (active).* ***b-d*** *HAT-AID tagged strains where there is no effect on the statistical distribution of the INO1 locus after treating the cells with auxin.* ***e-g*** *HAT-AID tagged strains where the addition of auxin results in disruption of the INO1 locus relocalization pattern to the nuclear periphery.* ***h*** *H3K14ac enrichment around and within the active INO1 gene, as determined by ChIP-qPCR and expressed as H3K14ac/H3 ratio, over the vicinity of DAS1, SNA3, INO1 and VPS35 gene loci for wild type and three different HAT-AID strains treated with auxin and under*

inositol activating conditions. ***i*** *mRNA levels as quantified by RT-qPCR, relative to ACT1, for DAS1, SNA3, INO1 and VPS35 loci in wild type and Gcn5-AID, Taf1-AID, and Rtt109-AID strains in the presence of auxin and INO1 activating conditions. Data represent mean ± SD (h and i); n = 3 biological samples. Data were analyzed by unpaired two-sided Student's t-test and p-values are shown for significant differences between wild type (grey) and Gcn5-AID mutant (blue). See also Figures S2.2-S2.4.*

To probe for HATs and other chromatin remodeling complexes proximal to specific GRSs, we developed a proximity-dependent biotinylation (BioID) approach, based on guide RNA (sgRNA)-directed catalytically dead (d)Cas9 (Figure 2.5 a) (Opitz et al., 2017). We created BirA*-dCas9 ligase fusions in different N- or C-terminal orientations and using short (12) or long (38) amino acid linkers. These constructions were used to provide for more or less steric constraint and flexibility and promiscuity of biotin labeling. The short linker was used in a previous BioID study in yeast (GSSGSSGSSGSS)(Opitz et al., 2017) and the long sequence in a CasID study in mammalian cells (LERPPLCWISAEFHHTGLVDPSSVPSLSLNRGSGSGSG) (Schmidtmann et al., 2016).

We transformed a *wild type* strain with the different plasmids encoding the BirA*-dCas9 constructs and four different sgRNAs targeting genomic sequences proximal to the GRS I site. We also generated control strains that were transformed with the BirA*-dCas9 constructs but not with sgRNAs (Tables S2.1-S2.3). Western blot confirmed the expression of the different fusion systems generated (Figure S2.5). Biotinylated proteins were pulled down on streptavidin-sepharose beads, bound proteins were trypsin digested, and resulting peptides were analyzed by tandem mass spectrometry (LC-MS/MS). We observed enrichment of peptides derived from proteins associated with several nuclear complexes in extracts from strains expressing *versus* those not expressing sgRNAs (Figure 2.5 b-e, Figure S2.6) (Table 2.1; Tables S2.4-S2.9). Five of the complexes are associated with chromatin remodeling activity including Ino80, Swr1, ASTRA, Set3, and FACT complexes (Table 2.1). Among the enriched peptides, those belonging to the ATP-

dependent DNA helicases Rvb1 and/or Rvb2 were enriched in all separate sgRNA-BirA*-dCas9 samples. Rvb1 and Rvb2 are components of Ino80 (Shen et al., 2000), Swr1 (Nguyen et al., 2013), and ASTRA (Nguyen et al., 2013) complexes and they are also linked to two (Gcn5 and Taf1) (Lakshminarasimhan et al., 2016; Lee et al., 2011; Sanders et al., 2002) of the three HAT catalytic subunits, whose depletion resulted in reduced partitioning of the active *INO1* towards the NE. Specifically, Gcn5 and Taf1 make protein-protein interactions with Rvb1 (Gcn5) and Rbv2 (Gcn5 and Taf1) and Taf1 also interacts with Ino80, another subunit of the Ino80 complex. Both subunits of the FACT complex Spt16 and Pob3 showed peptides enriched in one of the sgRNA-BirA*-dCas9 samples, and there are reported interactions of these proteins with several HATs including Gcn5 (Lee et al., 2011; Leng et al., 2021) and Rtt109 (Yang et al., 2016). Analysis of protein enrichment in the samples expressing sgRNAs revealed that some proteins were only enriched in one of the samples, or the enrichment of several proteins varied between samples. This may indicate steric label constraint or hindrance due to sgRNA localization on chromatin, BirA*-dCas9 fusion orientation and linker length (Figure S2.6, Tables S2.6-S2.8).

Taken together, our observations imply a probable role for these three HATs in initiating the cascade of histone acetylation and other remodeling activities that results in increased histone exchange and decompaction of the *INO1* locus chromatin. That there are likely alternative sites of association of these HATs or other chromatin remodeling proteins is consistent with our observation that the GRSI,IIΔ double deletion only results in a partial decrease in histone H3 exchange at the *INO1* locus.

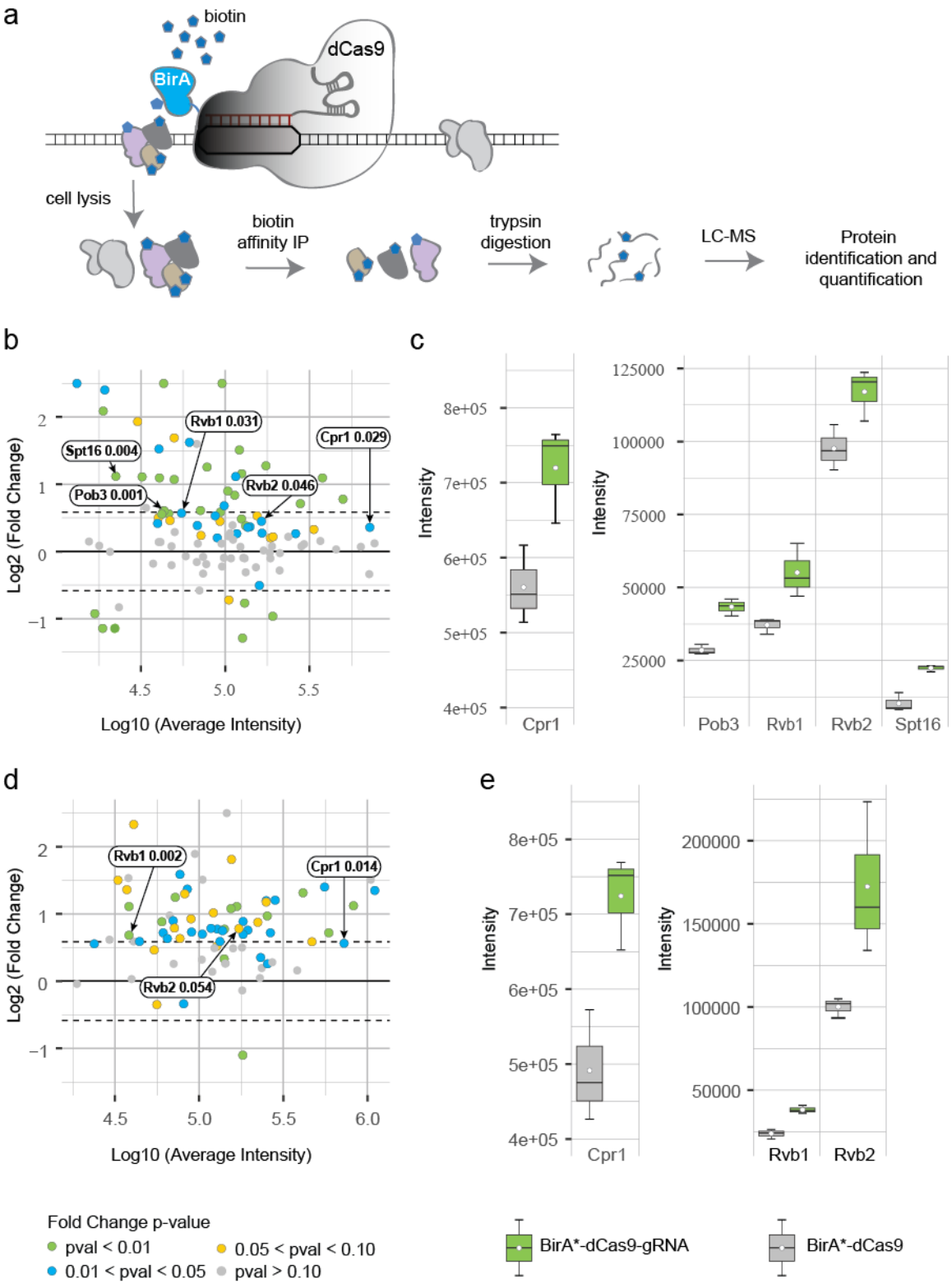

Figure 2.5 Chromatin remodeling subunits bind GRS site near INO1 locus

a *BirA*-dCas9 system generated to target the vicinity of GRS I site by using different sgRNAs for site-specific binding of BirA*-dCas9 and biotinylation of proximal proteins. Proteins were then affinity purified with streptavidin, digested, and analyzed by mass spectrometry.* ***b, d*** *Micro array (MA) plots representing average protein intensities from biological triplicates from sgRNA-BirA*-dCas9 samples S5 (b) and S7 (c) plotted against protein quantity fold changes from these sgRNA-BirA*-dCas9 samples over those from their respective negative control triplicates (BirA*-dCas9). Protein fold change p-values calculated from a two-sided unpaired Student's t-test with equal variance are color coded, and the grey dashed lines represent 1.5-fold quantity increase. p-values are indicated next to labels.* ***c, e*** *Box plots of measured protein intensities of candidates from sgRNA-BirA*-dCas9 samples S5 (d) and S7 (e) triplicates along with their respective negative control triplicates. Median is indicated as middle line, average as a white dot, 25th and 75th percentile as boxes and whiskers represent 5th and 95th percentile. False discovery rates thresholds for mass spectrometry identification of peptide spectrum match, peptides, and proteins were set to 0.1. See also Tables S2.4-S2.9 and Figures S2.5 and S2.6.*

Table 2.1 Enriched biotinylated proteins associated with chromatin remodeling and Histone Acetyltransferase (HAT) complexes

Enriched Biotinylated Proteins	Associated Chromatin Remodeling Complexes	HATs That Bind To Enriched Proteins[1]
Rvb1, Rvb2	ASTRA complex Ino80 complex R2TP complex Swr1 complex	Gcn5, Nut1, Sas2, Taf1
Spt16, Pob3	FACT Complex	Elp3, Esa1, Gcn5, Hat1, Rtt109, Sas3, Sua7
Acs2	histone acetylase complexes	Elp3, Esa1, Gcn5, Hat1, Sas2, Sas3
Cpr1	Set3 complex	Nut1, Taf1

	histone deacetylase complexes

[1]**Reported in the BioGRID DataBase.**

2.3.3.6 Decompacted chromosome segments can undergo polymer-polymer phase separation

Our results provide biochemical evidence for the mechanism by which changes in mechanical properties of the activated *INO1* gene locus is initiated (Bystricky et al., 2004; Verdaasdonk et al., 2013). How then are these changes in mechanical properties consistent with a phase transition that causes partitioning of the *INO1* locus to the NE? Would a change in properties of a single gene locus towards the middle of a chromosome arm cause such narrow localization of the locus to the NE? Phase separation of segments of polymers or polymer-polymer phase separation (PPPS) have been predicted based on Flory-Huggins theory, in which self-interacting ligand molecules occupy multiple sites throughout the polymer (Dormidontova et al., 1992). Phase separation between two segments of the polymer will occur if the density of ligands decreases in one region. The high ligand occupancy region forms a dense phase through the high valency ligand-ligand interactions and the low-density segment forms an expanded, “dilute” phase.

Bead-spring models of chromatin provide the means to explore the physical properties of the chromatin fiber and mechanisms responsible for polymer, including DNA phase separation. For instance, as predicted by Flory-Huggins theory (Flory and Gee, 1956; Huggins, 1942), invoking dynamic chromosome cross-linkers (bound ligand) into a model of the yeast genome recapitulates the segregation and morphology of the nucleolus (Hult et al., 2017). The physical basis for partitioning the *INO1* gene locus extends beyond recruitment to the NE. The radius of confinement and mobility of the locus are decreased, indicating a change in the polymeric state that accompanies its migration to the NE. While we can readily identify transcriptionally active domains relative to DNA sequence, we are just starting to appreciate how gene activity manifests in structural changes at the chromosome level. Active genes can be sequestered into chromosome loops

(topologically associated domains) or into membrane-less compartments (Gibson et al., 2019; Sanulli et al., 2019).

Although Flory-Huggins theory alone can explain segmental phase separation of a polymer as described above (Dormidontova et al., 1992), we also wanted to test if we could reproduce the dynamic behaviors of the *INO1* locus observed experimentally and observe segmental phase separation by including parameters in our bead-spring model that are known to accompany changes in gene expression. One of these parameters is the persistence length of the chromatin fiber. As discussed above, persistence length (L_p) is the length scale over which the polymer tends to remain linear and resist bending (expected value of cosine of angle θ from the horizontal at length L over L_p falls off exponentially according to Equation 2). For the large fraction of non-transcribed chromatin, persistence length measurements range in the hundreds of nanometers. In the case of transcribing gene loci or regions of reduced histone occupancy, these regions have a much shorter persistence length and therefore can explore a greater number of configurations (Chi et al., 2013; Rechendorff et al., 2009; Smith et al., 1996).

$$\langle cos\theta \rangle = e^{-\frac{L}{Lp}} \qquad (2)$$

To simulate the experimental condition of active genes flanked by inactive genes, we tuned the model such that the midsection of beads representing active genes has the lowest bending stiffness, L_p = 5 nm, flanked by sections of inactive chromatin with L_p = 250 nm. The MSD of the 5 nm L_p segment was considerably reduced relative to the 250 nm L_p segment (Figure 2.6 a), recapitulating our experimental observations (Figure 2.2). Likewise, the increase in k_s and reduced R_c of the 5 nm L_p segment further reflect our experimental results (Figure 2.6 b, c). The 5 nm L_p chain collapsed into a much smaller area compared to the 250 nm L_p segments, due to the increase in number of entropic states that they can explore. Consequently, the 5 nm L_p region appears spherical compared to the ellipsoid shape of the 250 nm L_p due to their increased randomness, and

hence increased shape symmetry. The result is that the 250 nm L_p segments show increased frequencies and amplitudes of expansion-contraction compared to the 5 nm L_p (Figure 2.6 d). These behaviors reflect our experimental observations of compression/expansion of the *INO1* locus in repressed *versus* activated states (Figure 2.2 k). Finally, simulations of chain dynamics reveal phase separation of the 5 and 250 nm L_p segments modeling the phase separation observed in the analytical model and in our experimental results for the active *INO1* locus (Supplementary Movie 1).

We can reproduce segmental changes in dynamics and phase separation of a model polymer, we cannot explain the dynamics itself, which are known to be driven by active, ATP-dependent processes that remain obscure, but we model as Brownian dynamics with tuning of temperature (Heun et al., 2001b; Tortora et al., 2020).

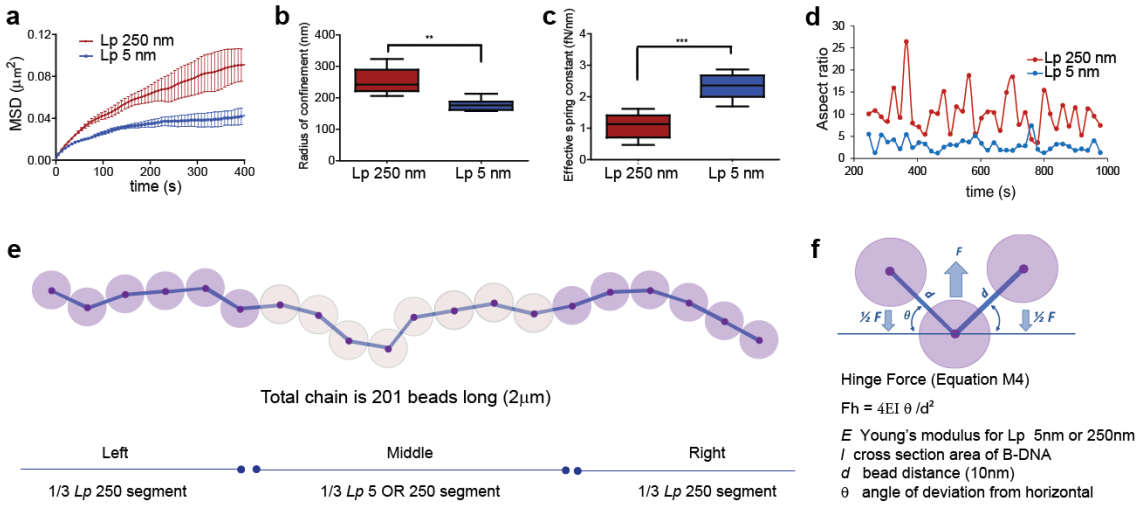

Figure 2.6 Elastic wormlike chain (bead-spring) modeling recapitulates activated (Lp = 5) and repressed (Lp = 250) chromatin

a *Aggregated MSDs for 26-bead subsegment within the high persistence length (L_p = 250 nm) segment represents repressed chromatin (red, n = 5 with SE bars), low persistence length (L_p 5nm) segment represents activated chromatin (blue, n = 6 with SE bars).* ***b, c***

Decreasing L_p to 5 nm reduces the radius of confinement (b) and increases apparent effective spring constant (k_s) for the 26-bead-subsegment by 2-fold (c), consistent with experimental observations in Figure 2.2, b and f. ***d*** *Aspect ratio of modeled fluorescent loci (occupied by the 26-beads) at 38 time points from the simulation averages.* ***e*** *Cartoon illustration of bead-spring model. At 10 nm rest length, springs experience no force. Beads are soft spheres 9 nm diameter that will resist compression via excluded volume force.* ***f*** *Hinge forces applied to beads proportional to varied persistence length will affect bead positions. In the box and whiskers plots* ***b, c****, the median is indicated as middle line, 25th and 75th percentile as boxes and the whiskers represent minimum and maximum values. *p < 0.05; **p < 0.01; ***p < 0.001.*

2.3.4 Discussion

Our results on the mechanics of *INO1* locus chromatin can now be put into molecular terms to explain the partitioning of the active gene to the NE. Recent evidence suggests that liquid-liquid phase separation (LLPS) of histones combines with PPPS of chromatin to form condensates, a potentially important mechanism by which the spatiotemporal organization of the genome can be regulated (Gibson et al., 2019; Sanulli et al., 2019). Specifically, acetylation-deacetylation of the histone tails in nucleosomal arrays has been shown to underlie PPPS in which deacetylated histones induce formation of a protein-DNA condensate and acetylation causes its dissolution (Gibson et al., 2019). We propose that the disruption of histone interactions that occurs due to acetylation in the active *INO1* locus causes it to "dissolve" out of the dense nucleoplasmic chromatin phase into the less dense chromatin phase adjacent to the NE, as predicted previously for a single copolymer chain (Dormidontova et al., 1992).

The increased spring stiffness of the active *INO1* locus we observed in experiments and simulations also have implications for LLPS of proteins associated with sub-compartmentalization of different processes in the nucleus. The contribution of PPPS to formation of chromatin-containing condensates has been considered both theoretically

(Erdel and Rippe, 2018) and most recently, demonstrated both *in vivo* and *in vitro* (Quail et al., 2021; Shin et al., 2018). Quail *et al.* recently showed that LLPS of a transcription factor required it to be bound to DNA in a tension-dependent manner. They presented evidence to support the postulate that less dense DNA forms an ideal template for nucleating LLPS of the bound protein and that protein-DNA co-condensation is associated with the difference in chemical potential of the DNA, as reflected in its difference in spring stiffness. Shin *et al.* observed that light-activated condensates in the nucleus selectively formed in regions of low-density chromatin as observed *in vitro* (Quail et al., 2021; Shin et al., 2018). Ribosomal DNA (rDNA) is another example of this phenomenon. rDNA is essential for the phase separation of the nucleolus (Lawrimore et al., 2021). When rDNA was made discontinuous (rDNA genes were expressed from individual plasmids *versus* genome repeats), nucleolus formation was disrupted upon transcriptional inactivation (Lawrimore et al., 2021). That is, rDNA is a PPPS that relies on transcription to remain phase separated from the bulk genome. Thus, combined protein-DNA LLPS-PPPS of chromatin could facilitate the nucleation of co-condensates that have been associated with transcription and its regulation(Henninger et al., 2021; Sabari et al., 2018), heterochromatin formation (Rudnizky et al., 2021; Strom et al., 2017), nucleolus assembly (Quinodoz and Guttman, 2021) and DNA repair (Pessina et al., 2019).

The work done to sub-compartmentalize the *INO1* and other active gene loci could also be driven by PPPS. Partitioning of the repressed locus into the nucleoplasm phase is driven by transduction of the chemical potential of PPPS into mechanical work on the non-condensed DNA (Quail et al., 2021). The work done in sub-compartmentalizing the active *INO1* locus to the nuclear periphery is simply equal and opposite to that driving condensation. It is also possible that the *INO*1 chromatin could nucleate LLPS of associated proteins combined with PPPS, resulting in a DNA-protein condensate.

The polymer modeling provides critical insight into mechanisms of translocation of the active locus. The means by which the sub-compartment comes to reside at the nuclear

periphery is that it is seeking the most thermodynamically favored state. Chains with self-similar properties tend to segregate as mixing of two chains is thermodynamically disfavored in a confined space, such as the nucleus (Hult et al., 2017; Jun and Mulder, 2006). In the case of the nucleus, segregation of dissimilar chains leads to their migration to the furthest distance from each other, which is the outer edge of the nucleus at the nuclear envelope.

Finally, the ability to partition the genome into discrete domains that transition between physical states, either through multivalent binding of DNA-associated proteins (dense and deformable) or disruption of histone association (dilute but less deformable active subcompartments) could lead to architectural changes that can be understood from the material properties of the components, as we have demonstrated in this study.

2.3.5 Acknowledgements

The authors thank Jason Brickner (Northwestern University), Tom Ellis (Imperial College London), Amine Nourani (Université Laval), Oliver Valerius (Georg-August-University), and Daniel Zenklusen (Université de Montréal) for providing reagents, plasmids and strains. The authors acknowledge support from Canadian Institutes of Health Research (CIHR) grant MOP-GMX-152556 and Human Frontier Science Program grant RGP0034/2017 (S.W.M.); CIHR grant PJT-153313 (M.O.); CIHR grant PJT-162334 (F.R.); and National Institutes of Health grant R37 GM32238 (K.B.).

Authors contributions

Conceptualization: L.G. and S.W.M.; Methodology: L.G., D.K., C.T., C.J.; Investigation: L.G., D.K., C.T., C.J.; Data analysis: L.G., D.K., C.T., C.J., F.R., M.O., K.B., S.W.M.; Writing-review: L.G., D.K., C.T., C.J., F.R., M.O., K.B., S.W.M.

Declaration of interests

The authors declare no competing interests.

2.3.6 Methods

2.3.6.1 Strains and plasmids

The LMY52 strain (Brickner et al., 2012) was used as a control for the statistical mapping and for the gene tracking experiments (provided by Jason Brickner, Northwestern University, USA) (Table S2.1). This strain contains a cassette of 128 repeats of the Lac operator binding site (LacO) into the *INO1* locus and expresses a GFP-Lac repressor (LacI), which binds to the LacO repeats. This strain also expresses the Nuclear Pore Complex (NPC) protein Nup49 fused to GFP and the nucleolar protein Nop1 fused to mCherry as reference markers for the NE and the nucleolus, respectively.

GRS I and II deletion mutants used for the statistical mapping and for the gene tracking experiments were generated in the LMY52 strain by employing a CRISPR-Cas9 based strategy developed by and with reagents provided by Tom Ellis at Imperial College London, UK (Shaw et al., 2019) (Table S2.2). This system consists of a sgRNA entry vector and a range of Cas9-sgRNA expression vectors with different selection markers that are transformed into yeast cells together with donor DNA fragments containing the desired sequence changes. In this case, each sgRNA entry vector (pWS082) was completed using small fragment Golden Gate assembly (Lee et al., 2015) with two 26-mer oligos each containing 20 nucleotide guide sequences selected to target each GRS to be deleted. Once assembled, the plasmid was digested with EcoRV to generate a linear sgRNA expression cassette. This linearized cassette contained homology arms to the Cas9-sgRNA expression vector that served for gap repair of the linearized plasmid in yeast to reconstitute a stable Cas9-sgRNA expression vector. The Cas9-sgRNA expression vector selected for each GRS was also linearized with a BsmBI restriction digest and gel purified. The different markers on each Cas9-sgRNA vector allowed selection for successfully transformed cells expressing both Cas9 under the strong *PGK1* promoter and a sgRNA. Each linear sgRNA expression cassette and the linear Cas9-sgRNA expression vector were transformed into LMY52 together with the corresponding donor sequence consisting of a double stranded

DNA sequence of around 100 bp obtained by synthesizing and annealing mutagenic primers containing the corresponding GRS mutated sites flanked by homology arms to the integration region at the *INO1* locus.

The YAN1001 strain (Rufiange et al., 2007) (Table S2.1) was used as control to measure the incorporation of newly synthesized histone H3 into nucleosomes (provided by Amine Nourani, Université Laval, Canada). In this strain, endogenous genes for histones H3 and H4 are deleted and expressed in two different ways: 1, constitutively from a plasmid, under the control of their own promoter, and 2, from another region in the genome under the control of the *GAL1-10* promoter, with H3 fused to a FLAG tag. This allows to measure incorporation of newly synthesized H3-FLAG into nucleosomes following galactose induction. GRS I and II (GRSI, IIΔ) deletion mutants (Table S2.1) were generated in the YAN1001 by the CRISPR-Cas9 strategy described above.

To measure the effect of rapid depletion of different HATs on active *INO1* localization to the NE, 12 known yeast HAT catalytic subunits were tagged with a degron peptide IAA17 (71/116) that targets the protein for proteasomal degradation in the presence of the plant hormone auxin (Morawska and Ulrich, 2013). First, the *TIR1* gene that mediates the auxin-IAA degradation was integrated into the genome of the LMY52 strain by transformation with the Yeast Integrating plasmid YIp204-PADH1-atTIR1-9myc (Addgene #99532, Table S2.2). This strain was used as background to tag each HAT 3' of the coding sequence to produce C-terminal fusion products with a cassette containing the IAA17 degron sequence as well as six FLAG epitopes amplified from a plasmid generated in a previous study (pHyg–AID*–6FLAG, Table S2.2) (Morawska and Ulrich, 2013). These FLAG tags allowed to verify the efficiency of degradation by Western Blot.

BirA*-dCas9 fusions to identify candidate GRS-binding proteins and specifically, histone acetyl transferases (HATs) were generated based on a previously described Proximity-dependent Biotin Identification (BioID) strategy that was successful in *S. cerevisiae* (Opitz

et al., 2017). The BirA* ligase sequence was provided in a plasmid vector by Oliver Valerius at Georg-August-University, Germany (Table S2.2). dCas9 mutant was first obtained in one of the Cas9-sgRNA expression vectors (pWS174) to introduce the mutations D10A and H840A resulting in a catalytically dead (d)Cas9. Then, by linearizing this vector at the selected fusion site and using the GeneArt Seamless Cloning and Assembly kit (ThermoFisher Scientific), the sequence encoding for BirA* with specific linker sequences (linker 1: GSSGSSGSSGSS or linker 2: LERPPLCWISAEFHHTGLVDPSSVPSLSLNRGSGSGSG) were fused 5' or 3' to the dCas9 gene to produce N-terminal or C-terminal fusion products, respectively. Once we obtained the desired BirA*-dCas9 expression vectors, the same procedure was performed as described above for CRISPR/Cas9 genome editing by transforming both BirA*-dCas9 and sgRNA linearized cassettes into the LMY52 strain to obtain the strains used in this approach (Table S2.1), this time without the need of using any donor DNA sequence. We also transformed the LMY52 strain with the different BirA*-dCas9 expression vectors alone with empty sgRNA cassettes as negative controls for non-targeted biotinylation of proteins.

2.3.6.2 Statistical mapping of the *INO1* locus

Statistical mapping of the *INO1* locus was performed as previously described (Brickner et al., 2012). Briefly, overnight cultures in synthetic, defined medium (SDC) without inositol or SDC containing 100 µM of inositol were diluted to 10^6 cells/mL and after two generations cells were immobilized on Concanavalin A-coated well slides (Malleshaiah et al., 2010). Images were acquired with a Zeiss Axio Observer Z1 Yokogawa spinning disk confocal microscope using a 100 × 1.40 NA oil objective. Z-stacks with a slice spacing of 250 nm were taken at an acquisition time of 50 ms for GFP (50 %, 3 mW 488 nm excitation), and 100 ms for mCherry (50 %, 3.3 mW 561 nm excitation). Images were processed by nucloc software modified to display probability density maps as percentiles using a kernel density estimate (Therizols et al., 2010).

2.3.6.3 Particle tracking of the *INO1* locus

To track the *INO1* locus in live yeast cells, LMY52 and GRS I or II mutant strains containing the gene tagged with the LacO array and expressing GFP-LacI as well as the NE tagged with Nup49-GFP were used. Images of the cells were also recorded on a Zeiss spinning disk Axio Observer Z1 confocal microscope at an acquisition time of 50 ms (50 %, 3 mW 488 nm excitation) for 1 minute at an interval of 500 ms. To check for possible stage-drift the GFP signal was also imaged in fixed cells.

Images of GFP foci corresponding to the *INO1* locus were automatically tracked using the WaveTracer tool in MetaMorph software (Kechkar et al., 2013). The algorithm segments circular objects with a particular size and intensity cut-off and then calculates the centroid position for each object in each frame through Gaussian fitting. For each locus monitored, the software quantifies the movement and calculated mean squared displacement (MSD). Only cells whose MSD curves exhibited a linear slope were included in subsequent analysis.

To calculate the radius of confinement, the MSD plateau values were used in each case since the plateau reached is proportional to the square of R_c, as previously described (Equation M1) (Neumann et al., 2012; Verdaasdonk et al., 2013).

$$R_c = \frac{5}{4}\sqrt{MSD_{plateau}} \quad \text{(M1)}$$

or independently, from the standard deviation of spot positions, σ, and the average squared deviation from the mean position, $\langle \Delta r_0^2 \rangle$, by applying the equipartition theorem (Methods, Equation M2) (Scheffold et al., 2010; Uhlenbeck, 1930; Verdaasdonk et al., 2013).

$$R_c = \frac{5}{4}\sqrt{2\sigma^2 + \langle \Delta r_0^2 \rangle} \quad \text{(M2)}$$

Effective spring constants (k_s) for the *INO1* locus in repressed *versus* activated conditions were determined by using the equipartition theorem to measure the standard deviation (σ) of each step from the mean position to calculate k_s (Equation M3) (Scheffold et al., 2010; Verdaasdonk et al., 2013).

$$k_s = \frac{k_B T}{\sigma^2} \qquad \text{(M3)}$$

Statistical differences for R_c and effective k_s in strains grown under different conditions were determined by Student's t-tests.

To analyze the rate and amplitude of *INO1* locus expansion-contraction, the GFP array was also acquired at same frequency as mentioned before but using a Zeiss Elyra PS.1 system. SIM images were acquired in this case with a 63 × 1.40 NA oil objective in the GFP channel (15 %, 20 mW 488 nm HR diode laser), exposure time 24 ms and 3 rotations. Each locus was then fitted to an ellipsoid function to quantify the ratio between long and short axes by using the Fiji software (Schindelin et al., 2012).

2.3.6.4 Chromatin polymer simulations

An elastic worm-like chain consisting of 201 beads (masses) connected by linear springs was sectored into three equal segments: two flanking segments composed of beads 1-67 and 135-201, and one middle segment with beads 68-134. Initially the chain was homogenized with L_p for all segments set to 250 nm (in n = 5 randomly seeded simulations). In the experimental condition we lowered the L_p for the middle segment to 5 nm (in n = 6, randomly seeded simulations) by adjusting the value of hinge force on the beads. Whenever three beads (or two springs) are not colinear, hinge forces act to restore the positions of the beads to lie on a line (see Figure 2.6, e and f). Hinge forces are based on the Euler-Bernoulli formula (Equation M4), where *E* is Young's modulus, proportional

to polymer's bending stiffness, and is in a linear relationship to persistence length (for more details see methods Lawrimore *et al.* (Lawrimore et al., 2016)). In our approach the Young's modulus (E) in Equation M4 is varied only in calculation of bending stiffness, and does not affect the tensile stiffness of individual DNA springs. Hinge forces were manually set to constant L_p = 250 nm for the flanking segments, and set to either L_p = 250 nm and L_p = 5 nm for the variable middle segment.

$$\mathrm{F}_h = \frac{4EI\,\theta}{d^2} \qquad \text{(M4)}$$

In the simulations we obtain 35,000 timepoints of bead position data (x_t, y_t, z_t) for a duration of 70 ms at 2 μsec resolution. With a working estimate of cellular nuclear viscosity of 141 Pa (Fisher et al., 2009) the model's parameters reflected a fluid environment set to 0.01 Pa allowing a 14,100X speedup of physical time for the simulation. An equilibration time corresponding to 25% of the total trajectories was set to allow for meaningful chain configurations from its starting linear confirmation. To eliminate the effects of drift on the entire chain, we considered individual bead positions relative to bead number 55 within the invariable portion of the chain (L_p 250 nm segments) throughout our analyses. Positions of a center of mass of a 26-bead long subsegment (beads 90 – 115) within the middle segment representing a fluorescent segment (virtual LacO array segment), were tracked for each of 15,000 time intervals (t values) amounting to 35 ms of simulation time (equivalent to 423 sec of real time), and MSD was computed for each independent experiment in MATLAB with *computespotmsd.m* (Equation M5). Average MSD with standard error bars for a spot (26-bead subsegment) within L_p 250 (n = 5) compared to spot within L_p 5 nm (n = 6) chain segments are displayed in Figure 2.6 a.

$$MSD = \langle |x_t - x_o|^2 \rangle \quad \text{(M5)}$$

We computed R_c, for the simulated with Equation M2 (Verdaasdonk et al., 2013).

$$R_c = \frac{5}{4}\sqrt{2\sigma^2 + \langle \Delta r_0^2 \rangle} \quad \text{(M2)}$$

Considering 35 ms of simulation time and using the standard deviation of spot position, σ, and the averaged square deviations from the mean position, $\langle \Delta r_0^2 \rangle$ we compared spatial confinements of L_p 250 nm (n = 5) to L_p 5 nm segments (n = 6). Effective spring constants were estimated by using the standard deviations obtained from simulation's spot positions, σ, as in Equation M3.

$$k_s = \frac{k_B T}{\sigma^2} \qquad \text{(M3)}$$

We used principal component analysis to estimate 2D shapes of simulated fluorescent spots (26-beads) to obtain their aspect ratios. Given averaged bead position data at 38 regularly spaced time intervals we used MATLAB *aspect_ratio.m* to calculate the aspect ratio for the point cloud representing the fluorescent spot (26-bead subsegment) by taking the square root of the ratio of the first principal component's scaling factor over the second.

2.3.6.5 ChIP experiments

(i) Cell cultures and crosslinking

ChIP experiments were performed in four biological replicates. YAN1001 or the corresponding GRS mutant strains were inoculated on 100 mL SDC + 2 % glucose with or without 100 µM inositol medium and incubated until they reached OD_{600} 0.2-0.3. Cells were recovered by centrifugation and switched to 100 mL medium with 2 % raffinose and incubated overnight. In the morning, cell cycle was arrested with 5 mM α-factor for 3.5 hours and inositol was added again to 100 µM inositol final concentration to the repressed cells. Efficient G1 arrest (at least 90 % of cells) was confirmed by microscope as

percentage of cells with shmoo morphology. Cells were collected by centrifugation at 2000 × g, 5 min switched to 2 % galactose medium and incubated for 1 hour. At every step, OD_{600} cells were grown only long enough to reach values of < 0.5, to avoid losing the repressed phenotype.

After 1 hour incubation in galactose, cells were crosslinked with 1 % formaldehyde for 30 minutes with gentle rotation at room temperature. To quench formaldehyde, 2.5 M glycine was added to a final concentration of 125 mM. Crosslinked cells were recovered by centrifugation and washed twice with 25 mL ice cold 1X Tris-buffered saline (TBS: 20 mM Tris, 150 mM NaCl, pH 7.6). Pellets were resuspended in the remaining liquid and transferred to 1.5 mL tubes. Cells were harvested by centrifugation at 2000 × g, 4°C, 5 min, immediately frozen in liquid nitrogen and stored at -80°C until processed.

(ii) Chromatin immunoprecipitation (ChIP) and quantitative PCR (qPCR)

Immunoprecipitation assays were performed as previously described (Jeronimo et al., 2019) with slight modifications. Cells were resuspended in 700 µl of lysis buffer (50 mM HEPES-KOH pH 7.5, 140 mM NaCl, 1 mM EDTA, 1 % Triton X-100, 0.1 % Na-deoxycholate, 1 mM PMSF, 1 mM Benzamidine, 10 µg/mL Aprotinin, 1 µg/mL Leupeptin, 1 µg/mL Pepstatin) and mechanically lysed with glass bead beating. Cells were spun at 5000 × g for 10 seconds and supernatants were transferred to new tubes. Cells were sonicated in a Sonic dismembrator Model 100 equipped with a micro probe (Fisher Scientific), 4 × 20 seconds at output of 7 Watts, with a 1-minute break between sonication cycles. Supernatants containing solubilized chromatin fragments were recovered by centrifugation at 16000 × g, 5 min and transferred to new tubes. An aliquot of 5 µl (1 %) per sample of this whole-cell extract was kept at -20°C to be used as input sample, which represents the amount of chromatin used in the ChIP, usually 1 % of starting chromatin. 500 µl of the remaining material was used for immunoprecipitation (IP). For each IP sample, 50 µl of Dynabeads™ Pan Mouse IgG (ThermoFisher Scientific) pre-coupled to 5

µg of mouse Monoclonal Anti-FLAG M2 antibody (Sigma) was added to the 500 µl of chromatin sample and incubated overnight at 4°C.

Beads were washed twice with Lysis buffer, twice with Lysis buffer 500 (Lysis buffer + 360 mM NaCl), twice with Wash buffer (10 mM Tris-HCl pH 8.0, 250 mM LiCl, 0.5 % NP40, 0.5 % Na-deoxycholate, 1 mM EDTA) and once with TE (10 mM Tris-HCl pH 8.0, 1 mM EDTA). Immunoprecipitated chromatin was eluted and reverse-crosslinked with 50 µL TE/SDS (TE + 1 % SDS) by incubating overnight at 65°C. Input samples were also reverse-crosslinked with 50 µL TE/SDS and incubated overnight at 65°C. Eluted chromatin as well as Input samples were treated with RNase A (345 µL TE, 3 µL 10 mg/mL RNase A, 2 µL 20 mg/mL Glycogen) at 37°C, for 2 hours and subsequently digested with Proteinase K (15 µL 10 % SDS, 7.5 µL 20 mg/mL Proteinase K) at 37°C for 2 hours. Samples were extracted twice with phenol/chloroform/isoamyl alcohol (25:24:1) and precipitated with 200 mM NaCl and 70 % EtOH. Precipitated DNA was resuspended in 50 µL of TE before being used for ChIP-qPCR experiments.

The immunoprecipitated DNA and DNA from 1 % of the Input samples were analyzed by quantitative PCR on a ViiA 7 Real-Time PCR System (Thermo Fisher Scientific) using the PowerUp™ SYBR™ Green Master (Thermo Fisher Scientific). The amount of newly synthesized FLAG-H3 incorporated at the nucleosomes was calculated as the percent of Input using the following formula: $100*2\hat{}(Ct_{Input}-6.644-Ct_{IP})$, Ct being the value where the PCR curve crosses the threshold line above background levels of detection. Subtracting 6.644 from Ct_{Input} allows to adjust for the fact that 1 % of Input was used. In this case since the starting input fraction is 1 %, then a dilution factor of 100 or 6.644 cycles (log_2 of 100) is subtracted from the Ct value of diluted input.

2.3.6.6 HATs depletion using an auxin degron system

All 12 HAT-AID fusion strains (Table S2.1) were generated to rapidly deplete specific HAT activity and the *wild type* cells were cultured in SDC medium without inositol until OD_{600}

0.3. At this point, cultures were split in two and auxin (I2886, Sigma-Aldrich) was added to one of the tubes for each sample to a final concentration of 500 µM. Cells were incubated with auxin for 1 hour 30 minutes followed by immobilization on ConA-coated Nunc 96 well Optical-Bottom plates (164588, ThermoFisher). Imaging and nucloc analysis were performed as previously described(Brickner et al., 2012) for the Statistical Mapping of the *INO1* locus *wild type* and the GRS mutants. Western Blots were performed on HAT-AID fusion strains to verify the degradation of the corresponding HAT once the auxin was added to growth medium.

ChIP-qPCR experiments for H3K14ac and H3 in the AID strains were performed in three biological replicates similarly as described before for the H3-FLAG with modifications for the sample preparation and the IP procedures. In this case, cells were grown in the same conditions as described for the AID experiments before crosslinking. For the IP protocols, 50 ul of Dynabeads™ Protein G beads (ThermoFisher Scientific) pre-coupled to 2µl of rabbit anti-H3K14ac (Millipore) or 2µg of rabbit anti-H3 (Abcam) were used per IP sample.

2.3.6.7 Reverse transcriptase real-time quantitative PCR (RT-qPCR)

Cells were prepared under the same conditions described before for AID and inositol starvation. Total RNA was isolated from yeast cells using TRIzol reagent (Invitrogen) following manufacturer's instructions. Approximately 2 µg of total RNA was reversed transcribed using All-In-One 5X RT MasterMix (abm). qPCR reactions were performed using FastStart Essential DNA Green Master (Roche Diagnostics) and gene expression levels were determined with a LightCycler 96 (software version 1.1). All assays were performed in biological triplicates.

2.3.6.8 dCas9-BioID assays

(i) Cell cultures and streptavidin affinity purification

The protocol for biotinylated proteins purification was modified from Opitz *et al*. (Opitz et al., 2017). LMY52 *wild type* and LMY52-BirA*-dCas9 with or without sgRNA mutants generated (Table S2.3) were inoculated in 4 L of SDC medium without inositol plus D-biotin (B4639, Sigma-Aldrich) added to final concentration of 10 µM. Cells were grown to OD_{600} of 0.8 and harvested by filtration using a Kontes™ Ultra-Ware™ Microfiltration Assembly with Fritted Glass Support (90 mm) and MF-Millipore™ Membrane Filters, 0.45 µm pore size (HAWP0900 Millipore). Pellets were immediately frozen in liquid nitrogen and kept at -80°C. Cell lysis was performed under cryogenic conditions using solid phase milling in a planetary ball mill (Retsch PM 100) producing a fine cell grindate (Oeffinger et al., 2007). Grindate samples were stored at −80°C until processed. Biotinylated proteins were purified using streptavidin-sepharose beads (GE Healthcare, 17-5113-01). For each sample, 0.7 g of crude extract was resuspended in 6.3 ml of buffer A: commercial buffer W (100 mM Tris-Cl, 150 M NaCl, pH 8, 2-1003-100, IBA) containing 0.1 % SDS, 0.5 % Sodium Deoxycholate, and protease inhibitors mixture (cOmplete™, Mini, EDTA-free Protease Inhibitor Cocktail, 11836170001, Roche). Samples were homogenized with a vortex agitator, polytron (PT1200E, for 30 seconds, one time), and incubated at 65°C for 5 minutes in a water bath. Subsequent clarification was performed by two rounds of centrifugation at 2,465 × g, 4°C, 5 minutes, and 20,292 × g, 4°C, 20 minutes, respectively. Triplicates for each sample were prepared; clear extracts were incubated with 30 µl of beads previously equilibrated with buffer A. Samples with beads were incubated for 3 hours at 4°C and gentle mixing (VWR® Nutating Mixer). Beads were washed with buffer A and transferred to 1.5 ml Protein LoBind tubes (Eppendorf, 0030108422) and three consecutive washes with buffer A were performed, followed by four quick washes with 50 mM Ammonium Bicarbonate pH 8 (ABC). 30 µL of 50 mM ABC pH 8 containing 6 mM fresh DTT were added to each tube followed by 30 minutes incubation at 37°C with gentle agitation in a ThermoMixer (Eppendorf) at 350 rpm. Samples were spun quickly and 5ul

IAA 126 mM dissolved in ABC 50 mM pH 8 were added to each tube and incubated for another 30 minutes in the dark at room temperature. Tubes were quickly spun again and 5 µl Trypsin/LysC Mix (Promega, V5073) dissolved in ABC 50 mM pH 8 at 200 ng/µl were added to each one. Samples were digested on-beads overnight at 37°C, 350 rpm. The next day, after a quick spin, 60 µl of MS grade H_2O were added to the beads, mixed, and centrifuged at low speed (1 min, 400 × g). 80 µl of the peptides digests were transferred to new labeled Protein LoBind tubes before adding formic acid (FA) to a final concentration of 4 % v/v. The peptides were dried in a SpeedVac at room temperature and then stored at −80°C.

(ii) Mass spectrometry and data analysis

Samples were resuspended in 11 µl of 2 % acetonitrile (ACN) and 1 % FA containing 0.5X of iRT standard peptides (Biognosys, Ki-3002-1), of which, 2 µl of each sample was further diluted 1/5 in the same buffer. Diluted samples were loaded (2.5 µl each) at 450 nL/min on a 17 cm × 75 µm i.d. PicoFrit fused silica capillary column (New Objective), packed in-house with Jupiter 5 µm C18 300 Å (Phenomenex). The column was mounted in an Easy-nLC II system (Proxeon Biosystems) and coupled to an Orbitrap Fusion mass spectrometer (ThermoFisher Scientific) equipped with a Nanospray Flex Ion source (Proxeon Biosystems). Peptides were eluted at a flow rate of 250 nL/min on 2-slope gradient made with 0.2 % FA in water (buffer A) and 0.2 % FA in 100 % ACN (buffer B). Concentration of buffer B first increased from 2 % to 36 % over 105 minutes, and from 36 % to 80 % over 12 minutes. The mass spectrometer was operated in data-independent acquisition mode. Full MS scans in the range of 400-1000 m/z range were acquired in the Orbitrap at a resolution of 120 K. Each full scan was followed by 25 MS2 acquisition windows with 24 m/z increments and 0.5 m/z overlaps, covering each full scan. Matching MS2 m/z window precursor ions were fragmented by HCD at a 30 % collision energy and acquired in the Orbitrap at a 30 K resolution. Both MS and MS2 AGC target were set to 4e5 with maximum fill times of 60 ms. The lock mass option (lock mass: m/z 371.101233) was used for internal

calibration. MS RAW files were analyzed with Spectronaut v15.1.210713 (Biognosys) by directDIA. The Fasta database was downloaded from Uniprot and consisted of all Saccharomyces cerevisiae S288c verified nuclear proteins entries (1749). Considered peptide length for Pulsar search was 6-52 amino acids with two missed cleavages tolerance, using the semi-specific Trypsin/P rules. Carbamidomethylation of cysteines was set as fixed modifications while oxidation of methionines, protein N-termini acetylation, biotinylation of lysines and protein N-termini as well as phosphorylation (STY) were set as variable modifications, with a maximum of five. Peptide spectrum match, peptides, and protein group FDR were set at 0.01. Machine learning was applied per run and both precursor and protein were identified at a Qvalue cutoff of 0.01. Proteins were quantified at the MS2 level on stripped peptide median qucas9ties. Unique peptides were used for quantification. Only proteins for which values from all biological triplicates were measured in the sgRNA-BirA*-dCas9 were kept for quantification, and no values were imputed during the analysis. The resulting protein datasets were crosschecked with a list of chromatin and transcription related proteins obtained from Uniprot (Table S2.8). The protein list and associated ontologies was built from searches using the keyword chromatin (461 reviewed entries), and transcription (1211 reviewed entries) in *S. cerevisiae*. After merging both lists and removing duplicates, 1320 entries remained (Table S2.9). A two-sided unpaired Student's t-test with equal variance was used to help in the evaluation of significant protein enrichment from sgRNA-BirA*-dCas9 triplicates. Analyses of evidence for association of chromatin remodeling subunits with nuclear protein complexes was performed for all significant candidates with definitions of subunit compositions of protein complexes taken from the Saccharomyces Genome Database (SGD) (Cherry et al., 2012) and UniProt (The UniProt, 2021), and protein-protein interactions were identified in The Biological General Repository for Interaction Datasets (BioGrid) (Oughtred et al., 2021). For representation clarity, proteins having a log2 fold change above 2.5 were limited at the 2.5 value on MA plots (Figure 2.5). We removed two sgRNA-BirA*-dCas9 samples out of a total of 4 because they did not reveal significant fold changes for many or most of the candidates that were identified in the samples kept for

further analysis. Both MA and box plots were made in RStudio (v2022.07.2) using the ggplot2 package (v3.3.6). Data are available via ProteomeXchange with identifier PXD029913. Project Name: Adaptive partitioning of the *INO1* locus to the nuclear envelope is driven by polymer-polymer phase separation. Project accession: PXD029913. Project DOI: Not applicable

Reviewer account details:

Username: reviewer_pxd029913@ebi.ac.uk<mailto:reviewer_pxd029913@ebi.ac.uk>

Password: NFJ2V4Et

Data Availability

Mass spectrometric data are publicly available *via* ProteomeXchange. Project accession: PXD029913. Project DOI: Not applicable. Reviewer account details: Username: reviewer_pxd029913@ebi.ac.uk<mailto:reviewer_pxd029913@ebi.ac.uk>.

The data supporting the results presented in this work are available in the main article and the supplementary information. Any additional information is available upon request from the corresponding author. Source data are provided with this paper.

Code Availability

All original code for matlab methods specifically referenced in the text are accessible in a GitHub repository publicly available: https://github.com/kolbincode/INO1-paper. DOI: 10.5281/zenodo.7492891.

2.3.7 Supplementary information

Figure S 2.1

INO1 and proximal loci positions in chromosome X*. Black bars indicate positions where the incorporation of newly synthesized FLAG-H3 into nucleosomes was measured by ChIP-qPCR assays.*

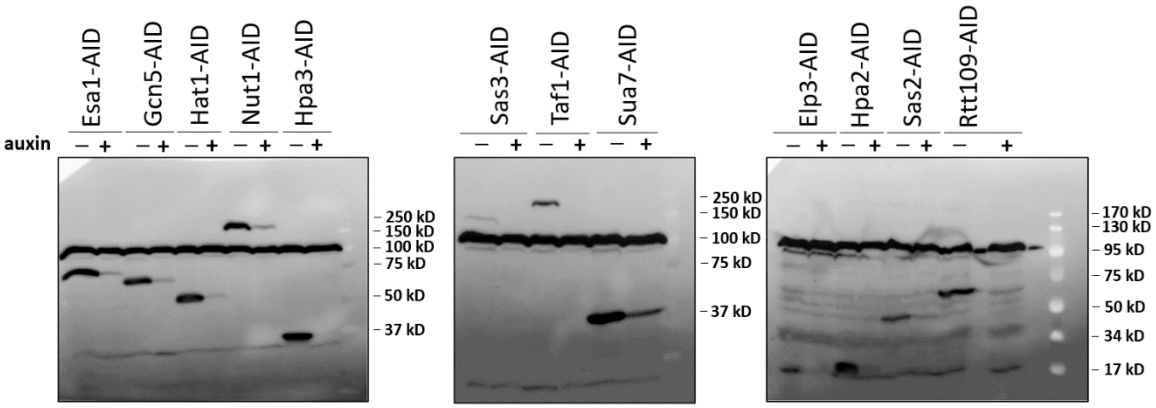

Figure S 2.2

Detection of HATs-AID*-6FLAG proteins in the presence and absence of auxin*. Protein levels of 12 different HATs carrying a C-terminal AID* tag extended by a FLAG epitope, analyzed by western blotting with an anti-Flag M2 antibody. Where indicated, cultures were treated with 500 µM auxin for 1 h 30 min before preparation of the lysates.*

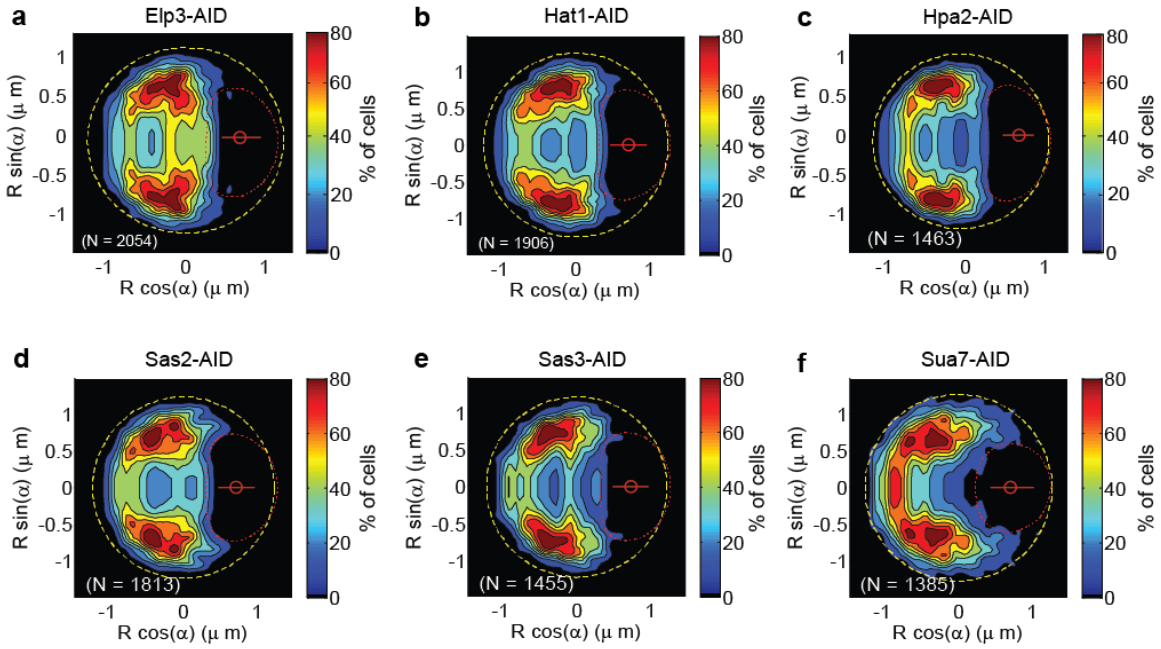

Figure S 2.3

Statistical distribution of the INO1 locus in strains expressing different HAT-AID grown in the absence of inositol (active) and after treating the cells with auxin. a-f *INO1 locus probability maps after nucloc software analysis of thousands of nuclei per strain.*

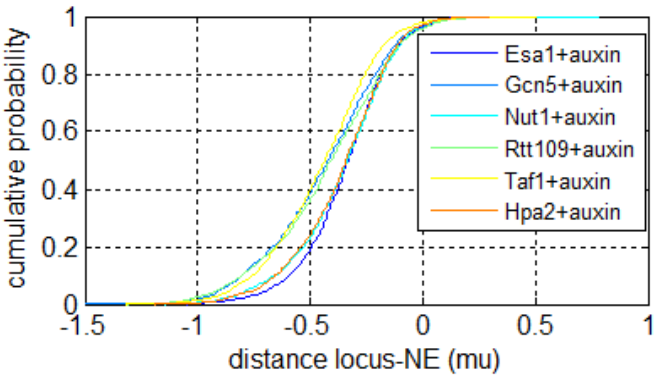

Figure S 2.4

Cumulative distributions of distances to the nuclear envelope for the active INO1 locus in six auxin-induced histone deacetylase degradation strains. *Distributions shifted closer to 0 µm indicate that active loci are closer to the nuclear envelope.*

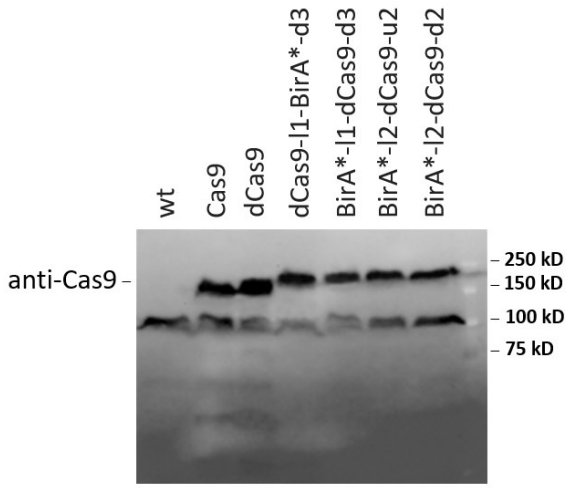

Figure S 2.5

Detection of different Cas9 and BirA*-dCas9 fusions in yeast strains*. Protein levels of Cas9, dCas9 and different BirA*-dCas9 fusions with BirA* in different N- or C-terminal positions and using short or long linker sequences, examined by western blotting with a mouse monoclonal Cas9 antibody 7A9-3A3 (Santa Cruz Biotechnology).*

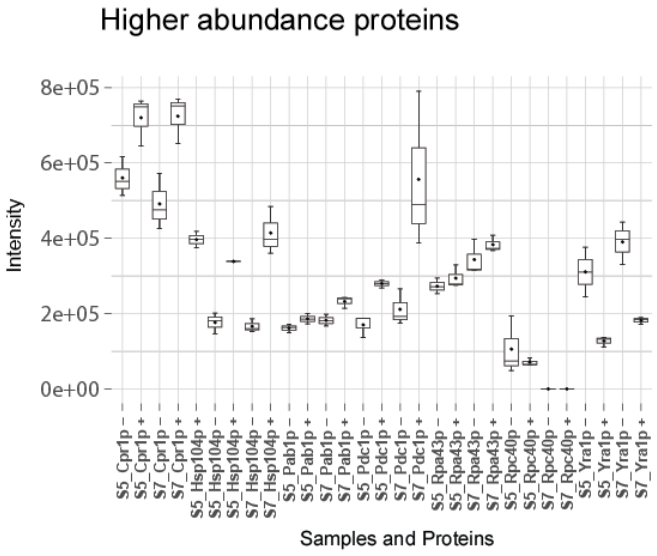
Higher abundance proteins
Intensity
8e+05
6e+05
4e+05
2e+05
0e+00
Samples and Proteins

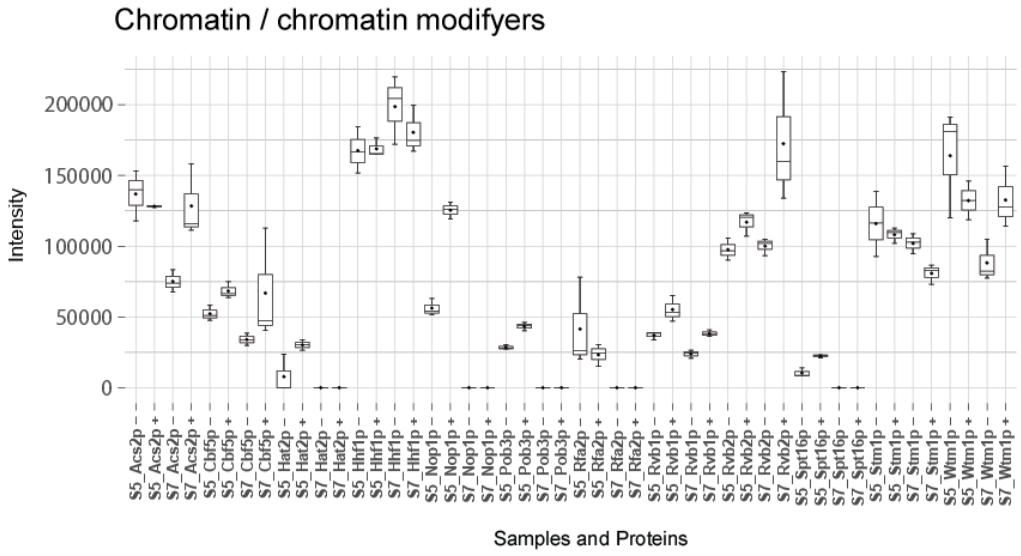
Chromatin / chromatin modifyers
Intensity
200000
150000
100000
50000
0
Samples and Proteins

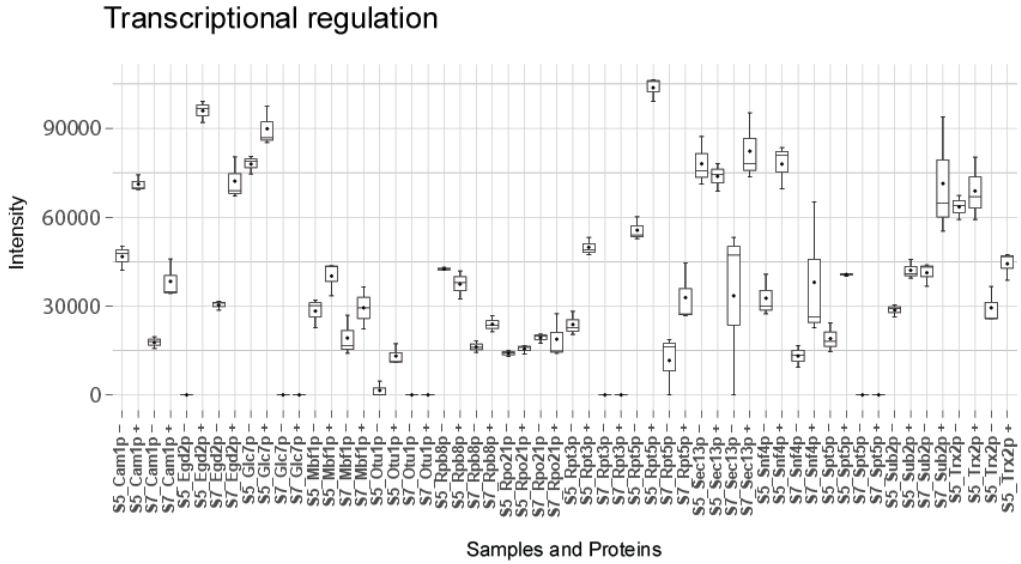
Transcriptional regulation
Intensity
90000
60000
30000
0
Samples and Proteins

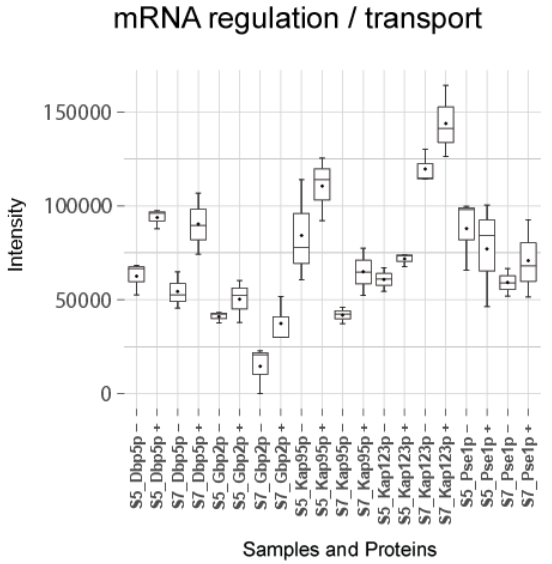
mRNA regulation / transport
Intensity
150000
100000
50000
0
Samples and Proteins

Figure S 2.6

Box plots of proteins intensities measured by MS for all proteins related to chromatin or transcription meeting quantification criteria. *Purified protein measurements from biological triplicates expressing either gRNAs-BirA*-dCas9 (S5 and S7; +) along with their respective BirA*-dCas9 negative controls (S5 and S7; -) are shown side by side. Median is indicated as middle line, average as a black dot, 25th and 75th percentile as boxes and whiskers represent 5th and 95th percentile. For plotting, proteins were grouped by function, and proteins with significantly higher abundance compared to their corresponding group were plotted separately. See also Tables S2.6-S2.8.*

Table S 2.1 Yeast strains used in this study

Strain	Genotype	Reference
LMY52	*MAT***a** *ade2-1 can1-100 his3-11,15::LacI-GFP:HIS3 leu2-3,112 trp1-1 ura3-1 INO1:LacO128:URA3 SEC63-13myc::kan^r ADE2:Nup49GFP_Nop1RFP*	Brickner et al.(Brickner et al., 2012)
JBY397	*MAT***a** *ade2-1 can1-100 his3-11,15::LacI-GFP:HIS3 leu2-3,112 trp1-1 ura3-1 INO1:LacO128:URA3 SEC63-13myc::kan^r*	Brickner et al.(Brickner and Walter, 2004)
ML1	*MAT***a** *ade2-1 can1-100 his3-11,15::LacI-GFP:HIS3 leu2-3,112 trp1-1 ura3-1 INO1:LacO128:URA3 SEC63-13myc::kan^r ADE2:Nup49GFP_Nop1RFP grsIΔ* pWS171-sgRNA-GRSI	This study
ML2	*MAT***a** *ade2-1 can1-100 his3-11,15::LacI-GFP:HIS3 leu2-3,112 trp1-1 ura3-1 INO1:LacO128:URA3 SEC63-13myc::kan^r ADE2:Nup49GFP_Nop1RFP grsIIΔ* pWS171-sgRNA-GRSII	This study
ML3	*MAT***a** *ade2-1 can1-100 his3-11,15::LacI-GFP:HIS3 leu2-3,112 trp1-1 ura3-1 INO1:LacO128:URA3 SEC63-13myc::kan^r ADE2:Nup49GFP_Nop1RFP grsIΔ-grsIIΔ* pWS171-sgRNA-GRSI pWS175-sgRNA-GRSII	This study
YAN1001	*MAT***a** *ura3-52::HHF1-*p*GAL1/10-* Flag-*HHT1-URA3 lys2-801 his3*Δ*200 leu2*Δ*1 hht1-hhf1*::*LEU2 hht2-hhf2*::HIS3 *trp1*Δ*63 bar1*Δ*::NATMX4* /pNOY 439 [CEN6 ARS4-TRP1 *HHF2* MYC-*HHT2*]	Rufiange et al.,(Rufiange et al., 2007)
ML4	*MAT***a** *ura3-52::HHF1-*p*GAL1/10-* Flag-*HHT1-URA3 lys2-801 his3*Δ*200 leu2*Δ*1 hht1-hhf1*::*LEU2 hht2-hhf2*::HIS3 *trp1*Δ*63 bar1*Δ*::NATMX4* /pNOY 439 [CEN6 ARS4-TRP1 *HHF2* MYC-*HHT2*] *grsIΔ* pWS175-sgRNA-GRSI	This study
ML5	*MAT***a** *ura3-52::HHF1-*p*GAL1/10-* Flag-*HHT1-URA3 lys2-801 his3*Δ*200 leu2*Δ*1 hht1-hhf1*::*LEU2 hht2-hhf2*::HIS3 *trp1*Δ*63 bar1*Δ*::NATMX4* /pNOY 439 [CEN6 ARS4-TRP1 *HHF2* MYC-*HHT2*] *grsIIΔ* pWS175-sgRNA-GRSII	This study
ML6	*MAT***a** *ura3-52::HHF1-*p*GAL1/10-* Flag-*HHT1-URA3 lys2-801 his3*Δ*200 leu2*Δ*1 hht1-hhf1*::*LEU2 hht2-hhf2*::HIS3 *trp1*Δ*63 bar1*Δ*::NATMX4* /pNOY 439 [CEN6 ARS4-TRP1 *HHF2* MYC-*HHT2*] *grsIΔ-grsIIΔ* pWS175-sgRNA-GRSI pWS175-sgRNA-GRSII	This study
ML7	*MAT***a** *ade2-1 can1-100 his3-11,15::LacI-GFP:HIS3 leu2-3,112 trp1-1 ura3-1 INO1:LacO128:URA3 SEC63-13myc::kan^r ADE2:Nup49GFP_Nop1RFP* pWS174	This study

ML8	*MAT***a** *ade2-1 can1-100 his3-11,15::LacI-GFP:HIS3 leu2-3,112 trp1-1 ura3-1 INO1:LacO128:URA3 SEC63-13myc::kan^r ADE2:Nup49GFP_Nop1RFP* pWS174-dCa9	This study
ML9	*MAT***a** *ade2-1 can1-100 his3-11,15::LacI-GFP:HIS3 leu2-3,112 trp1-1 ura3-1 INO1:LacO128:URA3 SEC63-13myc::kan^r ADE2:Nup49GFP_Nop1RFP* pWS174-dCas9-l1-BirA*	This study
ML10	*MAT***a** *ade2-1 can1-100 his3-11,15::LacI-GFP:HIS3 leu2-3,112 trp1-1 ura3-1 INO1:LacO128:URA3 SEC63-13myc::kan^r ADE2:Nup49GFP_Nop1RFP* pWS174-BirA*-l1-dCas9	This study
ML11	*MAT***a** *ade2-1 can1-100 his3-11,15::LacI-GFP:HIS3 leu2-3,112 trp1-1 ura3-1 INO1:LacO128:URA3 SEC63-13myc::kan^r ADE2:Nup49GFP_Nop1RFP* pWS174-BirA*-l2-dCas9	This study
ML12	*MAT***a** *ade2-1 can1-100 his3-11,15::LacI-GFP:HIS3 leu2-3,112 trp1-1 ura3-1 INO1:LacO128:URA3 SEC63-13myc::kan^r ADE2:Nup49GFP_Nop1RFP* pWS174-dCas9-l1-BirA*-d3	This study
ML13	*MAT***a** *ade2-1 can1-100 his3-11,15::LacI-GFP:HIS3 leu2-3,112 trp1-1 ura3-1 INO1:LacO128:URA3 SEC63-13myc::kan^r ADE2:Nup49GFP_Nop1RFP* pWS174-BirA*-l1-dCas9-d3	This study
ML14	*MAT***a** *ade2-1 can1-100 his3-11,15::LacI-GFP:HIS3 leu2-3,112 trp1-1 ura3-1 INO1:LacO128:URA3 SEC63-13myc::kan^r ADE2:Nup49GFP_Nop1RFP* pWS174-BirA*-l2-dCas9-u2	This study
ML15	*MAT***a** *ade2-1 can1-100 his3-11,15::LacI-GFP:HIS3 leu2-3,112 trp1-1 ura3-1 INO1:LacO128:URA3 SEC63-13myc::kan^r ADE2:Nup49GFP_Nop1RFP* pWS174-BirA*-l2-dCas9-d2	This study
ML16	*MAT***a** *ade2-1 can1-100 his3-11,15::LacI-GFP:HIS3 leu2-3,112 trp1-1::ADH1-AtTIR1^{9myc}:TRP1 ura3-1 INO1:LacO128:URA3 SEC63-13myc::kan^r ADE2:Nup49GFP_Nop1RFP*	This study
ML17	*MAT***a** *ade2-1 can1-100 his3-11,15::LacI-GFP:HIS3 leu2-3,112 trp1-1::ADH1-AtTIR1^{9myc}:TRP1 ura3-1 INO1:LacO128:URA3 SEC63-13myc::kan^r ADE2:Nup49GFP_Nop1RFP ELP3$^{AID*-6FLAG::HygR}$*	This study
ML18	*MAT***a** *ade2-1 can1-100 his3-11,15::LacI-GFP:HIS3 leu2-3,112 trp1-1::ADH1-AtTIR1^{9myc}:TRP1 ura3-1 INO1:LacO128:URA3 SEC63-13myc::kan^r ADE2:Nup49GFP_Nop1RFP ESA1$^{AID*-6FLAG::HygR}$*	This study

ML19	*MAT***a** *ade2-1 can1-100 his3-11,15::LacI-GFP:HIS3 leu2-3,112 trp1-1::ADH1-AtTIR1^{9myc}:TRP1 ura3-1 INO1:LacO128:URA3 SEC63-13myc::kan^{r} ADE2:Nup49GFP_Nop1RFP GCN5$^{AID*-6FLAG::HygR}$*	This study
ML20	*MAT***a** *ade2-1 can1-100 his3-11,15::LacI-GFP:HIS3 leu2-3,112 trp1-1::ADH1-AtTIR1^{9myc}:TRP1 ura3-1 INO1:LacO128:URA3 SEC63-13myc::kan^{r} ADE2:Nup49GFP_Nop1RFP HAT1$^{AID*-6FLAG::HygR}$*	This study
ML21	*MAT***a** *ade2-1 can1-100 his3-11,15::LacI-GFP:HIS3 leu2-3,112 trp1-1::ADH1-AtTIR1^{9myc}:TRP1 ura3-1 INO1:LacO128:URA3 SEC63-13myc::kan^{r} ADE2:Nup49GFP_Nop1RFP HPA2$^{AID*-6FLAG::HygR}$*	This study
ML22	*MAT***a** *ade2-1 can1-100 his3-11,15::LacI-GFP:HIS3 leu2-3,112 trp1-1::ADH1-AtTIR1^{9myc}:TRP1 ura3-1 INO1:LacO128:URA3 SEC63-13myc::kan^{r} ADE2:Nup49GFP_Nop1RFP HPA3$^{AID*-6FLAG::HygR}$*	This study
ML23	*MAT***a** *ade2-1 can1-100 his3-11,15::LacI-GFP:HIS3 leu2-3,112 trp1-1::ADH1-AtTIR1^{9myc}:TRP1 ura3-1 INO1:LacO128:URA3 SEC63-13myc::kan^{r} ADE2:Nup49GFP_Nop1RFP NUT1$^{AID*-6FLAG::HygR}$*	This study
ML24	*MAT***a** *ade2-1 can1-100 his3-11,15::LacI-GFP:HIS3 leu2-3,112 trp1-1::ADH1-AtTIR1^{9myc}:TRP1 ura3-1 INO1:LacO128:URA3 SEC63-13myc::kan^{r} ADE2:Nup49GFP_Nop1RFP RTT109$^{AID*-6FLAG::HygR}$*	This study
ML25	*MAT***a** *ade2-1 can1-100 his3-11,15::LacI-GFP:HIS3 leu2-3,112 trp1-1::ADH1-AtTIR1^{9myc}:TRP1 ura3-1 INO1:LacO128:URA3 SEC63-13myc::kan^{r} ADE2:Nup49GFP_Nop1RFP SAS2$^{AID*-6FLAG::HygR}$*	This study
ML26	*MAT***a** *ade2-1 can1-100 his3-11,15::LacI-GFP:HIS3 leu2-3,112 trp1-1::ADH1-AtTIR1^{9myc}:TRP1 ura3-1 INO1:LacO128:URA3 SEC63-13myc::kan^{r} ADE2:Nup49GFP_Nop1RFP SAS3$^{AID*-6FLAG::HygR}$*	This study
ML27	*MAT***a** *ade2-1 can1-100 his3-11,15::LacI-GFP:HIS3 leu2-3,112 trp1-1::ADH1-AtTIR1^{9myc}:TRP1 ura3-1 INO1:LacO128:URA3 SEC63-13myc::kan^{r} ADE2:Nup49GFP_Nop1RFP SUA7$^{AID*-6FLAG::HygR}$*	This study
ML28	*MAT***a** *ade2-1 can1-100 his3-11,15::LacI-GFP:HIS3 leu2-3,112 trp1-1::ADH1-AtTIR1^{9myc}:TRP1 ura3-1 INO1:LacO128:URA3 SEC63-13myc::kan^{r} ADE2:Nup49GFP_Nop1RFP TAF1$^{AID*-6FLAG::HygR}$*	This study

Table S 2.2 Plasmids used in this study

Plasmid	Description	Reference
pWS082	sgRNA entry vector	Addgene 90516, Shaw *et al*. (Shaw et al., 2019)
pWS082-GRSI	sgRNA GRSI	This study
pWS082-GRSII	sgRNA GRSII	This study
pWS171	Cas9 gap repair vector - LEU2	Addgene 90518, Shaw *et al.* (Shaw et al., 2019)
pWS175	Cas9 gap repair vector - Hyg^R	Addgene 90962, Shaw *et al.* (Shaw et al., 2019)
pWS174	Cas9 gap repair vector - Nat^R	Addgene 90961, Shaw *et al.* (Shaw et al., 2019)
pME4478	ASC1-birA*	Opitz *et al.,* (Opitz et al., 2017)
pWS082-GRSI-u2	sgRNA GRSI upstream 2	This study
pWS082-GRSI-d2	sgRNA GRSI downstream 2	This study
pWS082-GRSI-d3	sgRNA GRSI downstream 3	This study
pWS174-dCas9	dCas9 vector – Nat^R	This study
pWS174-dCas9-l1-BirA*	dCas9 vector – Nat^R C-terminal fused by linker 1 to BirA*	This study
pWS174-BirA*-l1-dCas9	dCas9 vector – Nat^R N-terminal fused by linker 1 to BirA*	This study
pWS174-BirA*-l2-dCas9	dCas9 vector – Nat^R N-terminal fused by linker 2 to BirA*	This study
YIp204-PADH1-atTIR1-9myc	F-box protein TIR1-9myc (for use with the AID degron system)	Addgene 99532, unpublished Ulrich lab
pHyg–AID*–6FLAG	C-terminal AID*-6FLAG degron cassette - Hyg^R	Morawska and Ulrich (Morawska and Ulrich, 2013)

Table S 2.3 Samples used for mass spectrometry analysis

Sample	Name	Description	Controls correspondence
S2	BirA*-l1-dCas9	BirA* N-terminal to dCas9, short linker	Negative for sample S7
S3	BirA*-l2-dCas9	BirA* N-terminal to dCas9, long linker	Negative for samples S5, S6
S4	dCas9-l1-BirA*	BirA* C-terminal to dCas9, short linker	Negative for sample S8
S5	BirA*-l2-dCas9-u2	BirA* N-terminal to dCas9, long linker, guide u2 (24bp upstream GRSI site)	
S6	BirA*-l2-dCas9-d2	BirA* N-terminal to dCas9, long linker, guide d2 (35bp downstream GRSI site)	
S7	BirA*-l1-dCas9-d3	BirA* N-terminal to dCas9, short linker, guide d3 (15bp downstream GRSI site)	
S8	dCas9-l1-BirA*-d3	BirA* C-terminal to dCas9, short linker, guide d3 (15bp downstream GRSI site)	

Table S 2.4 (separate file)

Raw Spectronaut output of the mass spectrometry analysis between biological triplicates of BirA*-l2-dCas9-u2 (samples S5) and corresponding negative controls BirA*-l2-dCas9 (samples S3).

Table S 2.5 (separate file)

Raw Spectronaut output of the mass spectrometry analysis between biological triplicates of BirA*-l1-dCas9-d3 (samples S7) and corresponding negative controls BirA*-l1-dCas9 (samples S2).

Table S 2.6 (separate file)

Protein candidates meeting quantification requirements as described in the mass spectrometry method section for samples 5 and 3 biological triplicates, along with their intensities, average intensities, standard deviations, variation coefficients, fold changes, and associated p-values.

Table S 2.7 (separate file)

Protein candidates meeting quantification requirements as described in the mass spectrometry method section for samples 7 and 2 biological triplicates, along with their intensities, average intensities, standard deviations, variation coefficients, fold changes, and associated p-values.

Table S 2.8 (separate file)

Protein candidates list from both mass spectrometry datasets matching the Uniprot chromatin and transcription related proteins list, along with their ontologies.

Table S 2.9 (separate file)

Uniprot search output of chromatin and transcription related proteins in *S. cerevisiae*, along with their ontologies.

Supplementary Movie 1. ChromoShake simulation of 2um heterogeneous DNA chain.

Related to Figure 2.5. This video shows a single run of ChromoShake simulation for 2µm of DNA modeled as a bead-springs polymer with regions of heterogenous persistence length. Simulation begins with an extended linear polymer chain that quickly collapses to an equilibrium conformation due to thermal fluctuations and inherent (modelled) physical parameters. The stiffer segments of persistence length 250 nm are flanking the wigglier middle segment, which has persistence length of 5 nm and contains a highlighted region (green beads) to which all the statistical analyses in this paper (MSDs, spring constants, radii of gyration, and aspect ratio) are applied. Positions of blue beads are used for reference only and are not included in the statistical calculation.

Chapitre 3 Retro-evolutionary engineering of budding yeast chromatin decreases global mutation and recombination rate

3.1 Context of the research

Heterochromatin constitutes a well-known example of chromatin organization that regulates genome function in different ways. Several recent studies have demonstrated that compact heterochromatin domains form through LLPS, highlighting the importance of chromatin material properties to defining nuclear organization, and consequently function. *S. cerevisiae* and other budding yeast species have a less compact genome due to the loss during evolution of histone H3 K9 methylation and associated binding to the chromodomain-containing homolog of the protein HP1. To understand the implications of genome compaction in *S. cerevisiae*, we have analyzed the effects of expressing the *S. pombe* HP1 homolog *Sp*Swi6 and H3 K9 methyltransferase *Sp*Clr4. We measured global compaction of the chromatin and nuclear architecture, observing significantly increased compaction, compression of nuclear morphology, likely due to contraction of chromosomes arms, and decreases in chromatin effective spring stiffness and confinement, consistent with increased compaction. Finally, we observed significantly reduced mutation and meiotic recombination rates.

3.2 Authors contributions

For this study, S.W.M. and L.G. conceptualized and designed the study. L.G. generated all the strains employed in all the different assays. L.G. performed and analyzed the chromatin compaction and nuclear morphology measurements, the statistical mapping, the particle tracking assays and all the mutation rate measurements and sequencing analysis. For the recombination rate measurements, L.G. performed the sporulation assays and participated in the flow cytometry analysis done by the facility manager. S.W.M and L.G. wrote the manuscript.

Article 2. Retro-evolutionary engineering of budding yeast chromatin decreases global mutation and recombination rate

Authors: Lidice González[1], Stephen W. Michnick[1]*

[1]Département de Biochimie, Université de Montréal ; C.P. 6128, Succursale centre-ville, Montréal, Québec H3C 3J7, Canada.

* Corresponding author. Email: stephen.michnick@umontreal.ca

3.3 Text of the article

3.3.1 Abstract

Chromatin compaction defines genome topology, evolution, and function. The Saccharomycotina subphylum, including the bread fermenting yeast *Saccharomyces cerevisiae* have a decompacted genome, possibly because they lost two genes mediating a specific histone lysine methylation and histone binding protein heterochromatin protein 1 (HP1) (Hickman et al., 2011; Lomberk et al., 2006). The decompaction caused accelerated speciation, perhaps due to increased mutation and meiotic recombination rates. To test this hypothesis, we retro-engineered *S. cerevisiae* to compact the genome by expressing the HP1 homologue of *Schizosaccharomyces pombe Sp*Swi6 and H3K9 methyltransferase *Sp*Clr4. The resulting mutant had significantly more compact and relaxed chromatin and point and insertion/deletion mutations, and meiotic recombination rates were all significantly reduced. These results may reflect how organisms in this subphylum evolved to become such important models and tools for biotechnology and synthetic biology. The resulting strain may be valuable for maintaining metabolically engineered strains that are prone to losses of activities due to genetic instability.

3.3.2 Introduction

DNA compaction is essential to control genome organization and expression. Well known examples of chromatin organization comprise the existence of chromosome territories as well as the separation into domains of transcriptionally active and repressed regions, including the compartmentalization of the ribosomal DNA genes (Cremer and Cremer, 2001). By quantifying the interactions between genomic loci that are close in 3D space with Hi-C experiments, it has been possible to observe the presence of other structural elements such as the topologically associating domains (TADs) (Dekker et al., 2002; Duan et al., 2010; Lieberman-Aiden et al., 2009). These domains, found in many organisms and ranging from hundreds of kilobases to several megabases in length, are believed to constitute regulatory regions defined by specific contacts between different DNA elements to form enhancers, promoters, and heterochromatin components among others (Crane et al., 2015; Dong et al., 2017; Dong et al., 2018; Lieberman-Aiden et al., 2009; Sexton et al., 2012). All this evidence suggests that chromatin compaction is essential for eukaryotic cell genome regulation.

The formation of heterochromatin domains regulates genome organization in different ways, for instance, by modulating gene expression and changing the physico-chemical properties of the nucleoplasm (Allshire and Madhani, 2018; Stephens et al., 2018). A well characterized and abundant type of heterochromatin in eukaryotes contains the heterochromatin protein 1 (HP1), a chromodomain-containing protein that binds histone H3 methylated on lysine 9 (H3K9me) among other components (Bannister et al., 2001; Nakayama et al., 2001; Sanulli et al., 2019; Stewart et al., 2005). This mechanism of heterochromatin formation is well conserved in most eukaryotic organisms (Mizuguchi et al., 2015). Furthermore, it was recently demonstrated that the *Schizosaccharomyces pombe* (*S. pombe*) homologue of HP1, *Sp*Swi6 induces self-association and compaction of nucleosome arrays and undergoes phase separation to form high density chromatin droplets (Sanulli et al., 2019).

Some eukaryotes, however, have little such genomic organization. Fungi of the Ascomycota subphylum Saccharomycotina lack the lysine 9-methylated histone H3 form of eukaryotic heterochromatin, resulting in mostly decompacted chromatin (Hickman et al., 2011; Lomberk et al., 2006). This occurred because of loss of the ancestral genes encoding the present day *Schizosaccharomyces pombe Sp*Clr4 (H3K9 methyltransferase), and *Sp*Swi6 about 300 million years ago (Figure 3.1 a). For instance, the fermenting yeast *Saccharomyces cerevisiae* (*S. cerevisiae*) does not form compact structures in interphase or mitosis, which is consistent with the fact that most of its genes are in an open configuration and either actively transcribed or primed to be rapidly induced (Chen et al., 2016; Grunstein and Gasser, 2013). Hi-C experiments in this organism have not revealed TAD structures (Duan et al., 2010), although more recent results obtained with Micro-C techniques showed the presence of much shorter self-associating regions with an approximate size of 5 kb (Hsieh et al., 2015). Additionally, the presence of heterochromatin in budding yeast is mainly constrained to telomeric regions and the mating type loci (Hickman et al., 2011).

It is interesting to speculate about how loss of the ancestors of *Spswi6* and *Spclr4* may have contributed to the evolution of *S. cerevisiae*, such as an increased rate of speciation, mating type switching, loss of intergenic DNA resulting in a very compact genome, and adaptions that may have followed a whole-genome duplication (WGD) and subsequent rapid loss of duplicate genes (Dietrich et al., 2004; Dujon et al., 2004; Goffeau et al., 1996; Kellis et al., 2004; Wolfe and Shields, 1997). For instance, could an increased rate of insertion/deletion mutations have made adaption to the WGD possible and metabolic innovation more likely? Furthermore, eukaryotes exhibit meiotic recombination rates that are inversely proportional to genome size (Segura et al., 2013; Tiley and Burleigh, 2015; Wilfert et al., 2007), but the *S. cerevisiae* recombination rate is three times higher than expected (She and Jarosz, 2018). Could the open configuration of the genome make recombination more probable?

We have performed a retro-engineering of *S. cerevisiae* by expressing *Spswi6/Spclr4* (*Sp*Swi6/*Sp*Clr4) to create a pseudo-ancestral state where we hypothesized that the *S. cerevisiae* chromatin would become more compact and stable. Increased compaction of the chromatin occurred in cells expressing *Sp*Swi6/*Sp*Clr4 with reduction in mutation and recombination rates. These findings have implications to synthetic biology applications where difficulties to maintain strains that harbor exogenous genes may be overcome.

3.3.3 Results

3.3.3.1 *Sp*Swi6/*Sp*Clr4 expression induces global chromatin compaction

*Sp*Swi6 and *Sp*Clr4 were expressed in a W303 strain of *S. cerevisiae* under control of regulatable promoters TetO (7 sites) and MET17, respectively. To measure chromatin compaction, we quantitated 4',6-diamidino-2-phenylindole (DAPI) binding to the minor groove of DNA, which is sensitive to chromatin structure and increases with chromatin compaction (Imai et al., 2017; Linhoff et al., 2015). We observed increased DAPI binding on cells expressing the *Sp*Swi6/*Sp*Clr4 proteins (Figure 3.1 b, c).

Most striking, was a narrowing of the nucleus along the axis orthogonal to that defined by the nucleolus and Spindle Pole Body (SPB) in cells expressing *Sp*Swi6/*Sp*Clr4 along with additional markers for nuclear envelope (Nup49-GFP) and the nucleolus (Nop1-mCherry) (Figure 3.1 d). These results are consistent with compaction of the chromatin in the Rabl configuration of chromosomes, with centromeres associated to the SPB clustered on one side of the nuclear envelope and telomeres located at the nuclear periphery at positions determined by the length of the chromosome arms (Figure 3.1 d) (Berger et al., 2008; Jin et al., 2000; Pouokam et al., 2019; Rabl, 1885; Spector, 2003; Therizols et al., 2010). Consequently, compaction of the chromosomal arms between centromeres and telomeres induced by *Sp*Swi6/*Sp*Clr4 results in the nuclear envelope being drawn inward, resulting in an ellipsoid nuclear shape with the long axis determined by the SPB-nucleolar positions (Duan et al., 2010; Mizuguchi et al., 2015; Wong et al., 2012).

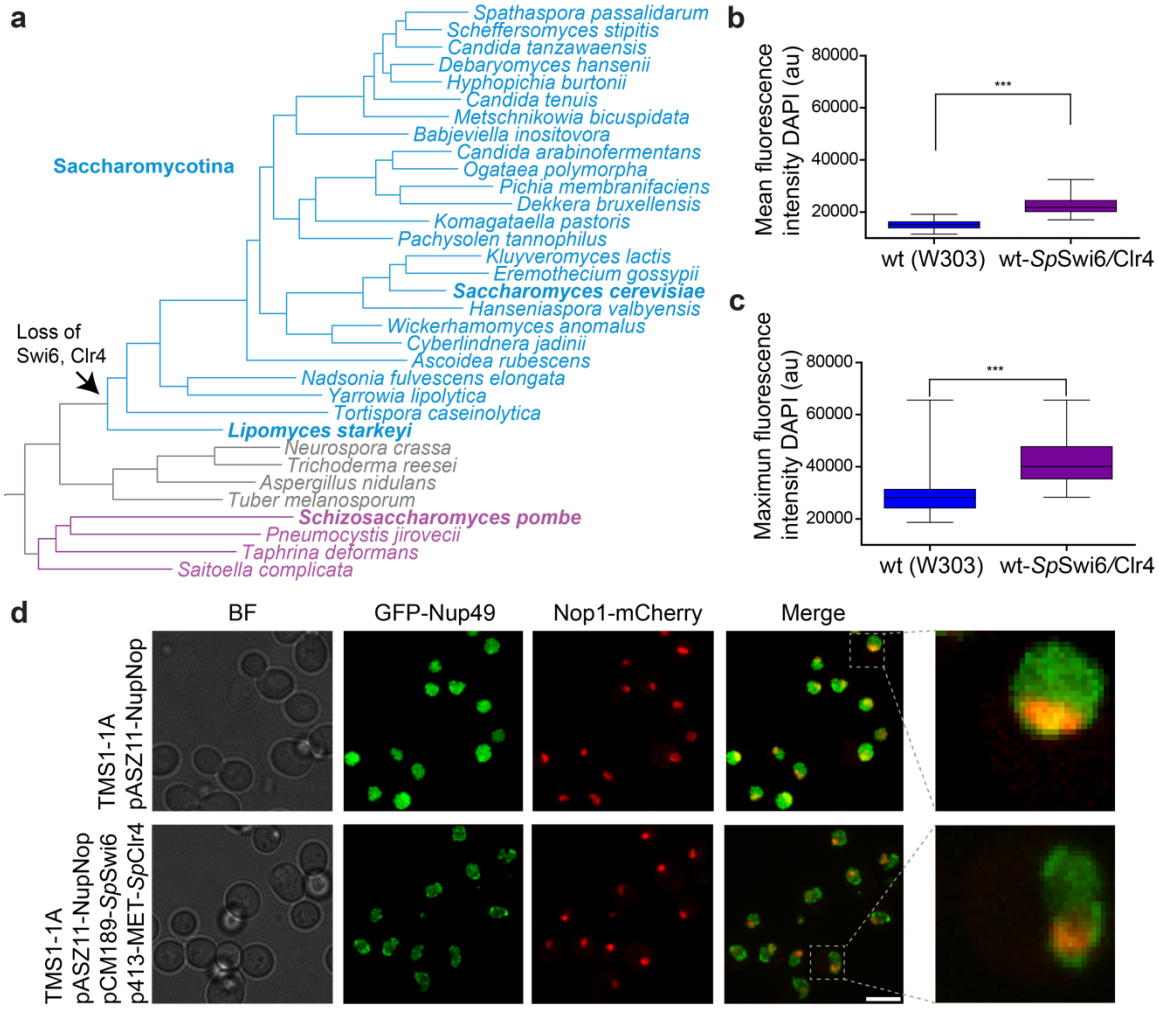

Figure 3.1 Expressing SpSwi6/SpClr4 proteins increases chromatin compaction in S. cerevisiae

a, *Phylogenetic tree of yeast species. The arrow indicates where yeast HP1 and H3K9 methyltransferases were lost during evolution, ~300 million years ago. Blue and purple highlighted regions indicate organisms mentioned in this study (modified from Riley et al., (Riley et al., 2016)).* ***b***, ***c****, Mean and maximum fluorescence intensity of chromatin stained with DAPI significantly increases in SpSwi6/SpClr4 expressing cells versus wild type (t-test, p < 0.0001).* ***d****, Live cell imaging of GFP-Nup49 (green) and Nop1-mCherry (red) nuclear envelope (NE) and nucleolus (NO) markers, respectively, in wild type and cells expressing the SpSwi6/SpClr4 proteins (maximum projection of 250 nm Z stacks). BF, brightfield*

images of the cells. Grey dashed square highlights representative nuclei in both wild type and SpSwi6/SpClr4 expressing cells. Scale bar represents 5 µm.

3.3.3.2 *Sp*Swi6/*Sp*Clr4 expression results in reduced stiffness, characteristic of dense chromatin

Chromatin stiffness increases with decompaction of chromatin, for instance, as occurs during nucleosome depletion and gene induction. Stiffening of the chromatin does work that drives separation of sister chromatids and partitioning of chromatin to different regions of the nucleus (Bystricky et al., 2004; Neumann et al., 2012; Verdaasdonk et al., 2013). For example, it has been shown that depletion of nucleosomes that accompanies replication and mitosis results in stiffening of the chromatin as measured by an increase in effective spring constant (k_s) (Verdaasdonk et al., 2013). The increase in k_s is the consequence of the inverse relationship between k_s and the persistence length (L_p) of chromatin, which increases with increasing chromatin density.

The mechanical stiffness and radius of confinement (R_c) of chromatin can be measured by spatiotemporal tracking of individual chromatin regions with site-specific fluorescent probes integrated into the genome. Well-established relationships have been derived from polymer theory to calculate k_s and R_c from plots of mean-squared displacements (MSD) (See Methods, Equations 1 and 2) (Bystricky et al., 2004; Neumann et al., 2012; Verdaasdonk et al., 2013). We chose to probe the spatiotemporal dynamics of the metabolic stress-response gene *INO1* locus. We chose this locus because we could measure two effects of *Sp*Swi6/*Sp*Clr4 expression: changes in chromatin stiffness and the adaptive response of *INO1* activation: nucleoplasm to the nuclear envelope (NE) translocation resulting in more efficient *INO1* expression (Chapter 2).

To probe the locus spatiotemporal dynamics, we used a strain in which an array of 128 LacO sites is inserted into the genome adjacent to the *INO1* locus and the LacO-binding LacI protein fused to GFP is expressed. A bright fluorescent focus arising from the array-

bound LacI-GFP can then be tracked. We also labeled the nuclear pore complex (NPC) protein Nup49 with GFP and Nop1 with mCherry for nuclear envelope and nucleolar reference markers, respectively (Figure 3.2 a, b). The mean squared displacement values (MSD) for the *INO1*-LacI-GFP signal as a function of time were significantly higher for the activated state of the gene in the strain expressing *Sp*Swi6/*Sp*Clr4 compared to the *wild type* strain also growing under activating conditions, and similar to repressed conditions for both type of cells (Figure 3.2 c). This indicated that in the presence of these heterochromatin forming proteins the locus behaved as if the cells were growing under repressed conditions. The values obtained for R_c and k_s also confirmed these results, with the gene showing a higher area of distribution and lower effective spring constant for cells expressing *Sp*Swi6/*Sp*Clr4 compared to *wild type* cells, which means the locus is more flexible than expected in the activated state (Figure 3.2 d-g).

We have demonstrated that partitioning of the *INO1* locus to the NE from the nucleoplasm is accompanied by an increase in locus chromatin stiffness causing it to phase separate from the denser nucleoplasm chromatin to less dense perinuclear chromatin (Chapter 2). We therefore predicted that expression of *Sp*Swi6/*Sp*Clr4 could prevent this partitioning. We calculated maps of the statistical distribution of the *INO1* locus under repressed and activated conditions (Berger et al., 2008). Under activating conditions (inositol starvation), the locus appeared to be confined to a region adjacent to the NE, but under repressed conditions (presence of inositol) the locus was broadly distributed throughout the nucleoplasm (Figure 3.2 h, i). We observed, however, a reduction of NE localization of the *INO1* locus in the strain expressing *Sp*Swi6/*Sp*Clr4 under activating conditions similar to the repressed state of the gene (Figure 3.2 j, k).

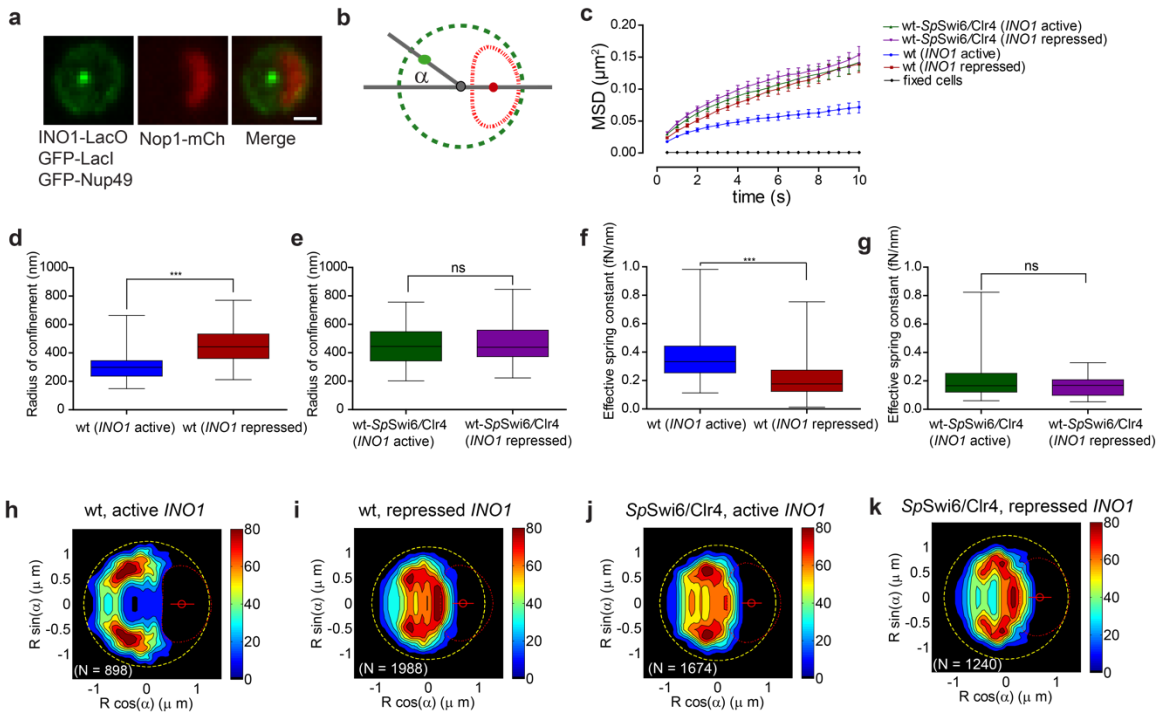

Figure 3.2 Active INO1 locus behave like condensed repressed chromatin in cells expressing SpSwi6/SpClr4 proteins

***a**, Representative images of a yeast strain nuclei in which the an array of 128 LacO sites are integrated next to the INO1 locus and the LacO-binding protein LacI-GFP is expressed. Additionally, the NE and the nucleolus in these nuclei are labeled with GFP (Nup49) and mCherry (Nop1), respectively. Images shown are maximum projections of 250 nm Z stacks. Scale bar equals 1 μm. **b**, Positioning of the nuclear landmarks used to track the INO1 gene and to generate the statistical distribution maps for the localization of the INO1 locus. Green dashed circle (NE), red dashed ellipsoid (nucleolus), grey circle (nucleus center) and red circle (center of the nucleolus). The green circle represents the position of the gene in the nucleoplasm and the grey lines, the axes that connect the center of the nucleus with the center of the nucleolus and the center of the nucleus with the gene; α is the angle between these axes. **c**, MSD curves for the INO1 locus in wild type and SpSwi6/SpClr4 strain under activating or repressed conditions (blue and red, and green and purple, respectively), and for the gene in a population of fixed cells (black curve). **d**, Radius of confinement (R_c) for the INO1 gene in an active state (blue) is significantly smaller than in*

the repressed state (red) for wild type cells (t-test, p < 0.0001). ***e****,* R_c *in the SpSwi6/SpClr4 strain under activating conditions (purple) does not show significant differences compared to the repressed state (grey).* ***f****,* ***g****, Spring constant (*k_s*) for the INO1 activated gene in the wild type (blue) significantly decreases compared to repressed cells (t-test, p = 0.0002), while there are no significant differences in* R_c *and* k_s *in the SpSwi6/SpClr4 strain under both conditions.* ***h****-****k****, Statistical maps for the INO1 localization obtained with nucloc software by superimposing nuclei of wild type and SpSwi6/SpClr4-expressing cells grown under activating or repressed conditions.*

3.3.3.3 *Sp*Swi6/*Sp*Clr4 expression increases genome stability to mutations

The mutation rate of the genome is among the primary sources of genetic variation that determines rates of evolution, speciation and on short time scales, genome stability (Martincorena et al., 2012; Zhu et al., 2014). We next asked whether *Sp*Swi6/*Sp*Clr4 expression and resulting compaction of chromatin would cause a decrease in rates of mutation. We measured single nucleotide and insertion/deletion (indel) mutations with the widely used *CAN1* mutator assay, which is based on counterselection of the *CAN1* gene that encodes for the arginine permease Can1, an amino acid transporter responsible for the uptake of arginine from the environment (Huang et al., 2003; Lang and Murray, 2008; Measday and Stirling, 2015; Stirling et al., 2014). Can1 also specifically transports the toxic arginine analog, canavanine. Consequently, we can select for individual clones containing *CAN1* mutations by growth on solid medium containing canavanine but not arginine (Figure 3.3 a) (Huang et al., 2003; Lang and Murray, 2008; Stirling et al., 2014).

To characterize the type and rate of mutations that occur in *wild type* versus *Sp*Swi6/*Sp*Clr4-expressing cells, we monitored the frequency of Can^r mutations (number of colonies) over several days of incubation (Figure 3.3 b). We used the DBY746 strain of *S. cerevisiae* for which the number of mutants with Can^r increases rapidly, after several days of growth (Fabrizio et al., 2004). For the first 5 days of incubation, we did not observe a significant difference in the frequency of mutants for *wild type* or *Sp*Swi6/*Sp*Clr4-

expressing strains although the values were always higher for the *wild type* strain. However, after day 7 the difference became significant, and the resulting frequencies of mutation were 3-4 times lower for the *Sp*Swi6/*Sp*Clr4-expressing than *wild type* cells by day 13 (Figure 3.3 b).

We also analyzed the type of mutations that appeared to confer resistance to canavanine for 10 of the Can^r mutants (Table S3.1). For one of the clones obtained from the *wild type* strain we were not able to amplify the *CAN1* locus which suggests that a large chromosomal rearrangement occurred in this clone. For the rest of the clones from *wild type*, sequencing of the *CAN1* gene showed that six contained single base substitutions, three single deletions and one exhibited a triple deletion (Table S3.1). Three of the clones contained two or more types of mutations. For the base substitutions four were transversions C → A or G → C, and four were transitions G → A or A → G. The deletions were ΔC or ΔT. For the DBY746 *Sp*Swi6/*Sp*Clr4-expressing strain, we were able to amplify and sequence the 10 colonies selected, indicating no chromosomal rearrangement. Additionally, all colonies exhibited only one single point mutation per strain. Most of the mutations observed were base substitutions present in eight of the 10 clones. The other two strains contained a single base deletion ΔC in both cases. The base substitutions were mainly transversions the type C → A, G → C, G → T and a single transition C → T (Table S3.1). It appears that expression of *Sp*Swi6/*Sp*Clr4 and consequent compaction of chromatin results in significantly decreased mutations in the genome, including large chromosomal rearrangements, during aging.

We used a second approach to determine the frequency of gross chromosomal rearrangement (GCR) based on an assay in which two counter-selectable markers are linked and the loss of both is measured by growing the cells in the presence of a double selection medium. In this case the markers are, *CAN1* and *URA3*, and the strains to analyze are grown in medium containing canavanine and 5-fluoroorotic acid (5-FOA) (Kanellis et al., 2007; Smith et al., 2004). The uracil biosynthesis pathway can convert the nontoxic 5-

FOA into toxic 5-fluoro-uracil and the *URA3* gene encodes for a product that catalyzes a key step in this synthesis. The treatment of cells with both canavanine and 5-FOA will thus select for *CAN1*- and *URA3*- inactive mutants. To avoid loss of cell viability by rearrangement or deletion of the whole cassette flanked by *CAN1–URA3*, these markers are usually inserted into a position proximal to the telomere in the chromosome arm (Figure 3.3 c). It is unlikely that point mutations can inactivate two different markers simultaneously, particularly if the genes are located in neighboring regions in the chromatin. Consequently, unless cells are also treated with DNA mutagens, the *CAN1–URA3* reporter likely measures GCRs(Chen and Kolodner, 1999; Kanellis et al., 2007; Madia et al., 2008; Smith et al., 2004).

We measured the GCR frequency for the *wild type* DBY746 and DBY746-*Sp*Swi6-*Sp*Clr4 grown for a period of 13 days. After day 5 there was a significant increase in GCR frequency for the *wild type* compared to the *Sp*Swi6/*Sp*Clr4-expressing strain that reached 10-fold by day 13 (Figure 3.3 d).

Overall, *Sp*Swi6/*Sp*Clr4 expression significantly decreases the mutation rate of *S. cerevisiae* to single nucleotide, up to GCR scales.

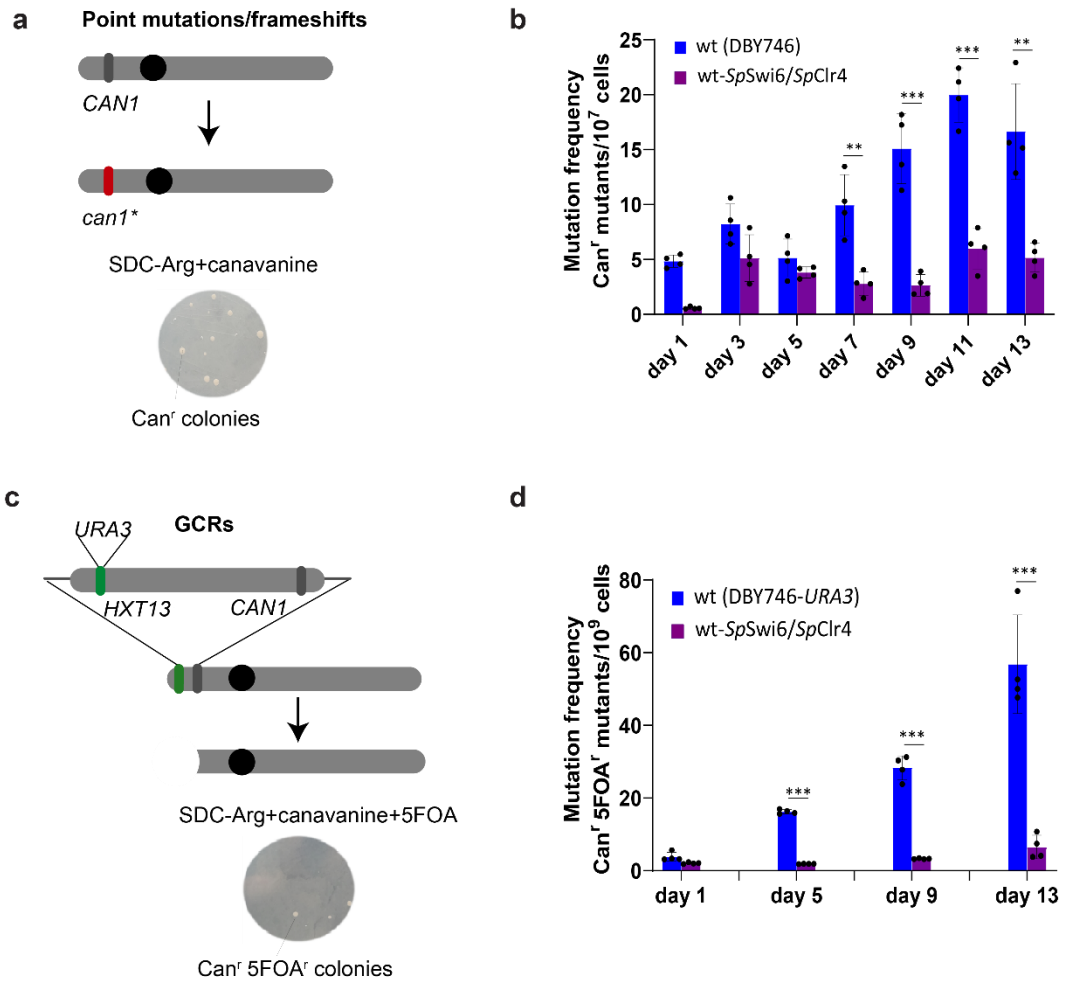

Figure 3.3 Genomic stability increases in SpSwi6/SpClr4 mutants

***a**, CAN1 mutator assay. Mutations in the CAN1 gene confer resistance to canavanine, a toxic arginine analog. Mutation rate is quantified by measuring the frequency of canavanine resistant mutants on plates of synthetic medium lacking arginine and containing canavanine. **b**, Mutation frequency for the CAN1 gene in wild type (DBY746) versus the DBY746-SpSwi6-SpClr4 strain, measured as Can^r mutants/10^7 cells, on cultures incubated over 13 days. **c**, Gross Chromosomal Rearrangement (GCR) assay. The rate of large chromosomal rearrangements is quantified by determining the frequency of mutations for two linked loci, URA3 and CAN1. Mutants are counter-selected on plates containing canavanine and 5-fluoroorotic acid (5-FOA), which is converted by the URA3 gene product to toxic 5-fluorouracil. **d**, GCR frequency, measured as Can^r 5-FOA^r*

mutants/10^9, in wild type (DBY746-URA3) versus the SpSwi6/SpClr4 strain, for cells cultured over 13 days. Experiments were performed in four biological replicates. Error bars represent standard deviations and asterisks represent the significance of the p-values calculated with Student's t-tests.

3.3.3.4 Global meiotic recombination rates decrease in *Sp*Swi6/*Sp*Clr4 expressing cells

Meiotic recombination is another important driver of genetic variation, a key source of genome evolution in organisms that reproduce sexually. This process provides new allelic combinations that serve as pools for natural selection as well as artificial selection of high-performing genotypes for industrial purposes (Raffoux et al., 2018). *S. cerevisiae* is unique in that its rate of recombination is so high that it can reach nearly 100 % linkage equilibrium within 6 generations of inbred crosses (Datta et al., 1996; Ji et al., 2020; Lichten and Haber, 1989; McIlwraith and West, 2008; She and Jarosz, 2018). Indeed, mitotic recombination between artificially constructed ectopic repeats can occur as efficiently as allelic recombination in *S. cerevisiae* (Lichten and Haber, 1989). Among eukaryotic organisms, recombination rates vary inversely with genome size over several orders of magnitude but for *S. cerevisiae* it is 3 times higher than predicted (Segura et al., 2013; She and Jarosz, 2018; Tiley and Burleigh, 2015; Wilfert et al., 2007). We next asked whether expression of *Sp*Swi6/*Sp*Clr4 would affect rates of meiotic recombination.

To quantify the recombination rate for *S. cerevisiae* we used a high-throughput and low-cost strategy in which three fluorescent marker protein-coding genes are integrated into chromosomes in different positions and flow cytometry is used to measure recombination rates and crossover patterns, based on compositions of fluorescent proteins expressed in spores (Raffoux et al., 2018). The fluorescent protein-coding genes were integrated at optimal distances from each other in a particular chromosome to measure recombination rates. These strains were crossed with non-marker strains to obtain diploids that would produce spores with different rearrangement patterns depending on the recombination events that occur in the chromosomes (Figure 3.4 a). By

calculating the frequencies of these events per segment, we were able to quantify the values for rate of recombination between each different pair of markers in each strain (See Methods, Equation 3).

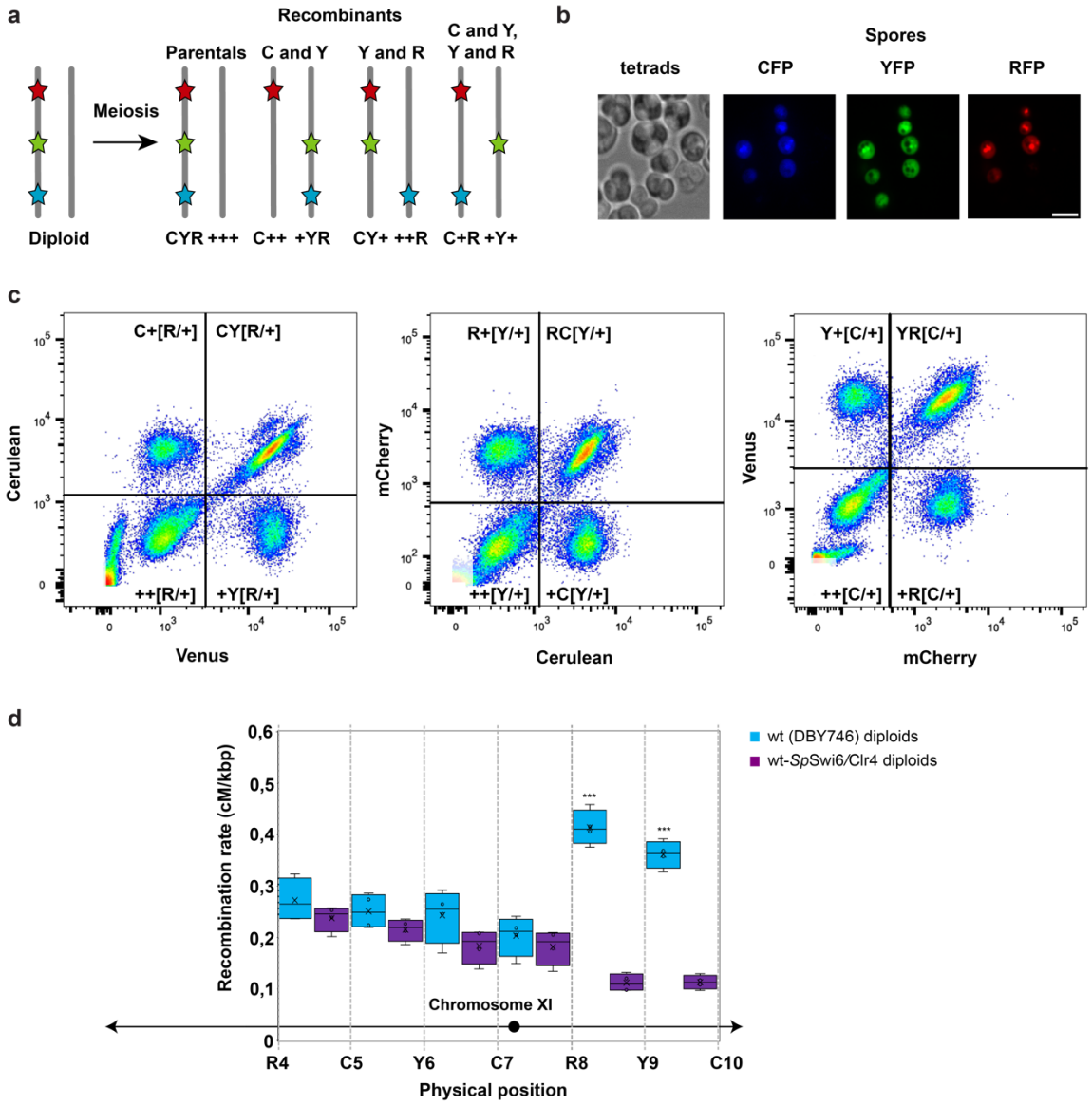

Figure 3.4 Global recombination rate decreases in S. cerevisiae cells expressing SpSwi6-heterochromatin

***a**, Meiotic chromosome segregation for three linked markers. Spores were classified into different classes according to the pattern of the markers they contained by using the three*

letters C (cerulean), Y (yellow), and R (red). The symbol '+' was used to indicate the absence of a particular marker. Thus, for a distribution pattern CYR, parental spores were denominated CYR and +++, recombinant spores between C and Y, or between Y and R, were designated as C++ and +YR, or CY+ and ++R, respectively. Finally double recombinant spores were named C+R and +Y+. ***b****, Imaging of tetrads and fluorescent spores following sporulation and spore isolation, respectively. Scale bar represents 5 µm.* ***c****, Examples of projections obtained for one sample representing the fluorescent intensities for the different pairs of markers: Venus versus Cerulean (left), Cerulean versus mCherry (middle), and mCherry versus Venus (right). Indicated in each quadrant per projection are the classifications of the spores, with the symbol [X/+] representing that the designated marker may be present or not at this position.* ***d****, Recombination rates for the different wild type and SpSwi6/SpClr4 containing diploids along chromosome XI of S. cerevisiae. The centromere of the chromosome is indicated with a black circle and the extremes with black arrows. Four biological replicates were used to calculate these results. Asterisks represent levels of significance for the p-values obtained from Student's t-tests between strains.*

We transformed the strains containing the three fluorescent markers spanning a total of 7 different consecutive sites in chromosome XI with the *Sp*Swi6/*Sp*Clr4 expression cassette. These and *wild type* tri-fluorescent strains were crossed with either *Sp*Swi6/*Sp*Clr4-expressing or *wild type* W303 strains, respectively, to obtain diploids. These diploids were induced to sporulate, followed by spore isolation, and finally FACS analysis of the spores (Figure 3.4 b, c). Each spore was classified according to its fluorescent pattern, which allowed to calculate values of recombination rates for all consecutive sites in each strain (Figure 3.4 d, See Methods, Equation 3). Recombination rates ranged from 0.26 to 0.41 cM/kbp among the 7 intervals on chromosome XI for the *wild type* diploids, and from 0.11 to 0.23 cM/kbp for the *Sp*Swi6/*Sp*Clr4 containing diploids (Figure 3.4 d). In both cases higher values of recombination rate were observed towards the end of the chromosome arm as expected (Barton et al., 2008). On average the values obtained for *wild type* strains were in the range of previously obtained values

for *S. cerevisiae* strains, however the averages for strains expressing the *Sp*Swi6/*Sp*Clr4 factors were almost two times lower than previously reported (Raffoux et al., 2018; She and Jarosz, 2018). This difference was mainly due to large decreases in the rates of recombination in the peripheral right arm of the chromosome, but all regions showed significant decreases (Figure 3.4 d).

3.3.4 Discussion

How chromatin topology affects mutation rate is not understood. Results linking mutation rate to chromatin compaction varies depending on which cells are studied and the type of mutation (Makova and Hardison, 2015; Pich et al., 2018). The relationship between recombination rate and chromatin compaction is clearer, where open euchromatin has higher recombination rates than compacted heterochromatin (Henderson and Bomblies, 2021). Our results suggest that increased compaction of chromatin on a local scale decreases mutation rates in the genome. This effect could be even more significant if increased efficiency of compensating DNA repair mechanisms had not evolved in *S. cerevisiae* reflected, for example in high rates of homologous recombination.

We describe our study as a retro-evolutionary engineering exercise, though more precisely, it is pseudo-retro-engineering in that *S. cerevisiae* is approximately 290 million years removed from the last common ancestor to possess homologues of *Sp*Swi6/*Sp*Clr4 and 330 to 420 million years from *S. pombe*. It is not possible to do a true retro-evolutionary engineering experiment by creating a strain in which the entire genome and *Sp*Swi6/*Sp*Clr4 homologs recreate the last common ancestor with these genes. One could, however, study the effects on genome structure, mechanics, and stability by knocking out the *Sp*Swi6/*Sp*Clr4 homologs in *Lipomyces starkeyi*, the only Saccharomycotina species to express these genes. In mouse embryonic fibroblasts, knockouts of all six SET domain lysine methyltransferase genes lacked all H3K9 methylation states, derepressed nearly all families of repeat elements and displayed genomic instabilities. Furthermore, mutant cells no longer maintained heterochromatin organization and lost all electron-dense

heterochromatin (Montavon et al., 2021). Nonetheless, it is likely the physical and functional consequences of *Sp*Swi6/*Sp*Clr4 expression would be similar in all Saccharomycotina, regardless of evolutionary distance from the last common ancestor to possess them. Furthermore, a remnant of the H3K9 methylation system was recently identified in *S. cerevisiae*, an H3K9-specific demethylase Rph1(Klose et al., 2007). It would be interesting to see if knocking out this enzyme would enhance the effects of expressing *Sp*Swi6/*Sp*Clr4 on genome compaction.

Our results have implications to basic research and industrial applications of yeast for which their low cost of maintenance, fast growth and great consistency and precision of editing its genome have made it an ideal organism as a model system of eukaryotes. Additionally, the ability to adapt to harsh fermentation conditions including low pH, high osmotic pressure, high alcohol concentration, and phage contamination have also made possible the great success of budding yeast in wine, beer, and biofuel fermentations as well as to express pathways to produce more complex chemical compounds. However, different industrial practices and the harsh conditions these cells are kept in, including long incubation times and recycling, make these strains susceptible to genetic instability. Consequently, this can cause the loss of beneficial traits or the appearance of phenotypes such as cellular aggregation that can be harmful for production (Rodrigues-Prause et al., 2018). In fact, studies that characterize the genomes of *S. cerevisiae* isolates coming from different industrial sources have shown high intra-strain variability (Argueso et al., 2009; Borneman et al., 2011). Moreover, chromosomal rearrangements in strains from different industrial backgrounds can result in mutations in the genome that remove desirable traits or genes that have been engineered into a strain for some industrial application (Basso et al., 2008; Carro and Piña, 2001; Querol and Bond, 2009).

The expression of *Sp*Swi6/*Sp*Clr4 or mutants engineered for optimal expression in biotechnologically important strains could help to stabilize their genomes (St Charles and Petes, 2013). The losses in productivity that these problems create could be tackled by

expressing *Sp*Swi6/*Sp*Clr4, induced under specific conditions either for fermentation purposes or for the process to prepare the strains for long periods of storage.

3.3.5 Acknowledgements

The authors thank Geeta J. Narlikar (University of California, San Francisco), Jason Brickner (Northwestern University), Matt Kaeberlein (University of Washington), and Matthieu Falque (Université Paris-Saclay, France) for providing reagents, plasmids, and strains.

Funding: This work was supported by Canadian Institutes of Health Research (CIHR) grant MOP-GMX-152556 and Human Frontiers Science Program grant RGP0034/2017 (S.W.M).

Author contributions

Conceptualization: L.G. and S.W.M.; Methodology: L.G.; Data Analysis-Writing-Review: L.G. and S.W.M.

Declaration of interests

The authors declare no competing interests.

3.3.6 Methods

3.3.6.1 Strains and plasmids

S. cerevisiae W303 strain was used as control to quantify DAPI both signal and relative chromatin compaction (Table S3.2). To analyze the effects of *Sp*Swi6 and *Sp*Clr4 expression on genome compaction of *S. cerevisiae,* two plasmids were generated to express these genes in the W303 strain (Table S3.2). Briefly, plasmids containing *Spswi6* and *Spclr4* sequences (pET30a-*Sp*Swi6 and 2CT[1]- *Sp*Clr4) were provided by Geeta J. Narlikar at the University of California, San Francisco (Table S3.3). *Spswi6* was subcloned into pCM189 under the control of the CYC1 promoter and a tet operator array containing 7 tetO sites, while *Spclr4* was subcloned into a p413-ADH1 vector where the ADH1 promoter had been previously replaced by a MET17 promoter. Both pCM189-tetO7-*Sp*Swi6 and p413-MET-*Sp*Clr4 were transformed in W303 (Table S3.3).

To analyze nuclear morphology, a strain (TMS1-1A) containing a plasmid (pASZ11-NupNop) expressing GFP-Nup49 and mCherry-Nop1 to mark the NE and the nucleolus, respectively, was imaged as control(Albert et al., 2013). This strain was transformed with the plasmids pCM189-*Sp*Swi6 and p413-MET-*Sp*Clr4 previously obtained Table S3.2).

To create an integration cassette containing both tetO7-*Sp*Swi6 and MET-*Sp*Clr4 expression cassettes, that could be inserted into different strains, the backbone of the yeast integration plasmid YIp204-PADH1-atTIR1-9myc was used (Addgene, Plasmid #99532) (Table S3.3). In this case, any cassette subcloned into this plasmid can be inserted into the genome of *S. cerevisiae* by linearizing the plasmid at the *TRP1* locus (Bsu36I site) and then transforming the linearized vector into a tryptophan auxotroph strain. Briefly, the sequence that encodes for the TIR1-9myc protein was first removed by reverse PCR and then both tetO7-*Sp*Swi6 and MET17-*Sp*Clr4 expression cassettes were cloned consecutively at this site by using the GeneArt Seamless Cloning and Assembly kit (ThermoFisher Scientific) (Table S3.3). By employing the same strategy, a 6-FLAG tag was

inserted at the coding sequence for the C-terminus of *Sp*Swi6 to allow for detecting the expression of the protein by Western blot (Figures S3.1, S3.2). The plasmid generated (YIp204-tetO7-*Sp*Swi6-6FLAG-MET17-*Sp*Clr4) was then linearized at the *TRP1* locus, purified, and stored for transformation (Table S3.3).

To quantify the statistical distribution and mechanical properties of the *INO1* gene, the LMY52 strain (Brickner et al., 2012) (Table S3.2) was employed as control (provided by Jason Brickner, Northwestern University, USA). This strain contains an array of 128 LacO sites fused to the *INO1* locus and expresses LacI-GFP and NE and nucleolus proteins fused to fluorescent proteins (GFP-Nup49 and mCherry-Nop1). To insert *Sp*Swi6/*Sp*Cl4 in the genome of LMY52, this strain was transformed with the YIp204-tetO7-*Sp*Swi6-6FLAG-MET17-*Sp*Clr4 linearized plasmid.

The *S. cerevisiae* DBY746 strain (Table S3.2) (provided by Matt Kaeberlein, University of Washington, USA) was used as background to measure mutation rates driven by small base substitutions/deletions/insertions. To assay the effect of *Sp*Swi6/*Sp*Cl4 expression on mutation frequency, the integration plasmid YIp204-*tetO7*-*Sp*Swi6-6FLAG-MET-*Sp*Clr4 was transformed into this strain. To measure large chromosomal rearrangements in the DBY746 and DBY746-*Sp*Swi6-S*p*Clr4 strains, both were transformed with a *URA3* cassette designed with flanking homologous regions to replace the *HXT13* locus situated 7.5 kb upstream of the *CAN1* locus.

For recombination rate measurements, tri-fluorescent tester strains (Table S3.2): 348 (SK1-XI-R4C5Y6), 400 (SK1-XI-Y6C7R8), 369 (SK1-XI-R8Y9C10) were provided by Matthieu Falque at Université Paris-Saclay, France (Raffoux et al., 2018). These strains containing different arrangements of three-colored fluorescent protein-coding genes (Cerulean, Venus and mCherry) in chromosome XI were crossed with a W303-*MAT***a** strain (Table S3.2) to generate control diploids to use for sporulation in the recombination rate assays. These tri-fluorescent testers and W303-*MAT***a** haploids were also transformed separately

with the yeast integration plasmid YIp204-tetO7-*Sp*Swi6-6FLAG-MET17-*Sp*Clr4 to integrate *Spswi6/Spclr4* into their genomes. Next, each tri-fluorescent tester strain expressing *Sp*Swi6/*Sp*Clr4 proteins was crossed with the W303-*MAT***a** strain also expressing these proteins to obtain *Sp*Swi6/*Sp*Cl4 diploids for the recombination tests (Table S3.2).

3.3.6.2 Chromatin compaction analysis

To analyze chromatin compaction, cells were stained with 4',6-diamidino-2-phenylindole (DAPI) and values of fluorescent intensities were compared among strains. Briefly, cells were grown overnight in synthetic complete (SC) medium lacking adenine (SC-ade) for the wild type (W303) and SC lacking adenine, uracil, and histidine (SC-ade-ura-his) for the W303 strain expressing *Sp*Swi6/*Sp*Clr4. The next day, fresh media was inoculated with the overnight cultures and cells were incubated for 4 h. Cells were immobilized in Concanavalin A-coated well slides and fixation was performed by adding 4% paraformaldehyde (EMS 15714S), prepared in phosphate-buffered saline (PBS), and incubating 10 min. Next, cells were permeabilized with 0.2 % Triton X-100 in PBS, washed three times with PBS, and incubated with a DAPI aqueous solution 2 µg/ml (Sigma, D8417) for 5 min. After removing the DAPI solution and washing the cells with PBS, mounting media was added to the well slides before imaging. Microscopy was performed on a Zeiss Elyra PS.1 system. Structured illumination microscopy (SIM) images were acquired with a 63 × 1.46 NA oil objective in the DAPI channel with an exposure of 100 ms and 10 % laser power (4.1 mW 405 nm HR diode laser). Each image was acquired using 3 rotations and 5 phases per rotation. Images were processed using Zen Black structured illumination reconstruction algorithm.

3.3.6.3 Nuclear morphology assessment

To visualize the nuclear envelope and nucleolus morphology, wild type (TMS1-1A) and mutant strains expressing fluorescent protein-fused marker proteins for both landmarks

in the nucleus, Nup49-GFP and Nop1-mCherry, were grown in SC-ade or SC-ade-ura-his, respectively. Overnight cultures of these strains were used to inoculate fresh media and cells were incubated until late logarithmic phase (OD_{600} 1 – 1.5). Cells were then immobilized on ConA-coated well slides, and imaging was performed in a Zeiss Axio-Observer Z1 Yokogawa spinning disk confocal microscope using a 100 × 1.43 NA oil objective. For this, 10 Z-stack slices were recorded at a spacing of 300 nm and exposure times 50 ms and 100 ms, for GFP (50 %, 3 mW 488 nm excitation) and mCherry (50%, 3.3 mW 561 nm excitation) channels, respectively. Images were analyzed with Fiji software (Schindelin et al., 2012).

3.3.6.4 *INO1* locus statistical distribution

The procedure for the statistical mapping of the *INO1* locus was similar to previously described by Brickner *et al*. (Brickner et al., 2012) with slight modifications. In this case, the wild type and *Sp*Swi6/*Sp*Clr4-expressing mutant strains with the *INO1* tagged with the 128 LacO array and the same nuclear landmark protein-fluorescent protein fusions described above were grown overnight in synthetic defined medium without inositol or containing freshly prepared 100 µM *myo*-inositol. The next day, these cultures were diluted in fresh medium and incubated for approximately two generations. Cells were then immobilized in ConA-coated well slides and microscopy was performed as described for the nuclear morphology analysis but in this case 32 Z-stack slices were recorded for each field at a spacing of 250 nm. Nucloc software was used to process images in a modified mode where probability maps are presented as percentiles using a kernel density estimate (Therizols et al., 2010).

3.3.6.5 *INO1* tracking and mechanical properties

In order to track the *INO1* gene, the same strains and culture conditions used for the statistical distribution of the locus analysis were reproduced. Cells were also immobilized on ConA-coated wells but in this case, time-lapsed images of each field in the GFP channel

(100 mW 488 nm excitation) were recorded at intervals of 500 ms for 1 min. Fixed cells were also imaged with the same settings as controls for microscope stage drift. The WaveTracer tool on the Metamorph software was used to track the locus for each cell in each time-lapse set of images (Kechkar et al., 2013). This tool enabled automatic segmentation and positioning of the loci in each slide to determine Mean Squared displacement (MSD) values for each locus as well as discard curves that do not have linear slopes.

Two mechanical properties of the *INO1* locus were calculated by using these MSD values and tracking coordinates. First, the radius of confinement (Rc) was calculated from the MSD plateaus (equation 1) (Neumann et al., 2012; Verdaasdonk et al., 2012).

$$R_c = \frac{5}{4}\sqrt{MSD_{plateau}} \quad (1)$$

Second, the effective spring constant (k_s) for the locus was calculated by quantifying the standard deviation (σ) of each step from the mean position by applying the equipartition theorem (Equation 2) (Scheffold et al., 2010; Verdaasdonk et al., 2013).

$$k_s = \frac{k_B T}{\sigma^2} \quad (2)$$

Student's t-tests analyses were performed between the different strains and conditions to determine statistical differences for both *Rc* and k_s parameters in each case.

3.3.6.6 Mutation rate measurements

Can^r mutator assay

To measure the spontaneous mutation rate of a DBY746 *Sp*Swi6/*Sp*Cl4 expressing strain versus *wild type*, we quantified the frequency of mutation of the *CAN1* (YEL063) gene. For

this, both *wild type* and *Sp*Swi6/*Sp*Clr4 mutant strains were incubated overnight and inoculated in 50 mL SC. Cells were incubated over 13 days at 30°C and 200 rpm. To measure cell viability, every two days, samples of each culture were diluted to a final concentration of 10^3 cells/ml and 100 µl of this suspension was inoculated on solid Yeast Extract–Peptone–Dextrose (YPD) medium. Colony-forming units (CFUs) were counted after 48 h. To quantify canavanine-resistant mutants (Can^r), every two days, approximately 2 x 10^7 cells were taken from each culture, washed with sterile H_2O, and plated in SC lacking arginine (SC-arg) supplemented with 60 µg/ml L-canavanine sulfate. In this case colonies were counted after 3 to 4 days of incubation. To calculate frequency of mutants, the ratio of Can^r/total viable cells was determined.

CAN1 sequencing

Sequencing was performed for 10 clones of the Can^r mutants obtained for each DBY746 and DBY746-*Sp*Swi6-*Sp*Cl4 strains after 9 days incubation in canavanine plates. Mutant colonies were collected, and genomic DNA was isolated by using a simple lithium acetate (LiOAc)-SDS procedure previously described(Lõoke et al., 2011). A set of primers was used to amplify a region of 2082 bp including the whole *CAN1* open reading frame: CAN1-5UTR-Fw (5'- CAGAGTAAACCGAATCAGGGAATCCC -3') and CAN1-3UTR-Rev (5'-GCTCATTGATCCCTTAAACTTTCTTTTCGG-3'). PCR products were purified and sent for sequencing using the amplification primers plus additional ones to completely cover the 2 kb fragment: CAN1-296-Fw (5'- AGACATATTGGTATGATTGCCCTTGG -3'), CAN1-562-Fw (5'- ATCACTTTTGCCCTGGAACTTAGTGTAG -3'), CAN1-989-Fw (5'-GAGCCATCAAAAAAGTTGTTTTCCGTATCTTAAC -3').

Frequency of gross chromosomal rearrangement (GCRs)

To quantify GCRs, cultures with the DBY746 *wild type* and DBY746-*Sp*Swi6-*Sp*Cl4 mutant strains transformed with the *URA3* cassette that replaced the *HXT13* locus, were prepared

as described before for the Can^r mutator assay. Cell viability was also measured by plating cells dilutions in YPD plates. To detect large rearrangements in the region containing both *CAN1* and *URA3,* every 4 days, approximately 10^8 cells from each culture were washed with sterile H_2O and plated in SC-arg plates containing 60 ug/ml L-canavanine and 1 mg/ml 5-fluoroorotic acid (5FOA). Colonies were counted after 3 to 4 days of incubation and the frequency of GCR events was calculated in a similar way as done for the Can^r mutants.

To calculate statistical differences for mutation frequencies between the different strains and conditions Student's t-tests analyses were performed.

3.3.3.7 Recombination rate measurements

Sporulation and flow cytometry procedure

Sporulation and flow cytometry analysis of the spores was performed as described before (Raffoux et al., 2018) with some variations. Diploids strains were inoculated on 5 ml YPD and incubated overnight at 30°C, 200 rpm. Cells were harvested at 2000 rpm, 2 min and resuspended in 600 µl of sterile H_2O, and 150 µl of each preparation was plated on four different plates containing sporulation medium (2 % potassium acetate, 1.2 % agar, and 10 µg/ml of L adenine, L arginine, L histidine, L leucine, L lysine, L phenylalanine, L threonine, L tryptophan, L uracil, L valine). Plates were incubated for 10 days at 30°C. After this time, cells were recovered using polystyrene scraper loops and were resuspended in tubes containing 5 mg/ml zymolyase 100T (Zym002.250, Bioshop) in 750 µl of sterile H_2O and 100 µl glass beads (Glass beads, acid-washed, 425-600 µm, G8772, Sigma). Tetrads were then disrupted by vortexing the tubes in a Mini-BeadBeater-16 (Biospec), for 1 min, followed by incubation at 30°C for 60 min, and another cycle of vortexing for 1 min. Samples were centrifuged 5 min at 4500 rpm and pellets were resuspended by vortexing in 200 µl of sterile H_2O. Samples were centrifuged again and the supernatants containing mainly vegetative cells were discarded. Spores were

resuspended by vortexing in 600 µl sterile H_2O containing 0.01% nonidet NP40. Spores were analyzed on a Bio-Rad YETI (ZE5) Cell analyzer and the Everest 3.0 acquisition software. A gate was set on the FSC *versus* SSC plot to only allow the analysis of events corresponding to spores (Figure S3.3). Cerulean, Venus and mCherry fluorescent markers were excited using a 405 nm, 488 nm and 561 nm laser respectively and read through a 525/50, 549/15 and 615/24 bandpass filter (Figure S3.4). Data were then analyzed using FlowJo V10 software.

Analysis of fluorescent patterns

As described above(Raffoux et al., 2018), each of the tester strains contain three fluorescent markers corresponding to cerulean, yellow, and red (C, Y or R) channels. Thus, diploids cells that were obtained by crosses with haploids not containing any fluorescent marker produced eight different classes of spores (Figure 3.4 a). When analyzing the data from flow cytometry, each class was denoted by stating the markers presence in a consecutive array, and in the absence of fluorescence for any marker the symbol '+' was used. For example, if the arrangement of the markers in the tri-fluorescent haploid parental strain was CYR, then parental spores containing all three markers or none were indicated as CYR and +++, respectively. The rest of the classes corresponded to single recombination events between C and Y markers (C++ and +YR), Y and R markers (CY+ and ++R), or double recombination events (C+R and +Y+) (Figure 3.4 a). Three projections were used to represent the intensities of two different fluorescence markers (Figure 3.4 c) where the nomenclature [X/+] specifies that the X marker might be present or not. As done previously, to classify each spore in one of the eight different classes that could be obtained, the following rules to analyze the quadrants in each projection were applied:

CYR: spores in quadrants CY[R/+] and C[Y/+]R and [C/+]YR.

+++: spores in quadrants ++[R/+] and +[Y/+]+ and [C/+]++.

C++: spores in quadrants C+[R/+] and C[Y/+]+ and [C/+]++.

+YR: spores in quadrants +Y[R/+] and +[Y/+]R and [C/+]YR.

CY+: spores in quadrants CY[R/+] and C[Y/+]+ and [C/+]Y+.

++C: spores in quadrants ++[R/+] and +[Y/+]R and [C/+]+R.

C+R: spores in quadrants C+[R/+] and C[Y/+]R and [C/+]+R.

+Y+: spores in quadrants +Y[R/+] and +[Y/+]+ and [C/+]Y+.

Recombination rate quantification

To calculate the recombination rates for two linked markers, for example C and Y, the following equation (3) was used:

$$R_{CY} = \frac{-50\ln(1-2\,(f_{\mathrm{C+[}R\mathrm{+]}} + f_{\mathrm{+Y[}R\mathrm{+]}}))}{d_{CY}} \quad (3)$$

In this case *d*CY represents the distance in kbp between the markers, and *f*XYZ is the frequency of the particular XYZ class of spores. The values for recombination rate were expressed in centiMorgan (cM) per kilobase.

3.3.7 Supplementary information

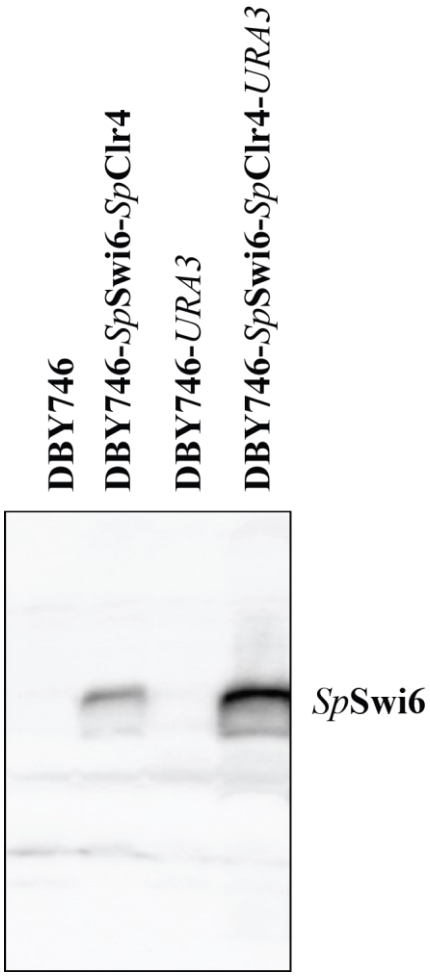

Figure S 3.1

Detection of SpSwi6-6FLAG in DBY746 strain and mutants. *Protein levels in lysates from DBY746 strains used for the mutation rate assays, carrying SpSwi6 tagged at C-terminal position with an array of 6 FLAG epitopes. Membranes were analyzed by western blotting with an anti-Flag M2 antibody.*

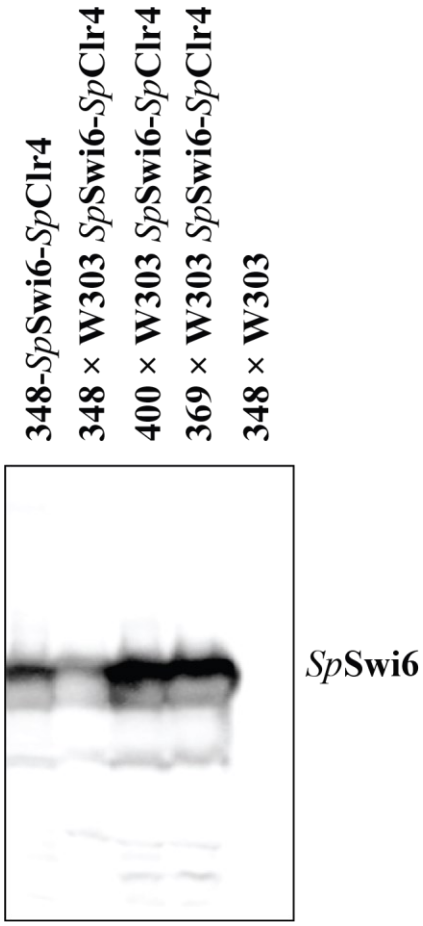

Figure S 3.2

Detection of SpSwi6-6FLAG in tri-fluorescent tester strains and mutants. *Protein levels in cell extracts from different tri-fluorescent haploid and diploid strains used for the recombination rate assays, expressing SpSwi6 fused to an array of 6 FLAG epitopes at C-terminal position, and analyzed by western blotting with an anti-Flag M2 antibody.*

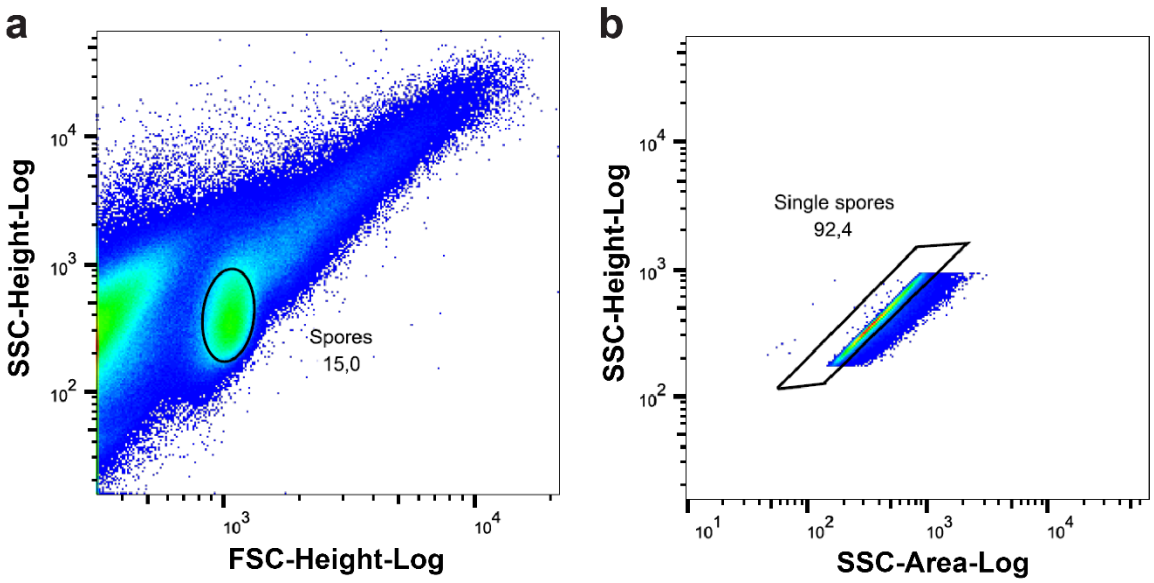

Figure S 3.3

Spore events selection based on scattered light. ***a****, Spores selection by using gates in the SSC-Height-Log versus FSC-Height-Log graph based on their size.* ***b****, Selection of single spores by using gates in the SSC-Height-Log versus SSC-Area-Log graph since events that correspond to doublets generate a lower ratio height vs area. Warm colors indicate highest density of spores.*

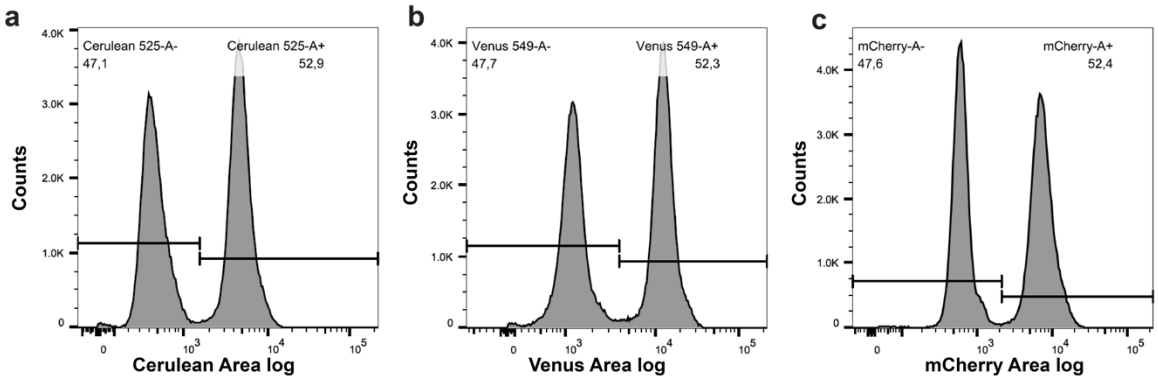

Figure S 3.4

Fluorescence intensity distribution in spores. *Example of spore from a 348 × W303 diploid hemizygote for markers C, Y, and R.*

Table S 3.1 Mutation patterns obtained in Canr colonies from day 9 incubation

Clone	Mutation type			Position from ATG	Sequence
DBY746					
1	Base substitution	G → A	Stop codon	530	TCTT**G**GGCA
2	Deletion	C	Frameshift	1042	GAC**C**CTAAA
	Deletion	T		1173	GCAAA**T**TCA
3	Base substitution	A → G	Ile → Val	1600	TCT**A**TTTTC
	Base substitution	C → A	Ala → Asp	290	ATTG**C**CCTT
4	Base substitution	C → A	Ser → Tyr	1193	GGTT**C**CCGT
5	Base substitution	C → A	Ala → Asp	1094	ATTG**C**TATT
6	No PCR				
7	Base substitution	A → G	Thr → Ala	538	ATC**A**CTTTT
8	Base substitution	A → G	Glu → Gly	32	ATAG**A**GGAG
	Base substitution	G → C	Ala → Pro	1429	CAA**G**CTTTG
	Deletion	T	Frameshift	1433	GCTT**T**GAAA
9	Deletion	T	Frameshift	1324	GAGACA**T**CT
10	Deletion	TAT	Frameshift		CTAT**TAT**TC
DBY746-*Sp*Swi6-*Sp*Clr4					
1	Base substitution	C → A	Thr → Lys	311	GGTA**C**AGGT
2	Deletion	C	Frameshift	1042	GAC**C**CTAAA
3	Base substitution	G → C	Ala → Pro	691	GTC**G**CTTCC
4	Base substitution	G → T	Gly → Cys	670	TAC**G**GTGAA
5	Base substitution	G → T	Val → Phe	1264	GGT**G**TTCCA
6	Base substitution	C → A	Stop codon	1035	CCATA**C**AAT
7	Deletion	C	Frameshift	1587	GCTGC**C**GCC
8	Base substitution	C → T	Ser → Phe	1163	ATTT**C**TGCC
9	Base substitution	C → A	Thr → Lys	887	TTCA**C**ATTT
10	Base substitution	G → T	Gly → Val	671	TACG**G**TGAA

Table S 3.2 Yeast strains used in this study

Strain	Genotype	Reference
W303	*MATa leu2-3,112 trp1-1 can1-100 ura3-1 ade2-1 his3-11,15*	Rothstein et al. (Rothstein, 1983)
ML29	*MATa leu2-3,112 trp1-1 can1-100 ura3-1 ade2-1 his3-11,15 pCM189-SpSwi6 p413-MET-SpClr4*	This study
TMS1-1A	*MATa his3-Δ1 leu2-Δ1 ura3-Δ0 ade2-801 lys2-801 LYS2::TETR-GFP nup49-Δ::HPHMX6 pASZ11-NupNop*	Albert et al. (Albert et al., 2013)
ML30	*MATa his3-Δ1 leu2-Δ1 ura3-Δ0 ade2-801 lys2-801 LYS2::TETR-GFP nup49-Δ::HPHMX6 pASZ11-NupNop pCM189-SpSwi6 p413-MET-SpClr4*	This study
LMY52	*MATa ade2-1 can1-100 his3-11,15::LacI-GFP:HIS3 leu2-3,112 trp1-1 ura3-1 INO1:LacO128:URA3 SEC63-13myc::kan^r ADE2:Nup49GFP_Nop1RFP*	Brickner et al. (Brickner et al., 2012)
ML31	*MATa ade2-1 can1-100 his3-11,15::LacI-GFP:HIS3 leu2-3,112 ura3-1 INO1:LacO128:URA3 SEC63-13myc::kan^r ADE2:Nup49GFP_Nop1RFP trp1-1::SpSwi6^{6FLAG}-SpClr4:TRP1*	This study
DBY746	*MATα leu2-3,112 his3Δ1 trp1-289a ura3-52 GAL+*	Wei et al (Wei et al., 2008)
ML32	*MATα leu2-3,112 his3Δ1 ura3-52 GAL+ trp1-289a::SpSwi6^{6FLAG}-SpClr4:TRP1*	This study
ML33	*MATα leu2-3,112 his3Δ1 trp1-289a ura3-52 GAL+ hxt13::URA3*	This study
ML34	*MATα leu2-3,112 his3Δ1 ura3-52 GAL+ trp1-289a::SpSwi6^{6FLAG}-SpClr4:TRP1 hxt13::URA3*	This study
348 (SK1-XI-R4C5Y6)	*MATα URA$^+$ NatMX KanMX hygro^s trp1-1 XI-R4C5Y6*	Raffoux et al. (Raffoux et al., 2018)
400 (SK1-XI-Y6C7R8)	*MATα URA$^+$ NatMX KanMX hygro^s trp1-1 XI-Y6C7R8*	Raffoux et al. (Raffoux et al., 2018)
369 (SK1-XI-R8Y9C10)	*MATα URA$^+$ NatMX KanMX hygro^s trp1-1 XI-R8Y9C10*	Raffoux et al. (Raffoux et al., 2018)

ML34	*MATα URA^{+} NatMX KanMX hygro^{s} XI-R4C5Y6 trp1-1::SpSwi6^{6FLAG}-SpClr4:TRP1*	This study
ML35	*MATα URA^{+} NatMX KanMX hygro^{s} trp1-1 XI-Y6C7R8 trp1-1::SpSwi6^{6FLAG}-SpClr4:TRP1*	This study
ML36	*MATα URA^{+} NatMX KanMX hygro^{s} trp1-1 XI-R8Y9C10 trp1-1::SpSwi6^{6FLAG}-SpClr4:TRP1*	This study
ML37	*MATa leu2-3,112 can1-100 ura3-1 ade2-1 his3-11,15 trp1-1::SpSwi6^{6FLAG}-SpClr4:TRP1*	This study
ML38	*348 × W303*	This study
ML39	*400 × W303*	This study
ML40	*369 × W303*	This study
ML41	*348- trp1-1::SpSwi6^{6FLAG}-SpClr4:TRP1 × W303- trp1-1::SpSwi6^{6FLAG}-SpClr4:TRP1*	This study
ML42	*400- trp1-1::SpSwi6^{6FLAG}-SpClr4:TRP1 × W303- trp1-1::SpSwi6^{6FLAG}-SpClr4:TRP1*	This study
ML43	*369- trp1-1::SpSwi6^{6FLAG}-SpClr4:TRP1 × W303- trp1-1::SpSwi6^{6FLAG}-SpClr4:TRP1*	This study

Table S 3.3 Plasmids used in this study

Plasmid	Description	Reference
pET30a-*Sp*Swi6	*Sp*Swi6 expression in bacteria	Canzio et al. (Canzio et al., 2011)
2CT[1]-*Sp*Clr4	*Sp*Clr4 cloning vector	Geeta Narlikar, UCSF, USA
pCM189	Yeast centromeric expression vector driven by the tetO-CYC1 promoter	ATCC 87661
p413-ADH1	Low copy number shuttle expression vector ADH1 promoter	ATCC 87370
p413-MET17	Low copy number shuttle expression vector MET17 promoter	This study
pCM189-*Sp*Swi6	*Sp*Swi6 expression under tetO-CYC1	This study
p413-MET-*Sp*Clr4	*Sp*Clr4 expression under MET17	This study
YIp204-PADH1-atTIR1-9myc	for integration of the F-box protein TIR1-9myc cassette	Addgene 99532, unpublished Ulrich lab
YIp204-MET17-*Sp*Clr4	for integration of the *Sp*Clr4 cassette	This study
YIp204-tetO7-*Sp*Swi6-MET17-*Sp*Clr4	for integration of the *Sp*swi6-*Sp*Clr4 cassette	This study
YIp204-tetO7-*Sp*Swi6-6FLAG-MET17-*Sp*Clr4	for integration of the *Sp*Swi6-6FLAG-*Sp*Clr4 cassette	This study

Chapitre 4 Discussion

How the eukaryotic cell organizes and reorganizes its genome under changing conditions remains an open question. By studying environmental and evolutionary adaptations driven by chromatin organization, I hope that the work I describe here contributes to understanding of their underlying biochemical mechanisms and how these are reflected in chromatin mechanical properties and phase separation on local to global levels. On immediate time scales we have shown that local changes in the mechanics of a gene locus reflect post-translational modifications of histones that mediate phase separation of the transcriptionally active chromatin and its partitioning to nuclear envelope, an adaptation that results in efficient coupling of transcription-transport-translation. On the evolutionary scale, we have asked how a specific characteristic of the *S. cerevisiae* genome, its decompaction, may have contributed to evolutionary adaptations. These adaptations include the dense gene structure and removal of vast numbers of duplicate genes following a whole genome duplication process, that may have occurred due to a high rate of genome rearrangements that we show occurs in the less compact *S. cerevisiae* genome. Below, I further discuss implications of these phenomena and where we go from here to answer outstanding questions about functional genome organization and dynamics.

4.1 The generality of locus PPPS of chromatin to NE partitioning of other stress genes

In the first part of this dissertation, I describe how we discovered a mechanism by which the stress inducible gene *INO1* partitions to the NE and we showed how the *cis* elements (GRSs) position the chromatin modifying enzymes necessary to induce local PPPS. GRSs have been described in other loci that partition to the NE, including *TSA2* and the *GAL1-10* (Ahmed et al., 2010; Brickner et al., 2016). In the case of *GAL1-10*, two main GRSs have been characterized, GRS4 and GRS5, both located in the shared promoter of these genes

(Brickner et al., 2016). Previous studies have also shown that *GAL1-10* loci show similar dynamic behavior as *INO1* in repressed *versus* induced conditions (Cabal et al., 2006), with confined and stiffer movement closer to the NE when activated and less confined and more flexible when repressed. Additionally, SAGA complex subunits have been shown to be essential for this relocalization event, highlighting the role of chromatin remodeling and probably acetylation for changes in the local mechanical properties of chromatin at these loci. There are more than 280 GRSI sites in the yeast genome and more than a third are located in promoters, suggesting that a large number of gene loci could undergo nucleoplasm-NE partitioning. Additionally, analyses of the locations of GRSI sites correlate with locations of heat shock-responsive genes (Ahmed et al., 2010). If, as for *INO1*, these GRSs are nucleation sites for chromatin remodeling complexes that promote phase separation of the local chromatin, then nucleoplasm-NE partitioning may be more common than currently known. Furthermore, GRSs need not be in promoters. For instance, the GRSII site is located in the middle of the coding region of a gene upstream of the *INO1* locus. The fact that such a *cis* element may not be located in the promoter of the gene they control means that many more of these sites could regulate local chromatin properties in this context to make more efficient responses to different stresses.

4.2 *INO1* transcriptional memory, another phase separated domain?

A problem that remains to be answered about *INO1* expression is the mechanism of memory for NE localization. Upon repression of previously activated and NE partitioned genes, these loci remain at the nuclear periphery for several generations. For example, *INO1* remains at the NE for about 12h (about 6 cell cycles) after repression and *GAL1-10* for the replicative lifespan of yeast. Transcriptional memory also depends on local nucleosome structure and histone composition. For instance, the histone variant H2A.Z is incorporated into nucleosomes of the *INO1* promoter after cells are returned to repressing conditions, and this modification has been proven essential to transcriptional memory for both *INO1* and *GAL1* loci (Brickner et al., 2007). For instance, nucleosome positioning and occupancy analyses at the *INO1* promoter during different phases of its

activation-repression has revealed that the protection in the short-term repressed state decreases compared to the long-term repressed state. According to our observations of the dynamics of the histone turnover for the activation *versus* repressed states of the *INO1* locus, the new H2A.Z present at the gene could maintain the chromatin in its decompacted state. It would thus be interesting to investigate whether H2A.Z association with nucleosomes could maintain the phase separation of *INO1* locus from the nucleoplasm in the repressed state. Interestingly, another *cis* element called the "memory recruitment sequence" (MRS) encompassing 11 base pairs in the *INO1* promoter has been described to control both NE localization memory as well as H2A.Z incorporation after recent repression (Light et al., 2010). Also, chromatin remodeling proteins such as the Swr1 complex are essential to maintain this memory state. We hypothesize that H2A.Z-mediated memory represents a different epigenetic state than that of the activated and repressed genes that, like histone acetylation, disrupts multivalent histone-histone and histone-DNA interactions necessary for the *INO1* locus to partition to the nucleoplasmic phase (Gibson et al., 2019). Our theory is that this could constitute another domain that is also phase separated from the surrounding chromatin with its own set of epigenetic histone modifications and remodeling complexes recognizing and binding to the local chromatin.

4.3 Role of Swi6-heterochromatin in shaping *S. cerevisiae* genome architecture

In the second part of this work, we have shown that expressing the heterochromatin proteins *Sp*Swi6/*Sp*Clr4 that were lost during evolution, could re-establish chromatin compaction in *S. cerevisiae*, could change genome stability and possibly explain how this organism was able to evolve as it did. Studies using different techniques, including advanced chromatin conformation capture (Duan et al., 2010; Hsieh et al., 2015), and electron microscopy (Chen et al., 2016) have not shown any kind of compact chromatin structures in budding yeast. The ovoid shape that the nucleus adopts after expressing the *Sp*Swi6/*Sp*Clr4 proteins suggests that the nuclear envelope has lost components necessary to maintain its shape. The collapse of the nucleus into an ovoid structure

following expression of *Sp*Swi6/*Sp*Clr4 could reflect compaction of the chromosome arms. This follows from the Rabl configuration of the yeast chromosomes, in which centromeres are clustered and attached to the SPB and telomeres are tethered to the NE (Berger et al., 2008; Bystricky et al., 2005; Cremer and Cremer, 2001; Rabl, 1885; Verdaasdonk et al., 2013). Like a shrinking cone, the compaction of the chromosomes should compress the NE axis orthogonal to the SPB-nucleolar axis.

Telomeres, located at the nuclear periphery, are among the different components defining yeast genome architecture. It has been observed that some telomeres are clustered at the nuclear periphery, depending on the length of each specific chromosome arm, with some short arms with similar length having more contacts. For example, the right and left arms of the short chromosomes III and VI show more contacts with each other than with other chromosomes (Bystricky et al., 2005). However, this is not a general rule since other chromosome arms with the same length are located far apart from each other and all telomere ends are dynamic and can be found at different positions at the periphery or in the nucleoplasm. We do not know if by expressing the *Sp*Swi6/*Sp*Clr4 proteins, all chromosomes are equally affected and whether clustering of telomeres could be rearranged. Since it has been ruled out that conserved terminal $TG_{1–3}$ sequences and subtelomeric X and/or Y' elements are the cause behind these telomere interactions (Bystricky et al., 2005; Schober et al., 2008), it would be interesting to study how expression of *Sp*Swi6/*Sp*Clr4 affects the positioning of telomeres and the architecture of the nucleus. One could do this by imaging telomeres in cells expressing the *Sp*Swi6/*Sp*Clr4 by directly tagging both right and left telomeres of each chromosome with LacO/LacI-GFP arrays to determine how their anchoring to the nuclear periphery changes.

Chromosome conformation capture studies of the budding yeast nucleus have shown that there is a weakly defined spatial distribution of chromosomes that resembles nuclear territories found in many higher eukaryotes (Duan et al., 2010). Additionally, it has also been shown that the shorter chromosomes (I, III and VI) are more prone to interact with

others while the larger ones, such as XII and IV, are mainly isolated. This may be because the shorter arms are crowded towards one of the poles that the bundle of chromosomes adopt in the Rabl conformation, which increases the probabilities of their interacting. Conversely, the remote regions where the long chromosome arms are located are less crowded, making the probability of contacts with other chromosomes lower. It will be interesting to see whether shortening of the chromosome arms in the cells expressing *Sp*Swi6/*Sp*Clr4 could result in structures resembling other eukaryotes. A recent higher resolution study of the *S. cerevisiae* genome interactions (Micro-C) has also revealed that there are self-associating domains that were not observed before but are much smaller (around 5 kb) than those of other eukaryotes (Hsieh et al., 2015). It would be interesting as well to analyze how the contacts between different chromosomal regions are arranged and if the sizes of the domains increase in cells expressing *Sp*Swi6/*Sp*Clr4.

Another feature observed in conformation capture studies in *S. cerevisiae* is the remarkably different configuration of chromosome XII. Apart from being completely separated from the rest of the genome, the pattern of intra-chromosomal interactions is split into three distinct segments, with rDNA acting as a barrier to interactions between the chromosome ends (Duan et al., 2010). Nucleolus imaging in the *Sp*Swi6*/Sp*Clr4 expressing cells did not show any change in nucleolus morphology, but this organelle appears to be smaller, a feature worth further study with super resolution imaging.

4.4 Biotechnological applications of a more stable genome in yeast

Though already discussed in Chapter 3, other applications of an *S. cerevisiae* strain expressing *Sp*Swi6*/Sp*Clr4 can be imagined. For example, considering the many yeast species that could be exploited for research and biotechnology, only a few have seen applications in biotechnology. For instance, many species in the Saccharomycotina subphylum have potential with this purpose, given the variety of carbon sources they can ferment. Examples include species that can utilize D-xylose (*Scheffersomyces (P.) stipitis* and *Spathaspora passalidarum*), methanol (*K. pastoris)*, and other unconventional carbon

sources to grow, as well as the capacity to produce complex compounds such as vitamins (*Eremothecium gossypii*) and lipids (*Yarrowia lipolytica)* in large quantities. Also, different clades in this subphylum express a set of enzymes and pathways that could be exploited to produce compounds difficult to synthesize. Furthermore, the capacity for sexual recombination across Ascomycota, a trait that may have contributed to metabolic adaptability, can also be exploited to select for fitter strains that produce higher yields of desired products. However, the maintenance of desired traits in these species can be difficult, due to the high rates of recombination resulting in deletions of integrated genes. Expression of *Sp*Swi6*/Sp*Clr4 could enhance stability of such engineered yeasts.

References

A, P., and Weber, S.C. (2019). Evidence for and against Liquid-Liquid Phase Separation in the Nucleus. Noncoding RNA *5*, 50.

Abbott, D.W., Ivanova, V.S., Wang, X., Bonner, W.M., and Ausio, J. (2001). Characterization of the stability and folding of H2A.Z chromatin particles: implications for transcriptional activation. The Journal of biological chemistry *276*, 41945-41949.

Abshiru, N., Ippersiel, K., Tang, Y., Yuan, H., Marmorstein, R., Verreault, A., and Thibault, P. (2013). Chaperone-mediated acetylation of histones by Rtt109 identified by quantitative proteomics. Journal of proteomics *81*, 80-90.

Ahmed, S., Brickner, D.G., Light, W.H., Cajigas, I., McDonough, M., Froyshteter, A.B., Volpe, T., and Brickner, J.H. (2010). DNA zip codes control an ancient mechanism for gene targeting to the nuclear periphery. Nature cell biology *12*, 111-118.

Ahmed, S., and Brickner, J.H. (2010). A role for DNA sequence in controlling the spatial organization of the genome. Nucleus (Austin, Tex) *1*, 402-406.

Albert, B., Mathon, J., Shukla, A., Saad, H., Normand, C., Léger-Silvestre, I., Villa, D., Kamgoue, A., Mozziconacci, J., Wong, H.*, et al.* (2013). Systematic characterization of the conformation and dynamics of budding yeast chromosome XII. The Journal of cell biology *202*, 201-210.

Albert, I., Mavrich, T.N., Tomsho, L.P., Qi, J., Zanton, S.J., Schuster, S.C., and Pugh, B.F. (2007). Translational and rotational settings of H2A.Z nucleosomes across the Saccharomyces cerevisiae genome. Nature *446*, 572-576.

Alberti, S., Gladfelter, A., and Mittag, T. (2019). Considerations and Challenges in Studying Liquid-Liquid Phase Separation and Biomolecular Condensates. Cell *176*, 419-434.

Allshire, R.C., and Madhani, H.D. (2018). Ten principles of heterochromatin formation and function. Nat Rev Mol Cell Biol *19*, 229-244.

Altmeyer, M., Neelsen, K.J., Teloni, F., Pozdnyakova, I., Pellegrino, S., Grofte, M., Rask, M.B., Streicher, W., Jungmichel, S., Nielsen, M.L.*, et al.* (2015). Liquid demixing of intrinsically disordered proteins is seeded by poly(ADP-ribose). Nature communications *6*, 8088.

Arents, G., Burlingame, R.W., Wang, B.C., Love, W.E., and Moudrianakis, E.N. (1991). The nucleosomal core histone octamer at 3.1 A resolution: a tripartite protein assembly and a left-handed superhelix. Proceedings of the National Academy of Sciences of the United States of America *88*, 10148-10152.

Arents, G., and Moudrianakis, E.N. (1995). The histone fold: a ubiquitous architectural motif utilized in DNA compaction and protein dimerization. Proceedings of the National Academy of Sciences of the United States of America *92*, 11170-11174.

Argueso, J.L., Carazzolle, M.F., Mieczkowski, P.A., Duarte, F.M., Netto, O.V., Missawa, S.K., Galzerani, F., Costa, G.G., Vidal, R.O., Noronha, M.F.*, et al.* (2009). Genome structure of a Saccharomyces cerevisiae strain widely used in bioethanol production. Genome Res *19*, 2258-2270.

Backlund, M.P., Joyner, R., Weis, K., and Moerner, W.E. (2014). Correlations of three-dimensional motion of chromosomal loci in yeast revealed by the double-helix point spread function microscope. Molecular biology of the cell *25*, 3619-3629.

Banani, S.F., Lee, H.O., Hyman, A.A., and Rosen, M.K. (2017). Biomolecular condensates: organizers of cellular biochemistry. Nature Reviews Molecular Cell Biology *18*, 285.

Bannister, A.J., and Kouzarides, T. (2011). Regulation of chromatin by histone modifications. Cell research *21*, 381-395.

Bannister, A.J., Zegerman, P., Partridge, J.F., Miska, E.A., Thomas, J.O., Allshire, R.C., and Kouzarides, T. (2001). Selective recognition of methylated lysine 9 on histone H3 by the HP1 chromo domain. Nature *410*, 120-124.
Barton, A.B., Pekosz, M.R., Kurvathi, R.S., and Kaback, D.B. (2008). Meiotic recombination at the ends of chromosomes in Saccharomyces cerevisiae. Genetics *179*, 1221-1235.
Basso, L.C., de Amorim, H.V., de Oliveira, A.J., and Lopes, M.L. (2008). Yeast selection for fuel ethanol production in Brazil. FEMS Yeast Res *8*, 1155-1163.
Becker, P.B., and Horz, W. (2002). ATP-dependent nucleosome remodeling. Annual review of biochemistry *71*, 247-273.
Berger, A.B., Cabal, G.G., Fabre, E., Duong, T., Buc, H., Nehrbass, U., Olivo-Marin, J.C., Gadal, O., and Zimmer, C. (2008). High-resolution statistical mapping reveals gene territories in live yeast. Nat Methods *5*, 1031-1037.
Bergeron-Sandoval, L.P., Safaee, N., and Michnick, S.W. (2016). Mechanisms and Consequences of Macromolecular Phase Separation. Cell *165*, 1067-1079.
Berndsen, C.E., Tsubota, T., Lindner, S.E., Lee, S., Holton, J.M., Kaufman, P.D., Keck, J.L., and Denu, J.M. (2008). Molecular functions of the histone acetyltransferase chaperone complex Rtt109-Vps75. Nature structural & molecular biology *15*, 948-956.
Bernstein, B.E., Kamal, M., Lindblad-Toh, K., Bekiranov, S., Bailey, D.K., Huebert, D.J., McMahon, S., Karlsson, E.K., Kulbokas, E.J., 3rd, Gingeras, T.R.*, et al.* (2005). Genomic maps and comparative analysis of histone modifications in human and mouse. Cell *120*, 169-181.
Blobel, G. (1985). Gene gating: a hypothesis. Proceedings of the National Academy of Sciences of the United States of America *82*, 8527-8529.
Bloom, K., and Kolbin, D. (2022). Mechanisms of DNA Mobilization and Sequestration. Genes *13*.
Bloom, K.S. (2008). Beyond the code: the mechanical properties of DNA as they relate to mitosis. Chromosoma *117*, 103-110.
Boeynaems, S., Alberti, S., Fawzi, N.L., Mittag, T., Polymenidou, M., Rousseau, F., Schymkowitz, J., Shorter, J., Wolozin, B., Van Den Bosch, L.*, et al.* (2018). Protein Phase Separation: A New Phase in Cell Biology. Trends in cell biology *28*, 420-435.
Bolzer, A., Kreth, G., Solovei, I., Koehler, D., Saracoglu, K., Fauth, C., Müller, S., Eils, R., Cremer, C., Speicher, M.R.*, et al.* (2005). Three-Dimensional Maps of All Chromosomes in Human Male Fibroblast Nuclei and Prometaphase Rosettes. PLoS biology *3*, e157.
Borneman, A.R., Desany, B.A., Riches, D., Affourtit, J.P., Forgan, A.H., Pretorius, I.S., Egholm, M., and Chambers, P.J. (2011). Whole-genome comparison reveals novel genetic elements that characterize the genome of industrial strains of Saccharomyces cerevisiae. PLoS Genet *7*, e1001287.
Boulon, S., Westman, B.J., Hutten, S., Boisvert, F.M., and Lamond, A.I. (2010). The nucleolus under stress. Molecular cell *40*, 216-227.
Brackley, C.A., Johnson, J., Kelly, S., Cook, P.R., and Marenduzzo, D. (2016). Simulated binding of transcription factors to active and inactive regions folds human chromosomes into loops, rosettes and topological domains. Nucleic acids research *44*, 3503-3512.
Brangwynne, C.P. (2013). Phase transitions and size scaling of membrane-less organelles. The Journal of cell biology *203*, 875-881.
Brangwynne, C.P., Eckmann, C.R., Courson, D.S., Rybarska, A., Hoege, C., Gharakhani, J., Julicher, F., and Hyman, A.A. (2009). Germline P granules are liquid droplets that localize by controlled dissolution/condensation. Science (New York, NY) *324*, 1729-1732.
Brangwynne, C.P., Mitchison, T.J., and Hyman, A.A. (2011). Active liquid-like behavior of nucleoli determines their size and shape in Xenopus laevis oocytes. Proceedings of the National Academy of Sciences of the United States of America *108*, 4334-4339.

Brickner, D.G., Ahmed, S., Meldi, L., Thompson, A., Light, W., Young, M., Hickman, T.L., Chu, F., Fabre, E., and Brickner, J.H. (2012). Transcription factor binding to a DNA zip code controls interchromosomal clustering at the nuclear periphery. Developmental cell *22*, 1234-1246.
Brickner, D.G., Cajigas, I., Fondufe-Mittendorf, Y., Ahmed, S., Lee, P.C., Widom, J., and Brickner, J.H. (2007). H2A.Z-mediated localization of genes at the nuclear periphery confers epigenetic memory of previous transcriptional state. PLoS biology *5*, e81.
Brickner, D.G., Sood, V., Tutucci, E., Coukos, R., Viets, K., Singer, R., and Brickner, J.H. (2016). Subnuclear positioning and interchromosomal clustering of the GAL1-10 locus are controlled by separable, interdependent mechanisms. Molecular biology of the cell.
Brickner, J.H., and Walter, P. (2004). Gene recruitment of the activated INO1 locus to the nuclear membrane. PLoS biology *2*, e342.
Brown, C.R., Kennedy, C.J., Delmar, V.A., Forbes, D.J., and Silver, P.A. (2008). Global histone acetylation induces functional genomic reorganization at mammalian nuclear pore complexes. Genes & development *22*, 627-639.
Brown, K.E., Baxter, J., Graf, D., Merkenschlager, M., and Fisher, A.G. (1999). Dynamic repositioning of genes in the nucleus of lymphocytes preparing for cell division. Molecular cell *3*, 207-217.
Brownell, J.E., Zhou, J., Ranalli, T., Kobayashi, R., Edmondson, D.G., Roth, S.Y., and Allis, C.D. (1996). Tetrahymena histone acetyltransferase A: a homolog to yeast Gcn5p linking histone acetylation to gene activation. Cell *84*, 843-851.
Bystricky, K., Heun, P., Gehlen, L., Langowski, J., and Gasser, S.M. (2004). Long-range compaction and flexibility of interphase chromatin in budding yeast analyzed by high-resolution imaging techniques. Proc Natl Acad Sci U S A *101*, 16495-16500.
Bystricky, K., Laroche, T., van Houwe, G., Blaszczyk, M., and Gasser, S.M. (2005). Chromosome looping in yeast: telomere pairing and coordinated movement reflect anchoring efficiency and territorial organization. The Journal of cell biology *168*, 375-387.
Cabal, G.G., Genovesio, A., Rodriguez-Navarro, S., Zimmer, C., Gadal, O., Lesne, A., Buc, H., Feuerbach-Fournier, F., Olivo-Marin, J.C., Hurt, E.C*., et al.* (2006). SAGA interacting factors confine sub-diffusion of transcribed genes to the nuclear envelope. Nature *441*, 770-773.
Canzio, D., Chang, E.Y., Shankar, S., Kuchenbecker, K.M., Simon, M.D., Madhani, H.D., Narlikar, G.J., and Al-Sady, B. (2011). Chromodomain-mediated oligomerization of HP1 suggests a nucleosome-bridging mechanism for heterochromatin assembly. Molecular cell *41*, 67-81.
Carro, D., and Piña, B. (2001). Genetic analysis of the karyotype instability in natural wine yeast strains. Yeast *18*, 1457-1470.
Casolari, J.M., Brown, C.R., Komili, S., West, J., Hieronymus, H., and Silver, P.A. (2004). Genome-wide localization of the nuclear transport machinery couples transcriptional status and nuclear organization. Cell *117*, 427-439.
Chang, B., Chen, Y., Zhao, Y., and Bruick, R.K. (2007). JMJD6 is a histone arginine demethylase. Science (New York, NY) *318*, 444-447.
Chen, C., and Kolodner, R.D. (1999). Gross chromosomal rearrangements in Saccharomyces cerevisiae replication and recombination defective mutants. Nature Genetics *23*, 81-85.
Chen, C., Lim, H.H., Shi, J., Tamura, S., Maeshima, K., Surana, U., and Gan, L. (2016). Budding yeast chromatin is dispersed in a crowded nucleoplasm in vivo. Molecular biology of the cell *27*, 3357-3368.
Chen, C.C., Carson, J.J., Feser, J., Tamburini, B., Zabaronick, S., Linger, J., and Tyler, J.K. (2008). Acetylated lysine 56 on histone H3 drives chromatin assembly after repair and signals for the completion of repair. Cell *134*, 231-243.

Chen, D., Ma, H., Hong, H., Koh, S.S., Huang, S.M., Schurter, B.T., Aswad, D.W., and Stallcup, M.R. (1999). Regulation of transcription by a protein methyltransferase. Science (New York, NY) *284*, 2174-2177.
Cheng, T.M., Heeger, S., Chaleil, R.A., Matthews, N., Stewart, A., Wright, J., Lim, C., Bates, P.A., and Uhlmann, F. (2015). A simple biophysical model emulates budding yeast chromosome condensation. eLife *4*, e05565.
Cherry, J.M., Hong, E.L., Amundsen, C., Balakrishnan, R., Binkley, G., Chan, E.T., Christie, K.R., Costanzo, M.C., Dwight, S.S., Engel, S.R*., et al.* (2012). Saccharomyces Genome Database: the genomics resource of budding yeast. Nucleic Acids Res *40*, D700-705.
Chi, Q., Wang, G., and Jiang, J. (2013). The persistence length and length per base of single-stranded DNA obtained from fluorescence correlation spectroscopy measurements using mean field theory. Physica A: Statistical Mechanics and its Applications *392*, 1072-1079.
Clapier, C.R., and Cairns, B.R. (2009). The biology of chromatin remodeling complexes. Annual review of biochemistry *78*, 273-304.
Crane, E., Bian, Q., McCord, R.P., Lajoie, B.R., Wheeler, B.S., Ralston, E.J., Uzawa, S., Dekker, J., and Meyer, B.J. (2015). Condensin-driven remodelling of X chromosome topology during dosage compensation. Nature *523*, 240-244.
Cremer, T., and Cremer, C. (2001). Chromosome territories, nuclear architecture and gene regulation in mammalian cells. Nature reviews Genetics *2*, 292-301.
Cui, Y., and Bustamante, C. (2000). Pulling a single chromatin fiber reveals the forces that maintain its higher-order structure. Proceedings of the National Academy of Sciences of the United States of America *97*, 127-132.
Dao, T.P., Kolaitis, R.-M., Kim, H.J., O'Donovan, K., Martyniak, B., Colicino, E., Hehnly, H., Taylor, J.P., and Castañeda, C.A. (2018). Ubiquitin Modulates Liquid-Liquid Phase Separation of UBQLN2 via Disruption of Multivalent Interactions. Molecular cell *69*, 965-978.e966.
Datta, A., Adjiri, A., New, L., Crouse, G.F., and Jinks Robertson, S. (1996). Mitotic crossovers between diverged sequences are regulated by mismatch repair proteins in Saccaromyces cerevisiae. Mol Cell Biol *16*, 1085-1093.
Dekker, J., Rippe, K., Dekker, M., and Kleckner, N. (2002). Capturing chromosome conformation. Science *295*, 1306-1311.
Dietrich, F.S., Voegeli, S., Brachat, S., Lerch, A., Gates, K., Steiner, S., Mohr, C., Pöhlmann, R., Luedi, P., Choi, S*., et al.* (2004). The Ashbya gossypii genome as a tool for mapping the ancient Saccharomyces cerevisiae genome. Science *304*, 304-307.
Dion, M.F., Altschuler, S.J., Wu, L.F., and Rando, O.J. (2005). Genomic characterization reveals a simple histone H4 acetylation code. Proceedings of the National Academy of Sciences of the United States of America *102*, 5501-5506.
Dixon, J.R., Selvaraj, S., Yue, F., Kim, A., Li, Y., Shen, Y., Hu, M., Liu, J.S., and Ren, B. (2012). Topological domains in mammalian genomes identified by analysis of chromatin interactions. Nature *485*, 376-380.
Dong, P., Tu, X., Chu, P.Y., Lu, P., Zhu, N., Grierson, D., Du, B., Li, P., and Zhong, S. (2017). 3D Chromatin Architecture of Large Plant Genomes Determined by Local A/B Compartments. Mol Plant *10*, 1497-1509.
Dong, Q., Li, N., Li, X., Yuan, Z., Xie, D., Wang, X., Li, J., Yu, Y., Wang, J., Ding, B*., et al.* (2018). Genome-wide Hi-C analysis reveals extensive hierarchical chromatin interactions in rice. The Plant journal : for cell and molecular biology *94*, 1141-1156.
Dormidontova, E.E., Grosberg, A.Y., and Khokhlov, A.R. (1992). Intramolecular phase separation of a copolymer chain with mobile primary structure. Macromolecular Theory and Simulations *1*, 375-385.

Downs, J.A., Kosmidou, E., Morgan, A., and Jackson, S.P. (2003). Suppression of homologous recombination by the Saccharomyces cerevisiae linker histone. Molecular cell *11*, 1685-1692.
Driscoll, R., Hudson, A., and Jackson, S.P. (2007). Yeast Rtt109 Promotes Genome Stability by Acetylating Histone H3 on Lysine 56. Science (New York, NY) *315*, 649-652.
Duan, M.R., and Smerdon, M.J. (2014). Histone H3 lysine 14 (H3K14) acetylation facilitates DNA repair in a positioned nucleosome by stabilizing the binding of the chromatin Remodeler RSC (Remodels Structure of Chromatin). The Journal of biological chemistry *289*, 8353-8363.
Duan, Z., Andronescu, M., Schutz, K., McIlwain, S., Kim, Y.J., Lee, C., Shendure, J., Fields, S., Blau, C.A., and Noble, W.S. (2010). A three-dimensional model of the yeast genome. Nature *465*, 363-367.
Dujon, B., Sherman, D., Fischer, G., Durrens, P., Casaregola, S., Lafontaine, I., De Montigny, J., Marck, C., Neuvéglise, C., Talla, E.*, et al.* (2004). Genome evolution in yeasts. Nature *430*, 35-44.
Durant, M., and Pugh, B.F. (2006). Genome-wide relationships between TAF1 and histone acetyltransferases in Saccharomyces cerevisiae. Molecular and cellular biology *26*, 2791-2802.
Eissenberg, J.C., and Elgin, S.C. (2014). HP1a: a structural chromosomal protein regulating transcription. Trends in genetics : TIG *30*, 103-110.
Elbaum-Garfinkle, S., Kim, Y., Szczepaniak, K., Chen, C.C., Eckmann, C.R., Myong, S., and Brangwynne, C.P. (2015). The disordered P granule protein LAF-1 drives phase separation into droplets with tunable viscosity and dynamics. Proceedings of the National Academy of Sciences of the United States of America *112*, 7189-7194.
Emre, N.C., Ingvarsdottir, K., Wyce, A., Wood, A., Krogan, N.J., Henry, K.W., Li, K., Marmorstein, R., Greenblatt, J.F., Shilatifard, A.*, et al.* (2005). Maintenance of low histone ubiquitylation by Ubp10 correlates with telomere-proximal Sir2 association and gene silencing. Molecular cell *17*, 585-594.
Erdel, F., and Rippe, K. (2011). Chromatin remodelling in mammalian cells by ISWI-type complexes--where, when and why? The FEBS journal *278*, 3608-3618.
Erdel, F., and Rippe, K. (2018). Formation of Chromatin Subcompartments by Phase Separation. Biophysical journal *114*, 2262-2270.
Fabrizio, P., Battistella, L., Vardavas, R., Gattazzo, C., Liou, L.L., Diaspro, A., Dossen, J.W., Gralla, E.B., and Longo, V.D. (2004). Superoxide is a mediator of an altruistic aging program in Saccharomyces cerevisiae. J Cell Biol *166*, 1055-1067.
Feric, M., and Brangwynne, C.P. (2013). A nuclear F-actin scaffold stabilizes ribonucleoprotein droplets against gravity in large cells. Nature cell biology *15*, 1253-1259.
Ferrai, C., de Castro, I.J., Lavitas, L., Chotalia, M., and Pombo, A. (2010). Gene positioning. Cold Spring Harbor perspectives in biology *2*, a000588.
Field, Y., Kaplan, N., Fondufe-Mittendorf, Y., Moore, I.K., Sharon, E., Lubling, Y., Widom, J., and Segal, E. (2008). Distinct modes of regulation by chromatin encoded through nucleosome positioning signals. PLoS computational biology *4*, e1000216.
Finn, E.H., Pegoraro, G., Brandão, H.B., Valton, A.L., Oomen, M.E., Dekker, J., Mirny, L., and Misteli, T. (2019). Extensive Heterogeneity and Intrinsic Variation in Spatial Genome Organization. Cell *176*, 1502-1515.e1510.
Fisher, J.K., Ballenger, M., O'Brien, E.T., Haase, J., Superfine, R., and Bloom, K. (2009). DNA relaxation dynamics as a probe for the intracellular environment. Proc Natl Acad Sci U S A *106*, 9250-9255.
Flavahan, W.A., Drier, Y., Liau, B.B., Gillespie, S.M., Venteicher, A.S., Stemmer-Rachamimov, A.O., Suva, M.L., and Bernstein, B.E. (2016). Insulator dysfunction and oncogene activation in IDH mutant gliomas. Nature *529*, 110-114.

Flory, P.J., and Gee, G. (1956). Statistical thermodynamics of semi-flexible chain molecules. Proceedings of the Royal Society of London Series A Mathematical and Physical Sciences *234*, 60-73.
Franke, M., Ibrahim, D.M., Andrey, G., Schwarzer, W., Heinrich, V., Schopflin, R., Kraft, K., Kempfer, R., Jerkovic, I., Chan, W.L*., et al.* (2016). Formation of new chromatin domains determines pathogenicity of genomic duplications. Nature *538*, 265-269.
Frottin, F., Schueder, F., Tiwary, S., Gupta, R., Körner, R., Schlichthaerle, T., Cox, J., Jungmann, R., Hartl, F.U., and Hipp, M.S. (2019). The nucleolus functions as a phase-separated protein quality control compartment. Science (New York, NY) *365*, 342-347.
Gasser, S.M. (2001). Positions of potential: nuclear organization and gene expression. Cell *104*, 639-642.
Gerhold, C.B., and Gasser, S.M. (2014). INO80 and SWR complexes: relating structure to function in chromatin remodeling. Trends in cell biology *24*, 619-631.
Giaimo, B.D., Ferrante, F., Herchenrother, A., Hake, S.B., and Borggrefe, T. (2019). The histone variant H2A.Z in gene regulation. Epigenetics & chromatin *12*, 37.
Gibson, B.A., Doolittle, L.K., Schneider, M.W.G., Jensen, L.E., Gamarra, N., Henry, L., Gerlich, D.W., Redding, S., and Rosen, M.K. (2019). Organization of Chromatin by Intrinsic and Regulated Phase Separation. Cell *179*, 470-484.e421.
Godde, J.S., and Wolffe, A.P. (1996). Nucleosome assembly on CTG triplet repeats. The Journal of biological chemistry *271*, 15222-15229.
Goffeau, A., Barrell, B.G., Bussey, H., Davis, R.W., Dujon, B., Feldmann, H., Galibert, F., Hoheisel, J.D., Jacq, C., Johnston, M*., et al.* (1996). Life with 6000 genes. Science *274*, 546, 563-547.
Grunstein, M., and Gasser, S.M. (2013). Epigenetics in Saccharomyces cerevisiae. Cold Spring Harb Perspect Biol *5*.
Guelen, L., Pagie, L., Brasset, E., Meuleman, W., Faza, M.B., Talhout, W., Eussen, B.H., de Klein, A., Wessels, L., de Laat, W*., et al.* (2008). Domain organization of human chromosomes revealed by mapping of nuclear lamina interactions. Nature *453*, 948-951.
Han, J., Zhou, H., Horazdovsky, B., Zhang, K., Xu, R.M., and Zhang, Z. (2007). Rtt109 acetylates histone H3 lysine 56 and functions in DNA replication. Science (New York, NY) *315*, 653-655.
He, Y., Lawrimore, J., Cook, D., Van Gorder, E.E., De Larimat, S.C., Adalsteinsson, D., Forest, M.G., and Bloom, K. (2020). Statistical mechanics of chromosomes: in vivo and in silico approaches reveal high-level organization and structure arise exclusively through mechanical feedback between loop extruders and chromatin substrate properties. Nucleic acids research *48*, 11284-11303.
Heard, E., and Bickmore, W. (2007). The ins and outs of gene regulation and chromosome territory organisation. Current opinion in cell biology *19*, 311-316.
Heintzman, N.D., Stuart, R.K., Hon, G., Fu, Y., Ching, C.W., Hawkins, R.D., Barrera, L.O., Van Calcar, S., Qu, C., Ching, K.A*., et al.* (2007). Distinct and predictive chromatin signatures of transcriptional promoters and enhancers in the human genome. Nature genetics *39*, 311-318.
Henderson, I.R., and Bomblies, K. (2021). Evolution and Plasticity of Genome-Wide Meiotic Recombination Rates. Annu Rev Genet *55*, 23-43.
Henikoff, S. (2009). Labile H3.3+H2A.Z nucleosomes mark 'nucleosome-free regions'. Nature genetics *41*, 865-866.
Henikoff, S., and Furuyama, T. (2012). The unconventional structure of centromeric nucleosomes. Chromosoma *121*, 341-352.
Henninger, J.E., Oksuz, O., Shrinivas, K., Sagi, I., LeRoy, G., Zheng, M.M., Andrews, J.O., Zamudio, A.V., Lazaris, C., Hannett, N.M*., et al.* (2021). RNA-Mediated Feedback Control of Transcriptional Condensates. Cell *184*, 207-225 e224.

Henry, K.W., Wyce, A., Lo, W.S., Duggan, L.J., Emre, N.C., Kao, C.F., Pillus, L., Shilatifard, A., Osley, M.A., and Berger, S.L. (2003). Transcriptional activation via sequential histone H2B ubiquitylation and deubiquitylation, mediated by SAGA-associated Ubp8. Genes & development *17*, 2648-2663.
Hergeth, S.P., and Schneider, R. (2015). The H1 linker histones: multifunctional proteins beyond the nucleosomal core particle. EMBO reports *16*, 1439-1453.
Hernandez-Verdun, D., Roussel, P., Thiry, M., Sirri, V., and Lafontaine, D.L. (2010). The nucleolus: structure/function relationship in RNA metabolism. Wiley interdisciplinary reviews RNA *1*, 415-431.
Heun, P., Laroche, T., Raghuraman, M.K., and Gasser, S.M. (2001a). The positioning and dynamics of origins of replication in the budding yeast nucleus. The Journal of cell biology *152*, 385-400.
Heun, P., Laroche, T., Shimada, K., Furrer, P., and Gasser Susan, M. (2001b). Chromosome Dynamics in the Yeast Interphase Nucleus. Science (New York, NY) *294*, 2181-2186.
Hickman, M.A., Froyd, C.A., and Rusche, L.N. (2011). Reinventing heterochromatin in budding yeasts: Sir2 and the origin recognition complex take center stage. Eukaryot Cell *10*, 1183-1192.
Hnisz, D., Shrinivas, K., Young, R.A., Chakraborty, A.K., and Sharp, P.A. (2017). A Phase Separation Model for Transcriptional Control. Cell *169*, 13-23.
Hnisz, D., Weintraub, A.S., Day, D.S., Valton, A.L., Bak, R.O., Li, C.H., Goldmann, J., Lajoie, B.R., Fan, Z.P., Sigova, A.A*., et al.* (2016). Activation of proto-oncogenes by disruption of chromosome neighborhoods. Science (New York, NY) *351*, 1454-1458.
Holehouse, A.S., Ginell, G.M., Griffith, D., and Böke, E. (2021). Clustering of Aromatic Residues in Prion-like Domains Can Tune the Formation, State, and Organization of Biomolecular Condensates. Biochemistry *60*, 3566-3581.
Hsieh, T.H., Weiner, A., Lajoie, B., Dekker, J., Friedman, N., and Rando, O.J. (2015). Mapping Nucleosome Resolution Chromosome Folding in Yeast by Micro-C. Cell *162*, 108-119.
Huang, M.E., Rio, A.G., Nicolas, A., and Kolodner, R.D. (2003). A genomewide screen in Saccharomyces cerevisiae for genes that suppress the accumulation of mutations. Proc Natl Acad Sci U S A *100*, 11529-11534.
Huggins, M.L. (1942). THERMODYNAMIC PROPERTIES OF SOLUTIONS OF LONG-CHAIN COMPOUNDS. Annals of the New York Academy of Sciences *43*, 1-32.
Hughes, A.L., and Rando, O.J. (2014). Mechanisms underlying nucleosome positioning in vivo. Annual review of biophysics *43*, 41-63.
Hult, C., Adalsteinsson, D., Vasquez, P.A., Lawrimore, J., Bennett, M., York, A., Cook, D., Yeh, E., Forest, M.G., and Bloom, K. (2017). Enrichment of dynamic chromosomal crosslinks drive phase separation of the nucleolus. Nucleic Acids Res *45*, 11159-11173.
Hyland, E.M., Cosgrove, M.S., Molina, H., Wang, D., Pandey, A., Cottee, R.J., and Boeke, J.D. (2005). Insights into the role of histone H3 and histone H4 core modifiable residues in Saccharomyces cerevisiae. Molecular and cellular biology *25*, 10060-10070.
Iarovaia, O.V., Minina, E.P., Sheval, E.V., Onichtchouk, D., Dokudovskaya, S., Razin, S.V., and Vassetzky, Y.S. (2019). Nucleolus: A Central Hub for Nuclear Functions. Trends in cell biology *29*, 647-659.
Iborra, F.J. (2007). Can visco-elastic phase separation, macromolecular crowding and colloidal physics explain nuclear organisation? Theoretical biology & medical modelling *4*, 15.
Imai, R., Nozaki, T., Tani, T., Kaizu, K., Hibino, K., Ide, S., Tamura, S., Takahashi, K., Shribak, M., and Maeshima, K. (2017). Density imaging of heterochromatin in live cells using orientation-independent-DIC microscopy. Molecular biology of the cell *28*, 3349-3359.

Ioshikhes, I.P., Albert, I., Zanton, S.J., and Pugh, B.F. (2006). Nucleosome positions predicted through comparative genomics. Nature genetics *38*, 1210-1215.
Jenuwein, T., and Allis, C.D. (2001). Translating the histone code. Science (New York, NY) *293*, 1074-1080.
Jeronimo, C., Poitras, C., and Robert, F. (2019). Histone Recycling by FACT and Spt6 during Transcription Prevents the Scrambling of Histone Modifications. Cell reports *28*, 1206-1218.e1208.
Ji, Q., Mai, J., Ding, Y., Wei, Y., Ledesma-Amaro, R., and Ji, X.-J. (2020). Improving the homologous recombination efficiency of Yarrowia lipolytica by grafting heterologous component from Saccharomyces cerevisiae. Metabolic engineering communications *11*, e00152-e00152.
Jin, Q.W., Fuchs, J., and Loidl, J. (2000). Centromere clustering is a major determinant of yeast interphase nuclear organization. J Cell Sci *113 (Pt 11)*, 1903-1912.
Jr., P.E.R. (1953). A Theory of the Linear Viscoelastic Properties of Dilute Solutions of Coiling Polymers. *21*, 1272-1280.
Jun, S., and Mulder, B. (2006). Entropy-driven spatial organization of highly confined polymers: lessons for the bacterial chromosome. Proceedings of the National Academy of Sciences of the United States of America *103*, 12388-12393.
Kadosh, D., and Struhl, K. (1998). Targeted recruitment of the Sin3-Rpd3 histone deacetylase complex generates a highly localized domain of repressed chromatin in vivo. Molecular and cellular biology *18*, 5121-5127.
Kalverda, B., Pickersgill, H., Shloma, V.V., and Fornerod, M. (2010). Nucleoporins directly stimulate expression of developmental and cell-cycle genes inside the nucleoplasm. Cell *140*, 360-371.
Kanellis, P., Gagliardi, M., Banath, J.P., Szilard, R.K., Nakada, S., Galicia, S., Sweeney, F.D., Cabelof, D.C., Olive, P.L., and Durocher, D. (2007). A screen for suppressors of gross chromosomal rearrangements identifies a conserved role for PLP in preventing DNA lesions. PLoS Genet *3*, e134.
Kaplan, N., Moore, I.K., Fondufe-Mittendorf, Y., Gossett, A.J., Tillo, D., Field, Y., LeProust, E.M., Hughes, T.R., Lieb, J.D., Widom, J.*, et al.* (2009). The DNA-encoded nucleosome organization of a eukaryotic genome. Nature *458*, 362-366.
Kawaguchi, T., Tanigawa, A., Naganuma, T., Ohkawa, Y., Souquere, S., Pierron, G., and Hirose, T. (2015). SWI/SNF chromatin-remodeling complexes function in noncoding RNA-dependent assembly of nuclear bodies. Proceedings of the National Academy of Sciences of the United States of America *112*, 4304-4309.
Kechkar, A., Nair, D., Heilemann, M., Choquet, D., and Sibarita, J.B. (2013). Real-time analysis and visualization for single-molecule based super-resolution microscopy. PLoS One *8*, e62918.
Kedersha, N., Ivanov, P., and Anderson, P. (2013). Stress granules and cell signaling: more than just a passing phase? Trends in biochemical sciences *38*, 494-506.
Kellis, M., Birren, B.W., and Lander, E.S. (2004). Proof and evolutionary analysis of ancient genome duplication in the yeast Saccharomyces cerevisiae. Nature *428*, 617-624.
Kim, S.H., McQueen, P.G., Lichtman, M.K., Shevach, E.M., Parada, L.A., and Misteli, T. (2004). Spatial genome organization during T-cell differentiation. Cytogenetic and genome research *105*, 292-301.
Kind, J., Pagie, L., de Vries, S.S., Nahidiazar, L., Dey, S.S., Bienko, M., Zhan, Y., Lajoie, B., de Graaf, C.A., Amendola, M.*, et al.* (2015). Genome-wide maps of nuclear lamina interactions in single human cells. Cell *163*, 134-147.

Klose, R.J., Gardner, K.E., Liang, G., Erdjument-Bromage, H., Tempst, P., and Zhang, Y. (2007). Demethylation of histone H3K36 and H3K9 by Rph1: a vestige of an H3K9 methylation system in Saccharomyces cerevisiae? Mol Cell Biol *27*, 3951-3961.
Kornberg, R.D. (1974). Chromatin structure: a repeating unit of histones and DNA. Science (New York, NY) *184*, 868-871.
Kornberg, R.D., and Klug, A. (1981). The nucleosome. Sci Am *244*, 52-64.
Kornberg, R.D., and Thomas, J.O. (1974). Chromatin structure; oligomers of the histones. Science (New York, NY) *184*, 865-868.
Kosak, S.T., Skok, J.A., Medina, K.L., Riblet, R., Le Beau, M.M., Fisher, A.G., and Singh, H. (2002). Subnuclear compartmentalization of immunoglobulin loci during lymphocyte development. Science (New York, NY) *296*, 158-162.
Kouzarides, T. (2007). Chromatin modifications and their function. Cell *128*, 693-705.
Kuo, M.H., Brownell, J.E., Sobel, R.E., Ranalli, T.A., Cook, R.G., Edmondson, D.G., Roth, S.Y., and Allis, C.D. (1996). Transcription-linked acetylation by Gcn5p of histones H3 and H4 at specific lysines. Nature *383*, 269-272.
Kuo, M.H., vom Baur, E., Struhl, K., and Allis, C.D. (2000). Gcn4 activator targets Gcn5 histone acetyltransferase to specific promoters independently of transcription. Molecular cell *6*, 1309-1320.
Lachner, M., O'Carroll, D., Rea, S., Mechtler, K., and Jenuwein, T. (2001). Methylation of histone H3 lysine 9 creates a binding site for HP1 proteins. Nature *410*, 116-120.
Lakshminarasimhan, M., Boanca, G., Banks, C.A., Hattem, G.L., Gabriel, A.E., Groppe, B.D., Smoyer, C., Malanowski, K.E., Peak, A., Florens, L.*, et al.* (2016). Proteomic and Genomic Analyses of the Rvb1 and Rvb2 Interaction Network upon Deletion of R2TP Complex Components. Molecular & cellular proteomics : MCP *15*, 960-974.
Lang, G.I., and Murray, A.W. (2008). Estimating the per-base-pair mutation rate in the yeast Saccharomyces cerevisiae. Genetics *178*, 67-82.
Langst, G., and Manelyte, L. (2015). Chromatin Remodelers: From Function to Dysfunction. Genes *6*, 299-324.
Larson, A.G., Elnatan, D., Keenen, M.M., Trnka, M.J., Johnston, J.B., Burlingame, A.L., Agard, D.A., Redding, S., and Narlikar, G.J. (2017a). Liquid droplet formation by HP1alpha suggests a role for phase separation in heterochromatin. Nature *547*, 236-240.
Larson, A.G., Elnatan, D., Keenen, M.M., Trnka, M.J., Johnston, J.B., Burlingame, A.L., Agard, D.A., Redding, S., and Narlikar, G.J. (2017b). Liquid droplet formation by HP1α suggests a role for phase separation in heterochromatin. Nature *547*, 236-240.
Lawrimore, J., Aicher, J.K., Hahn, P., Fulp, A., Kompa, B., Vicci, L., Falvo, M., Taylor, R.M., 2nd, and Bloom, K. (2016). ChromoShake: a chromosome dynamics simulator reveals that chromatin loops stiffen centromeric chromatin. Molecular biology of the cell *27*, 153-166.
Lawrimore, J., Kolbin, D., Stanton, J., Khan, M., de Larminat, S.C., Lawrimore, C., Yeh, E., and Bloom, K. (2021). The rDNA is biomolecular condensate formed by polymer-polymer phase separation and is sequestered in the nucleolus by transcription and R-loops. Nucleic acids research *49*, 4586-4598.
Lee, K.K., Sardiu, M.E., Swanson, S.K., Gilmore, J.M., Torok, M., Grant, P.A., Florens, L., Workman, J.L., and Washburn, M.P. (2011). Combinatorial depletion analysis to assemble the network architecture of the SAGA and ADA chromatin remodeling complexes. Molecular systems biology *7*, 503.
Lee, M.E., DeLoache, W.C., Cervantes, B., and Dueber, J.E. (2015). A Highly Characterized Yeast Toolkit for Modular, Multipart Assembly. ACS synthetic biology *4*, 975-986.

Lee, W., Tillo, D., Bray, N., Morse, R.H., Davis, R.W., Hughes, T.R., and Nislow, C. (2007). A high-resolution atlas of nucleosome occupancy in yeast. Nature genetics *39*, 1235-1244.
Leng, H., Liu, S., Lei, Y., Tang, Y., Gu, S., Hu, J., Chen, S., Feng, J., and Li, Q. (2021). FACT interacts with Set3 HDAC and fine-tunes GAL1 transcription in response to environmental stimulation. Nucleic acids research *49*, 5502-5519.
Li, G., Tian, Y., and Zhu, W.-G. (2020). The Roles of Histone Deacetylases and Their Inhibitors in Cancer Therapy. *8*.
Li, Q., Zhou, H., Wurtele, H., Davies, B., Horazdovsky, B., Verreault, A., and Zhang, Z. (2008). Acetylation of histone H3 lysine 56 regulates replication-coupled nucleosome assembly. Cell *134*, 244-255.
Lichten, M., and Haber, J.E. (1989). Position effects in ectopic and allelic mitotic recombination in Saccharomyces cerevisiae. Genetics *123*, 261-268.
Lieberman-Aiden, E., van Berkum, N.L., Williams, L., Imakaev, M., Ragoczy, T., Telling, A., Amit, I., Lajoie, B.R., Sabo, P.J., Dorschner, M.O*., et al.* (2009). Comprehensive mapping of long-range interactions reveals folding principles of the human genome. Science *326*, 289-293.
Lieleg, C., Krietenstein, N., Walker, M., and Korber, P. (2015). Nucleosome positioning in yeasts: methods, maps, and mechanisms. Chromosoma *124*, 131-151.
Light, W.H., Brickner, D.G., Brand, V.R., and Brickner, J.H. (2010). Interaction of a DNA zip code with the nuclear pore complex promotes H2A.Z incorporation and INO1 transcriptional memory. Molecular cell *40*, 112-125.
Linhoff, M.W., Garg, S.K., and Mandel, G. (2015). A high-resolution imaging approach to investigate chromatin architecture in complex tissues. Cell *163*, 246-255.
Liu, C.L., Kaplan, T., Kim, M., Buratowski, S., Schreiber, S.L., Friedman, N., and Rando, O.J. (2005). Single-nucleosome mapping of histone modifications in S. cerevisiae. PLoS biology *3*, e328.
Liu, N., Balliano, A., and Hayes, J.J. (2011). Mechanism(s) of SWI/SNF-induced nucleosome mobilization. Chembiochem : a European journal of chemical biology *12*, 196-204.
Lo, W.-S., Duggan, L., Tolga , N.C., Emre, Belotserkovskya, R., Lane, W.S., Shiekhattar, R., and Berger, S.L. (2001). Snf1--a Histone Kinase That Works in Concert with the Histone Acetyltransferase Gcn5 to Regulate Transcription. Science (New York, NY) *293*, 1142-1146.
Lomberk, G., Wallrath, L., and Urrutia, R. (2006). The Heterochromatin Protein 1 family. Genome biology *7*, 228.
Lõoke, M., Kristjuhan, K., and Kristjuhan, A. (2011). Extraction of genomic DNA from yeasts for PCR-based applications. BioTechniques *50*, 325-328.
Lowary, P.T., and Widom, J. (1998). New DNA sequence rules for high affinity binding to histone octamer and sequence-directed nucleosome positioning. Journal of molecular biology *276*, 19-42.
Luger, K., Mader, A.W., Richmond, R.K., Sargent, D.F., and Richmond, T.J. (1997). Crystal structure of the nucleosome core particle at 2.8 A resolution. Nature *389*, 251-260.
Lupianez, D.G., Kraft, K., Heinrich, V., Krawitz, P., Brancati, F., Klopocki, E., Horn, D., Kayserili, H., Opitz, J.M., Laxova, R*., et al.* (2015). Disruptions of topological chromatin domains cause pathogenic rewiring of gene-enhancer interactions. Cell *161*, 1012-1025.
Madia, F., Gattazzo, C., Wei, M., Fabrizio, P., Burhans, W.C., Weinberger, M., Galbani, A., Smith, J.R., Nguyen, C., Huey, S*., et al.* (2008). Longevity mutation in SCH9 prevents recombination errors and premature genomic instability in a Werner/Bloom model system. The Journal of cell biology *180*, 67-81.
Maeshima, K., Ide, S., and Babokhov, M. (2019). Dynamic chromatin organization without the 30-nm fiber. Current opinion in cell biology *58*, 95-104.

Maeshima, K., Ide, S., Hibino, K., and Sasai, M. (2016). Liquid-like behavior of chromatin. Current opinion in genetics & development *37*, 36-45.
Makova, K.D., and Hardison, R.C. (2015). The effects of chromatin organization on variation in mutation rates in the genome. Nature reviews Genetics *16*, 213-223.
Malinovska, L., Kroschwald, S., and Alberti, S. (2013). Protein disorder, prion propensities, and self-organizing macromolecular collectives. Biochimica et biophysica acta *1834*, 918-931.
Malleshaiah, M.K., Shahrezaei, V., Swain, P.S., and Michnick, S.W. (2010). The scaffold protein Ste5 directly controls a switch-like mating decision in yeast. Nature *465*, 101-105.
Manohar, M., Mooney, A.M., North, J.A., Nakkula, R.J., Picking, J.W., Edon, A., Fishel, R., Poirier, M.G., and Ottesen, J.J. (2009). Acetylation of histone H3 at the nucleosome dyad alters DNA-histone binding. The Journal of biological chemistry *284*, 23312-23321.
Martin, A.M., Pouchnik, D.J., Walker, J.L., and Wyrick, J.J. (2004). Redundant roles for histone H3 N-terminal lysine residues in subtelomeric gene repression in Saccharomyces cerevisiae. Genetics *167*, 1123-1132.
Martincorena, I., Seshasayee, A.S., and Luscombe, N.M. (2012). Evidence of non-random mutation rates suggests an evolutionary risk management strategy. Nature *485*, 95-98.
Mavrich, T.N., Jiang, C., Ioshikhes, I.P., Li, X., Venters, B.J., Zanton, S.J., Tomsho, L.P., Qi, J., Glaser, R.L., Schuster, S.C.*, et al.* (2008). Nucleosome organization in the Drosophila genome. Nature *453*, 358-362.
McBryant, S.J., Lu, X., and Hansen, J.C. (2010). Multifunctionality of the linker histones: an emerging role for protein-protein interactions. Cell research *20*, 519-528.
McIlwraith, M.J., and West, S.C. (2008). DNA Repair Synthesis Facilitates RAD52-Mediated Second-End Capture during DSB Repair. Molecular Cell *29*, 510-516.
Measday, V., and Stirling, P.C. (2015). Navigating yeast genome maintenance with functional genomics. Briefings in Functional Genomics *15*, 119-129.
Meister, P., Towbin, B.D., Pike, B.L., Ponti, A., and Gasser, S.M. (2010). The spatial dynamics of tissue-specific promoters during C. elegans development. Genes & development *24*, 766-782.
Meneghini, M.D., Wu, M., and Madhani, H.D. (2003). Conserved histone variant H2A.Z protects euchromatin from the ectopic spread of silent heterochromatin. Cell *112*, 725-736.
Mercy, G., Mozziconacci, J., Scolari, V.F., Yang, K., Zhao, G., Thierry, A., Luo, Y., Mitchell, L.A., Shen, M., Shen, Y.*, et al.* (2017). 3D organization of synthetic and scrambled chromosomes. Science (New York, NY) *355*.
Mersfelder, E.L., and Parthun, M.R. (2006). The tale beyond the tail: histone core domain modifications and the regulation of chromatin structure. Nucleic acids research *34*, 2653-2662.
Michieletto, D., Chiang, M., Colì, D., Papantonis, A., Orlandini, E., Cook, P.R., and Marenduzzo, D. (2017). Shaping epigenetic memory via genomic bookmarking. Nucleic acids research *46*, 83-93.
Miron, E., Oldenkamp, R., Brown, J.M., Pinto, D.M.S., Xu, C.S., Faria, A.R., Shaban, H.A., Rhodes, J.D.P., Innocent, C., de Ornellas, S.*, et al.* (2020). Chromatin arranges in chains of mesoscale domains with nanoscale functional topography independent of cohesin. Sci Adv *6*.
Mizuguchi, T., Barrowman, J., and Grewal, S.I.S. (2015). Chromosome domain architecture and dynamic organization of the fission yeast genome. FEBS letters *589*, 2975-2986.
Mizuguchi, T., Fudenberg, G., Mehta, S., Belton, J.M., Taneja, N., Folco, H.D., FitzGerald, P., Dekker, J., Mirny, L., Barrowman, J.*, et al.* (2014). Cohesin-dependent globules and heterochromatin shape 3D genome architecture in S. pombe. Nature *516*, 432-435.
Mizzen, C.A., Yang, X.J., Kokubo, T., Brownell, J.E., Bannister, A.J., Owen-Hughes, T., Workman, J., Wang, L., Berger, S.L., Kouzarides, T.*, et al.* (1996). The TAF(II)250 subunit of TFIID has histone acetyltransferase activity. Cell *87*, 1261-1270.

Montavon, T., Shukeir, N., Erikson, G., Engist, B., Onishi-Seebacher, M., Ryan, D., Musa, Y., Mittler, G., Meyer, A.G., Genoud, C.*, et al.* (2021). Complete loss of H3K9 methylation dissolves mouse heterochromatin organization. Nat Commun *12*, 4359.
Morawska, M., and Ulrich, H.D. (2013). An expanded tool kit for the auxin-inducible degron system in budding yeast. Yeast (Chichester, England) *30*, 341-351.
Muck, J.S., Kandasamy, K., Englmann, A., Gunther, M., and Zink, D. (2012). Perinuclear positioning of the inactive human cystic fibrosis gene depends on CTCF, A-type lamins and an active histone deacetylase. Journal of cellular biochemistry *113*, 2607-2621.
Nakayama, J., Rice, J.C., Strahl, B.D., Allis, C.D., and Grewal, S.I. (2001). Role of histone H3 lysine 9 methylation in epigenetic control of heterochromatin assembly. Science *292*, 110-113.
Neumann, F.R., Dion, V., Gehlen, L.R., Tsai-Pflugfelder, M., Schmid, R., Taddei, A., and Gasser, S.M. (2012). Targeted INO80 enhances subnuclear chromatin movement and ectopic homologous recombination. Genes Dev *26*, 369-383.
Ng, M.K., and Cheung, P. (2016). A brief histone in time: understanding the combinatorial functions of histone PTMs in the nucleosome context. Biochemistry and cell biology = Biochimie et biologie cellulaire *94*, 33-42.
Nguyen, V.Q., Ranjan, A., Stengel, F., Wei, D., Aebersold, R., Wu, C., and Leschziner, A.E. (2013). Molecular architecture of the ATP-dependent chromatin-remodeling complex SWR1. Cell *154*, 1220-1231.
Nora, E.P., Lajoie, B.R., Schulz, E.G., Giorgetti, L., Okamoto, I., Servant, N., Piolot, T., van Berkum, N.L., Meisig, J., Sedat, J.*, et al.* (2012). Spatial partitioning of the regulatory landscape of the X-inactivation centre. Nature *485*, 381-385.
Nott, T.J., Petsalaki, E., Farber, P., Jervis, D., Fussner, E., Plochowietz, A., Craggs, T.D., Bazett-Jones, D.P., Pawson, T., Forman-Kay, J.D.*, et al.* (2015). Phase transition of a disordered nuage protein generates environmentally responsive membraneless organelles. Molecular cell *57*, 936-947.
Oeffinger, M., Wei, K.E., Rogers, R., DeGrasse, J.A., Chait, B.T., Aitchison, J.D., and Rout, M.P. (2007). Comprehensive analysis of diverse ribonucleoprotein complexes. Nature methods *4*, 951-956.
Ogawa, L.M., and Baserga, S.J. (2017). Crosstalk between the nucleolus and the DNA damage response. Molecular bioSystems *13*, 443-455.
Olins, D.E., and Olins, A.L. (2003). Chromatin history: our view from the bridge. Nature Reviews Molecular Cell Biology *4*, 809-814.
Ong, C.T., and Corces, V.G. (2009). Insulators as mediators of intra- and inter-chromosomal interactions: a common evolutionary theme. Journal of biology *8*, 73.
Opitz, N., Schmitt, K., Hofer-Pretz, V., Neumann, B., Krebber, H., Braus, G.H., and Valerius, O. (2017). Capturing the Asc1p/Receptor for Activated C Kinase 1 (RACK1) Microenvironment at the Head Region of the 40S Ribosome with Quantitative BioID in Yeast. Molecular & cellular proteomics : MCP *16*, 2199-2218.
Orsztynowicz, M., Lechniak, D., Pawlak, P., Kociucka, B., Kubickova, S., Cernohorska, H., and Madeja, Z.E. (2017). Changes in chromosome territory position within the nucleus reflect alternations in gene expression related to embryonic lineage specification. PloS one *12*, e0182398.
Ou, H.D., Phan, S., Deerinck, T.J., Thor, A., Ellisman, M.H., and O'Shea, C.C. (2017). ChromEMT: Visualizing 3D chromatin structure and compaction in interphase and mitotic cells. Science (New York, NY) *357*.

Oughtred, R., Rust, J., Chang, C., Breitkreutz, B.J., Stark, C., Willems, A., Boucher, L., Leung, G., Kolas, N., Zhang, F.*, et al.* (2021). The BioGRID database: A comprehensive biomedical resource of curated protein, genetic, and chemical interactions. Protein Sci *30*, 187-200.
Parra, M.A., Kerr, D., Fahy, D., Pouchnik, D.J., and Wyrick, J.J. (2006). Deciphering the roles of the histone H2B N-terminal domain in genome-wide transcription. Molecular and cellular biology *26*, 3842-3852.
Pepenella, S., Murphy, K.J., and Hayes, J.J. (2014). Intra- and inter-nucleosome interactions of the core histone tail domains in higher-order chromatin structure. Chromosoma *123*, 3-13.
Pessina, F., Giavazzi, F., Yin, Y., Gioia, U., Vitelli, V., Galbiati, A., Barozzi, S., Garre, M., Oldani, A., Flaus, A.*, et al.* (2019). Functional transcription promoters at DNA double-strand breaks mediate RNA-driven phase separation of damage-response factors. Nature Cell Biology *21*, 1286-1299.
Petty, E.L., Collette, K.S., Cohen, A.J., Snyder, M.J., and Csankovszki, G. (2009). Restricting dosage compensation complex binding to the X chromosomes by H2A.Z/HTZ-1. PLoS Genet *5*, e1000699.
Phillips-Cremins, J.E., Sauria, M.E., Sanyal, A., Gerasimova, T.I., Lajoie, B.R., Bell, J.S., Ong, C.T., Hookway, T.A., Guo, C., Sun, Y.*, et al.* (2013). Architectural protein subclasses shape 3D organization of genomes during lineage commitment. Cell *153*, 1281-1295.
Phillips, D.M., and Johns, E.W. (1965). A FRACTIONATION OF THE HISTONES OF GROUP F2A FROM CALF THYMUS. The Biochemical journal *94*, 127-130.
Pich, O., Muiños, F., Sabarinathan, R., Reyes-Salazar, I., Gonzalez-Perez, A., and Lopez-Bigas, N. (2018). Somatic and Germline Mutation Periodicity Follow the Orientation of the DNA Minor Groove around Nucleosomes. Cell *175*, 1074-1087.e1018.
Pokholok, D.K., Harbison, C.T., Levine, S., Cole, M., Hannett, N.M., Lee, T.I., Bell, G.W., Walker, K., Rolfe, P.A., Herbolsheimer, E.*, et al.* (2005). Genome-wide map of nucleosome acetylation and methylation in yeast. Cell *122*, 517-527.
Pouokam, M., Cruz, B., Burgess, S., Segal, M.R., Vazquez, M., and Arsuaga, J. (2019). The Rabl configuration limits topological entanglement of chromosomes in budding yeast. Scientific Reports *9*, 6795.
Pulice, J.L., and Kadoch, C. (2017). Composition and Function of Mammalian SWI/SNF Chromatin Remodeling Complexes in Human Disease. Cold Spring Harbor symposia on quantitative biology.
Quail, T., Golfier, S., Elsner, M., Ishihara, K., Murugesan, V., Renger, R., Jülicher, F., and Brugués, J. (2021). Force generation by protein–DNA co-condensation. Nature Physics *17*, 1007-1012.
Querol, A., and Bond, U. (2009). The complex and dynamic genomes of industrial yeasts. FEMS Microbiol Lett *293*, 1-10.
Quinodoz, S.A., and Guttman, M. (2021). Essential Roles for RNA in Shaping Nuclear Organization. Cold Spring Harb Perspect Biol.
Rabl, C. (1885). Uber Zelltheilung. Morphol Jahrb *10*, 214-330.
Raffoux, X., Bourge, M., Dumas, F., Martin, O.C., and Falque, M. (2018). High-throughput measurement of recombination rates and genetic interference in Saccharomyces cerevisiae. Yeast *35*, 431-442.
Ragoczy, T., Bender, M.A., Telling, A., Byron, R., and Groudine, M. (2006). The locus control region is required for association of the murine beta-globin locus with engaged transcription factories during erythroid maturation. Genes & development *20*, 1447-1457.
Raisner, R.M., Hartley, P.D., Meneghini, M.D., Bao, M.Z., Liu, C.L., Schreiber, S.L., Rando, O.J., and Madhani, H.D. (2005). Histone variant H2A.Z marks the 5' ends of both active and inactive genes in euchromatin. Cell *123*, 233-248.
Randise-Hinchliff, C., Coukos, R., Sood, V., Sumner, M.C., Zdraljevic, S., Meldi Sholl, L., Garvey Brickner, D., Ahmed, S., Watchmaker, L., and Brickner, J.H. (2016). Strategies to regulate

transcription factor-mediated gene positioning and interchromosomal clustering at the nuclear periphery. The Journal of cell biology *212*, 633-646.
Rando, O.J. (2007). Global patterns of histone modifications. Current opinion in genetics & development *17*, 94-99.
Ransom, M., Dennehey, B.K., and Tyler, J.K. (2010). Chaperoning histones during DNA replication and repair. Cell *140*, 183-195.
Rao, S.S., Huntley, M.H., Durand, N.C., Stamenova, E.K., Bochkov, I.D., Robinson, J.T., Sanborn, A.L., Machol, I., Omer, A.D., Lander, E.S.*, et al.* (2014). A 3D map of the human genome at kilobase resolution reveals principles of chromatin looping. Cell *159*, 1665-1680.
Raveh-Sadka, T., Levo, M., Shabi, U., Shany, B., Keren, L., Lotan-Pompan, M., Zeevi, D., Sharon, E., Weinberger, A., and Segal, E. (2012). Manipulating nucleosome disfavoring sequences allows fine-tune regulation of gene expression in yeast. Nature genetics *44*, 743-750.
Rea, S., Eisenhaber, F., O'Carroll, D., Strahl, B.D., Sun, Z.W., Schmid, M., Opravil, S., Mechtler, K., Ponting, C.P., Allis, C.D.*, et al.* (2000). Regulation of chromatin structure by site-specific histone H3 methyltransferases. Nature *406*, 593-599.
Rechendorff, K., Witz, G., Adamcik, J., and Dietler, G. (2009). Persistence length and scaling properties of single-stranded DNA adsorbed on modified graphite. The Journal of chemical physics *131*, 095103.
Richmond, T.J., and Davey, C.A. (2003). The structure of DNA in the nucleosome core. Nature *423*, 145-150.
Riley, R., Haridas, S., Wolfe, K.H., Lopes, M.R., Hittinger, C.T., Göker, M., Salamov, A.A., Wisecaver, J.H., Long, T.M., Calvey, C.H.*, et al.* (2016). Comparative genomics of biotechnologically important yeasts. Proceedings of the National Academy of Sciences *113*, 9882.
Robzyk, K., Recht, J., and Osley, M.A. (2000). Rad6-dependent ubiquitination of histone H2B in yeast. Science (New York, NY) *287*, 501-504.
Rodrigues-Prause, A., Sampaio, N.M.V., Gurol, T.M., Aguirre, G.M., Sedam, H.N.C., Chapman, M.J., Malc, E.P., Ajith, V.P., Chakraborty, P., Tizei, P.A.*, et al.* (2018). A Case Study of Genomic Instability in an Industrial Strain of Saccharomyces cerevisiae. G3 (Bethesda, Md) *8*, 3703-3713.
Rohner, S., Kalck, V., Wang, X., Ikegami, K., Lieb, J.D., Gasser, S.M., and Meister, P. (2013). Promoter- and RNA polymerase II-dependent hsp-16 gene association with nuclear pores in Caenorhabditis elegans. The Journal of cell biology *200*, 589-604.
Roque, A., Iloro, I., Ponte, I., Arrondo, J.L., and Suau, P. (2005). DNA-induced secondary structure of the carboxyl-terminal domain of histone H1. The Journal of biological chemistry *280*, 32141-32147.
Rothstein, R.J. (1983). One-step gene disruption in yeast. Methods in enzymology *101*, 202-211.
Rudnizky, S., Khamis, H., Ginosar, Y., Goren, E., Melamed, P., and Kaplan, A. (2021). Extended and dynamic linker histone-DNA Interactions control chromatosome compaction. Mol Cell *81*, 3410-3421 e3414.
Rufiange, A., Jacques, P.E., Bhat, W., Robert, F., and Nourani, A. (2007). Genome-wide replication-independent histone H3 exchange occurs predominantly at promoters and implicates H3 K56 acetylation and Asf1. Mol Cell *27*, 393-405.
Sabari, B.R., Dall'Agnese, A., Boija, A., Klein, I.A., Coffey, E.L., Shrinivas, K., Abraham, B.J., Hannett, N.M., Zamudio, A.V., Manteiga, J.C.*, et al.* (2018). Coactivator condensation at super-enhancers links phase separation and gene control. Science *361*.
Sáez-Vásquez, J., and Gadal, O. (2010). Genome organization and function: a view from yeast and Arabidopsis. Molecular plant *3*, 678-690.

Sanders, S.L., Jennings, J., Canutescu, A., Link, A.J., and Weil, P.A. (2002). Proteomics of the eukaryotic transcription machinery: identification of proteins associated with components of yeast TFIID by multidimensional mass spectrometry. Molecular and cellular biology *22*, 4723-4738.
Sanulli, S., Trnka, M.J., Dharmarajan, V., Tibble, R.W., Pascal, B.D., Burlingame, A.L., Griffin, P.R., Gross, J.D., and Narlikar, G.J. (2019). HP1 reshapes nucleosome core to promote heterochromatin phase separation. Nature.
Sassone-Corsi, P., Mizzen, C.A., Cheung, P., Crosio, C., Monaco, L., Jacquot, S., Hanauer, A., and Allis, C.D. (1999). Requirement of Rsk-2 for epidermal growth factor-activated phosphorylation of histone H3. Science (New York, NY) *285*, 886-891.
Satchwell, S.C., Drew, H.R., and Travers, A.A. (1986). Sequence periodicities in chicken nucleosome core DNA. Journal of molecular biology *191*, 659-675.
Scheffold, F., Diaz-Leyva, P., Reufer, M., Ben Braham, N., Lynch, I., and Harden, J.L. (2010). Brushlike interactions between thermoresponsive microgel particles. Phys Rev Lett *104*, 128304.
Schindelin, J., Arganda-Carreras, I., Frise, E., Kaynig, V., Longair, M., Pietzsch, T., Preibisch, S., Rueden, C., Saalfeld, S., Schmid, B.*, et al.* (2012). Fiji: an open-source platform for biological-image analysis. Nature methods *9*, 676-682.
Schmidtmann, E., Anton, T., Rombaut, P., Herzog, F., and Leonhardt, H. (2016). Determination of local chromatin composition by CasID. Nucleus (Austin, Tex) *7*, 476-484.
Schober, H., Kalck, V., Vega-Palas, M.A., Van Houwe, G., Sage, D., Unser, M., Gartenberg, M.R., and Gasser, S.M. (2008). Controlled exchange of chromosomal arms reveals principles driving telomere interactions in yeast. Genome Res *18*, 261-271.
Schones, D.E., Cui, K., Cuddapah, S., Roh, T.Y., Barski, A., Wang, Z., Wei, G., and Zhao, K. (2008). Dynamic regulation of nucleosome positioning in the human genome. Cell *132*, 887-898.
Scott, D.D., and Oeffinger, M. (2016). Nucleolin and nucleophosmin: nucleolar proteins with multiple functions in DNA repair. Biochemistry and cell biology = Biochimie et biologie cellulaire *94*, 419-432.
Segal, E., Fondufe-Mittendorf, Y., Chen, L., Thastrom, A., Field, Y., Moore, I.K., Wang, J.P., and Widom, J. (2006). A genomic code for nucleosome positioning. Nature *442*, 772-778.
Segura, J., Ferretti, L., Ramos-Onsins, S., Capilla, L., Farre, M., Reis, F., Oliver-Bonet, M., Fernandez-Bellon, H., Garcia, F., Garcia-Caldes, M.*, et al.* (2013). Evolution of recombination in eutherian mammals: insights into mechanisms that affect recombination rates and crossover interference. Proc Biol Sci *280*, 20131945.
Sexton, T., Yaffe, E., Kenigsberg, E., Bantignies, F., Leblanc, B., Hoichman, M., Parrinello, H., Tanay, A., and Cavalli, G. (2012). Three-dimensional folding and functional organization principles of the Drosophila genome. Cell *148*, 458-472.
Shaban, H.A., Barth, R., and Bystricky, K. (2018). Formation of correlated chromatin domains at nanoscale dynamic resolution during transcription. Nucleic acids research *46*, e77.
Shaban, H.A., and Seeber, A. (2020). Monitoring the spatio-temporal organization and dynamics of the genome. Nucleic acids research *48*, 3423-3434.
Shaw, W.M., Yamauchi, H., Mead, J., Gowers, G.-O.F., Bell, D.J., Öling, D., Larsson, N., Wigglesworth, M., Ladds, G., and Ellis, T. (2019). Engineering a Model Cell for Rational Tuning of GPCR Signaling. Cell *177*, 782-796.e727.
She, R., and Jarosz, D.F. (2018). Mapping Causal Variants with Single-Nucleotide Resolution Reveals Biochemical Drivers of Phenotypic Change. Cell *172*, 478-490.e415.
Shen, X., Mizuguchi, G., Hamiche, A., and Wu, C. (2000). A chromatin remodelling complex involved in transcription and DNA processing. Nature *406*, 541-544.

Shin, Y., Chang, Y.-C., Lee, D.S.W., Berry, J., Sanders, D.W., Ronceray, P., Wingreen, N.S., Haataja, M., and Brangwynne, C.P. (2018). Liquid Nuclear Condensates Mechanically Sense and Restructure the Genome. Cell *175*, 1481-1491.e1413.
Singleton, M.R., Dillingham, M.S., and Wigley, D.B. (2007). Structure and mechanism of helicases and nucleic acid translocases. Annual review of biochemistry *76*, 23-50.
Skok, J.A., Brown, K.E., Azuara, V., Caparros, M.L., Baxter, J., Takacs, K., Dillon, N., Gray, D., Perry, R.P., Merkenschlager, M*., et al.* (2001). Nonequivalent nuclear location of immunoglobulin alleles in B lymphocytes. Nature immunology *2*, 848-854.
Smerdon, M.J. (1991). DNA repair and the role of chromatin structure. Current opinion in cell biology *3*, 422-428.
Smith, S., Hwang, J.Y., Banerjee, S., Majeed, A., Gupta, A., and Myung, K. (2004). Mutator genes for suppression of gross chromosomal rearrangements identified by a genome-wide screening in Saccharomyces cerevisiae. Proc Natl Acad Sci U S A *101*, 9039-9044.
Smith, S.B., Cui, Y., and Bustamante, C. (1996). Overstretching B-DNA: the elastic response of individual double-stranded and single-stranded DNA molecules. Science (New York, NY) *271*, 795-799.
Solovei, I., Kreysing, M., Lanctôt, C., Kösem, S., Peichl, L., Cremer, T., Guck, J., and Joffe, B. (2009). Nuclear architecture of rod photoreceptor cells adapts to vision in mammalian evolution. Cell *137*, 356-368.
Spector, D.L. (2003). The dynamics of chromosome organization and gene regulation. Annu Rev Biochem *72*, 573-608.
St Charles, J., and Petes, T.D. (2013). High-resolution mapping of spontaneous mitotic recombination hotspots on the 1.1 Mb arm of yeast chromosome IV. PLoS Genet *9*, e1003434.
Stanek, D., and Fox, A.H. (2017). Nuclear bodies: news insights into structure and function. Current opinion in cell biology *46*, 94-101.
Stephens, A.D., Liu, P.Z., Banigan, E.J., Almassalha, L.M., Backman, V., Adam, S.A., Goldman, R.D., and Marko, J.F. (2018). Chromatin histone modifications and rigidity affect nuclear morphology independent of lamins. Mol Biol Cell *29*, 220-233.
Sterner, D.E., and Berger, S.L. (2000). Acetylation of histones and transcription-related factors. Microbiology and molecular biology reviews : MMBR *64*, 435-459.
Stevens, T.J., Lando, D., Basu, S., Atkinson, L.P., Cao, Y., Lee, S.F., Leeb, M., Wohlfahrt, K.J., Boucher, W., O'Shaughnessy-Kirwan, A*., et al.* (2017). 3D structures of individual mammalian genomes studied by single-cell Hi-C. Nature *544*, 59-64.
Stewart, M.D., Li, J., and Wong, J. (2005). Relationship between histone H3 lysine 9 methylation, transcription repression, and heterochromatin protein 1 recruitment. Mol Cell Biol *25*, 2525-2538.
Stirling, P.C., Shen, Y., Corbett, R., Jones, S.J.M., and Hieter, P. (2014). Genome destabilizing mutator alleles drive specific mutational trajectories in Saccharomyces cerevisiae. Genetics *196*, 403-412.
Strahl, B.D., and Allis, C.D. (2000). The language of covalent histone modifications. Nature *403*, 41-45.
Strom, A.R., Emelyanov, A.V., Mir, M., Fyodorov, D.V., Darzacq, X., and Karpen, G.H. (2017). Phase separation drives heterochromatin domain formation. Nature *547*, 241-245.
Taddei, A., Van Houwe, G., Hediger, F., Kalck, V., Cubizolles, F., Schober, H., and Gasser, S.M. (2006). Nuclear pore association confers optimal expression levels for an inducible yeast gene. Nature *441*, 774-778.
Talbert, P.B., and Henikoff, S. (2010). Histone variants--ancient wrap artists of the epigenome. Nature reviews Molecular cell biology *11*, 264-275.

Taunton, J., Hassig, C.A., and Schreiber, S.L. (1996). A mammalian histone deacetylase related to the yeast transcriptional regulator Rpd3p. Science (New York, NY) *272*, 408-411.
Thastrom, A., Lowary, P.T., and Widom, J. (2004). Measurement of histone-DNA interaction free energy in nucleosomes. Methods (San Diego, Calif) *33*, 33-44.
The UniProt, C. (2021). UniProt: the universal protein knowledgebase in 2021. Nucleic Acids Research *49*, D480-D489.
Therizols, P., Duong, T., Dujon, B., Zimmer, C., and Fabre, E. (2010). Chromosome arm length and nuclear constraints determine the dynamic relationship of yeast subtelomeres. Proc Natl Acad Sci U S A *107*, 2025-2030.
Thomson, S., Clayton, A.L., Hazzalin, C.A., Rose, S., Barratt, M.J., and Mahadevan, L.C. (1999). The nucleosomal response associated with immediate-early gene induction is mediated via alternative MAP kinase cascades: MSK1 as a potential histone H3/HMG-14 kinase. The EMBO journal *18*, 4779-4793.
Tiley, G.P., and Burleigh, J.G. (2015). The relationship of recombination rate, genome structure, and patterns of molecular evolution across angiosperms. BMC Evol Biol *15*, 194.
Topal, S., Vasseur, P., Radman-Livaja, M., and Peterson, C.L. (2019). Distinct transcriptional roles for Histone H3-K56 acetylation during the cell cycle in Yeast. Nature communications *10*, 4372.
Toretsky, J.A., and Wright, P.E. (2014). Assemblages: functional units formed by cellular phase separation. The Journal of cell biology *206*, 579-588.
Tsukada, Y., Fang, J., Erdjument-Bromage, H., Warren, M.E., Borchers, C.H., Tempst, P., and Zhang, Y. (2006). Histone demethylation by a family of JmjC domain-containing proteins. Nature *439*, 811-816.
Turner, A.L., Watson, M., Wilkins, O.G., Cato, L., Travers, A., Thomas, J.O., and Stott, K. (2018). Highly disordered histone H1-DNA model complexes and their condensates. Proceedings of the National Academy of Sciences of the United States of America *115*, 11964-11969.
Tyagi, M., Imam, N., Verma, K., and Patel, A.K. (2016). Chromatin remodelers: We are the drivers!! Nucleus (Austin, Tex) *7*, 388-404.
Uhlenbeck, G.E., and Ornstein, L.S. (1930). On the Theory of the Brownian Motion. Phys Rev *36*, 823–841.
van Attikum, H., and Gasser, S.M. (2009). Crosstalk between histone modifications during the DNA damage response. Trends in cell biology *19*, 207-217.
van der Lee, R., Buljan, M., Lang, B., Weatheritt, R.J., Daughdrill, G.W., Dunker, A.K., Fuxreiter, M., Gough, J., Gsponer, J., Jones, D.T*., et al.* (2014). Classification of intrinsically disordered regions and proteins. Chemical reviews *114*, 6589-6631.
Van Holde, K.E., Allen, J.R., Tatchell, K., Weischet, W.O., and Lohr, D. (1980). DNA-histone interactions in nucleosomes. Biophysical journal *32*, 271-282.
Vasquez, P.A., and Bloom, K. (2014). Polymer models of interphase chromosomes. Nucleus (Austin, Tex) *5*, 376-390.
Vasquez, P.A., Hult, C., Adalsteinsson, D., Lawrimore, J., Forest, M.G., and Bloom, K. (2016). Entropy gives rise to topologically associating domains. Nucleic acids research *44*, 5540-5549.
Verdaasdonk, J.S., Gardner, R., Stephens, A.D., Yeh, E., and Bloom, K. (2012). Tension-dependent nucleosome remodeling at the pericentromere in yeast. Molecular biology of the cell *23*, 2560-2570.
Verdaasdonk, J.S., Vasquez, P.A., Barry, R.M., Barry, T., Goodwin, S., Forest, M.G., and Bloom, K. (2013). Centromere tethering confines chromosome domains. Mol Cell *52*, 819-831.
Vernarecci, S., Tosi, F., and Filetici, P. (2010). Tuning acetylated chromatin with HAT inhibitors: a novel tool for therapy. Epigenetics *5*, 105-111.

Vietri Rudan, M., Barrington, C., Henderson, S., Ernst, C., Odom, D.T., Tanay, A., and Hadjur, S. (2015). Comparative Hi-C reveals that CTCF underlies evolution of chromosomal domain architecture. Cell reports *10*, 1297-1309.
Wang, J., Choi, J.M., Holehouse, A.S., Lee, H.O., Zhang, X., Jahnel, M., Maharana, S., Lemaitre, R., Pozniakovsky, A., Drechsel, D*., et al.* (2018). A Molecular Grammar Governing the Driving Forces for Phase Separation of Prion-like RNA Binding Proteins. Cell *174*, 688-699.e616.
Wang, S., Su, J.H., Beliveau, B.J., Bintu, B., Moffitt, J.R., Wu, C.T., and Zhuang, X. (2016). Spatial organization of chromatin domains and compartments in single chromosomes. Science (New York, NY) *353*, 598-602.
Wang, Y.H., Amirhaeri, S., Kang, S., Wells, R.D., and Griffith, J.D. (1994). Preferential nucleosome assembly at DNA triplet repeats from the myotonic dystrophy gene. Science (New York, NY) *265*, 669-671.
Wang, Y.H., and Griffith, J. (1995). Expanded CTG triplet blocks from the myotonic dystrophy gene create the strongest known natural nucleosome positioning elements. Genomics *25*, 570-573.
Wapenaar, H., and Dekker, F.J. (2016). Histone acetyltransferases: challenges in targeting bi-substrate enzymes. Clinical Epigenetics *8*, 59.
Weber, S.C., and Brangwynne, C.P. (2015). Inverse size scaling of the nucleolus by a concentration-dependent phase transition. Current biology : CB *25*, 641-646.
Weber, S.C., Spakowitz, A.J., and Theriot, J.A. (2010). Bacterial chromosomal loci move subdiffusively through a viscoelastic cytoplasm. Phys Rev Lett *104*, 238102.
Weber, S.C., Spakowitz, A.J., and Theriot, J.A. (2012). Nonthermal ATP-dependent fluctuations contribute to the in vivo motion of chromosomal loci. Proceedings of the National Academy of Sciences of the United States of America *109*, 7338-7343.
Wei, M., Fabrizio, P., Hu, J., Ge, H., Cheng, C., Li, L., and Longo, V.D. (2008). Life span extension by calorie restriction depends on Rim15 and transcription factors downstream of Ras/PKA, Tor, and Sch9. PLoS genetics *4*, e13-e13.
Widom, J. (2001). Role of DNA sequence in nucleosome stability and dynamics. Quarterly reviews of biophysics *34*, 269-324.
Wilfert, L., Gadau, J., and Schmid-Hempel, P. (2007). Variation in genomic recombination rates among animal taxa and the case of social insects. Heredity (Edinb) *98*, 189-197.
Williams, R.R., Azuara, V., Perry, P., Sauer, S., Dvorkina, M., Jorgensen, H., Roix, J., McQueen, P., Misteli, T., Merkenschlager, M*., et al.* (2006). Neural induction promotes large-scale chromatin reorganisation of the Mash1 locus. Journal of cell science *119*, 132-140.
Wolfe, K.H., and Shields, D.C. (1997). Molecular evidence for an ancient duplication of the entire yeast genome. Nature *387*, 708-713.
Wong, H., Marie-Nelly, H., Herbert, S., Carrivain, P., Blanc, H., Koszul, R., Fabre, E., and Zimmer, C. (2012). A predictive computational model of the dynamic 3D interphase yeast nucleus. Curr Biol *22*, 1881-1890.
Wood, C.M., Nicholson, J.M., Lambert, S.J., Chantalat, L., Reynolds, C.D., and Baldwin, J.P. (2005). High-resolution structure of the native histone octamer. Acta crystallographica Section F, Structural biology and crystallization communications *61*, 541-545.
Xhemalce, B., Miller, K.M., Driscoll, R., Masumoto, H., Jackson, S.P., Kouzarides, T., Verreault, A., and Arcangioli, B. (2007). Regulation of histone H3 lysine 56 acetylation in Schizosaccharomyces pombe. The Journal of biological chemistry *282*, 15040-15047.
Xu, F., Zhang, K., and Grunstein, M. (2005). Acetylation in histone H3 globular domain regulates gene expression in yeast. Cell *121*, 375-385.

Yang, J., Zhang, X., Feng, J., Leng, H., Li, S., Xiao, J., Liu, S., Xu, Z., Xu, J., Li, D.*, et al.* (2016). The Histone Chaperone FACT Contributes to DNA Replication-Coupled Nucleosome Assembly. Cell reports *14*, 1128-1141.
Yang, X.-J., and Seto, E. (2008a). Lysine acetylation: codified crosstalk with other posttranslational modifications. Molecular cell *31*, 449-461.
Yang, X.-J., and Seto, E. (2008b). The Rpd3/Hda1 family of lysine deacetylases: from bacteria and yeast to mice and men. Nature Reviews Molecular Cell Biology *9*, 206-218.
Yang, X.J., and Grégoire, S. (2007). Metabolism, cytoskeleton and cellular signalling in the grip of protein Nepsilon - and O-acetylation. EMBO reports *8*, 556-562.
Yu, Q., Kuzmiak, H., Zou, Y., Olsen, L., Defossez, P.A., and Bi, X. (2009). Saccharomyces cerevisiae linker histone Hho1p functionally interacts with core histone H4 and negatively regulates the establishment of transcriptionally silent chromatin. The Journal of biological chemistry *284*, 740-750.
Yuan, G.C., Liu, Y.J., Dion, M.F., Slack, M.D., Wu, L.F., Altschuler, S.J., and Rando, O.J. (2005). Genome-scale identification of nucleosome positions in S. cerevisiae. Science (New York, NY) *309*, 626-630.
Zhang, H., Roberts, D.N., and Cairns, B.R. (2005). Genome-wide dynamics of Htz1, a histone H2A variant that poises repressed/basal promoters for activation through histone loss. Cell *123*, 219-231.
Zhu, L., and Brangwynne, C.P. (2015). Nuclear bodies: the emerging biophysics of nucleoplasmic phases. Current opinion in cell biology *34*, 23-30.
Zhu, Y.O., Siegal, M.L., Hall, D.W., and Petrov, D.A. (2014). Precise estimates of mutation rate and spectrum in yeast. Proc Natl Acad Sci U S A *111*, E2310-2318.
Zink, D., Amaral, M.D., Englmann, A., Lang, S., Clarke, L.A., Rudolph, C., Alt, F., Luther, K., Braz, C., Sadoni, N.*, et al.* (2004). Transcription-dependent spatial arrangements of CFTR and adjacent genes in human cell nuclei. The Journal of cell biology *166*, 815-825.
Zlatanova, J., Bishop, T.C., Victor, J.M., Jackson, V., and van Holde, K. (2009). The nucleosome family: dynamic and growing. Structure (London, England : 1993) *17*, 160-171.

A, P., and Weber, S.C. (2019). Evidence for and against Liquid-Liquid Phase Separation in the Nucleus. Noncoding RNA *5*, 50.
Abbott, D.W., Ivanova, V.S., Wang, X., Bonner, W.M., and Ausio, J. (2001). Characterization of the stability and folding of H2A.Z chromatin particles: implications for transcriptional activation. The Journal of biological chemistry *276*, 41945-41949.
Abshiru, N., Ippersiel, K., Tang, Y., Yuan, H., Marmorstein, R., Verreault, A., and Thibault, P. (2013). Chaperone-mediated acetylation of histones by Rtt109 identified by quantitative proteomics. Journal of proteomics *81*, 80-90.
Ahmed, S., Brickner, D.G., Light, W.H., Cajigas, I., McDonough, M., Froyshteter, A.B., Volpe, T., and Brickner, J.H. (2010). DNA zip codes control an ancient mechanism for gene targeting to the nuclear periphery. Nature cell biology *12*, 111-118.
Ahmed, S., and Brickner, J.H. (2010). A role for DNA sequence in controlling the spatial organization of the genome. Nucleus (Austin, Tex) *1*, 402-406.

Albert, B., Mathon, J., Shukla, A., Saad, H., Normand, C., Léger-Silvestre, I., Villa, D., Kamgoue, A., Mozziconacci, J., Wong, H.*, et al.* (2013). Systematic characterization of the conformation and dynamics of budding yeast chromosome XII. The Journal of cell biology *202*, 201-210.
Albert, I., Mavrich, T.N., Tomsho, L.P., Qi, J., Zanton, S.J., Schuster, S.C., and Pugh, B.F. (2007). Translational and rotational settings of H2A.Z nucleosomes across the Saccharomyces cerevisiae genome. Nature *446*, 572-576.
Alberti, S., Gladfelter, A., and Mittag, T. (2019). Considerations and Challenges in Studying Liquid-Liquid Phase Separation and Biomolecular Condensates. Cell *176*, 419-434.
Allshire, R.C., and Madhani, H.D. (2018). Ten principles of heterochromatin formation and function. Nat Rev Mol Cell Biol *19*, 229-244.
Altmeyer, M., Neelsen, K.J., Teloni, F., Pozdnyakova, I., Pellegrino, S., Grofte, M., Rask, M.B., Streicher, W., Jungmichel, S., Nielsen, M.L.*, et al.* (2015). Liquid demixing of intrinsically disordered proteins is seeded by poly(ADP-ribose). Nature communications *6*, 8088.
Arents, G., Burlingame, R.W., Wang, B.C., Love, W.E., and Moudrianakis, E.N. (1991). The nucleosomal core histone octamer at 3.1 A resolution: a tripartite protein assembly and a left-handed superhelix. Proceedings of the National Academy of Sciences of the United States of America *88*, 10148-10152.
Arents, G., and Moudrianakis, E.N. (1995). The histone fold: a ubiquitous architectural motif utilized in DNA compaction and protein dimerization. Proceedings of the National Academy of Sciences of the United States of America *92*, 11170-11174.
Argueso, J.L., Carazzolle, M.F., Mieczkowski, P.A., Duarte, F.M., Netto, O.V., Missawa, S.K., Galzerani, F., Costa, G.G., Vidal, R.O., Noronha, M.F.*, et al.* (2009). Genome structure of a Saccharomyces cerevisiae strain widely used in bioethanol production. Genome Res *19*, 2258-2270.
Backlund, M.P., Joyner, R., Weis, K., and Moerner, W.E. (2014). Correlations of three-dimensional motion of chromosomal loci in yeast revealed by the double-helix point spread function microscope. Molecular biology of the cell *25*, 3619-3629.
Banani, S.F., Lee, H.O., Hyman, A.A., and Rosen, M.K. (2017). Biomolecular condensates: organizers of cellular biochemistry. Nature Reviews Molecular Cell Biology *18*, 285.
Bannister, A.J., and Kouzarides, T. (2011). Regulation of chromatin by histone modifications. Cell research *21*, 381-395.
Bannister, A.J., Zegerman, P., Partridge, J.F., Miska, E.A., Thomas, J.O., Allshire, R.C., and Kouzarides, T. (2001). Selective recognition of methylated lysine 9 on histone H3 by the HP1 chromo domain. Nature *410*, 120-124.
Barton, A.B., Pekosz, M.R., Kurvathi, R.S., and Kaback, D.B. (2008). Meiotic recombination at the ends of chromosomes in Saccharomyces cerevisiae. Genetics *179*, 1221-1235.
Basso, L.C., de Amorim, H.V., de Oliveira, A.J., and Lopes, M.L. (2008). Yeast selection for fuel ethanol production in Brazil. FEMS Yeast Res *8*, 1155-1163.
Becker, P.B., and Horz, W. (2002). ATP-dependent nucleosome remodeling. Annual review of biochemistry *71*, 247-273.
Berger, A.B., Cabal, G.G., Fabre, E., Duong, T., Buc, H., Nehrbass, U., Olivo-Marin, J.C., Gadal, O., and Zimmer, C. (2008). High-resolution statistical mapping reveals gene territories in live yeast. Nature methods *5*, 1031-1037.
Bergeron-Sandoval, L.P., Safaee, N., and Michnick, S.W. (2016). Mechanisms and Consequences of Macromolecular Phase Separation. Cell *165*, 1067-1079.
Berndsen, C.E., Tsubota, T., Lindner, S.E., Lee, S., Holton, J.M., Kaufman, P.D., Keck, J.L., and Denu, J.M. (2008). Molecular functions of the histone acetyltransferase chaperone complex Rtt109-Vps75. Nature structural & molecular biology *15*, 948-956.

Bernstein, B.E., Kamal, M., Lindblad-Toh, K., Bekiranov, S., Bailey, D.K., Huebert, D.J., McMahon, S., Karlsson, E.K., Kulbokas, E.J., 3rd, Gingeras, T.R.*, et al.* (2005). Genomic maps and comparative analysis of histone modifications in human and mouse. Cell *120*, 169-181.
Blobel, G. (1985). Gene gating: a hypothesis. Proceedings of the National Academy of Sciences of the United States of America *82*, 8527-8529.
Bloom, K., and Kolbin, D. (2022). Mechanisms of DNA Mobilization and Sequestration. Genes *13*.
Bloom, K.S. (2008). Beyond the code: the mechanical properties of DNA as they relate to mitosis. Chromosoma *117*, 103-110.
Boeynaems, S., Alberti, S., Fawzi, N.L., Mittag, T., Polymenidou, M., Rousseau, F., Schymkowitz, J., Shorter, J., Wolozin, B., Van Den Bosch, L.*, et al.* (2018). Protein Phase Separation: A New Phase in Cell Biology. Trends in cell biology *28*, 420-435.
Bolzer, A., Kreth, G., Solovei, I., Koehler, D., Saracoglu, K., Fauth, C., Müller, S., Eils, R., Cremer, C., Speicher, M.R.*, et al.* (2005). Three-Dimensional Maps of All Chromosomes in Human Male Fibroblast Nuclei and Prometaphase Rosettes. PLoS biology *3*, e157.
Borneman, A.R., Desany, B.A., Riches, D., Affourtit, J.P., Forgan, A.H., Pretorius, I.S., Egholm, M., and Chambers, P.J. (2011). Whole-genome comparison reveals novel genetic elements that characterize the genome of industrial strains of Saccharomyces cerevisiae. PLoS Genet *7*, e1001287.
Boulon, S., Westman, B.J., Hutten, S., Boisvert, F.M., and Lamond, A.I. (2010). The nucleolus under stress. Molecular cell *40*, 216-227.
Brackley, C.A., Johnson, J., Kelly, S., Cook, P.R., and Marenduzzo, D. (2016). Simulated binding of transcription factors to active and inactive regions folds human chromosomes into loops, rosettes and topological domains. Nucleic acids research *44*, 3503-3512.
Brangwynne, C.P. (2013). Phase transitions and size scaling of membrane-less organelles. The Journal of cell biology *203*, 875-881.
Brangwynne, C.P., Eckmann, C.R., Courson, D.S., Rybarska, A., Hoege, C., Gharakhani, J., Julicher, F., and Hyman, A.A. (2009). Germline P granules are liquid droplets that localize by controlled dissolution/condensation. Science (New York, NY) *324*, 1729-1732.
Brangwynne, C.P., Mitchison, T.J., and Hyman, A.A. (2011). Active liquid-like behavior of nucleoli determines their size and shape in Xenopus laevis oocytes. Proceedings of the National Academy of Sciences of the United States of America *108*, 4334-4339.
Brickner, D.G., Ahmed, S., Meldi, L., Thompson, A., Light, W., Young, M., Hickman, T.L., Chu, F., Fabre, E., and Brickner, J.H. (2012). Transcription factor binding to a DNA zip code controls interchromosomal clustering at the nuclear periphery. Developmental cell *22*, 1234-1246.
Brickner, D.G., Cajigas, I., Fondufe-Mittendorf, Y., Ahmed, S., Lee, P.C., Widom, J., and Brickner, J.H. (2007). H2A.Z-mediated localization of genes at the nuclear periphery confers epigenetic memory of previous transcriptional state. PLoS biology *5*, e81.
Brickner, D.G., Sood, V., Tutucci, E., Coukos, R., Viets, K., Singer, R., and Brickner, J.H. (2016). Subnuclear positioning and interchromosomal clustering of the GAL1-10 locus are controlled by separable, interdependent mechanisms. Molecular biology of the cell.
Brickner, J.H., and Walter, P. (2004). Gene recruitment of the activated INO1 locus to the nuclear membrane. PLoS biology *2*, e342.
Brown, C.R., Kennedy, C.J., Delmar, V.A., Forbes, D.J., and Silver, P.A. (2008). Global histone acetylation induces functional genomic reorganization at mammalian nuclear pore complexes. Genes & development *22*, 627-639.
Brown, K.E., Baxter, J., Graf, D., Merkenschlager, M., and Fisher, A.G. (1999). Dynamic repositioning of genes in the nucleus of lymphocytes preparing for cell division. Molecular cell *3*, 207-217.

Brownell, J.E., Zhou, J., Ranalli, T., Kobayashi, R., Edmondson, D.G., Roth, S.Y., and Allis, C.D. (1996). Tetrahymena histone acetyltransferase A: a homolog to yeast Gcn5p linking histone acetylation to gene activation. Cell *84*, 843-851.
Bystricky, K., Heun, P., Gehlen, L., Langowski, J., and Gasser, S.M. (2004). Long-range compaction and flexibility of interphase chromatin in budding yeast analyzed by high-resolution imaging techniques. Proc Natl Acad Sci U S A *101*, 16495-16500.
Bystricky, K., Laroche, T., van Houwe, G., Blaszczyk, M., and Gasser, S.M. (2005). Chromosome looping in yeast: telomere pairing and coordinated movement reflect anchoring efficiency and territorial organization. The Journal of cell biology *168*, 375-387.
Cabal, G.G., Genovesio, A., Rodriguez-Navarro, S., Zimmer, C., Gadal, O., Lesne, A., Buc, H., Feuerbach-Fournier, F., Olivo-Marin, J.C., Hurt, E.C*., et al.* (2006). SAGA interacting factors confine sub-diffusion of transcribed genes to the nuclear envelope. Nature *441*, 770-773.
Canzio, D., Chang, E.Y., Shankar, S., Kuchenbecker, K.M., Simon, M.D., Madhani, H.D., Narlikar, G.J., and Al-Sady, B. (2011). Chromodomain-mediated oligomerization of HP1 suggests a nucleosome-bridging mechanism for heterochromatin assembly. Molecular cell *41*, 67-81.
Carro, D., and Piña, B. (2001). Genetic analysis of the karyotype instability in natural wine yeast strains. Yeast *18*, 1457-1470.
Casolari, J.M., Brown, C.R., Komili, S., West, J., Hieronymus, H., and Silver, P.A. (2004). Genome-wide localization of the nuclear transport machinery couples transcriptional status and nuclear organization. Cell *117*, 427-439.
Chang, B., Chen, Y., Zhao, Y., and Bruick, R.K. (2007). JMJD6 is a histone arginine demethylase. Science (New York, NY) *318*, 444-447.
Chen, C., and Kolodner, R.D. (1999). Gross chromosomal rearrangements in Saccharomyces cerevisiae replication and recombination defective mutants. Nature Genetics *23*, 81-85.
Chen, C., Lim, H.H., Shi, J., Tamura, S., Maeshima, K., Surana, U., and Gan, L. (2016). Budding yeast chromatin is dispersed in a crowded nucleoplasm in vivo. Molecular biology of the cell *27*, 3357-3368.
Chen, C.C., Carson, J.J., Feser, J., Tamburini, B., Zabaronick, S., Linger, J., and Tyler, J.K. (2008). Acetylated lysine 56 on histone H3 drives chromatin assembly after repair and signals for the completion of repair. Cell *134*, 231-243.
Chen, D., Ma, H., Hong, H., Koh, S.S., Huang, S.M., Schurter, B.T., Aswad, D.W., and Stallcup, M.R. (1999). Regulation of transcription by a protein methyltransferase. Science (New York, NY) *284*, 2174-2177.
Cheng, T.M., Heeger, S., Chaleil, R.A., Matthews, N., Stewart, A., Wright, J., Lim, C., Bates, P.A., and Uhlmann, F. (2015). A simple biophysical model emulates budding yeast chromosome condensation. eLife *4*, e05565.
Cherry, J.M., Hong, E.L., Amundsen, C., Balakrishnan, R., Binkley, G., Chan, E.T., Christie, K.R., Costanzo, M.C., Dwight, S.S., Engel, S.R*., et al.* (2012). Saccharomyces Genome Database: the genomics resource of budding yeast. Nucleic Acids Res *40*, D700-705.
Chi, Q., Wang, G., and Jiang, J. (2013). The persistence length and length per base of single-stranded DNA obtained from fluorescence correlation spectroscopy measurements using mean field theory. Physica A: Statistical Mechanics and its Applications *392*, 1072-1079.
Clapier, C.R., and Cairns, B.R. (2009). The biology of chromatin remodeling complexes. Annual review of biochemistry *78*, 273-304.
Crane, E., Bian, Q., McCord, R.P., Lajoie, B.R., Wheeler, B.S., Ralston, E.J., Uzawa, S., Dekker, J., and Meyer, B.J. (2015). Condensin-driven remodelling of X chromosome topology during dosage compensation. Nature *523*, 240-244.

Cremer, T., and Cremer, C. (2001). Chromosome territories, nuclear architecture and gene regulation in mammalian cells. Nature reviews Genetics *2*, 292-301.
Cui, Y., and Bustamante, C. (2000). Pulling a single chromatin fiber reveals the forces that maintain its higher-order structure. Proceedings of the National Academy of Sciences of the United States of America *97*, 127-132.
Dao, T.P., Kolaitis, R.-M., Kim, H.J., O'Donovan, K., Martyniak, B., Colicino, E., Hehnly, H., Taylor, J.P., and Castañeda, C.A. (2018). Ubiquitin Modulates Liquid-Liquid Phase Separation of UBQLN2 via Disruption of Multivalent Interactions. Molecular cell *69*, 965-978.e966.
Datta, A., Adjiri, A., New, L., Crouse, G.F., and Jinks Robertson, S. (1996). Mitotic crossovers between diverged sequences are regulated by mismatch repair proteins in Saccaromyces cerevisiae. Mol Cell Biol *16*, 1085-1093.
Dekker, J., Rippe, K., Dekker, M., and Kleckner, N. (2002). Capturing chromosome conformation. Science (New York, NY) *295*, 1306-1311.
Dietrich, F.S., Voegeli, S., Brachat, S., Lerch, A., Gates, K., Steiner, S., Mohr, C., Pöhlmann, R., Luedi, P., Choi, S*., et al.* (2004). The Ashbya gossypii genome as a tool for mapping the ancient Saccharomyces cerevisiae genome. Science *304*, 304-307.
Dion, M.F., Altschuler, S.J., Wu, L.F., and Rando, O.J. (2005). Genomic characterization reveals a simple histone H4 acetylation code. Proceedings of the National Academy of Sciences of the United States of America *102*, 5501-5506.
Dixon, J.R., Selvaraj, S., Yue, F., Kim, A., Li, Y., Shen, Y., Hu, M., Liu, J.S., and Ren, B. (2012). Topological domains in mammalian genomes identified by analysis of chromatin interactions. Nature *485*, 376-380.
Dong, P., Tu, X., Chu, P.Y., Lu, P., Zhu, N., Grierson, D., Du, B., Li, P., and Zhong, S. (2017). 3D Chromatin Architecture of Large Plant Genomes Determined by Local A/B Compartments. Mol Plant *10*, 1497-1509.
Dong, Q., Li, N., Li, X., Yuan, Z., Xie, D., Wang, X., Li, J., Yu, Y., Wang, J., Ding, B*., et al.* (2018). Genome-wide Hi-C analysis reveals extensive hierarchical chromatin interactions in rice. Plant J *94*, 1141-1156.
Dormidontova, E.E., Grosberg, A.Y., and Khokhlov, A.R. (1992). Intramolecular phase separation of a copolymer chain with mobile primary structure. Macromolecular Theory and Simulations *1*, 375-385.
Downs, J.A., Kosmidou, E., Morgan, A., and Jackson, S.P. (2003). Suppression of homologous recombination by the Saccharomyces cerevisiae linker histone. Molecular cell *11*, 1685-1692.
Driscoll, R., Hudson, A., and Jackson, S.P. (2007). Yeast Rtt109 Promotes Genome Stability by Acetylating Histone H3 on Lysine 56. Science (New York, NY) *315*, 649-652.
Duan, M.R., and Smerdon, M.J. (2014). Histone H3 lysine 14 (H3K14) acetylation facilitates DNA repair in a positioned nucleosome by stabilizing the binding of the chromatin Remodeler RSC (Remodels Structure of Chromatin). The Journal of biological chemistry *289*, 8353-8363.
Duan, Z., Andronescu, M., Schutz, K., McIlwain, S., Kim, Y.J., Lee, C., Shendure, J., Fields, S., Blau, C.A., and Noble, W.S. (2010). A three-dimensional model of the yeast genome. Nature *465*, 363-367.
Dujon, B., Sherman, D., Fischer, G., Durrens, P., Casaregola, S., Lafontaine, I., De Montigny, J., Marck, C., Neuvéglise, C., Talla, E*., et al.* (2004). Genome evolution in yeasts. Nature *430*, 35-44.
Durant, M., and Pugh, B.F. (2006). Genome-wide relationships between TAF1 and histone acetyltransferases in Saccharomyces cerevisiae. Molecular and cellular biology *26*, 2791-2802.
Eissenberg, J.C., and Elgin, S.C. (2014). HP1a: a structural chromosomal protein regulating transcription. Trends in genetics : TIG *30*, 103-110.

Elbaum-Garfinkle, S., Kim, Y., Szczepaniak, K., Chen, C.C., Eckmann, C.R., Myong, S., and Brangwynne, C.P. (2015). The disordered P granule protein LAF-1 drives phase separation into droplets with tunable viscosity and dynamics. Proceedings of the National Academy of Sciences of the United States of America *112*, 7189-7194.
Emre, N.C., Ingvarsdottir, K., Wyce, A., Wood, A., Krogan, N.J., Henry, K.W., Li, K., Marmorstein, R., Greenblatt, J.F., Shilatifard, A.*, et al.* (2005). Maintenance of low histone ubiquitylation by Ubp10 correlates with telomere-proximal Sir2 association and gene silencing. Molecular cell *17*, 585-594.
Erdel, F., and Rippe, K. (2011). Chromatin remodelling in mammalian cells by ISWI-type complexes--where, when and why? The FEBS journal *278*, 3608-3618.
Erdel, F., and Rippe, K. (2018). Formation of Chromatin Subcompartments by Phase Separation. Biophysical journal *114*, 2262-2270.
Fabrizio, P., Battistella, L., Vardavas, R., Gattazzo, C., Liou, L.L., Diaspro, A., Dossen, J.W., Gralla, E.B., and Longo, V.D. (2004). Superoxide is a mediator of an altruistic aging program in Saccharomyces cerevisiae. J Cell Biol *166*, 1055-1067.
Feric, M., and Brangwynne, C.P. (2013). A nuclear F-actin scaffold stabilizes ribonucleoprotein droplets against gravity in large cells. Nature cell biology *15*, 1253-1259.
Ferrai, C., de Castro, I.J., Lavitas, L., Chotalia, M., and Pombo, A. (2010). Gene positioning. Cold Spring Harbor perspectives in biology *2*, a000588.
Field, Y., Kaplan, N., Fondufe-Mittendorf, Y., Moore, I.K., Sharon, E., Lubling, Y., Widom, J., and Segal, E. (2008). Distinct modes of regulation by chromatin encoded through nucleosome positioning signals. PLoS computational biology *4*, e1000216.
Finn, E.H., Pegoraro, G., Brandão, H.B., Valton, A.L., Oomen, M.E., Dekker, J., Mirny, L., and Misteli, T. (2019). Extensive Heterogeneity and Intrinsic Variation in Spatial Genome Organization. Cell *176*, 1502-1515.e1510.
Fisher, J.K., Ballenger, M., O'Brien, E.T., Haase, J., Superfine, R., and Bloom, K. (2009). DNA relaxation dynamics as a probe for the intracellular environment. Proc Natl Acad Sci U S A *106*, 9250-9255.
Flavahan, W.A., Drier, Y., Liau, B.B., Gillespie, S.M., Venteicher, A.S., Stemmer-Rachamimov, A.O., Suva, M.L., and Bernstein, B.E. (2016). Insulator dysfunction and oncogene activation in IDH mutant gliomas. Nature *529*, 110-114.
Flory, P.J., and Gee, G. (1956). Statistical thermodynamics of semi-flexible chain molecules. Proceedings of the Royal Society of London Series A Mathematical and Physical Sciences *234*, 60-73.
Franke, M., Ibrahim, D.M., Andrey, G., Schwarzer, W., Heinrich, V., Schopflin, R., Kraft, K., Kempfer, R., Jerkovic, I., Chan, W.L.*, et al.* (2016). Formation of new chromatin domains determines pathogenicity of genomic duplications. Nature *538*, 265-269.
Frottin, F., Schueder, F., Tiwary, S., Gupta, R., Körner, R., Schlichthaerle, T., Cox, J., Jungmann, R., Hartl, F.U., and Hipp, M.S. (2019). The nucleolus functions as a phase-separated protein quality control compartment. Science (New York, NY) *365*, 342-347.
Gasser, S.M. (2001). Positions of potential: nuclear organization and gene expression. Cell *104*, 639-642.
Gerhold, C.B., and Gasser, S.M. (2014). INO80 and SWR complexes: relating structure to function in chromatin remodeling. Trends in cell biology *24*, 619-631.
Giaimo, B.D., Ferrante, F., Herchenrother, A., Hake, S.B., and Borggrefe, T. (2019). The histone variant H2A.Z in gene regulation. Epigenetics & chromatin *12*, 37.

Gibson, B.A., Doolittle, L.K., Schneider, M.W.G., Jensen, L.E., Gamarra, N., Henry, L., Gerlich, D.W., Redding, S., and Rosen, M.K. (2019). Organization of Chromatin by Intrinsic and Regulated Phase Separation. Cell *179*, 470-484.e421.
Godde, J.S., and Wolffe, A.P. (1996). Nucleosome assembly on CTG triplet repeats. The Journal of biological chemistry *271*, 15222-15229.
Goffeau, A., Barrell, B.G., Bussey, H., Davis, R.W., Dujon, B., Feldmann, H., Galibert, F., Hoheisel, J.D., Jacq, C., Johnston, M.*, et al.* (1996). Life with 6000 genes. Science *274*, 546, 563-547.
Grunstein, M., and Gasser, S.M. (2013). Epigenetics in Saccharomyces cerevisiae. Cold Spring Harb Perspect Biol *5*.
Guelen, L., Pagie, L., Brasset, E., Meuleman, W., Faza, M.B., Talhout, W., Eussen, B.H., de Klein, A., Wessels, L., de Laat, W.*, et al.* (2008). Domain organization of human chromosomes revealed by mapping of nuclear lamina interactions. Nature *453*, 948-951.
Han, J., Zhou, H., Horazdovsky, B., Zhang, K., Xu, R.M., and Zhang, Z. (2007). Rtt109 acetylates histone H3 lysine 56 and functions in DNA replication. Science (New York, NY) *315*, 653-655.
He, Y., Lawrimore, J., Cook, D., Van Gorder, E.E., De Larimat, S.C., Adalsteinsson, D., Forest, M.G., and Bloom, K. (2020). Statistical mechanics of chromosomes: in vivo and in silico approaches reveal high-level organization and structure arise exclusively through mechanical feedback between loop extruders and chromatin substrate properties. Nucleic acids research *48*, 11284-11303.
Heard, E., and Bickmore, W. (2007). The ins and outs of gene regulation and chromosome territory organisation. Current opinion in cell biology *19*, 311-316.
Heintzman, N.D., Stuart, R.K., Hon, G., Fu, Y., Ching, C.W., Hawkins, R.D., Barrera, L.O., Van Calcar, S., Qu, C., Ching, K.A.*, et al.* (2007). Distinct and predictive chromatin signatures of transcriptional promoters and enhancers in the human genome. Nature genetics *39*, 311-318.
Henderson, I.R., and Bomblies, K. (2021). Evolution and Plasticity of Genome-Wide Meiotic Recombination Rates. Annu Rev Genet *55*, 23-43.
Henikoff, S. (2009). Labile H3.3+H2A.Z nucleosomes mark 'nucleosome-free regions'. Nature genetics *41*, 865-866.
Henikoff, S., and Furuyama, T. (2012). The unconventional structure of centromeric nucleosomes. Chromosoma *121*, 341-352.
Henninger, J.E., Oksuz, O., Shrinivas, K., Sagi, I., LeRoy, G., Zheng, M.M., Andrews, J.O., Zamudio, A.V., Lazaris, C., Hannett, N.M.*, et al.* (2021). RNA-Mediated Feedback Control of Transcriptional Condensates. Cell *184*, 207-225 e224.
Henry, K.W., Wyce, A., Lo, W.S., Duggan, L.J., Emre, N.C., Kao, C.F., Pillus, L., Shilatifard, A., Osley, M.A., and Berger, S.L. (2003). Transcriptional activation via sequential histone H2B ubiquitylation and deubiquitylation, mediated by SAGA-associated Ubp8. Genes & development *17*, 2648-2663.
Hergeth, S.P., and Schneider, R. (2015). The H1 linker histones: multifunctional proteins beyond the nucleosomal core particle. EMBO reports *16*, 1439-1453.
Hernandez-Verdun, D., Roussel, P., Thiry, M., Sirri, V., and Lafontaine, D.L. (2010). The nucleolus: structure/function relationship in RNA metabolism. Wiley interdisciplinary reviews RNA *1*, 415-431.
Heun, P., Laroche, T., Raghuraman, M.K., and Gasser, S.M. (2001a). The positioning and dynamics of origins of replication in the budding yeast nucleus. The Journal of cell biology *152*, 385-400.
Heun, P., Laroche, T., Shimada, K., Furrer, P., and Gasser Susan, M. (2001b). Chromosome Dynamics in the Yeast Interphase Nucleus. Science (New York, NY) *294*, 2181-2186.

Hickman, M.A., Froyd, C.A., and Rusche, L.N. (2011). Reinventing heterochromatin in budding yeasts: Sir2 and the origin recognition complex take center stage. Eukaryot Cell *10*, 1183-1192.
Hnisz, D., Shrinivas, K., Young, R.A., Chakraborty, A.K., and Sharp, P.A. (2017). A Phase Separation Model for Transcriptional Control. Cell *169*, 13-23.
Hnisz, D., Weintraub, A.S., Day, D.S., Valton, A.L., Bak, R.O., Li, C.H., Goldmann, J., Lajoie, B.R., Fan, Z.P., Sigova, A.A*., et al.* (2016). Activation of proto-oncogenes by disruption of chromosome neighborhoods. Science (New York, NY) *351*, 1454-1458.
Holehouse, A.S., Ginell, G.M., Griffith, D., and Böke, E. (2021). Clustering of Aromatic Residues in Prion-like Domains Can Tune the Formation, State, and Organization of Biomolecular Condensates. Biochemistry *60*, 3566-3581.
Hsieh, T.H., Weiner, A., Lajoie, B., Dekker, J., Friedman, N., and Rando, O.J. (2015). Mapping Nucleosome Resolution Chromosome Folding in Yeast by Micro-C. Cell *162*, 108-119.
Huang, M.E., Rio, A.G., Nicolas, A., and Kolodner, R.D. (2003). A genomewide screen in Saccharomyces cerevisiae for genes that suppress the accumulation of mutations. Proc Natl Acad Sci U S A *100*, 11529-11534.
Huggins, M.L. (1942). THERMODYNAMIC PROPERTIES OF SOLUTIONS OF LONG-CHAIN COMPOUNDS. Annals of the New York Academy of Sciences *43*, 1-32.
Hughes, A.L., and Rando, O.J. (2014). Mechanisms underlying nucleosome positioning in vivo. Annual review of biophysics *43*, 41-63.
Hult, C., Adalsteinsson, D., Vasquez, P.A., Lawrimore, J., Bennett, M., York, A., Cook, D., Yeh, E., Forest, M.G., and Bloom, K. (2017). Enrichment of dynamic chromosomal crosslinks drive phase separation of the nucleolus. Nucleic Acids Res *45*, 11159-11173.
Hyland, E.M., Cosgrove, M.S., Molina, H., Wang, D., Pandey, A., Cottee, R.J., and Boeke, J.D. (2005). Insights into the role of histone H3 and histone H4 core modifiable residues in Saccharomyces cerevisiae. Molecular and cellular biology *25*, 10060-10070.
Iarovaia, O.V., Minina, E.P., Sheval, E.V., Onichtchouk, D., Dokudovskaya, S., Razin, S.V., and Vassetzky, Y.S. (2019). Nucleolus: A Central Hub for Nuclear Functions. Trends in cell biology *29*, 647-659.
Iborra, F.J. (2007). Can visco-elastic phase separation, macromolecular crowding and colloidal physics explain nuclear organisation? Theoretical biology & medical modelling *4*, 15.
Imai, R., Nozaki, T., Tani, T., Kaizu, K., Hibino, K., Ide, S., Tamura, S., Takahashi, K., Shribak, M., and Maeshima, K. (2017). Density imaging of heterochromatin in live cells using orientation-independent-DIC microscopy. Molecular biology of the cell *28*, 3349-3359.
Ioshikhes, I.P., Albert, I., Zanton, S.J., and Pugh, B.F. (2006). Nucleosome positions predicted through comparative genomics. Nature genetics *38*, 1210-1215.
Jenuwein, T., and Allis, C.D. (2001). Translating the histone code. Science (New York, NY) *293*, 1074-1080.
Jeronimo, C., Poitras, C., and Robert, F. (2019). Histone Recycling by FACT and Spt6 during Transcription Prevents the Scrambling of Histone Modifications. Cell reports *28*, 1206-1218.e1208.
Ji, Q., Mai, J., Ding, Y., Wei, Y., Ledesma-Amaro, R., and Ji, X.-J. (2020). Improving the homologous recombination efficiency of Yarrowia lipolytica by grafting heterologous component from Saccharomyces cerevisiae. Metabolic engineering communications *11*, e00152-e00152.
Jin, Q.W., Fuchs, J., and Loidl, J. (2000). Centromere clustering is a major determinant of yeast interphase nuclear organization. J Cell Sci *113 (Pt 11)*, 1903-1912.

Jun, S., and Mulder, B. (2006). Entropy-driven spatial organization of highly confined polymers: lessons for the bacterial chromosome. Proceedings of the National Academy of Sciences of the United States of America *103*, 12388-12393.
Kadosh, D., and Struhl, K. (1998). Targeted recruitment of the Sin3-Rpd3 histone deacetylase complex generates a highly localized domain of repressed chromatin in vivo. Molecular and cellular biology *18*, 5121-5127.
Kalverda, B., Pickersgill, H., Shloma, V.V., and Fornerod, M. (2010). Nucleoporins directly stimulate expression of developmental and cell-cycle genes inside the nucleoplasm. Cell *140*, 360-371.
Kanellis, P., Gagliardi, M., Banath, J.P., Szilard, R.K., Nakada, S., Galicia, S., Sweeney, F.D., Cabelof, D.C., Olive, P.L., and Durocher, D. (2007). A screen for suppressors of gross chromosomal rearrangements identifies a conserved role for PLP in preventing DNA lesions. PLoS Genet *3*, e134.
Kaplan, N., Moore, I.K., Fondufe-Mittendorf, Y., Gossett, A.J., Tillo, D., Field, Y., LeProust, E.M., Hughes, T.R., Lieb, J.D., Widom, J.*, et al.* (2009). The DNA-encoded nucleosome organization of a eukaryotic genome. Nature *458*, 362-366.
Kawaguchi, T., Tanigawa, A., Naganuma, T., Ohkawa, Y., Souquere, S., Pierron, G., and Hirose, T. (2015). SWI/SNF chromatin-remodeling complexes function in noncoding RNA-dependent assembly of nuclear bodies. Proceedings of the National Academy of Sciences of the United States of America *112*, 4304-4309.
Kechkar, A., Nair, D., Heilemann, M., Choquet, D., and Sibarita, J.B. (2013). Real-time analysis and visualization for single-molecule based super-resolution microscopy. PLoS One *8*, e62918.
Kedersha, N., Ivanov, P., and Anderson, P. (2013). Stress granules and cell signaling: more than just a passing phase? Trends in biochemical sciences *38*, 494-506.
Kellis, M., Birren, B.W., and Lander, E.S. (2004). Proof and evolutionary analysis of ancient genome duplication in the yeast Saccharomyces cerevisiae. Nature *428*, 617-624.
Kim, S.H., McQueen, P.G., Lichtman, M.K., Shevach, E.M., Parada, L.A., and Misteli, T. (2004). Spatial genome organization during T-cell differentiation. Cytogenetic and genome research *105*, 292-301.
Kind, J., Pagie, L., de Vries, S.S., Nahidiazar, L., Dey, S.S., Bienko, M., Zhan, Y., Lajoie, B., de Graaf, C.A., Amendola, M.*, et al.* (2015). Genome-wide maps of nuclear lamina interactions in single human cells. Cell *163*, 134-147.
Klose, R.J., Gardner, K.E., Liang, G., Erdjument-Bromage, H., Tempst, P., and Zhang, Y. (2007). Demethylation of histone H3K36 and H3K9 by Rph1: a vestige of an H3K9 methylation system in Saccharomyces cerevisiae? Mol Cell Biol *27*, 3951-3961.
Kornberg, R.D. (1974). Chromatin structure: a repeating unit of histones and DNA. Science (New York, NY) *184*, 868-871.
Kornberg, R.D., and Klug, A. (1981). The nucleosome. Sci Am *244*, 52-64.
Kornberg, R.D., and Thomas, J.O. (1974). Chromatin structure; oligomers of the histones. Science (New York, NY) *184*, 865-868.
Kosak, S.T., Skok, J.A., Medina, K.L., Riblet, R., Le Beau, M.M., Fisher, A.G., and Singh, H. (2002). Subnuclear compartmentalization of immunoglobulin loci during lymphocyte development. Science (New York, NY) *296*, 158-162.
Kouzarides, T. (2007). Chromatin modifications and their function. Cell *128*, 693-705.
Kuo, M.H., Brownell, J.E., Sobel, R.E., Ranalli, T.A., Cook, R.G., Edmondson, D.G., Roth, S.Y., and Allis, C.D. (1996). Transcription-linked acetylation by Gcn5p of histones H3 and H4 at specific lysines. Nature *383*, 269-272.

Kuo, M.H., vom Baur, E., Struhl, K., and Allis, C.D. (2000). Gcn4 activator targets Gcn5 histone acetyltransferase to specific promoters independently of transcription. Molecular cell *6*, 1309-1320.
Lachner, M., O'Carroll, D., Rea, S., Mechtler, K., and Jenuwein, T. (2001). Methylation of histone H3 lysine 9 creates a binding site for HP1 proteins. Nature *410*, 116-120.
Lakshminarasimhan, M., Boanca, G., Banks, C.A., Hattem, G.L., Gabriel, A.E., Groppe, B.D., Smoyer, C., Malanowski, K.E., Peak, A., Florens, L.*, et al.* (2016). Proteomic and Genomic Analyses of the Rvb1 and Rvb2 Interaction Network upon Deletion of R2TP Complex Components. Molecular & cellular proteomics : MCP *15*, 960-974.
Lang, G.I., and Murray, A.W. (2008). Estimating the per-base-pair mutation rate in the yeast Saccharomyces cerevisiae. Genetics *178*, 67-82.
Langst, G., and Manelyte, L. (2015). Chromatin Remodelers: From Function to Dysfunction. Genes *6*, 299-324.
Larson, A.G., Elnatan, D., Keenen, M.M., Trnka, M.J., Johnston, J.B., Burlingame, A.L., Agard, D.A., Redding, S., and Narlikar, G.J. (2017a). Liquid droplet formation by HP1alpha suggests a role for phase separation in heterochromatin. Nature *547*, 236-240.
Larson, A.G., Elnatan, D., Keenen, M.M., Trnka, M.J., Johnston, J.B., Burlingame, A.L., Agard, D.A., Redding, S., and Narlikar, G.J. (2017b). Liquid droplet formation by HP1α suggests a role for phase separation in heterochromatin. Nature *547*, 236-240.
Lawrimore, J., Aicher, J.K., Hahn, P., Fulp, A., Kompa, B., Vicci, L., Falvo, M., Taylor, R.M., 2nd, and Bloom, K. (2016). ChromoShake: a chromosome dynamics simulator reveals that chromatin loops stiffen centromeric chromatin. Molecular biology of the cell *27*, 153-166.
Lawrimore, J., Kolbin, D., Stanton, J., Khan, M., de Larminat, S.C., Lawrimore, C., Yeh, E., and Bloom, K. (2021). The rDNA is biomolecular condensate formed by polymer-polymer phase separation and is sequestered in the nucleolus by transcription and R-loops. Nucleic acids research *49*, 4586-4598.
Lee, K.K., Sardiu, M.E., Swanson, S.K., Gilmore, J.M., Torok, M., Grant, P.A., Florens, L., Workman, J.L., and Washburn, M.P. (2011). Combinatorial depletion analysis to assemble the network architecture of the SAGA and ADA chromatin remodeling complexes. Molecular systems biology *7*, 503.
Lee, M.E., DeLoache, W.C., Cervantes, B., and Dueber, J.E. (2015). A Highly Characterized Yeast Toolkit for Modular, Multipart Assembly. ACS synthetic biology *4*, 975-986.
Lee, W., Tillo, D., Bray, N., Morse, R.H., Davis, R.W., Hughes, T.R., and Nislow, C. (2007). A high-resolution atlas of nucleosome occupancy in yeast. Nature genetics *39*, 1235-1244.
Leng, H., Liu, S., Lei, Y., Tang, Y., Gu, S., Hu, J., Chen, S., Feng, J., and Li, Q. (2021). FACT interacts with Set3 HDAC and fine-tunes GAL1 transcription in response to environmental stimulation. Nucleic acids research *49*, 5502-5519.
Li, G., Tian, Y., and Zhu, W.-G. (2020). The Roles of Histone Deacetylases and Their Inhibitors in Cancer Therapy. *8*.
Li, Q., Zhou, H., Wurtele, H., Davies, B., Horazdovsky, B., Verreault, A., and Zhang, Z. (2008). Acetylation of histone H3 lysine 56 regulates replication-coupled nucleosome assembly. Cell *134*, 244-255.
Lichten, M., and Haber, J.E. (1989). Position effects in ectopic and allelic mitotic recombination in Saccharomyces cerevisiae. Genetics *123*, 261-268.
Lieberman-Aiden, E., van Berkum, N.L., Williams, L., Imakaev, M., Ragoczy, T., Telling, A., Amit, I., Lajoie, B.R., Sabo, P.J., Dorschner, M.O.*, et al.* (2009). Comprehensive mapping of long-range interactions reveals folding principles of the human genome. Science (New York, NY) *326*, 289-293.

Lieleg, C., Krietenstein, N., Walker, M., and Korber, P. (2015). Nucleosome positioning in yeasts: methods, maps, and mechanisms. Chromosoma *124*, 131-151.
Light, W.H., Brickner, D.G., Brand, V.R., and Brickner, J.H. (2010). Interaction of a DNA zip code with the nuclear pore complex promotes H2A.Z incorporation and INO1 transcriptional memory. Molecular cell *40*, 112-125.
Linhoff, M.W., Garg, S.K., and Mandel, G. (2015). A high-resolution imaging approach to investigate chromatin architecture in complex tissues. Cell *163*, 246-255.
Liu, C.L., Kaplan, T., Kim, M., Buratowski, S., Schreiber, S.L., Friedman, N., and Rando, O.J. (2005). Single-nucleosome mapping of histone modifications in S. cerevisiae. PLoS biology *3*, e328.
Liu, N., Balliano, A., and Hayes, J.J. (2011). Mechanism(s) of SWI/SNF-induced nucleosome mobilization. Chembiochem : a European journal of chemical biology *12*, 196-204.
Lo, W.-S., Duggan, L., Tolga , N.C., Emre, Belotserkovskya, R., Lane, W.S., Shiekhattar, R., and Berger, S.L. (2001). Snf1--a Histone Kinase That Works in Concert with the Histone Acetyltransferase Gcn5 to Regulate Transcription. Science (New York, NY) *293*, 1142-1146.
Lomberk, G., Wallrath, L., and Urrutia, R. (2006). The Heterochromatin Protein 1 family. Genome Biol *7*, 228.
Lõoke, M., Kristjuhan, K., and Kristjuhan, A. (2011). Extraction of genomic DNA from yeasts for PCR-based applications. BioTechniques *50*, 325-328.
Lowary, P.T., and Widom, J. (1998). New DNA sequence rules for high affinity binding to histone octamer and sequence-directed nucleosome positioning. Journal of molecular biology *276*, 19-42.
Luger, K., Mader, A.W., Richmond, R.K., Sargent, D.F., and Richmond, T.J. (1997). Crystal structure of the nucleosome core particle at 2.8 A resolution. Nature *389*, 251-260.
Lupianez, D.G., Kraft, K., Heinrich, V., Krawitz, P., Brancati, F., Klopocki, E., Horn, D., Kayserili, H., Opitz, J.M., Laxova, R.*, et al.* (2015). Disruptions of topological chromatin domains cause pathogenic rewiring of gene-enhancer interactions. Cell *161*, 1012-1025.
Madia, F., Gattazzo, C., Wei, M., Fabrizio, P., Burhans, W.C., Weinberger, M., Galbani, A., Smith, J.R., Nguyen, C., Huey, S.*, et al.* (2008). Longevity mutation in SCH9 prevents recombination errors and premature genomic instability in a Werner/Bloom model system. The Journal of cell biology *180*, 67-81.
Maeshima, K., Ide, S., and Babokhov, M. (2019). Dynamic chromatin organization without the 30-nm fiber. Current opinion in cell biology *58*, 95-104.
Maeshima, K., Ide, S., Hibino, K., and Sasai, M. (2016). Liquid-like behavior of chromatin. Current opinion in genetics & development *37*, 36-45.
Makova, K.D., and Hardison, R.C. (2015). The effects of chromatin organization on variation in mutation rates in the genome. Nature reviews Genetics *16*, 213-223.
Malinovska, L., Kroschwald, S., and Alberti, S. (2013). Protein disorder, prion propensities, and self-organizing macromolecular collectives. Biochimica et biophysica acta *1834*, 918-931.
Malleshaiah, M.K., Shahrezaei, V., Swain, P.S., and Michnick, S.W. (2010). The scaffold protein Ste5 directly controls a switch-like mating decision in yeast. Nature *465*, 101-105.
Manohar, M., Mooney, A.M., North, J.A., Nakkula, R.J., Picking, J.W., Edon, A., Fishel, R., Poirier, M.G., and Ottesen, J.J. (2009). Acetylation of histone H3 at the nucleosome dyad alters DNA-histone binding. The Journal of biological chemistry *284*, 23312-23321.
Martin, A.M., Pouchnik, D.J., Walker, J.L., and Wyrick, J.J. (2004). Redundant roles for histone H3 N-terminal lysine residues in subtelomeric gene repression in Saccharomyces cerevisiae. Genetics *167*, 1123-1132.
Martincorena, I., Seshasayee, A.S., and Luscombe, N.M. (2012). Evidence of non-random mutation rates suggests an evolutionary risk management strategy. Nature *485*, 95-98.

Mavrich, T.N., Jiang, C., Ioshikhes, I.P., Li, X., Venters, B.J., Zanton, S.J., Tomsho, L.P., Qi, J., Glaser, R.L., Schuster, S.C.*, et al.* (2008). Nucleosome organization in the Drosophila genome. Nature *453*, 358-362.
McBryant, S.J., Lu, X., and Hansen, J.C. (2010). Multifunctionality of the linker histones: an emerging role for protein-protein interactions. Cell research *20*, 519-528.
McIlwraith, M.J., and West, S.C. (2008). DNA Repair Synthesis Facilitates RAD52-Mediated Second-End Capture during DSB Repair. Molecular Cell *29*, 510-516.
Measday, V., and Stirling, P.C. (2015). Navigating yeast genome maintenance with functional genomics. Briefings in Functional Genomics *15*, 119-129.
Meister, P., Towbin, B.D., Pike, B.L., Ponti, A., and Gasser, S.M. (2010). The spatial dynamics of tissue-specific promoters during C. elegans development. Genes & development *24*, 766-782.
Meneghini, M.D., Wu, M., and Madhani, H.D. (2003). Conserved histone variant H2A.Z protects euchromatin from the ectopic spread of silent heterochromatin. Cell *112*, 725-736.
Mercy, G., Mozziconacci, J., Scolari, V.F., Yang, K., Zhao, G., Thierry, A., Luo, Y., Mitchell, L.A., Shen, M., Shen, Y.*, et al.* (2017). 3D organization of synthetic and scrambled chromosomes. Science (New York, NY) *355*.
Mersfelder, E.L., and Parthun, M.R. (2006). The tale beyond the tail: histone core domain modifications and the regulation of chromatin structure. Nucleic acids research *34*, 2653-2662.
Michieletto, D., Chiang, M., Colì, D., Papantonis, A., Orlandini, E., Cook, P.R., and Marenduzzo, D. (2017). Shaping epigenetic memory via genomic bookmarking. Nucleic acids research *46*, 83-93.
Miron, E., Oldenkamp, R., Brown, J.M., Pinto, D.M.S., Xu, C.S., Faria, A.R., Shaban, H.A., Rhodes, J.D.P., Innocent, C., de Ornellas, S.*, et al.* (2020). Chromatin arranges in chains of mesoscale domains with nanoscale functional topography independent of cohesin. Sci Adv *6*.
Mizuguchi, T., Barrowman, J., and Grewal, S.I.S. (2015). Chromosome domain architecture and dynamic organization of the fission yeast genome. FEBS letters *589*, 2975-2986.
Mizuguchi, T., Fudenberg, G., Mehta, S., Belton, J.M., Taneja, N., Folco, H.D., FitzGerald, P., Dekker, J., Mirny, L., Barrowman, J.*, et al.* (2014). Cohesin-dependent globules and heterochromatin shape 3D genome architecture in S. pombe. Nature *516*, 432-435.
Mizzen, C.A., Yang, X.J., Kokubo, T., Brownell, J.E., Bannister, A.J., Owen-Hughes, T., Workman, J., Wang, L., Berger, S.L., Kouzarides, T.*, et al.* (1996). The TAF(II)250 subunit of TFIID has histone acetyltransferase activity. Cell *87*, 1261-1270.
Montavon, T., Shukeir, N., Erikson, G., Engist, B., Onishi-Seebacher, M., Ryan, D., Musa, Y., Mittler, G., Meyer, A.G., Genoud, C.*, et al.* (2021). Complete loss of H3K9 methylation dissolves mouse heterochromatin organization. Nat Commun *12*, 4359.
Morawska, M., and Ulrich, H.D. (2013). An expanded tool kit for the auxin-inducible degron system in budding yeast. Yeast (Chichester, England) *30*, 341-351.
Muck, J.S., Kandasamy, K., Englmann, A., Gunther, M., and Zink, D. (2012). Perinuclear positioning of the inactive human cystic fibrosis gene depends on CTCF, A-type lamins and an active histone deacetylase. Journal of cellular biochemistry *113*, 2607-2621.
Nakayama, J., Rice, J.C., Strahl, B.D., Allis, C.D., and Grewal, S.I. (2001). Role of histone H3 lysine 9 methylation in epigenetic control of heterochromatin assembly. Science *292*, 110-113.
Neumann, F.R., Dion, V., Gehlen, L.R., Tsai-Pflugfelder, M., Schmid, R., Taddei, A., and Gasser, S.M. (2012). Targeted INO80 enhances subnuclear chromatin movement and ectopic homologous recombination. Genes Dev *26*, 369-383.
Ng, M.K., and Cheung, P. (2016). A brief histone in time: understanding the combinatorial functions of histone PTMs in the nucleosome context. Biochemistry and cell biology = Biochimie et biologie cellulaire *94*, 33-42.

Nguyen, V.Q., Ranjan, A., Stengel, F., Wei, D., Aebersold, R., Wu, C., and Leschziner, A.E. (2013). Molecular architecture of the ATP-dependent chromatin-remodeling complex SWR1. Cell *154*, 1220-1231.
Nora, E.P., Lajoie, B.R., Schulz, E.G., Giorgetti, L., Okamoto, I., Servant, N., Piolot, T., van Berkum, N.L., Meisig, J., Sedat, J.*, et al.* (2012). Spatial partitioning of the regulatory landscape of the X-inactivation centre. Nature *485*, 381-385.
Nott, T.J., Petsalaki, E., Farber, P., Jervis, D., Fussner, E., Plochowietz, A., Craggs, T.D., Bazett-Jones, D.P., Pawson, T., Forman-Kay, J.D.*, et al.* (2015). Phase transition of a disordered nuage protein generates environmentally responsive membraneless organelles. Molecular cell *57*, 936-947.
Oeffinger, M., Wei, K.E., Rogers, R., DeGrasse, J.A., Chait, B.T., Aitchison, J.D., and Rout, M.P. (2007). Comprehensive analysis of diverse ribonucleoprotein complexes. Nature methods *4*, 951-956.
Ogawa, L.M., and Baserga, S.J. (2017). Crosstalk between the nucleolus and the DNA damage response. Molecular bioSystems *13*, 443-455.
Olins, D.E., and Olins, A.L. (2003). Chromatin history: our view from the bridge. Nature Reviews Molecular Cell Biology *4*, 809-814.
Ong, C.T., and Corces, V.G. (2009). Insulators as mediators of intra- and inter-chromosomal interactions: a common evolutionary theme. Journal of biology *8*, 73.
Opitz, N., Schmitt, K., Hofer-Pretz, V., Neumann, B., Krebber, H., Braus, G.H., and Valerius, O. (2017). Capturing the Asc1p/Receptor for Activated C Kinase 1 (RACK1) Microenvironment at the Head Region of the 40S Ribosome with Quantitative BioID in Yeast. Molecular & cellular proteomics : MCP *16*, 2199-2218.
Orsztynowicz, M., Lechniak, D., Pawlak, P., Kociucka, B., Kubickova, S., Cernohorska, H., and Madeja, Z.E. (2017). Changes in chromosome territory position within the nucleus reflect alternations in gene expression related to embryonic lineage specification. PloS one *12*, e0182398.
Ou, H.D., Phan, S., Deerinck, T.J., Thor, A., Ellisman, M.H., and O'Shea, C.C. (2017). ChromEMT: Visualizing 3D chromatin structure and compaction in interphase and mitotic cells. Science (New York, NY) *357*.
Oughtred, R., Rust, J., Chang, C., Breitkreutz, B.J., Stark, C., Willems, A., Boucher, L., Leung, G., Kolas, N., Zhang, F.*, et al.* (2021). The BioGRID database: A comprehensive biomedical resource of curated protein, genetic, and chemical interactions. Protein Sci *30*, 187-200.
Parra, M.A., Kerr, D., Fahy, D., Pouchnik, D.J., and Wyrick, J.J. (2006). Deciphering the roles of the histone H2B N-terminal domain in genome-wide transcription. Molecular and cellular biology *26*, 3842-3852.
Pepenella, S., Murphy, K.J., and Hayes, J.J. (2014). Intra- and inter-nucleosome interactions of the core histone tail domains in higher-order chromatin structure. Chromosoma *123*, 3-13.
Pessina, F., Giavazzi, F., Yin, Y., Gioia, U., Vitelli, V., Galbiati, A., Barozzi, S., Garre, M., Oldani, A., Flaus, A.*, et al.* (2019). Functional transcription promoters at DNA double-strand breaks mediate RNA-driven phase separation of damage-response factors. Nature Cell Biology *21*, 1286-1299.
Petty, E.L., Collette, K.S., Cohen, A.J., Snyder, M.J., and Csankovszki, G. (2009). Restricting dosage compensation complex binding to the X chromosomes by H2A.Z/HTZ-1. PLoS Genet *5*, e1000699.
Phillips-Cremins, J.E., Sauria, M.E., Sanyal, A., Gerasimova, T.I., Lajoie, B.R., Bell, J.S., Ong, C.T., Hookway, T.A., Guo, C., Sun, Y.*, et al.* (2013). Architectural protein subclasses shape 3D organization of genomes during lineage commitment. Cell *153*, 1281-1295.

Phillips, D.M., and Johns, E.W. (1965). A FRACTIONATION OF THE HISTONES OF GROUP F2A FROM CALF THYMUS. The Biochemical journal *94*, 127-130.
Pich, O., Muiños, F., Sabarinathan, R., Reyes-Salazar, I., Gonzalez-Perez, A., and Lopez-Bigas, N. (2018). Somatic and Germline Mutation Periodicity Follow the Orientation of the DNA Minor Groove around Nucleosomes. Cell *175*, 1074-1087.e1018.
Pokholok, D.K., Harbison, C.T., Levine, S., Cole, M., Hannett, N.M., Lee, T.I., Bell, G.W., Walker, K., Rolfe, P.A., Herbolsheimer, E.*, et al.* (2005). Genome-wide map of nucleosome acetylation and methylation in yeast. Cell *122*, 517-527.
Pouokam, M., Cruz, B., Burgess, S., Segal, M.R., Vazquez, M., and Arsuaga, J. (2019). The Rabl configuration limits topological entanglement of chromosomes in budding yeast. Scientific Reports *9*, 6795.
Pulice, J.L., and Kadoch, C. (2017). Composition and Function of Mammalian SWI/SNF Chromatin Remodeling Complexes in Human Disease. Cold Spring Harbor symposia on quantitative biology.
Quail, T., Golfier, S., Elsner, M., Ishihara, K., Murugesan, V., Renger, R., Jülicher, F., and Brugués, J. (2021). Force generation by protein–DNA co-condensation. Nature Physics *17*, 1007-1012.
Querol, A., and Bond, U. (2009). The complex and dynamic genomes of industrial yeasts. FEMS Microbiol Lett *293*, 1-10.
Quinodoz, S.A., and Guttman, M. (2021). Essential Roles for RNA in Shaping Nuclear Organization. Cold Spring Harb Perspect Biol.
Rabl, C. (1885). Uber Zelltheilung. Morphol Jahrb *10*, 214-330.
Raffoux, X., Bourge, M., Dumas, F., Martin, O.C., and Falque, M. (2018). High-throughput measurement of recombination rates and genetic interference in Saccharomyces cerevisiae. Yeast *35*, 431-442.
Ragoczy, T., Bender, M.A., Telling, A., Byron, R., and Groudine, M. (2006). The locus control region is required for association of the murine beta-globin locus with engaged transcription factories during erythroid maturation. Genes & development *20*, 1447-1457.
Raisner, R.M., Hartley, P.D., Meneghini, M.D., Bao, M.Z., Liu, C.L., Schreiber, S.L., Rando, O.J., and Madhani, H.D. (2005). Histone variant H2A.Z marks the 5' ends of both active and inactive genes in euchromatin. Cell *123*, 233-248.
Randise-Hinchliff, C., Coukos, R., Sood, V., Sumner, M.C., Zdraljevic, S., Meldi Sholl, L., Garvey Brickner, D., Ahmed, S., Watchmaker, L., and Brickner, J.H. (2016). Strategies to regulate transcription factor-mediated gene positioning and interchromosomal clustering at the nuclear periphery. The Journal of cell biology *212*, 633-646.
Rando, O.J. (2007). Global patterns of histone modifications. Current opinion in genetics & development *17*, 94-99.
Ransom, M., Dennehey, B.K., and Tyler, J.K. (2010). Chaperoning histones during DNA replication and repair. Cell *140*, 183-195.
Rao, S.S., Huntley, M.H., Durand, N.C., Stamenova, E.K., Bochkov, I.D., Robinson, J.T., Sanborn, A.L., Machol, I., Omer, A.D., Lander, E.S.*, et al.* (2014). A 3D map of the human genome at kilobase resolution reveals principles of chromatin looping. Cell *159*, 1665-1680.
Raveh-Sadka, T., Levo, M., Shabi, U., Shany, B., Keren, L., Lotan-Pompan, M., Zeevi, D., Sharon, E., Weinberger, A., and Segal, E. (2012). Manipulating nucleosome disfavoring sequences allows fine-tune regulation of gene expression in yeast. Nature genetics *44*, 743-750.
Rea, S., Eisenhaber, F., O'Carroll, D., Strahl, B.D., Sun, Z.W., Schmid, M., Opravil, S., Mechtler, K., Ponting, C.P., Allis, C.D.*, et al.* (2000). Regulation of chromatin structure by site-specific histone H3 methyltransferases. Nature *406*, 593-599.

Rechendorff, K., Witz, G., Adamcik, J., and Dietler, G. (2009). Persistence length and scaling properties of single-stranded DNA adsorbed on modified graphite. The Journal of chemical physics *131*, 095103.
Richmond, T.J., and Davey, C.A. (2003). The structure of DNA in the nucleosome core. Nature *423*, 145-150.
Riley, R., Haridas, S., Wolfe, K.H., Lopes, M.R., Hittinger, C.T., Göker, M., Salamov, A.A., Wisecaver, J.H., Long, T.M., Calvey, C.H.*, et al.* (2016). Comparative genomics of biotechnologically important yeasts. Proceedings of the National Academy of Sciences *113*, 9882.
Robzyk, K., Recht, J., and Osley, M.A. (2000). Rad6-dependent ubiquitination of histone H2B in yeast. Science (New York, NY) *287*, 501-504.
Rodrigues-Prause, A., Sampaio, N.M.V., Gurol, T.M., Aguirre, G.M., Sedam, H.N.C., Chapman, M.J., Malc, E.P., Ajith, V.P., Chakraborty, P., Tizei, P.A.*, et al.* (2018). A Case Study of Genomic Instability in an Industrial Strain of Saccharomyces cerevisiae. G3 (Bethesda, Md) *8*, 3703-3713.
Rohner, S., Kalck, V., Wang, X., Ikegami, K., Lieb, J.D., Gasser, S.M., and Meister, P. (2013). Promoter- and RNA polymerase II-dependent hsp-16 gene association with nuclear pores in Caenorhabditis elegans. The Journal of cell biology *200*, 589-604.
Roque, A., Iloro, I., Ponte, I., Arrondo, J.L., and Suau, P. (2005). DNA-induced secondary structure of the carboxyl-terminal domain of histone H1. The Journal of biological chemistry *280*, 32141-32147.
Rothstein, R.J. (1983). One-step gene disruption in yeast. Methods in enzymology *101*, 202-211.
Rouse, P.E. (1953). A Theory of the Linear Viscoelastic Properties of Dilute Solutions of Coiling Polymers. *21*, 1272-1280.
Rudnizky, S., Khamis, H., Ginosar, Y., Goren, E., Melamed, P., and Kaplan, A. (2021). Extended and dynamic linker histone-DNA Interactions control chromatosome compaction. Mol Cell *81*, 3410-3421 e3414.
Rufiange, A., Jacques, P.E., Bhat, W., Robert, F., and Nourani, A. (2007). Genome-wide replication-independent histone H3 exchange occurs predominantly at promoters and implicates H3 K56 acetylation and Asf1. Mol Cell *27*, 393-405.
Sabari, B.R., Dall'Agnese, A., Boija, A., Klein, I.A., Coffey, E.L., Shrinivas, K., Abraham, B.J., Hannett, N.M., Zamudio, A.V., Manteiga, J.C.*, et al.* (2018). Coactivator condensation at super-enhancers links phase separation and gene control. Science *361*.
Sáez-Vásquez, J., and Gadal, O. (2010). Genome organization and function: a view from yeast and Arabidopsis. Molecular plant *3*, 678-690.
Sanders, S.L., Jennings, J., Canutescu, A., Link, A.J., and Weil, P.A. (2002). Proteomics of the eukaryotic transcription machinery: identification of proteins associated with components of yeast TFIID by multidimensional mass spectrometry. Molecular and cellular biology *22*, 4723-4738.
Sanulli, S., Trnka, M.J., Dharmarajan, V., Tibble, R.W., Pascal, B.D., Burlingame, A.L., Griffin, P.R., Gross, J.D., and Narlikar, G.J. (2019). HP1 reshapes nucleosome core to promote heterochromatin phase separation. Nature.
Sassone-Corsi, P., Mizzen, C.A., Cheung, P., Crosio, C., Monaco, L., Jacquot, S., Hanauer, A., and Allis, C.D. (1999). Requirement of Rsk-2 for epidermal growth factor-activated phosphorylation of histone H3. Science (New York, NY) *285*, 886-891.
Satchwell, S.C., Drew, H.R., and Travers, A.A. (1986). Sequence periodicities in chicken nucleosome core DNA. Journal of molecular biology *191*, 659-675.
Scheffold, F., Diaz-Leyva, P., Reufer, M., Ben Braham, N., Lynch, I., and Harden, J.L. (2010). Brushlike interactions between thermoresponsive microgel particles. Phys Rev Lett *104*, 128304.

Schindelin, J., Arganda-Carreras, I., Frise, E., Kaynig, V., Longair, M., Pietzsch, T., Preibisch, S., Rueden, C., Saalfeld, S., Schmid, B.*, et al.* (2012). Fiji: an open-source platform for biological-image analysis. Nature methods *9*, 676-682.
Schmidtmann, E., Anton, T., Rombaut, P., Herzog, F., and Leonhardt, H. (2016). Determination of local chromatin composition by CasID. Nucleus (Austin, Tex) *7*, 476-484.
Schober, H., Kalck, V., Vega-Palas, M.A., Van Houwe, G., Sage, D., Unser, M., Gartenberg, M.R., and Gasser, S.M. (2008). Controlled exchange of chromosomal arms reveals principles driving telomere interactions in yeast. Genome Res *18*, 261-271.
Schones, D.E., Cui, K., Cuddapah, S., Roh, T.Y., Barski, A., Wang, Z., Wei, G., and Zhao, K. (2008). Dynamic regulation of nucleosome positioning in the human genome. Cell *132*, 887-898.
Scott, D.D., and Oeffinger, M. (2016). Nucleolin and nucleophosmin: nucleolar proteins with multiple functions in DNA repair. Biochemistry and cell biology = Biochimie et biologie cellulaire *94*, 419-432.
Segal, E., Fondufe-Mittendorf, Y., Chen, L., Thastrom, A., Field, Y., Moore, I.K., Wang, J.P., and Widom, J. (2006). A genomic code for nucleosome positioning. Nature *442*, 772-778.
Segura, J., Ferretti, L., Ramos-Onsins, S., Capilla, L., Farre, M., Reis, F., Oliver-Bonet, M., Fernandez-Bellon, H., Garcia, F., Garcia-Caldes, M.*, et al.* (2013). Evolution of recombination in eutherian mammals: insights into mechanisms that affect recombination rates and crossover interference. Proc Biol Sci *280*, 20131945.
Sexton, T., Yaffe, E., Kenigsberg, E., Bantignies, F., Leblanc, B., Hoichman, M., Parrinello, H., Tanay, A., and Cavalli, G. (2012). Three-dimensional folding and functional organization principles of the Drosophila genome. Cell *148*, 458-472.
Shaban, H.A., Barth, R., and Bystricky, K. (2018). Formation of correlated chromatin domains at nanoscale dynamic resolution during transcription. Nucleic acids research *46*, e77.
Shaban, H.A., and Seeber, A. (2020). Monitoring the spatio-temporal organization and dynamics of the genome. Nucleic acids research *48*, 3423-3434.
Shaw, W.M., Yamauchi, H., Mead, J., Gowers, G.-O.F., Bell, D.J., Öling, D., Larsson, N., Wigglesworth, M., Ladds, G., and Ellis, T. (2019). Engineering a Model Cell for Rational Tuning of GPCR Signaling. Cell *177*, 782-796.e727.
She, R., and Jarosz, D.F. (2018). Mapping Causal Variants with Single-Nucleotide Resolution Reveals Biochemical Drivers of Phenotypic Change. Cell *172*, 478-490.e415.
Shen, X., Mizuguchi, G., Hamiche, A., and Wu, C. (2000). A chromatin remodelling complex involved in transcription and DNA processing. Nature *406*, 541-544.
Shin, Y., Chang, Y.-C., Lee, D.S.W., Berry, J., Sanders, D.W., Ronceray, P., Wingreen, N.S., Haataja, M., and Brangwynne, C.P. (2018). Liquid Nuclear Condensates Mechanically Sense and Restructure the Genome. Cell *175*, 1481-1491.e1413.
Singleton, M.R., Dillingham, M.S., and Wigley, D.B. (2007). Structure and mechanism of helicases and nucleic acid translocases. Annual review of biochemistry *76*, 23-50.
Skok, J.A., Brown, K.E., Azuara, V., Caparros, M.L., Baxter, J., Takacs, K., Dillon, N., Gray, D., Perry, R.P., Merkenschlager, M.*, et al.* (2001). Nonequivalent nuclear location of immunoglobulin alleles in B lymphocytes. Nature immunology *2*, 848-854.
Smerdon, M.J. (1991). DNA repair and the role of chromatin structure. Current opinion in cell biology *3*, 422-428.
Smith, S., Hwang, J.Y., Banerjee, S., Majeed, A., Gupta, A., and Myung, K. (2004). Mutator genes for suppression of gross chromosomal rearrangements identified by a genome-wide screening in Saccharomyces cerevisiae. Proc Natl Acad Sci U S A *101*, 9039-9044.

Smith, S.B., Cui, Y., and Bustamante, C. (1996). Overstretching B-DNA: the elastic response of individual double-stranded and single-stranded DNA molecules. Science (New York, NY) *271*, 795-799.
Solovei, I., Kreysing, M., Lanctôt, C., Kösem, S., Peichl, L., Cremer, T., Guck, J., and Joffe, B. (2009). Nuclear architecture of rod photoreceptor cells adapts to vision in mammalian evolution. Cell *137*, 356-368.
Spector, D.L. (2003). The dynamics of chromosome organization and gene regulation. Annual review of biochemistry *72*, 573-608.
St Charles, J., and Petes, T.D. (2013). High-resolution mapping of spontaneous mitotic recombination hotspots on the 1.1 Mb arm of yeast chromosome IV. PLoS Genet *9*, e1003434.
Stanek, D., and Fox, A.H. (2017). Nuclear bodies: news insights into structure and function. Current opinion in cell biology *46*, 94-101.
Stephens, A.D., Liu, P.Z., Banigan, E.J., Almassalha, L.M., Backman, V., Adam, S.A., Goldman, R.D., and Marko, J.F. (2018). Chromatin histone modifications and rigidity affect nuclear morphology independent of lamins. Mol Biol Cell *29*, 220-233.
Sterner, D.E., and Berger, S.L. (2000). Acetylation of histones and transcription-related factors. Microbiology and molecular biology reviews : MMBR *64*, 435-459.
Stevens, T.J., Lando, D., Basu, S., Atkinson, L.P., Cao, Y., Lee, S.F., Leeb, M., Wohlfahrt, K.J., Boucher, W., O'Shaughnessy-Kirwan, A*., et al.* (2017). 3D structures of individual mammalian genomes studied by single-cell Hi-C. Nature *544*, 59-64.
Stewart, M.D., Li, J., and Wong, J. (2005). Relationship between histone H3 lysine 9 methylation, transcription repression, and heterochromatin protein 1 recruitment. Mol Cell Biol *25*, 2525-2538.
Stirling, P.C., Shen, Y., Corbett, R., Jones, S.J.M., and Hieter, P. (2014). Genome destabilizing mutator alleles drive specific mutational trajectories in Saccharomyces cerevisiae. Genetics *196*, 403-412.
Strahl, B.D., and Allis, C.D. (2000). The language of covalent histone modifications. Nature *403*, 41-45.
Strom, A.R., Emelyanov, A.V., Mir, M., Fyodorov, D.V., Darzacq, X., and Karpen, G.H. (2017). Phase separation drives heterochromatin domain formation. Nature *547*, 241-245.
Taddei, A., Van Houwe, G., Hediger, F., Kalck, V., Cubizolles, F., Schober, H., and Gasser, S.M. (2006). Nuclear pore association confers optimal expression levels for an inducible yeast gene. Nature *441*, 774-778.
Talbert, P.B., and Henikoff, S. (2010). Histone variants--ancient wrap artists of the epigenome. Nature reviews Molecular cell biology *11*, 264-275.
Taunton, J., Hassig, C.A., and Schreiber, S.L. (1996). A mammalian histone deacetylase related to the yeast transcriptional regulator Rpd3p. Science (New York, NY) *272*, 408-411.
Thastrom, A., Lowary, P.T., and Widom, J. (2004). Measurement of histone-DNA interaction free energy in nucleosomes. Methods (San Diego, Calif) *33*, 33-44.
The UniProt, C. (2021). UniProt: the universal protein knowledgebase in 2021. Nucleic Acids Research *49*, D480-D489.
Therizols, P., Duong, T., Dujon, B., Zimmer, C., and Fabre, E. (2010). Chromosome arm length and nuclear constraints determine the dynamic relationship of yeast subtelomeres. Proceedings of the National Academy of Sciences of the United States of America *107*, 2025-2030.
Thomson, S., Clayton, A.L., Hazzalin, C.A., Rose, S., Barratt, M.J., and Mahadevan, L.C. (1999). The nucleosomal response associated with immediate-early gene induction is mediated via alternative MAP kinase cascades: MSK1 as a potential histone H3/HMG-14 kinase. The EMBO journal *18*, 4779-4793.

Tiley, G.P., and Burleigh, J.G. (2015). The relationship of recombination rate, genome structure, and patterns of molecular evolution across angiosperms. BMC Evol Biol *15*, 194.
Topal, S., Vasseur, P., Radman-Livaja, M., and Peterson, C.L. (2019). Distinct transcriptional roles for Histone H3-K56 acetylation during the cell cycle in Yeast. Nature communications *10*, 4372.
Toretsky, J.A., and Wright, P.E. (2014). Assemblages: functional units formed by cellular phase separation. The Journal of cell biology *206*, 579-588.
Tsukada, Y., Fang, J., Erdjument-Bromage, H., Warren, M.E., Borchers, C.H., Tempst, P., and Zhang, Y. (2006). Histone demethylation by a family of JmjC domain-containing proteins. Nature *439*, 811-816.
Turner, A.L., Watson, M., Wilkins, O.G., Cato, L., Travers, A., Thomas, J.O., and Stott, K. (2018). Highly disordered histone H1-DNA model complexes and their condensates. Proceedings of the National Academy of Sciences of the United States of America *115*, 11964-11969.
Tyagi, M., Imam, N., Verma, K., and Patel, A.K. (2016). Chromatin remodelers: We are the drivers!! Nucleus (Austin, Tex) *7*, 388-404.
Uhlenbeck, G.E., and Ornstein, L.S. (1930). On the Theory of the Brownian Motion. Phys Rev *36*, 823–841.
van Attikum, H., and Gasser, S.M. (2009). Crosstalk between histone modifications during the DNA damage response. Trends in cell biology *19*, 207-217.
van der Lee, R., Buljan, M., Lang, B., Weatheritt, R.J., Daughdrill, G.W., Dunker, A.K., Fuxreiter, M., Gough, J., Gsponer, J., Jones, D.T.*, et al.* (2014). Classification of intrinsically disordered regions and proteins. Chemical reviews *114*, 6589-6631.
Van Holde, K.E., Allen, J.R., Tatchell, K., Weischet, W.O., and Lohr, D. (1980). DNA-histone interactions in nucleosomes. Biophysical journal *32*, 271-282.
Vasquez, P.A., and Bloom, K. (2014). Polymer models of interphase chromosomes. Nucleus (Austin, Tex) *5*, 376-390.
Vasquez, P.A., Hult, C., Adalsteinsson, D., Lawrimore, J., Forest, M.G., and Bloom, K. (2016). Entropy gives rise to topologically associating domains. Nucleic acids research *44*, 5540-5549.
Verdaasdonk, J.S., Gardner, R., Stephens, A.D., Yeh, E., and Bloom, K. (2012). Tension-dependent nucleosome remodeling at the pericentromere in yeast. Molecular biology of the cell *23*, 2560-2570.
Verdaasdonk, J.S., Vasquez, P.A., Barry, R.M., Barry, T., Goodwin, S., Forest, M.G., and Bloom, K. (2013). Centromere tethering confines chromosome domains. Mol Cell *52*, 819-831.
Vernarecci, S., Tosi, F., and Filetici, P. (2010). Tuning acetylated chromatin with HAT inhibitors: a novel tool for therapy. Epigenetics *5*, 105-111.
Vietri Rudan, M., Barrington, C., Henderson, S., Ernst, C., Odom, D.T., Tanay, A., and Hadjur, S. (2015). Comparative Hi-C reveals that CTCF underlies evolution of chromosomal domain architecture. Cell reports *10*, 1297-1309.
Wang, J., Choi, J.M., Holehouse, A.S., Lee, H.O., Zhang, X., Jahnel, M., Maharana, S., Lemaitre, R., Pozniakovsky, A., Drechsel, D.*, et al.* (2018). A Molecular Grammar Governing the Driving Forces for Phase Separation of Prion-like RNA Binding Proteins. Cell *174*, 688-699.e616.
Wang, S., Su, J.H., Beliveau, B.J., Bintu, B., Moffitt, J.R., Wu, C.T., and Zhuang, X. (2016). Spatial organization of chromatin domains and compartments in single chromosomes. Science (New York, NY) *353*, 598-602.
Wang, Y.H., Amirhaeri, S., Kang, S., Wells, R.D., and Griffith, J.D. (1994). Preferential nucleosome assembly at DNA triplet repeats from the myotonic dystrophy gene. Science (New York, NY) *265*, 669-671.

Wang, Y.H., and Griffith, J. (1995). Expanded CTG triplet blocks from the myotonic dystrophy gene create the strongest known natural nucleosome positioning elements. Genomics *25*, 570-573.
Wapenaar, H., and Dekker, F.J. (2016). Histone acetyltransferases: challenges in targeting bi-substrate enzymes. Clinical Epigenetics *8*, 59.
Weber, S.C., and Brangwynne, C.P. (2015). Inverse size scaling of the nucleolus by a concentration-dependent phase transition. Current biology : CB *25*, 641-646.
Weber, S.C., Spakowitz, A.J., and Theriot, J.A. (2010). Bacterial chromosomal loci move subdiffusively through a viscoelastic cytoplasm. Phys Rev Lett *104*, 238102.
Weber, S.C., Spakowitz, A.J., and Theriot, J.A. (2012). Nonthermal ATP-dependent fluctuations contribute to the in vivo motion of chromosomal loci. Proceedings of the National Academy of Sciences of the United States of America *109*, 7338-7343.
Wei, M., Fabrizio, P., Hu, J., Ge, H., Cheng, C., Li, L., and Longo, V.D. (2008). Life span extension by calorie restriction depends on Rim15 and transcription factors downstream of Ras/PKA, Tor, and Sch9. PLoS genetics *4*, e13-e13.
Widom, J. (2001). Role of DNA sequence in nucleosome stability and dynamics. Quarterly reviews of biophysics *34*, 269-324.
Wilfert, L., Gadau, J., and Schmid-Hempel, P. (2007). Variation in genomic recombination rates among animal taxa and the case of social insects. Heredity (Edinb) *98*, 189-197.
Williams, R.R., Azuara, V., Perry, P., Sauer, S., Dvorkina, M., Jorgensen, H., Roix, J., McQueen, P., Misteli, T., Merkenschlager, M.*, et al.* (2006). Neural induction promotes large-scale chromatin reorganisation of the Mash1 locus. Journal of cell science *119*, 132-140.
Wolfe, K.H., and Shields, D.C. (1997). Molecular evidence for an ancient duplication of the entire yeast genome. Nature *387*, 708-713.
Wong, H., Marie-Nelly, H., Herbert, S., Carrivain, P., Blanc, H., Koszul, R., Fabre, E., and Zimmer, C. (2012). A predictive computational model of the dynamic 3D interphase yeast nucleus. Curr Biol *22*, 1881-1890.
Wood, C.M., Nicholson, J.M., Lambert, S.J., Chantalat, L., Reynolds, C.D., and Baldwin, J.P. (2005). High-resolution structure of the native histone octamer. Acta crystallographica Section F, Structural biology and crystallization communications *61*, 541-545.
Xhemalce, B., Miller, K.M., Driscoll, R., Masumoto, H., Jackson, S.P., Kouzarides, T., Verreault, A., and Arcangioli, B. (2007). Regulation of histone H3 lysine 56 acetylation in Schizosaccharomyces pombe. The Journal of biological chemistry *282*, 15040-15047.
Xu, F., Zhang, K., and Grunstein, M. (2005). Acetylation in histone H3 globular domain regulates gene expression in yeast. Cell *121*, 375-385.
Yang, J., Zhang, X., Feng, J., Leng, H., Li, S., Xiao, J., Liu, S., Xu, Z., Xu, J., Li, D.*, et al.* (2016). The Histone Chaperone FACT Contributes to DNA Replication-Coupled Nucleosome Assembly. Cell reports *14*, 1128-1141.
Yang, X.-J., and Seto, E. (2008a). Lysine acetylation: codified crosstalk with other posttranslational modifications. Molecular cell *31*, 449-461.
Yang, X.-J., and Seto, E. (2008b). The Rpd3/Hda1 family of lysine deacetylases: from bacteria and yeast to mice and men. Nature Reviews Molecular Cell Biology *9*, 206-218.
Yang, X.J., and Grégoire, S. (2007). Metabolism, cytoskeleton and cellular signalling in the grip of protein Nepsilon - and O-acetylation. EMBO reports *8*, 556-562.
Yu, Q., Kuzmiak, H., Zou, Y., Olsen, L., Defossez, P.A., and Bi, X. (2009). Saccharomyces cerevisiae linker histone Hho1p functionally interacts with core histone H4 and negatively regulates the establishment of transcriptionally silent chromatin. The Journal of biological chemistry *284*, 740-750.

Yuan, G.C., Liu, Y.J., Dion, M.F., Slack, M.D., Wu, L.F., Altschuler, S.J., and Rando, O.J. (2005). Genome-scale identification of nucleosome positions in S. cerevisiae. Science (New York, NY) *309*, 626-630.
Zhang, H., Roberts, D.N., and Cairns, B.R. (2005). Genome-wide dynamics of Htz1, a histone H2A variant that poises repressed/basal promoters for activation through histone loss. Cell *123*, 219-231.
Zhu, L., and Brangwynne, C.P. (2015). Nuclear bodies: the emerging biophysics of nucleoplasmic phases. Current opinion in cell biology *34*, 23-30.
Zhu, Y.O., Siegal, M.L., Hall, D.W., and Petrov, D.A. (2014). Precise estimates of mutation rate and spectrum in yeast. Proc Natl Acad Sci U S A *111*, E2310-2318.
Zink, D., Amaral, M.D., Englmann, A., Lang, S., Clarke, L.A., Rudolph, C., Alt, F., Luther, K., Braz, C., Sadoni, N*., et al.* (2004). Transcription-dependent spatial arrangements of CFTR and adjacent genes in human cell nuclei. The Journal of cell biology *166*, 815-825.
Zlatanova, J., Bishop, T.C., Victor, J.M., Jackson, V., and van Holde, K. (2009). The nucleosome family: dynamic and growing. Structure (London, England : 1993) *17*, 160-171.

A, P., and Weber, S.C. (2019). Evidence for and against Liquid-Liquid Phase Separation in the Nucleus. Noncoding RNA *5*, 50.
Abbott, D.W., Ivanova, V.S., Wang, X., Bonner, W.M., and Ausio, J. (2001). Characterization of the stability and folding of H2A.Z chromatin particles: implications for transcriptional activation. The Journal of biological chemistry *276*, 41945-41949.
Abshiru, N., Ippersiel, K., Tang, Y., Yuan, H., Marmorstein, R., Verreault, A., and Thibault, P. (2013). Chaperone-mediated acetylation of histones by Rtt109 identified by quantitative proteomics. Journal of proteomics *81*, 80-90.
Ahmed, S., Brickner, D.G., Light, W.H., Cajigas, I., McDonough, M., Froyshteter, A.B., Volpe, T., and Brickner, J.H. (2010). DNA zip codes control an ancient mechanism for gene targeting to the nuclear periphery. Nature cell biology *12*, 111-118.
Ahmed, S., and Brickner, J.H. (2010). A role for DNA sequence in controlling the spatial organization of the genome. Nucleus (Austin, Tex) *1*, 402-406.
Albert, B., Mathon, J., Shukla, A., Saad, H., Normand, C., Léger-Silvestre, I., Villa, D., Kamgoue, A., Mozziconacci, J., Wong, H*., et al.* (2013). Systematic characterization of the conformation and dynamics of budding yeast chromosome XII. The Journal of cell biology *202*, 201-210.
Albert, I., Mavrich, T.N., Tomsho, L.P., Qi, J., Zanton, S.J., Schuster, S.C., and Pugh, B.F. (2007). Translational and rotational settings of H2A.Z nucleosomes across the Saccharomyces cerevisiae genome. Nature *446*, 572-576.
Alberti, S., Gladfelter, A., and Mittag, T. (2019). Considerations and Challenges in Studying Liquid-Liquid Phase Separation and Biomolecular Condensates. Cell *176*, 419-434.
Allshire, R.C., and Madhani, H.D. (2018). Ten principles of heterochromatin formation and function. Nat Rev Mol Cell Biol *19*, 229-244.
Altmeyer, M., Neelsen, K.J., Teloni, F., Pozdnyakova, I., Pellegrino, S., Grofte, M., Rask, M.B., Streicher, W., Jungmichel, S., Nielsen, M.L*., et al.* (2015). Liquid demixing of intrinsically disordered proteins is seeded by poly(ADP-ribose). Nature communications *6*, 8088.
Arents, G., Burlingame, R.W., Wang, B.C., Love, W.E., and Moudrianakis, E.N. (1991). The nucleosomal core histone octamer at 3.1 A resolution: a tripartite protein assembly and a left-

handed superhelix. Proceedings of the National Academy of Sciences of the United States of America *88*, 10148-10152.
Arents, G., and Moudrianakis, E.N. (1995). The histone fold: a ubiquitous architectural motif utilized in DNA compaction and protein dimerization. Proceedings of the National Academy of Sciences of the United States of America *92*, 11170-11174.
Argueso, J.L., Carazzolle, M.F., Mieczkowski, P.A., Duarte, F.M., Netto, O.V., Missawa, S.K., Galzerani, F., Costa, G.G., Vidal, R.O., Noronha, M.F*., et al.* (2009). Genome structure of a Saccharomyces cerevisiae strain widely used in bioethanol production. Genome Res *19*, 2258-2270.
Backlund, M.P., Joyner, R., Weis, K., and Moerner, W.E. (2014). Correlations of three-dimensional motion of chromosomal loci in yeast revealed by the double-helix point spread function microscope. Molecular biology of the cell *25*, 3619-3629.
Banani, S.F., Lee, H.O., Hyman, A.A., and Rosen, M.K. (2017). Biomolecular condensates: organizers of cellular biochemistry. Nature Reviews Molecular Cell Biology *18*, 285.
Bannister, A.J., and Kouzarides, T. (2011). Regulation of chromatin by histone modifications. Cell research *21*, 381-395.
Bannister, A.J., Zegerman, P., Partridge, J.F., Miska, E.A., Thomas, J.O., Allshire, R.C., and Kouzarides, T. (2001). Selective recognition of methylated lysine 9 on histone H3 by the HP1 chromo domain. Nature *410*, 120-124.
Barton, A.B., Pekosz, M.R., Kurvathi, R.S., and Kaback, D.B. (2008). Meiotic recombination at the ends of chromosomes in Saccharomyces cerevisiae. Genetics *179*, 1221-1235.
Basso, L.C., de Amorim, H.V., de Oliveira, A.J., and Lopes, M.L. (2008). Yeast selection for fuel ethanol production in Brazil. FEMS Yeast Res *8*, 1155-1163.
Becker, P.B., and Horz, W. (2002). ATP-dependent nucleosome remodeling. Annual review of biochemistry *71*, 247-273.
Berger, A.B., Cabal, G.G., Fabre, E., Duong, T., Buc, H., Nehrbass, U., Olivo-Marin, J.C., Gadal, O., and Zimmer, C. (2008). High-resolution statistical mapping reveals gene territories in live yeast. Nat Methods *5*, 1031-1037.
Bergeron-Sandoval, L.P., Safaee, N., and Michnick, S.W. (2016). Mechanisms and Consequences of Macromolecular Phase Separation. Cell *165*, 1067-1079.
Berndsen, C.E., Tsubota, T., Lindner, S.E., Lee, S., Holton, J.M., Kaufman, P.D., Keck, J.L., and Denu, J.M. (2008). Molecular functions of the histone acetyltransferase chaperone complex Rtt109-Vps75. Nature structural & molecular biology *15*, 948-956.
Bernstein, B.E., Kamal, M., Lindblad-Toh, K., Bekiranov, S., Bailey, D.K., Huebert, D.J., McMahon, S., Karlsson, E.K., Kulbokas, E.J., 3rd, Gingeras, T.R*., et al.* (2005). Genomic maps and comparative analysis of histone modifications in human and mouse. Cell *120*, 169-181.
Blobel, G. (1985). Gene gating: a hypothesis. Proceedings of the National Academy of Sciences of the United States of America *82*, 8527-8529.
Bloom, K., and Kolbin, D. (2022). Mechanisms of DNA Mobilization and Sequestration. Genes *13*.
Bloom, K.S. (2008). Beyond the code: the mechanical properties of DNA as they relate to mitosis. Chromosoma *117*, 103-110.
Boeynaems, S., Alberti, S., Fawzi, N.L., Mittag, T., Polymenidou, M., Rousseau, F., Schymkowitz, J., Shorter, J., Wolozin, B., Van Den Bosch, L*., et al.* (2018). Protein Phase Separation: A New Phase in Cell Biology. Trends in cell biology *28*, 420-435.
Bolzer, A., Kreth, G., Solovei, I., Koehler, D., Saracoglu, K., Fauth, C., Müller, S., Eils, R., Cremer, C., Speicher, M.R*., et al.* (2005). Three-Dimensional Maps of All Chromosomes in Human Male Fibroblast Nuclei and Prometaphase Rosettes. PLoS biology *3*, e157.

Borneman, A.R., Desany, B.A., Riches, D., Affourtit, J.P., Forgan, A.H., Pretorius, I.S., Egholm, M., and Chambers, P.J. (2011). Whole-genome comparison reveals novel genetic elements that characterize the genome of industrial strains of Saccharomyces cerevisiae. PLoS Genet *7*, e1001287.
Boulon, S., Westman, B.J., Hutten, S., Boisvert, F.M., and Lamond, A.I. (2010). The nucleolus under stress. Molecular cell *40*, 216-227.
Brackley, C.A., Johnson, J., Kelly, S., Cook, P.R., and Marenduzzo, D. (2016). Simulated binding of transcription factors to active and inactive regions folds human chromosomes into loops, rosettes and topological domains. Nucleic acids research *44*, 3503-3512.
Brangwynne, C.P. (2013). Phase transitions and size scaling of membrane-less organelles. The Journal of cell biology *203*, 875-881.
Brangwynne, C.P., Eckmann, C.R., Courson, D.S., Rybarska, A., Hoege, C., Gharakhani, J., Julicher, F., and Hyman, A.A. (2009). Germline P granules are liquid droplets that localize by controlled dissolution/condensation. Science (New York, NY) *324*, 1729-1732.
Brangwynne, C.P., Mitchison, T.J., and Hyman, A.A. (2011). Active liquid-like behavior of nucleoli determines their size and shape in Xenopus laevis oocytes. Proceedings of the National Academy of Sciences of the United States of America *108*, 4334-4339.
Brickner, D.G., Ahmed, S., Meldi, L., Thompson, A., Light, W., Young, M., Hickman, T.L., Chu, F., Fabre, E., and Brickner, J.H. (2012). Transcription factor binding to a DNA zip code controls interchromosomal clustering at the nuclear periphery. Developmental cell *22*, 1234-1246.
Brickner, D.G., Cajigas, I., Fondufe-Mittendorf, Y., Ahmed, S., Lee, P.C., Widom, J., and Brickner, J.H. (2007). H2A.Z-mediated localization of genes at the nuclear periphery confers epigenetic memory of previous transcriptional state. PLoS biology *5*, e81.
Brickner, D.G., Sood, V., Tutucci, E., Coukos, R., Viets, K., Singer, R., and Brickner, J.H. (2016). Subnuclear positioning and interchromosomal clustering of the GAL1-10 locus are controlled by separable, interdependent mechanisms. Molecular biology of the cell.
Brickner, J.H., and Walter, P. (2004). Gene recruitment of the activated INO1 locus to the nuclear membrane. PLoS biology *2*, e342.
Brown, C.R., Kennedy, C.J., Delmar, V.A., Forbes, D.J., and Silver, P.A. (2008). Global histone acetylation induces functional genomic reorganization at mammalian nuclear pore complexes. Genes & development *22*, 627-639.
Brown, K.E., Baxter, J., Graf, D., Merkenschlager, M., and Fisher, A.G. (1999). Dynamic repositioning of genes in the nucleus of lymphocytes preparing for cell division. Molecular cell *3*, 207-217.
Brownell, J.E., Zhou, J., Ranalli, T., Kobayashi, R., Edmondson, D.G., Roth, S.Y., and Allis, C.D. (1996). Tetrahymena histone acetyltransferase A: a homolog to yeast Gcn5p linking histone acetylation to gene activation. Cell *84*, 843-851.
Bystricky, K., Heun, P., Gehlen, L., Langowski, J., and Gasser, S.M. (2004). Long-range compaction and flexibility of interphase chromatin in budding yeast analyzed by high-resolution imaging techniques. Proc Natl Acad Sci U S A *101*, 16495-16500.
Bystricky, K., Laroche, T., van Houwe, G., Blaszczyk, M., and Gasser, S.M. (2005). Chromosome looping in yeast: telomere pairing and coordinated movement reflect anchoring efficiency and territorial organization. The Journal of cell biology *168*, 375-387.
Cabal, G.G., Genovesio, A., Rodriguez-Navarro, S., Zimmer, C., Gadal, O., Lesne, A., Buc, H., Feuerbach-Fournier, F., Olivo-Marin, J.C., Hurt, E.C*., et al.* (2006). SAGA interacting factors confine sub-diffusion of transcribed genes to the nuclear envelope. Nature *441*, 770-773.

Canzio, D., Chang, E.Y., Shankar, S., Kuchenbecker, K.M., Simon, M.D., Madhani, H.D., Narlikar, G.J., and Al-Sady, B. (2011). Chromodomain-mediated oligomerization of HP1 suggests a nucleosome-bridging mechanism for heterochromatin assembly. Molecular cell *41*, 67-81.
Carro, D., and Piña, B. (2001). Genetic analysis of the karyotype instability in natural wine yeast strains. Yeast *18*, 1457-1470.
Casolari, J.M., Brown, C.R., Komili, S., West, J., Hieronymus, H., and Silver, P.A. (2004). Genome-wide localization of the nuclear transport machinery couples transcriptional status and nuclear organization. Cell *117*, 427-439.
Chang, B., Chen, Y., Zhao, Y., and Bruick, R.K. (2007). JMJD6 is a histone arginine demethylase. Science (New York, NY) *318*, 444-447.
Chen, C., and Kolodner, R.D. (1999). Gross chromosomal rearrangements in Saccharomyces cerevisiae replication and recombination defective mutants. Nature Genetics *23*, 81-85.
Chen, C., Lim, H.H., Shi, J., Tamura, S., Maeshima, K., Surana, U., and Gan, L. (2016). Budding yeast chromatin is dispersed in a crowded nucleoplasm in vivo. Molecular biology of the cell *27*, 3357-3368.
Chen, C.C., Carson, J.J., Feser, J., Tamburini, B., Zabaronick, S., Linger, J., and Tyler, J.K. (2008). Acetylated lysine 56 on histone H3 drives chromatin assembly after repair and signals for the completion of repair. Cell *134*, 231-243.
Chen, D., Ma, H., Hong, H., Koh, S.S., Huang, S.M., Schurter, B.T., Aswad, D.W., and Stallcup, M.R. (1999). Regulation of transcription by a protein methyltransferase. Science (New York, NY) *284*, 2174-2177.
Cheng, T.M., Heeger, S., Chaleil, R.A., Matthews, N., Stewart, A., Wright, J., Lim, C., Bates, P.A., and Uhlmann, F. (2015). A simple biophysical model emulates budding yeast chromosome condensation. eLife *4*, e05565.
Cherry, J.M., Hong, E.L., Amundsen, C., Balakrishnan, R., Binkley, G., Chan, E.T., Christie, K.R., Costanzo, M.C., Dwight, S.S., Engel, S.R*., et al.* (2012). Saccharomyces Genome Database: the genomics resource of budding yeast. Nucleic Acids Res *40*, D700-705.
Chi, Q., Wang, G., and Jiang, J. (2013). The persistence length and length per base of single-stranded DNA obtained from fluorescence correlation spectroscopy measurements using mean field theory. Physica A: Statistical Mechanics and its Applications *392*, 1072-1079.
Clapier, C.R., and Cairns, B.R. (2009). The biology of chromatin remodeling complexes. Annual review of biochemistry *78*, 273-304.
Crane, E., Bian, Q., McCord, R.P., Lajoie, B.R., Wheeler, B.S., Ralston, E.J., Uzawa, S., Dekker, J., and Meyer, B.J. (2015). Condensin-driven remodelling of X chromosome topology during dosage compensation. Nature *523*, 240-244.
Cremer, T., and Cremer, C. (2001). Chromosome territories, nuclear architecture and gene regulation in mammalian cells. Nat Rev Genet *2*, 292-301.
Cui, Y., and Bustamante, C. (2000). Pulling a single chromatin fiber reveals the forces that maintain its higher-order structure. Proceedings of the National Academy of Sciences of the United States of America *97*, 127-132.
Dao, T.P., Kolaitis, R.-M., Kim, H.J., O'Donovan, K., Martyniak, B., Colicino, E., Hehnly, H., Taylor, J.P., and Castañeda, C.A. (2018). Ubiquitin Modulates Liquid-Liquid Phase Separation of UBQLN2 via Disruption of Multivalent Interactions. Molecular cell *69*, 965-978.e966.
Datta, A., Adjiri, A., New, L., Crouse, G.F., and Jinks Robertson, S. (1996). Mitotic crossovers between diverged sequences are regulated by mismatch repair proteins in Saccaromyces cerevisiae. Mol Cell Biol *16*, 1085-1093.
Dekker, J., Rippe, K., Dekker, M., and Kleckner, N. (2002). Capturing chromosome conformation. Science *295*, 1306-1311.

Dietrich, F.S., Voegeli, S., Brachat, S., Lerch, A., Gates, K., Steiner, S., Mohr, C., Pöhlmann, R., Luedi, P., Choi, S*., et al.* (2004). The Ashbya gossypii genome as a tool for mapping the ancient Saccharomyces cerevisiae genome. Science *304*, 304-307.
Dion, M.F., Altschuler, S.J., Wu, L.F., and Rando, O.J. (2005). Genomic characterization reveals a simple histone H4 acetylation code. Proceedings of the National Academy of Sciences of the United States of America *102*, 5501-5506.
Dixon, J.R., Selvaraj, S., Yue, F., Kim, A., Li, Y., Shen, Y., Hu, M., Liu, J.S., and Ren, B. (2012). Topological domains in mammalian genomes identified by analysis of chromatin interactions. Nature *485*, 376-380.
Dong, P., Tu, X., Chu, P.Y., Lu, P., Zhu, N., Grierson, D., Du, B., Li, P., and Zhong, S. (2017). 3D Chromatin Architecture of Large Plant Genomes Determined by Local A/B Compartments. Mol Plant *10*, 1497-1509.
Dong, Q., Li, N., Li, X., Yuan, Z., Xie, D., Wang, X., Li, J., Yu, Y., Wang, J., Ding, B*., et al.* (2018). Genome-wide Hi-C analysis reveals extensive hierarchical chromatin interactions in rice. Plant J *94*, 1141-1156.
Dormidontova, E.E., Grosberg, A.Y., and Khokhlov, A.R. (1992). Intramolecular phase separation of a copolymer chain with mobile primary structure. Macromolecular Theory and Simulations *1*, 375-385.
Downs, J.A., Kosmidou, E., Morgan, A., and Jackson, S.P. (2003). Suppression of homologous recombination by the Saccharomyces cerevisiae linker histone. Molecular cell *11*, 1685-1692.
Driscoll, R., Hudson, A., and Jackson, S.P. (2007). Yeast Rtt109 Promotes Genome Stability by Acetylating Histone H3 on Lysine 56. Science (New York, NY) *315*, 649-652.
Duan, M.R., and Smerdon, M.J. (2014). Histone H3 lysine 14 (H3K14) acetylation facilitates DNA repair in a positioned nucleosome by stabilizing the binding of the chromatin Remodeler RSC (Remodels Structure of Chromatin). The Journal of biological chemistry *289*, 8353-8363.
Duan, Z., Andronescu, M., Schutz, K., McIlwain, S., Kim, Y.J., Lee, C., Shendure, J., Fields, S., Blau, C.A., and Noble, W.S. (2010). A three-dimensional model of the yeast genome. Nature *465*, 363-367.
Dujon, B., Sherman, D., Fischer, G., Durrens, P., Casaregola, S., Lafontaine, I., De Montigny, J., Marck, C., Neuvéglise, C., Talla, E*., et al.* (2004). Genome evolution in yeasts. Nature *430*, 35-44.
Durant, M., and Pugh, B.F. (2006). Genome-wide relationships between TAF1 and histone acetyltransferases in Saccharomyces cerevisiae. Molecular and cellular biology *26*, 2791-2802.
Eissenberg, J.C., and Elgin, S.C. (2014). HP1a: a structural chromosomal protein regulating transcription. Trends in genetics : TIG *30*, 103-110.
Elbaum-Garfinkle, S., Kim, Y., Szczepaniak, K., Chen, C.C., Eckmann, C.R., Myong, S., and Brangwynne, C.P. (2015). The disordered P granule protein LAF-1 drives phase separation into droplets with tunable viscosity and dynamics. Proceedings of the National Academy of Sciences of the United States of America *112*, 7189-7194.
Emre, N.C., Ingvarsdottir, K., Wyce, A., Wood, A., Krogan, N.J., Henry, K.W., Li, K., Marmorstein, R., Greenblatt, J.F., Shilatifard, A*., et al.* (2005). Maintenance of low histone ubiquitylation by Ubp10 correlates with telomere-proximal Sir2 association and gene silencing. Molecular cell *17*, 585-594.
Erdel, F., and Rippe, K. (2011). Chromatin remodelling in mammalian cells by ISWI-type complexes--where, when and why? The FEBS journal *278*, 3608-3618.
Erdel, F., and Rippe, K. (2018). Formation of Chromatin Subcompartments by Phase Separation. Biophysical journal *114*, 2262-2270.

Fabrizio, P., Battistella, L., Vardavas, R., Gattazzo, C., Liou, L.L., Diaspro, A., Dossen, J.W., Gralla, E.B., and Longo, V.D. (2004). Superoxide is a mediator of an altruistic aging program in Saccharomyces cerevisiae. J Cell Biol *166*, 1055-1067.
Feric, M., and Brangwynne, C.P. (2013). A nuclear F-actin scaffold stabilizes ribonucleoprotein droplets against gravity in large cells. Nature cell biology *15*, 1253-1259.
Ferrai, C., de Castro, I.J., Lavitas, L., Chotalia, M., and Pombo, A. (2010). Gene positioning. Cold Spring Harbor perspectives in biology *2*, a000588.
Field, Y., Kaplan, N., Fondufe-Mittendorf, Y., Moore, I.K., Sharon, E., Lubling, Y., Widom, J., and Segal, E. (2008). Distinct modes of regulation by chromatin encoded through nucleosome positioning signals. PLoS computational biology *4*, e1000216.
Finn, E.H., Pegoraro, G., Brandão, H.B., Valton, A.L., Oomen, M.E., Dekker, J., Mirny, L., and Misteli, T. (2019). Extensive Heterogeneity and Intrinsic Variation in Spatial Genome Organization. Cell *176*, 1502-1515.e1510.
Fisher, J.K., Ballenger, M., O'Brien, E.T., Haase, J., Superfine, R., and Bloom, K. (2009). DNA relaxation dynamics as a probe for the intracellular environment. Proc Natl Acad Sci U S A *106*, 9250-9255.
Flavahan, W.A., Drier, Y., Liau, B.B., Gillespie, S.M., Venteicher, A.S., Stemmer-Rachamimov, A.O., Suva, M.L., and Bernstein, B.E. (2016). Insulator dysfunction and oncogene activation in IDH mutant gliomas. Nature *529*, 110-114.
Flory, P.J., and Gee, G. (1956). Statistical thermodynamics of semi-flexible chain molecules. Proceedings of the Royal Society of London Series A Mathematical and Physical Sciences *234*, 60-73.
Franke, M., Ibrahim, D.M., Andrey, G., Schwarzer, W., Heinrich, V., Schopflin, R., Kraft, K., Kempfer, R., Jerkovic, I., Chan, W.L.*, et al.* (2016). Formation of new chromatin domains determines pathogenicity of genomic duplications. Nature *538*, 265-269.
Frottin, F., Schueder, F., Tiwary, S., Gupta, R., Körner, R., Schlichthaerle, T., Cox, J., Jungmann, R., Hartl, F.U., and Hipp, M.S. (2019). The nucleolus functions as a phase-separated protein quality control compartment. Science (New York, NY) *365*, 342-347.
Gasser, S.M. (2001). Positions of potential: nuclear organization and gene expression. Cell *104*, 639-642.
Gerhold, C.B., and Gasser, S.M. (2014). INO80 and SWR complexes: relating structure to function in chromatin remodeling. Trends in cell biology *24*, 619-631.
Giaimo, B.D., Ferrante, F., Herchenrother, A., Hake, S.B., and Borggrefe, T. (2019). The histone variant H2A.Z in gene regulation. Epigenetics & chromatin *12*, 37.
Gibson, B.A., Doolittle, L.K., Schneider, M.W.G., Jensen, L.E., Gamarra, N., Henry, L., Gerlich, D.W., Redding, S., and Rosen, M.K. (2019). Organization of Chromatin by Intrinsic and Regulated Phase Separation. Cell *179*, 470-484.e421.
Godde, J.S., and Wolffe, A.P. (1996). Nucleosome assembly on CTG triplet repeats. The Journal of biological chemistry *271*, 15222-15229.
Goffeau, A., Barrell, B.G., Bussey, H., Davis, R.W., Dujon, B., Feldmann, H., Galibert, F., Hoheisel, J.D., Jacq, C., Johnston, M.*, et al.* (1996). Life with 6000 genes. Science *274*, 546, 563-547.
Grunstein, M., and Gasser, S.M. (2013). Epigenetics in Saccharomyces cerevisiae. Cold Spring Harb Perspect Biol *5*.
Guelen, L., Pagie, L., Brasset, E., Meuleman, W., Faza, M.B., Talhout, W., Eussen, B.H., de Klein, A., Wessels, L., de Laat, W.*, et al.* (2008). Domain organization of human chromosomes revealed by mapping of nuclear lamina interactions. Nature *453*, 948-951.
Han, J., Zhou, H., Horazdovsky, B., Zhang, K., Xu, R.M., and Zhang, Z. (2007). Rtt109 acetylates histone H3 lysine 56 and functions in DNA replication. Science (New York, NY) *315*, 653-655.

He, Y., Lawrimore, J., Cook, D., Van Gorder, E.E., De Larimat, S.C., Adalsteinsson, D., Forest, M.G., and Bloom, K. (2020). Statistical mechanics of chromosomes: in vivo and in silico approaches reveal high-level organization and structure arise exclusively through mechanical feedback between loop extruders and chromatin substrate properties. Nucleic acids research *48*, 11284-11303.
Heard, E., and Bickmore, W. (2007). The ins and outs of gene regulation and chromosome territory organisation. Current opinion in cell biology *19*, 311-316.
Heintzman, N.D., Stuart, R.K., Hon, G., Fu, Y., Ching, C.W., Hawkins, R.D., Barrera, L.O., Van Calcar, S., Qu, C., Ching, K.A*., et al.* (2007). Distinct and predictive chromatin signatures of transcriptional promoters and enhancers in the human genome. Nature genetics *39*, 311-318.
Henderson, I.R., and Bomblies, K. (2021). Evolution and Plasticity of Genome-Wide Meiotic Recombination Rates. Annu Rev Genet *55*, 23-43.
Henikoff, S. (2009). Labile H3.3+H2A.Z nucleosomes mark 'nucleosome-free regions'. Nature genetics *41*, 865-866.
Henikoff, S., and Furuyama, T. (2012). The unconventional structure of centromeric nucleosomes. Chromosoma *121*, 341-352.
Henninger, J.E., Oksuz, O., Shrinivas, K., Sagi, I., LeRoy, G., Zheng, M.M., Andrews, J.O., Zamudio, A.V., Lazaris, C., Hannett, N.M*., et al.* (2021). RNA-Mediated Feedback Control of Transcriptional Condensates. Cell *184*, 207-225 e224.
Henry, K.W., Wyce, A., Lo, W.S., Duggan, L.J., Emre, N.C., Kao, C.F., Pillus, L., Shilatifard, A., Osley, M.A., and Berger, S.L. (2003). Transcriptional activation via sequential histone H2B ubiquitylation and deubiquitylation, mediated by SAGA-associated Ubp8. Genes & development *17*, 2648-2663.
Hergeth, S.P., and Schneider, R. (2015). The H1 linker histones: multifunctional proteins beyond the nucleosomal core particle. EMBO reports *16*, 1439-1453.
Hernandez-Verdun, D., Roussel, P., Thiry, M., Sirri, V., and Lafontaine, D.L. (2010). The nucleolus: structure/function relationship in RNA metabolism. Wiley interdisciplinary reviews RNA *1*, 415-431.
Heun, P., Laroche, T., Raghuraman, M.K., and Gasser, S.M. (2001a). The positioning and dynamics of origins of replication in the budding yeast nucleus. The Journal of cell biology *152*, 385-400.
Heun, P., Laroche, T., Shimada, K., Furrer, P., and Gasser, S.M. (2001b). Chromosome dynamics in the yeast interphase nucleus. Science (New York, NY) *294*, 2181-2186.
Heun, P., Laroche, T., Shimada, K., Furrer, P., and Gasser Susan, M. (2001c). Chromosome Dynamics in the Yeast Interphase Nucleus. Science (New York, NY) *294*, 2181-2186.
Hickman, M.A., Froyd, C.A., and Rusche, L.N. (2011). Reinventing heterochromatin in budding yeasts: Sir2 and the origin recognition complex take center stage. Eukaryotic cell *10*, 1183-1192.
Hnisz, D., Shrinivas, K., Young, R.A., Chakraborty, A.K., and Sharp, P.A. (2017). A Phase Separation Model for Transcriptional Control. Cell *169*, 13-23.
Hnisz, D., Weintraub, A.S., Day, D.S., Valton, A.L., Bak, R.O., Li, C.H., Goldmann, J., Lajoie, B.R., Fan, Z.P., Sigova, A.A*., et al.* (2016). Activation of proto-oncogenes by disruption of chromosome neighborhoods. Science (New York, NY) *351*, 1454-1458.
Holehouse, A.S., Ginell, G.M., Griffith, D., and Böke, E. (2021). Clustering of Aromatic Residues in Prion-like Domains Can Tune the Formation, State, and Organization of Biomolecular Condensates. Biochemistry *60*, 3566-3581.
Hsieh, T.H., Weiner, A., Lajoie, B., Dekker, J., Friedman, N., and Rando, O.J. (2015). Mapping Nucleosome Resolution Chromosome Folding in Yeast by Micro-C. Cell *162*, 108-119.

Huang, M.E., Rio, A.G., Nicolas, A., and Kolodner, R.D. (2003). A genomewide screen in Saccharomyces cerevisiae for genes that suppress the accumulation of mutations. Proc Natl Acad Sci U S A *100*, 11529-11534.
Huggins, M.L. (1942). THERMODYNAMIC PROPERTIES OF SOLUTIONS OF LONG-CHAIN COMPOUNDS. Annals of the New York Academy of Sciences *43*, 1-32.
Hughes, A.L., and Rando, O.J. (2014). Mechanisms underlying nucleosome positioning in vivo. Annual review of biophysics *43*, 41-63.
Hult, C., Adalsteinsson, D., Vasquez, P.A., Lawrimore, J., Bennett, M., York, A., Cook, D., Yeh, E., Forest, M.G., and Bloom, K. (2017). Enrichment of dynamic chromosomal crosslinks drive phase separation of the nucleolus. Nucleic Acids Res *45*, 11159-11173.
Hyland, E.M., Cosgrove, M.S., Molina, H., Wang, D., Pandey, A., Cottee, R.J., and Boeke, J.D. (2005). Insights into the role of histone H3 and histone H4 core modifiable residues in Saccharomyces cerevisiae. Molecular and cellular biology *25*, 10060-10070.
Iarovaia, O.V., Minina, E.P., Sheval, E.V., Onichtchouk, D., Dokudovskaya, S., Razin, S.V., and Vassetzky, Y.S. (2019). Nucleolus: A Central Hub for Nuclear Functions. Trends in cell biology *29*, 647-659.
Iborra, F.J. (2007). Can visco-elastic phase separation, macromolecular crowding and colloidal physics explain nuclear organisation? Theoretical biology & medical modelling *4*, 15.
Imai, R., Nozaki, T., Tani, T., Kaizu, K., Hibino, K., Ide, S., Tamura, S., Takahashi, K., Shribak, M., and Maeshima, K. (2017). Density imaging of heterochromatin in live cells using orientation-independent-DIC microscopy. Molecular biology of the cell *28*, 3349-3359.
Ioshikhes, I.P., Albert, I., Zanton, S.J., and Pugh, B.F. (2006). Nucleosome positions predicted through comparative genomics. Nature genetics *38*, 1210-1215.
Jenuwein, T., and Allis, C.D. (2001). Translating the histone code. Science (New York, NY) *293*, 1074-1080.
Jeronimo, C., Poitras, C., and Robert, F. (2019). Histone Recycling by FACT and Spt6 during Transcription Prevents the Scrambling of Histone Modifications. Cell reports *28*, 1206-1218.e1208.
Ji, Q., Mai, J., Ding, Y., Wei, Y., Ledesma-Amaro, R., and Ji, X.-J. (2020). Improving the homologous recombination efficiency of Yarrowia lipolytica by grafting heterologous component from Saccharomyces cerevisiae. Metabolic engineering communications *11*, e00152-e00152.
Jin, Q.W., Fuchs, J., and Loidl, J. (2000). Centromere clustering is a major determinant of yeast interphase nuclear organization. J Cell Sci *113 (Pt 11)*, 1903-1912.
Jun, S., and Mulder, B. (2006). Entropy-driven spatial organization of highly confined polymers: lessons for the bacterial chromosome. Proceedings of the National Academy of Sciences of the United States of America *103*, 12388-12393.
Kadosh, D., and Struhl, K. (1998). Targeted recruitment of the Sin3-Rpd3 histone deacetylase complex generates a highly localized domain of repressed chromatin in vivo. Molecular and cellular biology *18*, 5121-5127.
Kalverda, B., Pickersgill, H., Shloma, V.V., and Fornerod, M. (2010). Nucleoporins directly stimulate expression of developmental and cell-cycle genes inside the nucleoplasm. Cell *140*, 360-371.
Kanellis, P., Gagliardi, M., Banath, J.P., Szilard, R.K., Nakada, S., Galicia, S., Sweeney, F.D., Cabelof, D.C., Olive, P.L., and Durocher, D. (2007). A screen for suppressors of gross chromosomal rearrangements identifies a conserved role for PLP in preventing DNA lesions. PLoS Genet *3*, e134.

Kaplan, N., Moore, I.K., Fondufe-Mittendorf, Y., Gossett, A.J., Tillo, D., Field, Y., LeProust, E.M., Hughes, T.R., Lieb, J.D., Widom, J.*, et al.* (2009). The DNA-encoded nucleosome organization of a eukaryotic genome. Nature *458*, 362-366.
Kawaguchi, T., Tanigawa, A., Naganuma, T., Ohkawa, Y., Souquere, S., Pierron, G., and Hirose, T. (2015). SWI/SNF chromatin-remodeling complexes function in noncoding RNA-dependent assembly of nuclear bodies. Proceedings of the National Academy of Sciences of the United States of America *112*, 4304-4309.
Kechkar, A., Nair, D., Heilemann, M., Choquet, D., and Sibarita, J.B. (2013). Real-time analysis and visualization for single-molecule based super-resolution microscopy. PloS one *8*, e62918.
Kedersha, N., Ivanov, P., and Anderson, P. (2013). Stress granules and cell signaling: more than just a passing phase? Trends in biochemical sciences *38*, 494-506.
Kellis, M., Birren, B.W., and Lander, E.S. (2004). Proof and evolutionary analysis of ancient genome duplication in the yeast Saccharomyces cerevisiae. Nature *428*, 617-624.
Kim, S.H., McQueen, P.G., Lichtman, M.K., Shevach, E.M., Parada, L.A., and Misteli, T. (2004). Spatial genome organization during T-cell differentiation. Cytogenetic and genome research *105*, 292-301.
Kind, J., Pagie, L., de Vries, S.S., Nahidiazar, L., Dey, S.S., Bienko, M., Zhan, Y., Lajoie, B., de Graaf, C.A., Amendola, M.*, et al.* (2015). Genome-wide maps of nuclear lamina interactions in single human cells. Cell *163*, 134-147.
Klose, R.J., Gardner, K.E., Liang, G., Erdjument-Bromage, H., Tempst, P., and Zhang, Y. (2007). Demethylation of histone H3K36 and H3K9 by Rph1: a vestige of an H3K9 methylation system in Saccharomyces cerevisiae? Mol Cell Biol *27*, 3951-3961.
Kornberg, R.D. (1974). Chromatin structure: a repeating unit of histones and DNA. Science (New York, NY) *184*, 868-871.
Kornberg, R.D., and Klug, A. (1981). The nucleosome. Sci Am *244*, 52-64.
Kornberg, R.D., and Thomas, J.O. (1974). Chromatin structure; oligomers of the histones. Science (New York, NY) *184*, 865-868.
Kosak, S.T., Skok, J.A., Medina, K.L., Riblet, R., Le Beau, M.M., Fisher, A.G., and Singh, H. (2002). Subnuclear compartmentalization of immunoglobulin loci during lymphocyte development. Science (New York, NY) *296*, 158-162.
Kouzarides, T. (2007). Chromatin modifications and their function. Cell *128*, 693-705.
Kuo, M.H., Brownell, J.E., Sobel, R.E., Ranalli, T.A., Cook, R.G., Edmondson, D.G., Roth, S.Y., and Allis, C.D. (1996). Transcription-linked acetylation by Gcn5p of histones H3 and H4 at specific lysines. Nature *383*, 269-272.
Kuo, M.H., vom Baur, E., Struhl, K., and Allis, C.D. (2000). Gcn4 activator targets Gcn5 histone acetyltransferase to specific promoters independently of transcription. Molecular cell *6*, 1309-1320.
Lachner, M., O'Carroll, D., Rea, S., Mechtler, K., and Jenuwein, T. (2001). Methylation of histone H3 lysine 9 creates a binding site for HP1 proteins. Nature *410*, 116-120.
Lakshminarasimhan, M., Boanca, G., Banks, C.A., Hattem, G.L., Gabriel, A.E., Groppe, B.D., Smoyer, C., Malanowski, K.E., Peak, A., Florens, L.*, et al.* (2016). Proteomic and Genomic Analyses of the Rvb1 and Rvb2 Interaction Network upon Deletion of R2TP Complex Components. Molecular & cellular proteomics : MCP *15*, 960-974.
Lang, G.I., and Murray, A.W. (2008). Estimating the per-base-pair mutation rate in the yeast Saccharomyces cerevisiae. Genetics *178*, 67-82.
Langst, G., and Manelyte, L. (2015). Chromatin Remodelers: From Function to Dysfunction. Genes *6*, 299-324.

Larson, A.G., Elnatan, D., Keenen, M.M., Trnka, M.J., Johnston, J.B., Burlingame, A.L., Agard, D.A., Redding, S., and Narlikar, G.J. (2017a). Liquid droplet formation by HP1alpha suggests a role for phase separation in heterochromatin. Nature *547*, 236-240.
Larson, A.G., Elnatan, D., Keenen, M.M., Trnka, M.J., Johnston, J.B., Burlingame, A.L., Agard, D.A., Redding, S., and Narlikar, G.J. (2017b). Liquid droplet formation by HP1α suggests a role for phase separation in heterochromatin. Nature *547*, 236-240.
Lawrimore, J., Aicher, J.K., Hahn, P., Fulp, A., Kompa, B., Vicci, L., Falvo, M., Taylor, R.M., 2nd, and Bloom, K. (2016). ChromoShake: a chromosome dynamics simulator reveals that chromatin loops stiffen centromeric chromatin. Molecular biology of the cell *27*, 153-166.
Lawrimore, J., Kolbin, D., Stanton, J., Khan, M., de Larminat, S.C., Lawrimore, C., Yeh, E., and Bloom, K. (2021). The rDNA is biomolecular condensate formed by polymer-polymer phase separation and is sequestered in the nucleolus by transcription and R-loops. Nucleic acids research *49*, 4586-4598.
Lee, K.K., Sardiu, M.E., Swanson, S.K., Gilmore, J.M., Torok, M., Grant, P.A., Florens, L., Workman, J.L., and Washburn, M.P. (2011). Combinatorial depletion analysis to assemble the network architecture of the SAGA and ADA chromatin remodeling complexes. Molecular systems biology *7*, 503.
Lee, M.E., DeLoache, W.C., Cervantes, B., and Dueber, J.E. (2015). A Highly Characterized Yeast Toolkit for Modular, Multipart Assembly. ACS synthetic biology *4*, 975-986.
Lee, W., Tillo, D., Bray, N., Morse, R.H., Davis, R.W., Hughes, T.R., and Nislow, C. (2007). A high-resolution atlas of nucleosome occupancy in yeast. Nature genetics *39*, 1235-1244.
Leng, H., Liu, S., Lei, Y., Tang, Y., Gu, S., Hu, J., Chen, S., Feng, J., and Li, Q. (2021). FACT interacts with Set3 HDAC and fine-tunes GAL1 transcription in response to environmental stimulation. Nucleic acids research *49*, 5502-5519.
Li, G., Tian, Y., and Zhu, W.-G. (2020). The Roles of Histone Deacetylases and Their Inhibitors in Cancer Therapy. *8*.
Li, Q., Zhou, H., Wurtele, H., Davies, B., Horazdovsky, B., Verreault, A., and Zhang, Z. (2008). Acetylation of histone H3 lysine 56 regulates replication-coupled nucleosome assembly. Cell *134*, 244-255.
Lichten, M., and Haber, J.E. (1989). Position effects in ectopic and allelic mitotic recombination in Saccharomyces cerevisiae. Genetics *123*, 261-268.
Lieberman-Aiden, E., van Berkum, N.L., Williams, L., Imakaev, M., Ragoczy, T., Telling, A., Amit, I., Lajoie, B.R., Sabo, P.J., Dorschner, M.O*., et al.* (2009). Comprehensive mapping of long-range interactions reveals folding principles of the human genome. Science *326*, 289-293.
Lieleg, C., Krietenstein, N., Walker, M., and Korber, P. (2015). Nucleosome positioning in yeasts: methods, maps, and mechanisms. Chromosoma *124*, 131-151.
Light, W.H., Brickner, D.G., Brand, V.R., and Brickner, J.H. (2010). Interaction of a DNA zip code with the nuclear pore complex promotes H2A.Z incorporation and INO1 transcriptional memory. Molecular cell *40*, 112-125.
Linhoff, M.W., Garg, S.K., and Mandel, G. (2015). A high-resolution imaging approach to investigate chromatin architecture in complex tissues. Cell *163*, 246-255.
Liu, C.L., Kaplan, T., Kim, M., Buratowski, S., Schreiber, S.L., Friedman, N., and Rando, O.J. (2005). Single-nucleosome mapping of histone modifications in S. cerevisiae. PLoS biology *3*, e328.
Liu, N., Balliano, A., and Hayes, J.J. (2011). Mechanism(s) of SWI/SNF-induced nucleosome mobilization. Chembiochem : a European journal of chemical biology *12*, 196-204.
Lo, W.-S., Duggan, L., Tolga , N.C., Emre, Belotserkovskya, R., Lane, W.S., Shiekhattar, R., and Berger, S.L. (2001). Snf1--a Histone Kinase That Works in Concert with the Histone Acetyltransferase Gcn5 to Regulate Transcription. Science (New York, NY) *293*, 1142-1146.

Lomberk, G., Wallrath, L., and Urrutia, R. (2006). The Heterochromatin Protein 1 family. Genome Biol *7*, 228.
Lõoke, M., Kristjuhan, K., and Kristjuhan, A. (2011). Extraction of genomic DNA from yeasts for PCR-based applications. BioTechniques *50*, 325-328.
Lowary, P.T., and Widom, J. (1998). New DNA sequence rules for high affinity binding to histone octamer and sequence-directed nucleosome positioning. Journal of molecular biology *276*, 19-42.
Luger, K., Mader, A.W., Richmond, R.K., Sargent, D.F., and Richmond, T.J. (1997). Crystal structure of the nucleosome core particle at 2.8 A resolution. Nature *389*, 251-260.
Lupianez, D.G., Kraft, K., Heinrich, V., Krawitz, P., Brancati, F., Klopocki, E., Horn, D., Kayserili, H., Opitz, J.M., Laxova, R.*, et al.* (2015). Disruptions of topological chromatin domains cause pathogenic rewiring of gene-enhancer interactions. Cell *161*, 1012-1025.
Madia, F., Gattazzo, C., Wei, M., Fabrizio, P., Burhans, W.C., Weinberger, M., Galbani, A., Smith, J.R., Nguyen, C., Huey, S.*, et al.* (2008). Longevity mutation in SCH9 prevents recombination errors and premature genomic instability in a Werner/Bloom model system. The Journal of cell biology *180*, 67-81.
Maeshima, K., Ide, S., and Babokhov, M. (2019). Dynamic chromatin organization without the 30-nm fiber. Current opinion in cell biology *58*, 95-104.
Maeshima, K., Ide, S., Hibino, K., and Sasai, M. (2016). Liquid-like behavior of chromatin. Current opinion in genetics & development *37*, 36-45.
Makova, K.D., and Hardison, R.C. (2015). The effects of chromatin organization on variation in mutation rates in the genome. Nature reviews Genetics *16*, 213-223.
Malinovska, L., Kroschwald, S., and Alberti, S. (2013). Protein disorder, prion propensities, and self-organizing macromolecular collectives. Biochimica et biophysica acta *1834*, 918-931.
Malleshaiah, M.K., Shahrezaei, V., Swain, P.S., and Michnick, S.W. (2010). The scaffold protein Ste5 directly controls a switch-like mating decision in yeast. Nature *465*, 101-105.
Manohar, M., Mooney, A.M., North, J.A., Nakkula, R.J., Picking, J.W., Edon, A., Fishel, R., Poirier, M.G., and Ottesen, J.J. (2009). Acetylation of histone H3 at the nucleosome dyad alters DNA-histone binding. The Journal of biological chemistry *284*, 23312-23321.
Martin, A.M., Pouchnik, D.J., Walker, J.L., and Wyrick, J.J. (2004). Redundant roles for histone H3 N-terminal lysine residues in subtelomeric gene repression in Saccharomyces cerevisiae. Genetics *167*, 1123-1132.
Martincorena, I., Seshasayee, A.S., and Luscombe, N.M. (2012). Evidence of non-random mutation rates suggests an evolutionary risk management strategy. Nature *485*, 95-98.
Mavrich, T.N., Jiang, C., Ioshikhes, I.P., Li, X., Venters, B.J., Zanton, S.J., Tomsho, L.P., Qi, J., Glaser, R.L., Schuster, S.C.*, et al.* (2008). Nucleosome organization in the Drosophila genome. Nature *453*, 358-362.
McBryant, S.J., Lu, X., and Hansen, J.C. (2010). Multifunctionality of the linker histones: an emerging role for protein-protein interactions. Cell research *20*, 519-528.
McIlwraith, M.J., and West, S.C. (2008). DNA Repair Synthesis Facilitates RAD52-Mediated Second-End Capture during DSB Repair. Molecular Cell *29*, 510-516.
Measday, V., and Stirling, P.C. (2015). Navigating yeast genome maintenance with functional genomics. Briefings in Functional Genomics *15*, 119-129.
Meister, P., Towbin, B.D., Pike, B.L., Ponti, A., and Gasser, S.M. (2010). The spatial dynamics of tissue-specific promoters during C. elegans development. Genes & development *24*, 766-782.
Meneghini, M.D., Wu, M., and Madhani, H.D. (2003). Conserved histone variant H2A.Z protects euchromatin from the ectopic spread of silent heterochromatin. Cell *112*, 725-736.

Mercy, G., Mozziconacci, J., Scolari, V.F., Yang, K., Zhao, G., Thierry, A., Luo, Y., Mitchell, L.A., Shen, M., Shen, Y.*, et al.* (2017). 3D organization of synthetic and scrambled chromosomes. Science (New York, NY) *355*.
Mersfelder, E.L., and Parthun, M.R. (2006). The tale beyond the tail: histone core domain modifications and the regulation of chromatin structure. Nucleic acids research *34*, 2653-2662.
Michieletto, D., Chiang, M., Colì, D., Papantonis, A., Orlandini, E., Cook, P.R., and Marenduzzo, D. (2017). Shaping epigenetic memory via genomic bookmarking. Nucleic acids research *46*, 83-93.
Miron, E., Oldenkamp, R., Brown, J.M., Pinto, D.M.S., Xu, C.S., Faria, A.R., Shaban, H.A., Rhodes, J.D.P., Innocent, C., de Ornellas, S.*, et al.* (2020). Chromatin arranges in chains of mesoscale domains with nanoscale functional topography independent of cohesin. Sci Adv *6*.
Mizuguchi, T., Barrowman, J., and Grewal, S.I.S. (2015). Chromosome domain architecture and dynamic organization of the fission yeast genome. FEBS letters *589*, 2975-2986.
Mizuguchi, T., Fudenberg, G., Mehta, S., Belton, J.M., Taneja, N., Folco, H.D., FitzGerald, P., Dekker, J., Mirny, L., Barrowman, J.*, et al.* (2014). Cohesin-dependent globules and heterochromatin shape 3D genome architecture in S. pombe. Nature *516*, 432-435.
Mizzen, C.A., Yang, X.J., Kokubo, T., Brownell, J.E., Bannister, A.J., Owen-Hughes, T., Workman, J., Wang, L., Berger, S.L., Kouzarides, T.*, et al.* (1996). The TAF(II)250 subunit of TFIID has histone acetyltransferase activity. Cell *87*, 1261-1270.
Montavon, T., Shukeir, N., Erikson, G., Engist, B., Onishi-Seebacher, M., Ryan, D., Musa, Y., Mittler, G., Meyer, A.G., Genoud, C.*, et al.* (2021). Complete loss of H3K9 methylation dissolves mouse heterochromatin organization. Nat Commun *12*, 4359.
Morawska, M., and Ulrich, H.D. (2013). An expanded tool kit for the auxin-inducible degron system in budding yeast. Yeast (Chichester, England) *30*, 341-351.
Muck, J.S., Kandasamy, K., Englmann, A., Gunther, M., and Zink, D. (2012). Perinuclear positioning of the inactive human cystic fibrosis gene depends on CTCF, A-type lamins and an active histone deacetylase. Journal of cellular biochemistry *113*, 2607-2621.
Nakayama, J., Rice, J.C., Strahl, B.D., Allis, C.D., and Grewal, S.I. (2001). Role of histone H3 lysine 9 methylation in epigenetic control of heterochromatin assembly. Science *292*, 110-113.
Neumann, F.R., Dion, V., Gehlen, L.R., Tsai-Pflugfelder, M., Schmid, R., Taddei, A., and Gasser, S.M. (2012). Targeted INO80 enhances subnuclear chromatin movement and ectopic homologous recombination. Genes Dev *26*, 369-383.
Ng, M.K., and Cheung, P. (2016). A brief histone in time: understanding the combinatorial functions of histone PTMs in the nucleosome context. Biochemistry and cell biology = Biochimie et biologie cellulaire *94*, 33-42.
Nguyen, V.Q., Ranjan, A., Stengel, F., Wei, D., Aebersold, R., Wu, C., and Leschziner, A.E. (2013). Molecular architecture of the ATP-dependent chromatin-remodeling complex SWR1. Cell *154*, 1220-1231.
Nora, E.P., Lajoie, B.R., Schulz, E.G., Giorgetti, L., Okamoto, I., Servant, N., Piolot, T., van Berkum, N.L., Meisig, J., Sedat, J.*, et al.* (2012). Spatial partitioning of the regulatory landscape of the X-inactivation centre. Nature *485*, 381-385.
Nott, T.J., Petsalaki, E., Farber, P., Jervis, D., Fussner, E., Plochowietz, A., Craggs, T.D., Bazett-Jones, D.P., Pawson, T., Forman-Kay, J.D.*, et al.* (2015). Phase transition of a disordered nuage protein generates environmentally responsive membraneless organelles. Molecular cell *57*, 936-947.
Oeffinger, M., Wei, K.E., Rogers, R., DeGrasse, J.A., Chait, B.T., Aitchison, J.D., and Rout, M.P. (2007). Comprehensive analysis of diverse ribonucleoprotein complexes. Nature methods *4*, 951-956.

Ogawa, L.M., and Baserga, S.J. (2017). Crosstalk between the nucleolus and the DNA damage response. Molecular bioSystems *13*, 443-455.
Olins, D.E., and Olins, A.L. (2003). Chromatin history: our view from the bridge. Nature Reviews Molecular Cell Biology *4*, 809-814.
Ong, C.T., and Corces, V.G. (2009). Insulators as mediators of intra- and inter-chromosomal interactions: a common evolutionary theme. Journal of biology *8*, 73.
Opitz, N., Schmitt, K., Hofer-Pretz, V., Neumann, B., Krebber, H., Braus, G.H., and Valerius, O. (2017). Capturing the Asc1p/Receptor for Activated C Kinase 1 (RACK1) Microenvironment at the Head Region of the 40S Ribosome with Quantitative BioID in Yeast. Molecular & cellular proteomics : MCP *16*, 2199-2218.
Orsztynowicz, M., Lechniak, D., Pawlak, P., Kociucka, B., Kubickova, S., Cernohorska, H., and Madeja, Z.E. (2017). Changes in chromosome territory position within the nucleus reflect alternations in gene expression related to embryonic lineage specification. PloS one *12*, e0182398.
Ou, H.D., Phan, S., Deerinck, T.J., Thor, A., Ellisman, M.H., and O'Shea, C.C. (2017). ChromEMT: Visualizing 3D chromatin structure and compaction in interphase and mitotic cells. Science (New York, NY) *357*.
Oughtred, R., Rust, J., Chang, C., Breitkreutz, B.J., Stark, C., Willems, A., Boucher, L., Leung, G., Kolas, N., Zhang, F.*, et al.* (2021). The BioGRID database: A comprehensive biomedical resource of curated protein, genetic, and chemical interactions. Protein Sci *30*, 187-200.
Parra, M.A., Kerr, D., Fahy, D., Pouchnik, D.J., and Wyrick, J.J. (2006). Deciphering the roles of the histone H2B N-terminal domain in genome-wide transcription. Molecular and cellular biology *26*, 3842-3852.
Pepenella, S., Murphy, K.J., and Hayes, J.J. (2014). Intra- and inter-nucleosome interactions of the core histone tail domains in higher-order chromatin structure. Chromosoma *123*, 3-13.
Pessina, F., Giavazzi, F., Yin, Y., Gioia, U., Vitelli, V., Galbiati, A., Barozzi, S., Garre, M., Oldani, A., Flaus, A.*, et al.* (2019). Functional transcription promoters at DNA double-strand breaks mediate RNA-driven phase separation of damage-response factors. Nature Cell Biology *21*, 1286-1299.
Petty, E.L., Collette, K.S., Cohen, A.J., Snyder, M.J., and Csankovszki, G. (2009). Restricting dosage compensation complex binding to the X chromosomes by H2A.Z/HTZ-1. PLoS Genet *5*, e1000699.
Phillips-Cremins, J.E., Sauria, M.E., Sanyal, A., Gerasimova, T.I., Lajoie, B.R., Bell, J.S., Ong, C.T., Hookway, T.A., Guo, C., Sun, Y.*, et al.* (2013). Architectural protein subclasses shape 3D organization of genomes during lineage commitment. Cell *153*, 1281-1295.
Phillips, D.M., and Johns, E.W. (1965). A FRACTIONATION OF THE HISTONES OF GROUP F2A FROM CALF THYMUS. The Biochemical journal *94*, 127-130.
Pich, O., Muiños, F., Sabarinathan, R., Reyes-Salazar, I., Gonzalez-Perez, A., and Lopez-Bigas, N. (2018). Somatic and Germline Mutation Periodicity Follow the Orientation of the DNA Minor Groove around Nucleosomes. Cell *175*, 1074-1087.e1018.
Pokholok, D.K., Harbison, C.T., Levine, S., Cole, M., Hannett, N.M., Lee, T.I., Bell, G.W., Walker, K., Rolfe, P.A., Herbolsheimer, E.*, et al.* (2005). Genome-wide map of nucleosome acetylation and methylation in yeast. Cell *122*, 517-527.
Pouokam, M., Cruz, B., Burgess, S., Segal, M.R., Vazquez, M., and Arsuaga, J. (2019). The Rabl configuration limits topological entanglement of chromosomes in budding yeast. Scientific Reports *9*, 6795.
Pulice, J.L., and Kadoch, C. (2017). Composition and Function of Mammalian SWI/SNF Chromatin Remodeling Complexes in Human Disease. Cold Spring Harbor symposia on quantitative biology.

Quail, T., Golfier, S., Elsner, M., Ishihara, K., Murugesan, V., Renger, R., Jülicher, F., and Brugués, J. (2021). Force generation by protein–DNA co-condensation. Nature Physics *17*, 1007-1012.
Querol, A., and Bond, U. (2009). The complex and dynamic genomes of industrial yeasts. FEMS Microbiol Lett *293*, 1-10.
Quinodoz, S.A., and Guttman, M. (2021). Essential Roles for RNA in Shaping Nuclear Organization. Cold Spring Harb Perspect Biol.
Rabl, C. (1885). Uber Zelltheilung. Morphol Jahrb *10*, 214-330.
Raffoux, X., Bourge, M., Dumas, F., Martin, O.C., and Falque, M. (2018). High-throughput measurement of recombination rates and genetic interference in Saccharomyces cerevisiae. Yeast *35*, 431-442.
Ragoczy, T., Bender, M.A., Telling, A., Byron, R., and Groudine, M. (2006). The locus control region is required for association of the murine beta-globin locus with engaged transcription factories during erythroid maturation. Genes & development *20*, 1447-1457.
Raisner, R.M., Hartley, P.D., Meneghini, M.D., Bao, M.Z., Liu, C.L., Schreiber, S.L., Rando, O.J., and Madhani, H.D. (2005). Histone variant H2A.Z marks the 5' ends of both active and inactive genes in euchromatin. Cell *123*, 233-248.
Randise-Hinchliff, C., Coukos, R., Sood, V., Sumner, M.C., Zdraljevic, S., Meldi Sholl, L., Garvey Brickner, D., Ahmed, S., Watchmaker, L., and Brickner, J.H. (2016). Strategies to regulate transcription factor-mediated gene positioning and interchromosomal clustering at the nuclear periphery. The Journal of cell biology *212*, 633-646.
Rando, O.J. (2007). Global patterns of histone modifications. Current opinion in genetics & development *17*, 94-99.
Ransom, M., Dennehey, B.K., and Tyler, J.K. (2010). Chaperoning histones during DNA replication and repair. Cell *140*, 183-195.
Rao, S.S., Huntley, M.H., Durand, N.C., Stamenova, E.K., Bochkov, I.D., Robinson, J.T., Sanborn, A.L., Machol, I., Omer, A.D., Lander, E.S.*, et al.* (2014). A 3D map of the human genome at kilobase resolution reveals principles of chromatin looping. Cell *159*, 1665-1680.
Raveh-Sadka, T., Levo, M., Shabi, U., Shany, B., Keren, L., Lotan-Pompan, M., Zeevi, D., Sharon, E., Weinberger, A., and Segal, E. (2012). Manipulating nucleosome disfavoring sequences allows fine-tune regulation of gene expression in yeast. Nature genetics *44*, 743-750.
Rea, S., Eisenhaber, F., O'Carroll, D., Strahl, B.D., Sun, Z.W., Schmid, M., Opravil, S., Mechtler, K., Ponting, C.P., Allis, C.D.*, et al.* (2000). Regulation of chromatin structure by site-specific histone H3 methyltransferases. Nature *406*, 593-599.
Rechendorff, K., Witz, G., Adamcik, J., and Dietler, G. (2009). Persistence length and scaling properties of single-stranded DNA adsorbed on modified graphite. The Journal of chemical physics *131*, 095103.
Richmond, T.J., and Davey, C.A. (2003). The structure of DNA in the nucleosome core. Nature *423*, 145-150.
Riley, R., Haridas, S., Wolfe, K.H., Lopes, M.R., Hittinger, C.T., Göker, M., Salamov, A.A., Wisecaver, J.H., Long, T.M., Calvey, C.H.*, et al.* (2016). Comparative genomics of biotechnologically important yeasts. Proceedings of the National Academy of Sciences *113*, 9882.
Robzyk, K., Recht, J., and Osley, M.A. (2000). Rad6-dependent ubiquitination of histone H2B in yeast. Science (New York, NY) *287*, 501-504.
Rodrigues-Prause, A., Sampaio, N.M.V., Gurol, T.M., Aguirre, G.M., Sedam, H.N.C., Chapman, M.J., Malc, E.P., Ajith, V.P., Chakraborty, P., Tizei, P.A.*, et al.* (2018). A Case Study of Genomic Instability in an Industrial Strain of Saccharomyces cerevisiae. G3 (Bethesda, Md) *8*, 3703-3713.

Rohner, S., Kalck, V., Wang, X., Ikegami, K., Lieb, J.D., Gasser, S.M., and Meister, P. (2013). Promoter- and RNA polymerase II-dependent hsp-16 gene association with nuclear pores in Caenorhabditis elegans. The Journal of cell biology *200*, 589-604.
Roque, A., Iloro, I., Ponte, I., Arrondo, J.L., and Suau, P. (2005). DNA-induced secondary structure of the carboxyl-terminal domain of histone H1. The Journal of biological chemistry *280*, 32141-32147.
Rothstein, R.J. (1983). One-step gene disruption in yeast. Methods in enzymology *101*, 202-211.
Rouse, P.E. (1953). A Theory of the Linear Viscoelastic Properties of Dilute Solutions of Coiling Polymers. *21*, 1272-1280.
Rudnizky, S., Khamis, H., Ginosar, Y., Goren, E., Melamed, P., and Kaplan, A. (2021). Extended and dynamic linker histone-DNA Interactions control chromatosome compaction. Mol Cell *81*, 3410-3421 e3414.
Rufiange, A., Jacques, P.E., Bhat, W., Robert, F., and Nourani, A. (2007). Genome-wide replication-independent histone H3 exchange occurs predominantly at promoters and implicates H3 K56 acetylation and Asf1. Mol Cell *27*, 393-405.
Sabari, B.R., Dall'Agnese, A., Boija, A., Klein, I.A., Coffey, E.L., Shrinivas, K., Abraham, B.J., Hannett, N.M., Zamudio, A.V., Manteiga, J.C.*, et al.* (2018). Coactivator condensation at super-enhancers links phase separation and gene control. Science *361*.
Sáez-Vásquez, J., and Gadal, O. (2010). Genome organization and function: a view from yeast and Arabidopsis. Molecular plant *3*, 678-690.
Sanders, S.L., Jennings, J., Canutescu, A., Link, A.J., and Weil, P.A. (2002). Proteomics of the eukaryotic transcription machinery: identification of proteins associated with components of yeast TFIID by multidimensional mass spectrometry. Molecular and cellular biology *22*, 4723-4738.
Sanulli, S., Trnka, M.J., Dharmarajan, V., Tibble, R.W., Pascal, B.D., Burlingame, A.L., Griffin, P.R., Gross, J.D., and Narlikar, G.J. (2019). HP1 reshapes nucleosome core to promote heterochromatin phase separation. Nature.
Sassone-Corsi, P., Mizzen, C.A., Cheung, P., Crosio, C., Monaco, L., Jacquot, S., Hanauer, A., and Allis, C.D. (1999). Requirement of Rsk-2 for epidermal growth factor-activated phosphorylation of histone H3. Science (New York, NY) *285*, 886-891.
Satchwell, S.C., Drew, H.R., and Travers, A.A. (1986). Sequence periodicities in chicken nucleosome core DNA. Journal of molecular biology *191*, 659-675.
Scheffold, F., Diaz-Leyva, P., Reufer, M., Ben Braham, N., Lynch, I., and Harden, J.L. (2010). Brushlike interactions between thermoresponsive microgel particles. Phys Rev Lett *104*, 128304.
Schindelin, J., Arganda-Carreras, I., Frise, E., Kaynig, V., Longair, M., Pietzsch, T., Preibisch, S., Rueden, C., Saalfeld, S., Schmid, B.*, et al.* (2012). Fiji: an open-source platform for biological-image analysis. Nature methods *9*, 676-682.
Schmidtmann, E., Anton, T., Rombaut, P., Herzog, F., and Leonhardt, H. (2016). Determination of local chromatin composition by CasID. Nucleus (Austin, Tex) *7*, 476-484.
Schober, H., Kalck, V., Vega-Palas, M.A., Van Houwe, G., Sage, D., Unser, M., Gartenberg, M.R., and Gasser, S.M. (2008). Controlled exchange of chromosomal arms reveals principles driving telomere interactions in yeast. Genome Res *18*, 261-271.
Schones, D.E., Cui, K., Cuddapah, S., Roh, T.Y., Barski, A., Wang, Z., Wei, G., and Zhao, K. (2008). Dynamic regulation of nucleosome positioning in the human genome. Cell *132*, 887-898.
Scott, D.D., and Oeffinger, M. (2016). Nucleolin and nucleophosmin: nucleolar proteins with multiple functions in DNA repair. Biochemistry and cell biology = Biochimie et biologie cellulaire *94*, 419-432.

Segal, E., Fondufe-Mittendorf, Y., Chen, L., Thastrom, A., Field, Y., Moore, I.K., Wang, J.P., and Widom, J. (2006). A genomic code for nucleosome positioning. Nature *442*, 772-778.
Segura, J., Ferretti, L., Ramos-Onsins, S., Capilla, L., Farre, M., Reis, F., Oliver-Bonet, M., Fernandez-Bellon, H., Garcia, F., Garcia-Caldes, M.*, et al.* (2013). Evolution of recombination in eutherian mammals: insights into mechanisms that affect recombination rates and crossover interference. Proc Biol Sci *280*, 20131945.
Sexton, T., Yaffe, E., Kenigsberg, E., Bantignies, F., Leblanc, B., Hoichman, M., Parrinello, H., Tanay, A., and Cavalli, G. (2012). Three-dimensional folding and functional organization principles of the Drosophila genome. Cell *148*, 458-472.
Shaban, H.A., Barth, R., and Bystricky, K. (2018). Formation of correlated chromatin domains at nanoscale dynamic resolution during transcription. Nucleic acids research *46*, e77.
Shaban, H.A., and Seeber, A. (2020). Monitoring the spatio-temporal organization and dynamics of the genome. Nucleic acids research *48*, 3423-3434.
Shaw, W.M., Yamauchi, H., Mead, J., Gowers, G.-O.F., Bell, D.J., Öling, D., Larsson, N., Wigglesworth, M., Ladds, G., and Ellis, T. (2019). Engineering a Model Cell for Rational Tuning of GPCR Signaling. Cell *177*, 782-796.e727.
She, R., and Jarosz, D.F. (2018). Mapping Causal Variants with Single-Nucleotide Resolution Reveals Biochemical Drivers of Phenotypic Change. Cell *172*, 478-490.e415.
Shen, X., Mizuguchi, G., Hamiche, A., and Wu, C. (2000). A chromatin remodelling complex involved in transcription and DNA processing. Nature *406*, 541-544.
Shin, Y., Chang, Y.-C., Lee, D.S.W., Berry, J., Sanders, D.W., Ronceray, P., Wingreen, N.S., Haataja, M., and Brangwynne, C.P. (2018). Liquid Nuclear Condensates Mechanically Sense and Restructure the Genome. Cell *175*, 1481-1491.e1413.
Singleton, M.R., Dillingham, M.S., and Wigley, D.B. (2007). Structure and mechanism of helicases and nucleic acid translocases. Annual review of biochemistry *76*, 23-50.
Skok, J.A., Brown, K.E., Azuara, V., Caparros, M.L., Baxter, J., Takacs, K., Dillon, N., Gray, D., Perry, R.P., Merkenschlager, M.*, et al.* (2001). Nonequivalent nuclear location of immunoglobulin alleles in B lymphocytes. Nature immunology *2*, 848-854.
Smerdon, M.J. (1991). DNA repair and the role of chromatin structure. Current opinion in cell biology *3*, 422-428.
Smith, S., Hwang, J.Y., Banerjee, S., Majeed, A., Gupta, A., and Myung, K. (2004). Mutator genes for suppression of gross chromosomal rearrangements identified by a genome-wide screening in Saccharomyces cerevisiae. Proc Natl Acad Sci U S A *101*, 9039-9044.
Smith, S.B., Cui, Y., and Bustamante, C. (1996). Overstretching B-DNA: the elastic response of individual double-stranded and single-stranded DNA molecules. Science (New York, NY) *271*, 795-799.
Solovei, I., Kreysing, M., Lanctôt, C., Kösem, S., Peichl, L., Cremer, T., Guck, J., and Joffe, B. (2009). Nuclear architecture of rod photoreceptor cells adapts to vision in mammalian evolution. Cell *137*, 356-368.
Spector, D.L. (2003). The dynamics of chromosome organization and gene regulation. Annual review of biochemistry *72*, 573-608.
St Charles, J., and Petes, T.D. (2013). High-resolution mapping of spontaneous mitotic recombination hotspots on the 1.1 Mb arm of yeast chromosome IV. PLoS Genet *9*, e1003434.
Stanek, D., and Fox, A.H. (2017). Nuclear bodies: news insights into structure and function. Current opinion in cell biology *46*, 94-101.
Stephens, A.D., Liu, P.Z., Banigan, E.J., Almassalha, L.M., Backman, V., Adam, S.A., Goldman, R.D., and Marko, J.F. (2018). Chromatin histone modifications and rigidity affect nuclear morphology independent of lamins. Mol Biol Cell *29*, 220-233.

Sterner, D.E., and Berger, S.L. (2000). Acetylation of histones and transcription-related factors. Microbiology and molecular biology reviews : MMBR *64*, 435-459.
Stevens, T.J., Lando, D., Basu, S., Atkinson, L.P., Cao, Y., Lee, S.F., Leeb, M., Wohlfahrt, K.J., Boucher, W., O'Shaughnessy-Kirwan, A*., et al.* (2017). 3D structures of individual mammalian genomes studied by single-cell Hi-C. Nature *544*, 59-64.
Stewart, M.D., Li, J., and Wong, J. (2005). Relationship between histone H3 lysine 9 methylation, transcription repression, and heterochromatin protein 1 recruitment. Mol Cell Biol *25*, 2525-2538.
Stirling, P.C., Shen, Y., Corbett, R., Jones, S.J.M., and Hieter, P. (2014). Genome destabilizing mutator alleles drive specific mutational trajectories in Saccharomyces cerevisiae. Genetics *196*, 403-412.
Strahl, B.D., and Allis, C.D. (2000). The language of covalent histone modifications. Nature *403*, 41-45.
Strom, A.R., Emelyanov, A.V., Mir, M., Fyodorov, D.V., Darzacq, X., and Karpen, G.H. (2017). Phase separation drives heterochromatin domain formation. Nature *547*, 241-245.
Taddei, A., Van Houwe, G., Hediger, F., Kalck, V., Cubizolles, F., Schober, H., and Gasser, S.M. (2006). Nuclear pore association confers optimal expression levels for an inducible yeast gene. Nature *441*, 774-778.
Talbert, P.B., and Henikoff, S. (2010). Histone variants--ancient wrap artists of the epigenome. Nature reviews Molecular cell biology *11*, 264-275.
Taunton, J., Hassig, C.A., and Schreiber, S.L. (1996). A mammalian histone deacetylase related to the yeast transcriptional regulator Rpd3p. Science (New York, NY) *272*, 408-411.
Thastrom, A., Lowary, P.T., and Widom, J. (2004). Measurement of histone-DNA interaction free energy in nucleosomes. Methods (San Diego, Calif) *33*, 33-44.
The UniProt, C. (2021). UniProt: the universal protein knowledgebase in 2021. Nucleic Acids Research *49*, D480-D489.
Therizols, P., Duong, T., Dujon, B., Zimmer, C., and Fabre, E. (2010). Chromosome arm length and nuclear constraints determine the dynamic relationship of yeast subtelomeres. Proc Natl Acad Sci U S A *107*, 2025-2030.
Thomson, S., Clayton, A.L., Hazzalin, C.A., Rose, S., Barratt, M.J., and Mahadevan, L.C. (1999). The nucleosomal response associated with immediate-early gene induction is mediated via alternative MAP kinase cascades: MSK1 as a potential histone H3/HMG-14 kinase. The EMBO journal *18*, 4779-4793.
Tiley, G.P., and Burleigh, J.G. (2015). The relationship of recombination rate, genome structure, and patterns of molecular evolution across angiosperms. BMC Evol Biol *15*, 194.
Topal, S., Vasseur, P., Radman-Livaja, M., and Peterson, C.L. (2019). Distinct transcriptional roles for Histone H3-K56 acetylation during the cell cycle in Yeast. Nature communications *10*, 4372.
Toretsky, J.A., and Wright, P.E. (2014). Assemblages: functional units formed by cellular phase separation. The Journal of cell biology *206*, 579-588.
Tortora, M.M., Salari, H., and Jost, D. (2020). Chromosome dynamics during interphase: a biophysical perspective. Current opinion in genetics & development *61*, 37-43.
Tsukada, Y., Fang, J., Erdjument-Bromage, H., Warren, M.E., Borchers, C.H., Tempst, P., and Zhang, Y. (2006). Histone demethylation by a family of JmjC domain-containing proteins. Nature *439*, 811-816.
Turner, A.L., Watson, M., Wilkins, O.G., Cato, L., Travers, A., Thomas, J.O., and Stott, K. (2018). Highly disordered histone H1-DNA model complexes and their condensates. Proceedings of the National Academy of Sciences of the United States of America *115*, 11964-11969.

Tyagi, M., Imam, N., Verma, K., and Patel, A.K. (2016). Chromatin remodelers: We are the drivers!! Nucleus (Austin, Tex) *7*, 388-404.
Uhlenbeck, G.E., and Ornstein, L.S. (1930). On the Theory of the Brownian Motion. Phys Rev *36*, 823–841.
van Attikum, H., and Gasser, S.M. (2009). Crosstalk between histone modifications during the DNA damage response. Trends in cell biology *19*, 207-217.
van der Lee, R., Buljan, M., Lang, B., Weatheritt, R.J., Daughdrill, G.W., Dunker, A.K., Fuxreiter, M., Gough, J., Gsponer, J., Jones, D.T*., et al.* (2014). Classification of intrinsically disordered regions and proteins. Chemical reviews *114*, 6589-6631.
Van Holde, K.E., Allen, J.R., Tatchell, K., Weischet, W.O., and Lohr, D. (1980). DNA-histone interactions in nucleosomes. Biophysical journal *32*, 271-282.
Vasquez, P.A., and Bloom, K. (2014). Polymer models of interphase chromosomes. Nucleus (Austin, Tex) *5*, 376-390.
Vasquez, P.A., Hult, C., Adalsteinsson, D., Lawrimore, J., Forest, M.G., and Bloom, K. (2016). Entropy gives rise to topologically associating domains. Nucleic acids research *44*, 5540-5549.
Verdaasdonk, J.S., Gardner, R., Stephens, A.D., Yeh, E., and Bloom, K. (2012). Tension-dependent nucleosome remodeling at the pericentromere in yeast. Molecular biology of the cell *23*, 2560-2570.
Verdaasdonk, J.S., Vasquez, P.A., Barry, R.M., Barry, T., Goodwin, S., Forest, M.G., and Bloom, K. (2013). Centromere tethering confines chromosome domains. Mol Cell *52*, 819-831.
Vernarecci, S., Tosi, F., and Filetici, P. (2010). Tuning acetylated chromatin with HAT inhibitors: a novel tool for therapy. Epigenetics *5*, 105-111.
Vietri Rudan, M., Barrington, C., Henderson, S., Ernst, C., Odom, D.T., Tanay, A., and Hadjur, S. (2015). Comparative Hi-C reveals that CTCF underlies evolution of chromosomal domain architecture. Cell reports *10*, 1297-1309.
Wang, J., Choi, J.M., Holehouse, A.S., Lee, H.O., Zhang, X., Jahnel, M., Maharana, S., Lemaitre, R., Pozniakovsky, A., Drechsel, D*., et al.* (2018). A Molecular Grammar Governing the Driving Forces for Phase Separation of Prion-like RNA Binding Proteins. Cell *174*, 688-699.e616.
Wang, S., Su, J.H., Beliveau, B.J., Bintu, B., Moffitt, J.R., Wu, C.T., and Zhuang, X. (2016). Spatial organization of chromatin domains and compartments in single chromosomes. Science (New York, NY) *353*, 598-602.
Wang, Y.H., Amirhaeri, S., Kang, S., Wells, R.D., and Griffith, J.D. (1994). Preferential nucleosome assembly at DNA triplet repeats from the myotonic dystrophy gene. Science (New York, NY) *265*, 669-671.
Wang, Y.H., and Griffith, J. (1995). Expanded CTG triplet blocks from the myotonic dystrophy gene create the strongest known natural nucleosome positioning elements. Genomics *25*, 570-573.
Wapenaar, H., and Dekker, F.J. (2016). Histone acetyltransferases: challenges in targeting bi-substrate enzymes. Clinical Epigenetics *8*, 59.
Weber, S.C., and Brangwynne, C.P. (2015). Inverse size scaling of the nucleolus by a concentration-dependent phase transition. Current biology : CB *25*, 641-646.
Weber, S.C., Spakowitz, A.J., and Theriot, J.A. (2010). Bacterial chromosomal loci move subdiffusively through a viscoelastic cytoplasm. Phys Rev Lett *104*, 238102.
Weber, S.C., Spakowitz, A.J., and Theriot, J.A. (2012). Nonthermal ATP-dependent fluctuations contribute to the in vivo motion of chromosomal loci. Proceedings of the National Academy of Sciences of the United States of America *109*, 7338-7343.

Wei, M., Fabrizio, P., Hu, J., Ge, H., Cheng, C., Li, L., and Longo, V.D. (2008). Life span extension by calorie restriction depends on Rim15 and transcription factors downstream of Ras/PKA, Tor, and Sch9. PLoS genetics *4*, e13-e13.
Widom, J. (2001). Role of DNA sequence in nucleosome stability and dynamics. Quarterly reviews of biophysics *34*, 269-324.
Wilfert, L., Gadau, J., and Schmid-Hempel, P. (2007). Variation in genomic recombination rates among animal taxa and the case of social insects. Heredity (Edinb) *98*, 189-197.
Williams, R.R., Azuara, V., Perry, P., Sauer, S., Dvorkina, M., Jorgensen, H., Roix, J., McQueen, P., Misteli, T., Merkenschlager, M.*, et al.* (2006). Neural induction promotes large-scale chromatin reorganisation of the Mash1 locus. Journal of cell science *119*, 132-140.
Wolfe, K.H., and Shields, D.C. (1997). Molecular evidence for an ancient duplication of the entire yeast genome. Nature *387*, 708-713.
Wong, H., Marie-Nelly, H., Herbert, S., Carrivain, P., Blanc, H., Koszul, R., Fabre, E., and Zimmer, C. (2012). A predictive computational model of the dynamic 3D interphase yeast nucleus. Curr Biol *22*, 1881-1890.
Wood, C.M., Nicholson, J.M., Lambert, S.J., Chantalat, L., Reynolds, C.D., and Baldwin, J.P. (2005). High-resolution structure of the native histone octamer. Acta crystallographica Section F, Structural biology and crystallization communications *61*, 541-545.
Xhemalce, B., Miller, K.M., Driscoll, R., Masumoto, H., Jackson, S.P., Kouzarides, T., Verreault, A., and Arcangioli, B. (2007). Regulation of histone H3 lysine 56 acetylation in Schizosaccharomyces pombe. The Journal of biological chemistry *282*, 15040-15047.
Xu, F., Zhang, K., and Grunstein, M. (2005). Acetylation in histone H3 globular domain regulates gene expression in yeast. Cell *121*, 375-385.
Yang, J., Zhang, X., Feng, J., Leng, H., Li, S., Xiao, J., Liu, S., Xu, Z., Xu, J., Li, D.*, et al.* (2016). The Histone Chaperone FACT Contributes to DNA Replication-Coupled Nucleosome Assembly. Cell reports *14*, 1128-1141.
Yang, X.-J., and Seto, E. (2008a). Lysine acetylation: codified crosstalk with other posttranslational modifications. Molecular cell *31*, 449-461.
Yang, X.-J., and Seto, E. (2008b). The Rpd3/Hda1 family of lysine deacetylases: from bacteria and yeast to mice and men. Nature Reviews Molecular Cell Biology *9*, 206-218.
Yang, X.J., and Grégoire, S. (2007). Metabolism, cytoskeleton and cellular signalling in the grip of protein Nepsilon - and O-acetylation. EMBO reports *8*, 556-562.
Yu, Q., Kuzmiak, H., Zou, Y., Olsen, L., Defossez, P.A., and Bi, X. (2009). Saccharomyces cerevisiae linker histone Hho1p functionally interacts with core histone H4 and negatively regulates the establishment of transcriptionally silent chromatin. The Journal of biological chemistry *284*, 740-750.
Yuan, G.C., Liu, Y.J., Dion, M.F., Slack, M.D., Wu, L.F., Altschuler, S.J., and Rando, O.J. (2005). Genome-scale identification of nucleosome positions in S. cerevisiae. Science (New York, NY) *309*, 626-630.
Zhang, H., Roberts, D.N., and Cairns, B.R. (2005). Genome-wide dynamics of Htz1, a histone H2A variant that poises repressed/basal promoters for activation through histone loss. Cell *123*, 219-231.
Zhu, L., and Brangwynne, C.P. (2015). Nuclear bodies: the emerging biophysics of nucleoplasmic phases. Current opinion in cell biology *34*, 23-30.
Zhu, Y.O., Siegal, M.L., Hall, D.W., and Petrov, D.A. (2014). Precise estimates of mutation rate and spectrum in yeast. Proc Natl Acad Sci U S A *111*, E2310-2318.

Zink, D., Amaral, M.D., Englmann, A., Lang, S., Clarke, L.A., Rudolph, C., Alt, F., Luther, K., Braz, C., Sadoni, N.*, et al.* (2004). Transcription-dependent spatial arrangements of CFTR and adjacent genes in human cell nuclei. The Journal of cell biology *166*, 815-825.
Zlatanova, J., Bishop, T.C., Victor, J.M., Jackson, V., and van Holde, K. (2009). The nucleosome family: dynamic and growing. Structure (London, England : 1993) *17*, 160-171.